UNIONE EUROPEA
Fondo sociale europeo

REGIONE AUTONOMA DELLA SARDEGNA

POR
SARDEGNA

Università degli Studi di Cagliari
Facoltà di Scienze MM. FF. NN.

Scuola di Dottorato in Ingegneria e Scienze per l'Ambiente e il Territorio

Dottorato in Scienze della Terra

Ciclo XXVII

Settori scientifici disciplinari di afferenza GEO/01, GEO/02

Selected Famennian (Late Devonian) events (Condroz, Annulata, Hangenberg) in Sardinia and in the Carnic Alps: conodont biostratigraphy, magnetic susceptibility and geochemistry.

Presentata da:	***Dott. Angelo Mossoni***
Coordinatore Dottorato	***Prof. Marcello Franceschelli***
Tutor/Relatore	***Prof. Carlo Corradini***

Esame finale anno accademico 2013 – 2014

SUMMARY

ABSTRACT

The Condroz, the *Annulata* and the Hangenberg are three events occurred in the Famennian. Causes and consequences are different for each one. The Condroz event is related to a sharp regression associated with an extinction of few ammonoid groups. The *Annulata* event to a transgression associated with a global spread of the ammonoid *Platyclymeniae annulata*. The Hangenberg event is a major event, that took place in a complex phase of eustatic variations that affected severely the fauna, and it is considered as one of the biggest extinction in the history of the earth.

A multidisciplinary approach is here provided to investigate the selected events. A biostratigraphic study based on conodonts was carried out to individuate the precise biostratigraphic position when the events occurred. The evolution of the low field magnetic susceptibility and the major elements geochemistry (Al, Si, K and Ti) have been investigated to study the evolution of the detrital input across the events.

Six different section were studied in two different areas of North Gondwana where the Famennian rocks are well exposed. Two sections bearing the Condroz and the *Annulata* events were studied in the Carnic Alps, four sections containing the three events were studied in the South East of Sardinia.

A detailed biostratigraphic study is here provided from both areas. More than 28 000 conodonts have been collected and discriminated into 101 taxa. Each taxon is described and illustrated. Ten conodont Zones, from the Upper *rhenana* Zone (Frasnian) to the Lower *expansa* Zone (Famennian) have been recognized in the Carnic Alps. Nineteen conodont Zones, from the Lower *crepida* Zone (Famennian) to the Upper *duplicata* Zone (Tournaisian) have been discriminated in the Sardinian sections.

The three events have been recognized in both areas. As for the Condroz and for the *Annulata* events, even if there is no change in lithology, the curves obtained by the MS and the major elements tends to show distinctive peaks time-equivalent to the events. In addition, a stratum rich in ammonoids marks the *Annulata* event in the field.

As for the Hangenberg event, marked in the field by a thin level of black shales, while the curves of the magnetic susceptibility and the major elements show a constant trend immediately before the main event (Hangenberg equivalent shales), in the earliest Carboniferous the magnetic curve shows distinctive fluctuations. These fluctuations are here explained by a phase of oceanic instability after the event. Despite there are no changes in the MS and in the major element data, the fauna is impoverished and seems to be affected by an earlier phase of the main event already in the Lower *praesulcata* Zone.

The major detrital input in the Carnic Alps sections may indicate a closer distance to the source for the latter respect to the Sardinia-Corsica microplate, therefore a new palaeogeographic interpretation for the two areas investigated in the Upper Devonian is here hypothesize.

INTRODUCTION

During the geological Eras, the Earth has gone through climatic changes that have affected the planet. These changes, caused by several factors, have interested big variations in the eustatic sea-level, and can be described as “Eustatic Events”. Few of these events have affected the living beings, sometimes severely, and can thus be considered as “Extinction Events”.

A multidisciplinary approach is necessary to study the events that have been registered in the rocks.

The study of the magnetic susceptibility is considered as an index of detrital input in sedimentary environments, also its potential as a tool for correlating sections from different basins was witnessed in several areas. This work has to be set within this context.

MS analysis as a tool to study sedimentary rocks

The low field magnetic susceptibility (MS) measure the intensity of magnetization of an object, induced by the presence of an external magnetic field. The MS of a rock sample ($\chi_{LF=}m^3/kg$) is measured at very low fields, not exceeding 500 mT, and measures the induced magnetization of diamagnetic, paramagnetic, antiferromagnetic and ferromagnetic minerals.

The use of magnetic susceptibility as a tool in different research fields has been extensively shown in the last 30 years, from enhanced magnetism of the soil for archaeological studies (Becker & Fassbinder 1999), environmental pollution (Flanders 1994), to different geological and stratigraphic fields.

The use of magnetic susceptibility as a palaeoclimatic proxy for Holocene, Pleistocene, and Tertiary sediments has been proved valuable since the eighties (e.g. Kent 1982, Mead & Tauxe 1986). Shackelton (1999) shows the use of MS to astronomically calibrate portions of geologic time scale; Boulila et al. (2008) to identify orbital forcing or even astronomical climate forcing (Husson et al. 2011, Lourens et al. 2005, Zeeden et al. 2013).

Bulk MS measurements have been used in Palaeozoic rocks for correlations and for reconstruction of sea level or climatic changes (Ellwood et al. 2006, 2007, 2008, Hladil et al.2002, 2010, Da Silva et al. 2009, 2010).

Magnetic susceptibility measures are considered as a proxy for the sedimentary detrital input, this is the reason why it can be considered useful for stratigraphy. For this purpose it must be verified whether the signal it is not affected by diagenetic processes, and therefore if it reflects a detrital origin. Some parameters have been proven useful to understand whether or not the diagenesis have affected the magnetic signal: the study of the hysteresis loop (Walden et al. 1999, Da Silva et al. 2010, Riquier et al. 2010), and the smectite-illite transformation (Katz et al. 2000, Zegers et al. 2003). In addition, to study the detrital input the the magnetic susceptibility can be compared with the evolution of major elements like Ti, Al, Zr (Tribovillard et al. 2006, Riquier et al. 2010, Da Silva et al. 2012).

Riquier et al. (2010) and Devleeschouwer et al. (2010) tried to identify the real nature and the origin of the differents components of the signal using the parameters mentioned before, but the papers dealing with this issue are not many.

The grain size and the type of particles (single domain, pseudosingle domain, multi domain or superparamagnetic) that generate the signal is another problem that has been assessed, and several models have been proposed in different papers (Day et al. 1977, Dunlop 2002, Tauxe et al. 2006, Spassov & Valet 2012).

The IGCP-580 project named "application of magnetic susceptibility as a palaeoclimatic proxy on Palaeozoic sedimentary rocks and characterization of the magnetic signal" was developed in this framework, and intends to consider the application of magnetic susceptibility in a pluri-disciplinary approach.

Several papers involving the studies of the MS in the Upper Devonian have been published through the last decades (Ellewood et al. 2000, Devleeschouwer et al. 2010, Riquier et al. 2010, De Vleeschouwer et al. 2012, Pas et al. 2014). Most of these works have as a purpose the study of a particular eustatic event (Punctata, Kellwasser, Annulata, Hangenberg) in different regions and use the low field magnetic susceptibility as a marker for palaeoenvironmental changes.

Famennian Events

The Devonian Period and in particular the Upper Devonian epoch, was a time of greenhouse conditions in which big sea-level changes caused by extensive volcanism and episodes of orogeny in different paeogeographycal settings took place.

During the Upper Devonian several "events" (House 2002) have been recognized in the last fifty years. Two of these have been included among the biggest mass extinction of the earth history: the "Kellwasser Event" in the late Frasnian and the "Hangenberg Event" in the latest Famennian. The others are considered as minor events, because the fauna was generally not severely affected by it.

While a general transgression that started in the Givetian age (Taghanic onlap) continued in the Frasnian, the Famennian shows a general regressive trend in which seven different events are registered (fig 1.1).

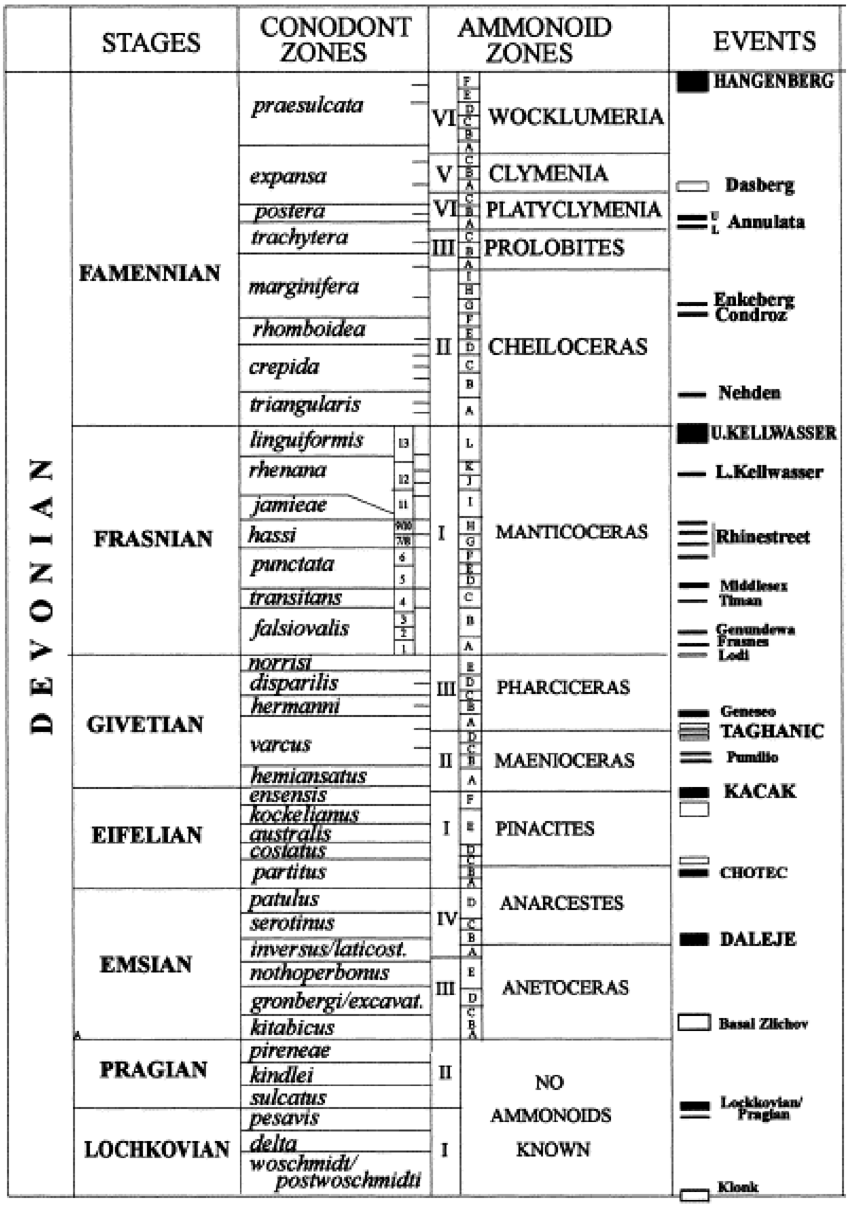

Figure 1.1. Devonian stages and events (House 2002, modified)

The Upper Kellwasser event coincide with the Frasnian/Fammenian boundary and is one of the "big Five" exctintion of the Phanerozoic Era (Buggisch 1991, Joachimski & Buggisch 1993, Becker & House 1994). The eustatic curve of Johnson et al. (1985) and that of Sandberg et al. (1988) show that events like Nehden (House 1985, 2002, Schülke & Popp 2005), *Annulata* (House 1985, 2002, Becker 1993a, Schülke & Popp 2005, Hartenfels 2011) and Dasberg (Becker 1993a, Hartenfels & Becker 2009, Girard et al. 2014) are related to marine transgressions. The Condroz event took place during a regressive phase (House 1985, 2002, Becker 1993a, Schülke & Popp 2005, Girard et al. 2014).

The Hangenberg event represent a complex phases of eustatic fluctuation (Walliser 1984, House 1985, 2002, Kaiser 2005, Schülke & Popp 2005, Kaiser et al. 2009).

The Condroz, the Annulata and the Hangenberg have been chosen among the seven Famennian events. In this work, these three events triggered by different factors and connected to different consequences, have been investigated in six different sections in Sardinia and in the Carnic Alps.

Condroz Event

The Condroz event was named after the Belgian Condroz "shelf" facies, it is marked at the top of UD II-D Ammonoid Zone (fig 1.1) and sees the extinction of over one third of ammonoid genera (many tornoceratids and cheiloceratids became extinct) (Becker 1993a, 1993b). It is not associated with anoxia spread, however it coincides with a regression that caused the end of the deposition of the *Cheiloceras* shales (Dreesen 1989, Walliser 1996).

Walliser (1996) and Schülke & Popp (2005) proposed a regressive phase in the eustatic cycle to be the trigger of this global event. This hypothesis has been well documented by Johnson et al. (1985) and Dopieralska (2003) that show respectively a sharp sea level fall and a significant amplitude regression within the *rhomboidea* Zone.

Becker & House (1997) identified two different regressive "pulses", and splitted the event in "Lower and Upper Condroz pulses". The "Lower Condroz pulse" coincides with a sharp sea level fall in the Uppermost *crepida* Zone (Johnson et al. 1985) and can be marked by a bioturbated shell-rich layer of cephalopod wackestone to packstone, with a various fossil content: goniatites, gastropods, trilobites, and bivalves (Schülke & Popp 2005).

The "Upper Condroz pulse" has been recorded in the Upper *rhomboidea* Zone (Becker & House 1997, Schülke & Popp 2005, Girard et al. 2014). This event has been registered at Col des Tribes section (France) and at Beringhauser Tunnel section (Rheinisches Schiefergebirge, Germany). It is associated with abundant ferruginous clays deposit and at least one hardground (Feist 2002, Schülke & Popp 2005, Girard et al. 2014).

Annulata Event

The *Annulata* event (Walliser 1984a, House 1985) represents a discrete sedimentary hypoxic to dysoxic perturbation in which a sudden proliferation of the ribbed ammonoid *Platyclymenia annulata* has been recorded worldwide (House 1985, Becker 1992a, 1992b, Becker & House 1997, Traghelen & Hartenels 2002).

According to Becker (1993), the *Annulata* event consists of two black shales levels riches in C_{org} or by dark limestones. It can be distincted into the Lower and Upper *Annulata* shales, biostratigraphically located in the Lower and Upper *trachytera* Zone (Walliser 1996, Hartenfels 2011).

Wilde & Berry (1984) hypothesize a short term flooding of oxygen depleted waters on continents due to a rise of anoxic layers as a cause of worldwide occurrence of these black shales. Regarding the eustatic sea level curve of Johnson et al. (1985), the Annulata horizon represents a transgressive phase or an early highstand condition (Becker & House 1997). At Col de Tribes (France) the *Annulata* event is not materialized by specific lithological changes, but its time-equivalent is marked by changes in the conodont biofacies and by the presence of deposits barren in the fauna content (Girard et al. 2014).

This event marks the last appearance of true *Platyclymenia* and *Trigonoclymenia* (House 1985, Korn 2004). However, it is not considered an event associated with extinction of fauna (about 20% of the ammonoid genera within the ammonoid zone, Korn 2004), but rather with a worldwide opportunistic bloom of some specialized species (Becker 1993, House 1996, Hartenfels 2011).

In addition, faunal groups such as stromatoporoids, thamnoporoids, several trilobites and favositid tabulate corals that were severely affected by biotic crisis during the Lower-Middle Famennian, have undergone a phase of recovery and spread only after the *Annulata* event (Becker et al. 2004).

The presence of hypoxia and the bloom of specialized species have been considered as a consequence of different phases of eutrophication influenced by eustatic changes driven by climatic processes (Hartenfels 2011).

Hangenberg Event

The Hangenberg event has been named by Walliser (1984a) after the black, organic rich marine Hangenberg Shales deposited slightly below the Devonian/Carboniferous boundary (fig 1.1) in the Rheinisches Schiefergebirge area (Germany). Because of its influence on the marine fauna is considered one of the greatest extinction events of the Phanerozoic. It is distinguished by high extinction and low origination rates (Walliser 1984a, Becker 1993): 21% of the marine genera and 16% of the families became extinct at the Hangenberg Event (Simakov 1993, Sepkoski 1996). Ammonoids, trilobites and conodonts were highly affected, and in a minor degree the agnathan fishes, placoderms, homalozoans, cystoids, foraminifera, brachiopods, corals, blastoids, stromatoporoids, acritarchs and ostracods (Walliser 1984a, 1984b, Bless et al. 1986, Simakov 1993). A significant drop in diversity and abundance of miospores (Streel 2000) and land plants, not time-equivalent to the initial phase of the marine extinction but close to the Devonian/Carboniferous boundary, have been registered in terrestrial ecosystem.

Kaiser et al. (2011) consider the Hangenberg black shales and its global-equivalents as the main extinction phase of the Hangenberg crisis. It represent a global litho-event occurred during a deep marine flooding surface at the base of a Transgressive Systems Tract. The MFS cause of the deposition of the shales and the subsequent polyphase regressive interval defines the *costatus-kockeli* Interregnum of the revised conodont zonation (Kaiser et al. 2009)

According to Becker (1993a, 1993b), the Hangenberg Event was triggered by a short-term sharp transgression, caused by a eustatic rise within the Middle *praesulcata* Zone (*costatus-kockeli* interregnum) at the base of the *Postclymenia evoluta* ammonoid Zone (Becker 1996) and LN miospore Zone (Higgs and Streel 1994). The successive major eustatic sea-level fall at the end of the Devonian has been marked by several authors (Johnson et al. 1985, Sandberg et al. 1988, Bless et al. 1993) and is considered time-equivalent to a glaciation pulse in Gondwana (Streel et al. 2000, Isaacson et al. 2008). Data from Southern Europe and Morocco (Kaiser 2005), show that the period across the D/C boundary was a time of eustatic fluctuations due to climate changes driven by the organic matter burial.

Aim

The aim of this work is to verify if the Condroz, the Annulata and the Hangenberg events are recognizable in the rocks and how they the detrital input has been affected by each event.

Six different sections from Sardinia and the Carnic Alps have been studied for conodont biostratigraphy. Considering the data from both areas, twenty-one conodont Zones have been recognized and more than 101 taxa have been described in the systematic chapter. In addition, the low field magnetic susceptibility measures and the major element geochemistry have been utilized to study the detrital input across the three selected events of the Famennian. Besides, considering the potential of the low field magnetic susceptibility, a tentatively correlation between the magnetic curves obtained measuring the low field magnetic susceptibility and the hysteresis loop is discussed.

In this work, new consideration about the relative palaeogeographic position of Sardinia and the Carnic Alps are presented.

This work is a contribution to IGCP-580 project “Application of magnetic susceptibility as a paleoclimatic proxy on Paleozoic sedimentary rocks and characterization of the magnetic signal” and to the IGCP-596 project “Climate change and biodiversity patterns in the mid-Palaeozoic”.

METHODS

The work started with a field work in which two different areas have been investigated. During this work a consistency number of samples have been collected during three years. The various samples have been prepared for different analysis: biostratigraphy, geophysics (magnetic susceptibility, hysteresis) and geochemistry (major element analysis).

Fieldwork

The fieldwork focused mainly on the Famennian and Tournaisian outcrops in Sardinia and in the Carnic Alps. Pelagic limestones with different tectonic imprint constitute the rocks that crop out in both areas. Several sections containing the selected events have been studied and measured in detail. Lithofacies and microfacies characteristics have been studied in the field as well as in thin sections.

Preparation of biostratigraphic samples

The samples, which have a weight ranging from one to three kilos, are first reduced in blocks of a few cm, to increase the surface on which the acid must act. The fragments are dipped in a bucket of water containing formic acid in solution, diluted to 4%. The concentration is low to avoid damaging the conodonts. The sample will remain immersed in this solution until the pH of the solution will be sufficient to dissolve the limestone, and will be replaced more times until the sample is completely melted.

At the end of the process, the residue is washed and sieved twice: first in a high-cut filter (2 mm), and then in a low-cut (120 µm). The dry sediment is ready for the final phase: the picking. The unsolved part of the rock is weighted in order to establish the exactly amount of conodonts per kilo.

The process of "picking" consists to manually separate the conodonts from the sediment. The conodonts are collected into a container (slight) where they can be studied throughout the binocular microscope.

Biostratigraphic work

The conodont zonation used in this thesis is the Late Devonian Standard Conodont Zonation (Ziegler & Sandberg, 1990) and the Late Devonian-Early Carboniferous Zonation of Sandberg et al. (1978). For the Sardinian sections has been used the scheme proposed for Sardinia by Corradini (2008), which is a rielaboration of the Standard conodont Zonations cited previously. The main differences regards the *postera* Zone and the Middle-Upper *praesulcata* Zones. The *postera* Zone has been excluded, and the *styriacus* Zone (Ziegler 1962) has been reintroduced because the marker of the *postera* Zone (*Pa. perl. postera*) is not present in Sardinia. The Middle *praesulcata* Zone is included in the Lower *praesulcata* Zone, because the base of the Zone is defined by a rare taxon (*Pa gracilis gonioclymeniae*) that in Sardinia is limited to an older interval (Corradini 2008). The Upper *praesulcata* have not yet been found in Sardinia. (Corradini 2008).

Preparation for geophysical samples

The samples for the magnetic studies have been collected from the various section in the nearby of the event that should be studied. The sampling have been performed with a gap of ten cm. wherever possible, and five cm. just across the event, to have a better detail.

Two different samples have been collected, for magnetic susceptibility and for hysteresis measures. The samples have been prepared using the cutter, with a measure of 2x2x3 cm for the magnetic susceptibility measures and 0,7x0,8x1,5 cm for hysteresis.

Low field MS measurements (χ_{LF} in m^3/kg) were performed on the KLY-3S Kappabridge (AGICO) at the University of Liege. Samples have been measured in a magnetic field intensity of 300 $A.m^{-1}$ at a frequency of 875 Hz. The bridge has a sensitivity of 3×10^{-8} SI.

The data presented in this work were processed to obtain an approximate conversion from dimensionless κ (SI) to χ in m3/kg. Here, the following approximation is used:

$$\chi_{LF} = (\kappa/((mass/10\ cm^3)\rho))/1000\ m^3/kg$$

where mass = the mass of the sample in grams, and ρ is the estimated density of the sample in g/cm3. This approach is necessary because the KLY-3S assumes a volume of 10 cm^3 for each sample measured, and because volume is so difficult to measure with precision (e.g., Ellwood et al. 1988).

The hysteresis parameters have been measured using the J-Coercivity “rotation” magnetometer (Dourbes IRM Geophysical Centre). The magnetising field have been increased from zero to +500mT then decreased to zero and then again to -500mT every 0.5mT, the remanent magnetization have been measured at each field increment/decrement. The slope at high-field, corresponding to the high-field magnetic susceptibility (X_{HF}), is indicative for paramagnetic and diamagnetic contributions to the low-field magnetic susceptibility (Devleeschouwer et al. 2010). The ferromagnetic susceptibility have been calculated subtracting the high field from the low field magnetic susceptibility ($\chi_{ferro} = \chi_{LF} - \chi_{HF}$).

The magnetic viscosity coefficient was calculated from the remanence decay, which was monitored for 100s after the field was removed.

A slope correction has been applied between 350/400 and 500 mT, in order to calculate the saturation magnetization Ms (mAm^2/Kg) and the coercive force Hc (mT). The coercivity of remanence (Hcr) were obtained by the back field curve.

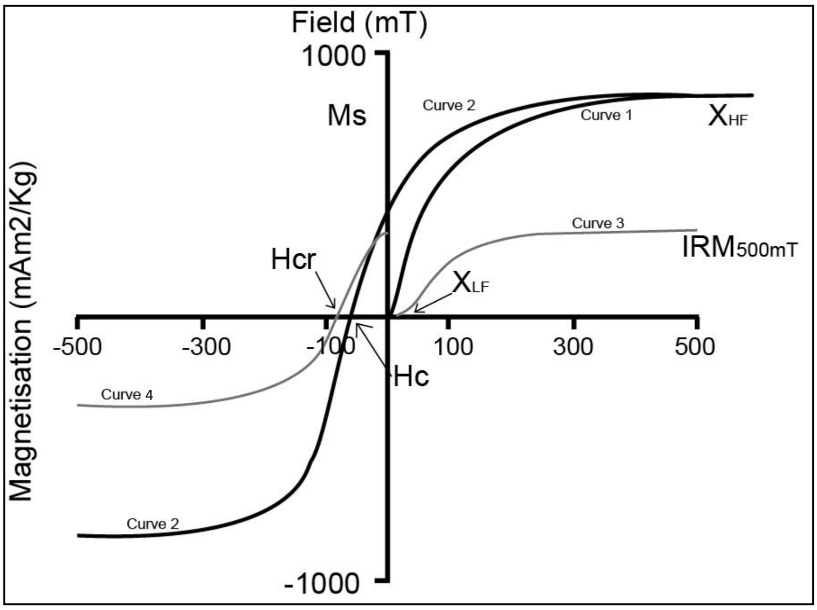

Figure 2.1. *Example of magnetisation curve measurements performed with the J-coercivity meter. Curve 1 (black) represents the initial hysteresis curve and curve 2 (black) the descending branch of the hystersis loop. From these curves (slope-corrected) the saturation magnetisation Ms, the coercive force Hc and the high-field magnetic susceptibility* X_{HF} *are calculated. Curve 3 (grey) represents the IRM acquisition from 0 to 500 mT and curve 4 (grey) is the backfield curve between 0 and -500mT.*

Preparation for geochemical samples

Analysis on major elements were performed on an X-Ray Fluorescence (Panalytical MagiX PW2540) device at the University of Cagliari. The powder disks were prepared using at least 20 grams of the minced sample mixed with polyvinyl alcohol, on a base of boric acid.

The total amount of oxides and LOI (loss on ignition) has been considered acceptable for samples with an error of ±2%. In order to have comparable results between the studied sections, all analyses were normalized to 100. In this way a small error percentage has been distributed between all the parameters measured.

STUDIED SECTIONS

This work was carried out by studying two different areas: the Carnic Alps and Sardinia (fig 3.1).
Six sections, two from the Carnic Alps (Pizzul West and Pramosio Bassa) and four from Sardinia (Bruncu Bullai, Monte Taccu, Corona Mizziu I and II). The sections were first studied from a biostratigraphic point of view, using conodonts. Then, the the evolution of the detrital input across the Condroz, Annulata and Hangenberg Events has been studied, using the low field magnetic susceptibility and the major element geochemistry.

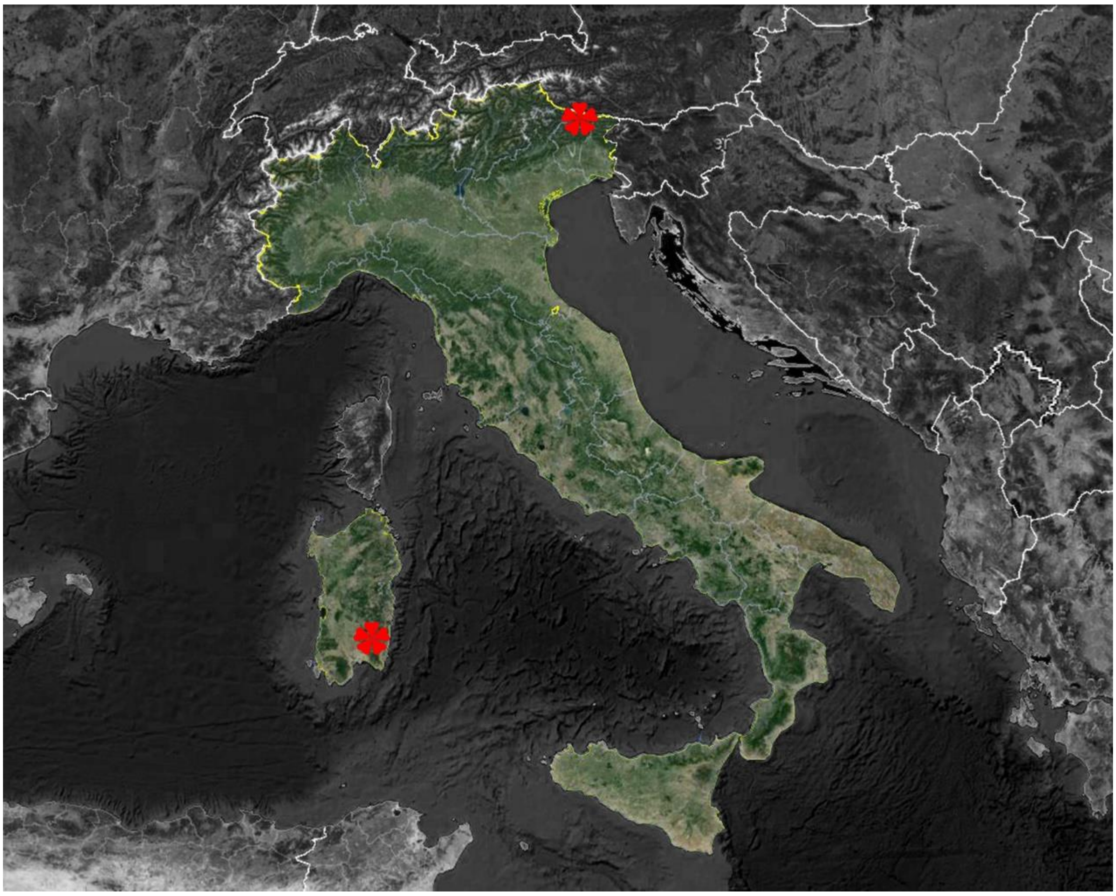

Figure 3.1. Location map of the studied areas.

CARNIC ALPS

Geographical setting

The area of work is located in the Carnic Alps: the western part of the Alpine chain across the Italy-Austria border (fig. 4.1). It correspond geographically to the northernmost part of the Friuli Venezia Giulia (Italy) and to the southern part of the Carinthia (Austria). The area is included in the tablets of the IGM Topographic Map of Italy, scale 1:25000, Paularo (14-IV-SE), Pontebba (14-I-SO) and Pizzo of Timau (14-V-NO). The sections studied are located in the area of Cason di Lanza (fig. 4.2A) and Pramosio Pass (fig 1.2B). The Cason di Lanza area is located in the heart of the Carnic Alps, along the mountain road connecting Paularo and Pontebba. The Pramosio Pass instead is a broad saddle that separates the Mount Avostanis from Mount Scarniz along the border with Austria.

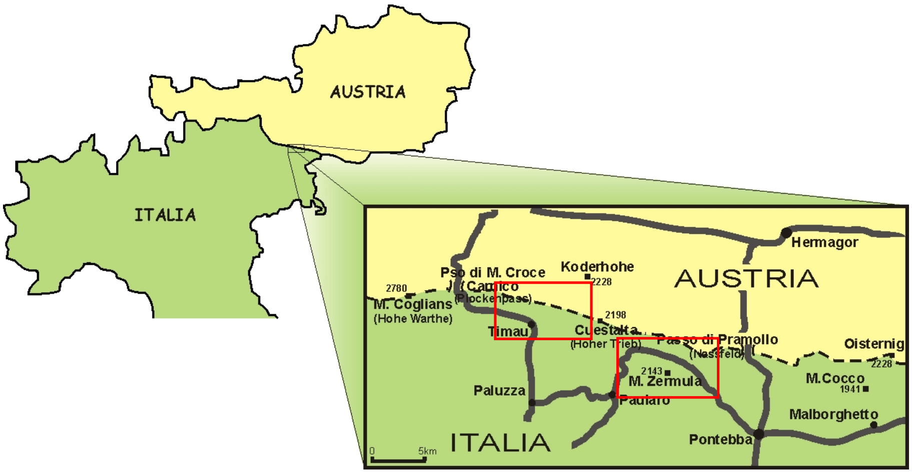

Figure 4.1. Location of the Carnic Alps. The red squares mark the studied areas.

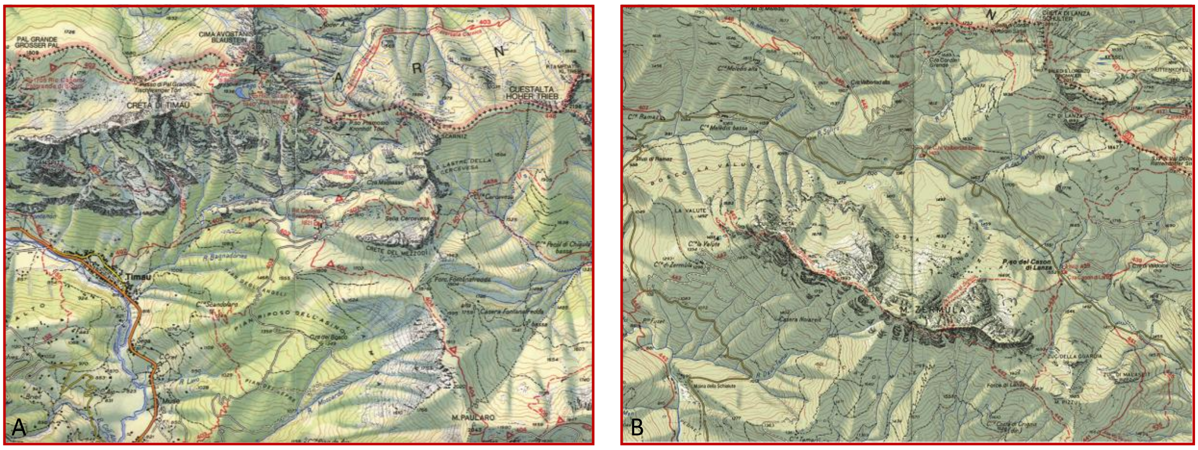

Figure 4.2. Studied areas: A. Pramosio Pass area, B. Cason di Lanza area.

Geological setting

The Palaeozoic of the Carnic Alps is organized into three sequences: the Variscan, the Permo–Carboniferous and the Alpine. The Variscan sequence includes rocks of Upper Ordovician to early Upper Carboniferous age, the Permo–Carboniferous sequence ranges from Late Carboniferous to Early Permian, and the "Alpine" sequence (Venturini 1990) is represented by Permo-Triassic rocks.

The Variscan sequence of the Carnic Alps is currently under revision in order to define formally the lithostratigraphic units. The succession ranges from the Darriwillian (Ordovician) to the lowermost part of the Upper Carboniferous (Corradini et al. 2012, 2013, Pondrelli et al. 2015) and represents one of the best sequences for studying the Palaeozoic in Europe (Selli 1963, Bandel 1972, Vai 1976, Schönlaub 1979, 1985).

The sequence is similar throughout the Carnic chain from the Middle Ordovician to the Lower Devonian (fig 4.3). From the Upper Lochkovian, the basin started to differentiate: in the shallower part a thick reefal sequence build up. Next to the reef a foreslope and a pelagic environments were estabilished (Pondrelli et al. 2015).

The changes in the basin are reflected in the lithology of the units, and it is possible to distinguish shallow water from pelagic units, with all the transitional units in between (fig 4.3).

The rocks were affected by the Variscan orogeny during the Westphalian and were disrupted and/or locally enhanced by at least three Alpine compressional phases (Venturini 1990, Läufer 1996). The different phases have been characterized using the stress tensor inversion method from fault striations (Gephart 1990, Gephart & Forsyth 1984, Pondrelli 1998).

This work focus on two different areas of the Carnic Alps: the Cason di Lanza and the Passo di Pramosio areas. The following paragraphs describe the geological successions in these two areas.

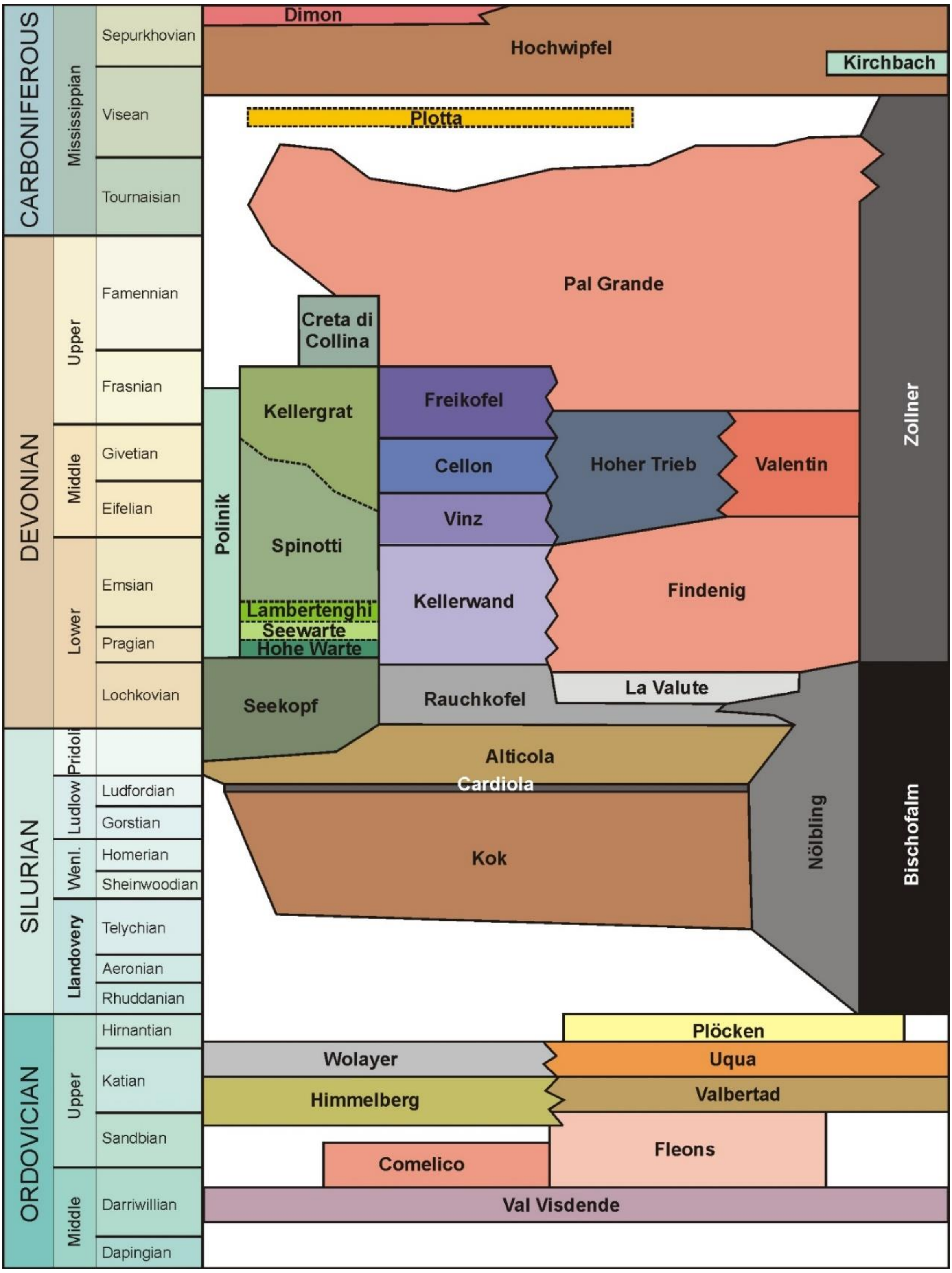

Figure 4.3. Litostratigraphic scheme of the Carnic Alps

Cason di Lanza area

The succession in the area of Cason di Lanza ranges from the Upper Ordovician to the Lower Permian. The three sequences are exposed: the Varisican and the Permo-Carboniferous sequences crops out widely in the area, while the Permo-Triassic sequence is represented only by few outcrop of Upper Permian rocks (Corradini et al. 2012).

The Varisican sequence starts in the Upper Ordovician (Sandbian-Katian) and represent almost a continuous sequence reaching the Lower Carboniferous. The oldest rocks are represented by the Valbertad Formation, which consist of highly fossiliferous thin to very thin-bedded light olive gray pelites, passing upward to arenaceous shales and then to very fine grained greywacke. The sequence continues with few meters of grey nodular mudstone and wackestone with very thin beds of light olive fine-grained greywacke interlayered ("Uqua formation”). Conodonts are the only fossils present, and age this unit to the *ordovicius* Zone (Schönlaub 1988, Bagnoli et al. 1998). Above, the Plöcken formation crops out. At the base of the unit, a few centimeters of shales are present, passing upward to dark gray thin to medium-bedded calcareous sandstone, with hummocky cross stratification structures and an evident thickening upward. The presence of conodonts and rare graptolites allow to assign this unit to the Hirnantian (Ferretti & Schönlaub 2001, Storch & Schönlaub 2012)

A disconformity, due probably to the Hirnantian glaciation, separate the Ordovician deposits from the Alticola Formation. The latter consists of prevalently thin to rarely medium-bedded medium dark gray cephalopod-bearing mudstone to wackestone. Beside cephalopods, the only abundant fossils observed are conodonts that date this unit from Ludlow to lowermost Lochkovian (Walliser 1964, Corriga & Corradini 2009, Corradini & Corriga 2010, 2012).

Compared to the older terms of the sequence, Devonian rocks are largely more abundant and differentiated. The oldest unit is the Rauchkofel Fm., constituted by very thin to medium-bedded interlayered mudstone-wackestone limestone with shales of grayish-black color interbedded. The presence of the crinoid loboliths in the Carnic Alps is considered to indicate a lowermost Lockhovian age, which has been confirmed by conodont data (*hesperius* Zone; Corradini et al. 2005).

The middle-upper Lochkovian La Valute Fm (Corriga et al. 2011) follows the Rauchkofel formation. It consists of thin-bedded medium dark grey and brownish grey nodular mud- to wackestone. In the uppermost couple of meters of the unit, the strata become very thin with silty and marly intercalations. Conodonts, trilobites, dacryoconarids, nautiloids, brachiopods, ostracods and sponge spiculae constitute the fossil association of this formation. Based on its conodont content, this unit can be assigned to the middle and upper Lochkovian (*carlsi* to *pandora* beta zones) (Carta 2011, Corriga 2011; Corriga et al. 2011).

The sequence continues with the Findenig formation, which consists of nodular purple-red mudstones and wackestones with thin to medium beige marly laminae intercalations. These marly intercalations are allodapic layers and have been interpreted either as tempestites (Vai 1980) or as turbidites (Bandel 1974). The fauna is dominated by dacryoconarids, while fragments of trilobites, ostracods, small orthocone nautiloids and crinoid stem-plates are less abundant (Corriga et al. 2011). The scarce conodont fauna data allow to date this formation from the Upper Lockovian to the Eifelian (Corriga et al. 2011, Pondrelli et al. 2015).

The Middle Devonian is represented by a reef (Mount Zermula) made up of thick-bedded *Amphipora* bafflestone, algal laminites, floatstone with micritic matrix and fenestral loferite (Ferrari and Vai, 1966).

In the deeper parts of the basin, gravitative driven deposits from the reef, intercalated with narrow pelagic levels, were deposited. These sediments belongs to the Vinz and Hoher Trieb formations.

The Vinz formation consists of various facies, all of them of medium grey color. The unit shows thick-bedded clast supported and disorganized breccia in a fine grained grainstone matrix; medium-bedded packstone to locally laminated grainstone with interlayered thin to medium-bedded fine grained breccia; very thick-bedded clast supported breccia locally displaying an erosional base; mostly crinoidal grainstone and/or fine grained breccia passing upward to clast supported breccia. Some clasts consists of mudstone, others are grainstone or fine grained breccia and yield fossils, mostly crinoids and corals. Silica replacement of corals is common. Iron-rich nodules are quite abundant in a portion of the unit (Pondrelli et al. 2015). Based on conodont data the central part of the unit belong to the late Eifelian (*kockelianus* Zone).

The Hoher Trieb formation consists of breccia levels of centimeter-scale thick clasts in a fine-grained grainstone matrix. These breccia levels are both matrix supported in the first levels and clast supported in the upper part. Breccias are interlayered with medium grey thin to thick-bedded grainstone to packstone, locally passing upward to wackestone and/or mudstone with thick laminae of silt/shale interbeds (Pondrelli et al. 2015). The fauna is dominated by the presence of conodonts (very abundant in some levels). Dacryoconarids, calcispheres, foraminifera, sponge spicules, algae, trilobites, bivalves, crinoids, brachiopods, ostracods have been detected in the wackestone to packstone beds, and reworked silicified corals within the breccia levels. Palynomorphs are also present.

During the Frasnian the Carnic basin underwent extensional tectonic pulses and the reefal facies collapsed and drowned (Venturini et al. 2009 and reference therein). The Upper Devonian is almost exclusively represented by the “Pal Grande Formation”.

The Varisican sequence ends with the Hochwipfel Formation: gravitative driven accumulation of breccias, conglomerates, sandstones and greywackes interbedded with dark grey laminated shales, originated by the Lower Carboniferous transtensional to transpressional tectonics (Spalletta et al.

1980). Plants remains are common. According to Venturini et al (2009), the Hochwipfel formation ranges from the middle Visean to the Bashkirian.

Passo di Pramosio area

The geological succession of the Passo di Pramosio area is not so various as the Cason di Lanza, only the upper part of the Varisican sequence (from the Middle Devonian to the Carboniferous) crops out in the area.

The Middle Devonian is represented by the Freikofel formation. It is made of meter thick floatstone and rudstone layers interlayered with decimetric thick grainstones to packstones often showing parting lineations, suggesting deposition in an upper flow regime. The base layers of the Freikofel Fm. is either erosional or sharp. Erosional surfaces are common within the breccia levels. This formation has been interpreted as result of gravity driven deposition (Pas et al. 2014). It spans a time from the Givetian to the Frasnian (Perri & Spalletta 1998, Pas et al. 2014)

The Upper Devonian-Lower Carboniferous is represented in the Passo di Pramosio area by the limestones of the “Pal Grande Formation” that crops out widely in the area, and it ends with the Hochwipfel formation of Carboniferous age.

The "Pal Grande Formation"

The “Pal Grande Formation” crops out widely in the Carnic Alps, and have been extensively studied by several authors. This unit of Frasnian-Tournaisian age is indicated in literature with various names, according to the different authors: Pal Fm., Gross Pal Fm., Calcari di Pramosio, etc (Pondrelli et al. 2015).

It consists of grey massive limestone, grey to moderate pink and red very thin to thin (rarely medium) bedded nodular mudstone to wackestone. In the lower part of the unit, a few levels of breccia occur in some localities. The upper limit is more problematic: due to sin-depositional tectonic the basin has been differentiated; the results were the deposition at places of a breccia limestone (Lower *expansa* Zone) documented (Mossoni et al. 2013a, Pondrelli et al. 2015), and the continuous sedimentation until the *homopunctatus* Zone in the lowermost Visean (Perri & Spalletta, 1998e). This correspond to the *Gnathodus* interregnum across the Tournaisian/Visean boundary described by Devuyst & Kalvoda (2007).

The thickness of the “Pal Grande formation” is about 20-25 meter, but due to tectonic apparently reach more than 200 meter.

The depositional environment is interpreted as pelagic (e.g., Schönlaub, 1992) with local gravitative-driven deposits near the base of the unit. Trilobites, ostracodes, radiolarians and conodonts, and less abundant echinoderms, mollusks, bivalves, brachiopods and fish teeth (Schönlaub 1992) represent the fossil content.

According to conodont data, this unit spans a time between the MN 3 and MN11 conodont Zones (Frasnian) to the *homopunctatus* Zone (Visean) (Perri & Spalletta, 1998e). A detailed biostratigraphy of the unit have been provided by several authors in the basis of the rich conodont associations (for a summary see Perri & Spalletta, 1998a).

Previous works

The Upper Devonian of Carnic Alps have been widely studied using conodonts from the sixties by Manzoni (1965, 1966) for biostratigraphic purposes.

The "Pal Grande Formation" is from a biostratigraphic point of view, one of most studied unit of Carnic Alps, because of the high abundance of conodonts. For the last fifty years many authors have worked using conodonts: Manzoni (1965, 1966, 1968), Gedik (1969), Pölser (1969), Schönlaub (1969, 1985), Schönlaub et al. (1992), Perri & Spalletta (1981a, 1981b, 1990, 1991, 1998a, 1998b, 1998c, 1998d, 1998e, 1998f), Spalletta & Perri (1998), Perri et al. (1998), Kreutzer (1990, 1992), Mossoni et al (2013a), Pas et al. (2014), Pondrelli et al. (2015). Thirty-five zones have been recognized from more than fifty sections of the Upper Devonian-Lower Carboniferous pelagic limestones of the Carnic Alps (Perri & Spalletta, 1998a).

Pizzul West section

The Pizzul West (PZW) section crops out on the western flank of Mt Pizzul, in a dugout from the First World War at coordinates 46° 33' 21,67'' N, 13° 18' 18,16''E.

It exposes about 24 metres of "Pal Grande Formation". Thirteen conodont samples have been collected from the section. It has been affected by some local tectonic movements, as the rest of the Mount Pizzul. Folds and/or faults affect particularly lower and central part of the section, below sample PZW 1. This is confirmed by conodont data and by field observation, where a fold is evident by S1 structures close to the axis of the fold. The upper part of the section shows almost no evidence of tectonic influence, a part from a small fault between samples PZW 5A and PZW 6 inside the Upper *rhomboidea* Zone.

Three different facies can be distinguished in the field:

- a light grey massive micritic limestone (fig 4.4);
- a dark red nodular limestone (fig 4.4);
- a grey-ochre nodular limestone (fig. 4.4).

In general, the massive grey limestones are more abundant in the lower part, whereas the red nodular limestone prevails in the upper part (fig 4.5).

A few thin pelitic levels are present in the section, i.e. between sample PZW 1 and sample PZW 4.

The microfacies of the grey limestone consists of a light grey coloured wackestone and few fossils remains scattered in the matrix (mostly ostracods and shells); some stylolite structures are also evident. The red nodular facies consists of a wackstone-packstone with nodules up to 1 cm of diameter, probably due to a synsedimentary diagenesis, with haematite precipitations (fig 4.4). The fossil content is higher and includes trilobites, small shells (brachiopods or bivalves), ostracods, a few cephalopods and sponge spiculae. The grey-ochre nodular limestone consists of a wackstone-packstone similar to the red one, but with less haematite precipitations that most probably give the red colour to the former facies (fig 4.4).

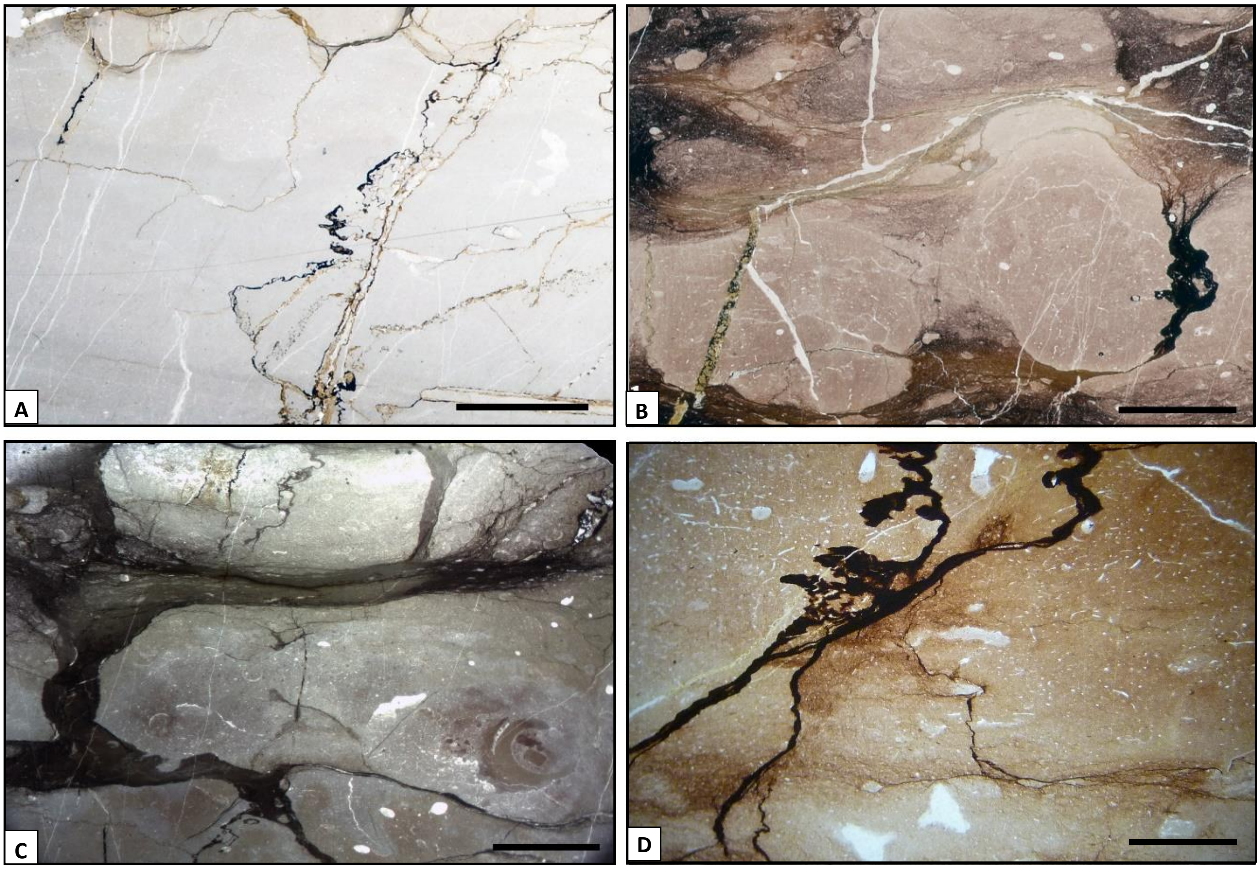

Figure 4.4. Microfacies of the Pizzul West section (scale bar 0,5 cm). A) Grey massive limestone with some stylolite structures from the sample PZW 1; B) Red nodular limestone with haematite precipitations and nodules (Sample PZW 5); C) Grey-ochre nodular facies of the sample PZW 5A; D) Red nodular limestone with haematite precipitations and fossil remains, mainly ammonoids and (Sample PZW 3).

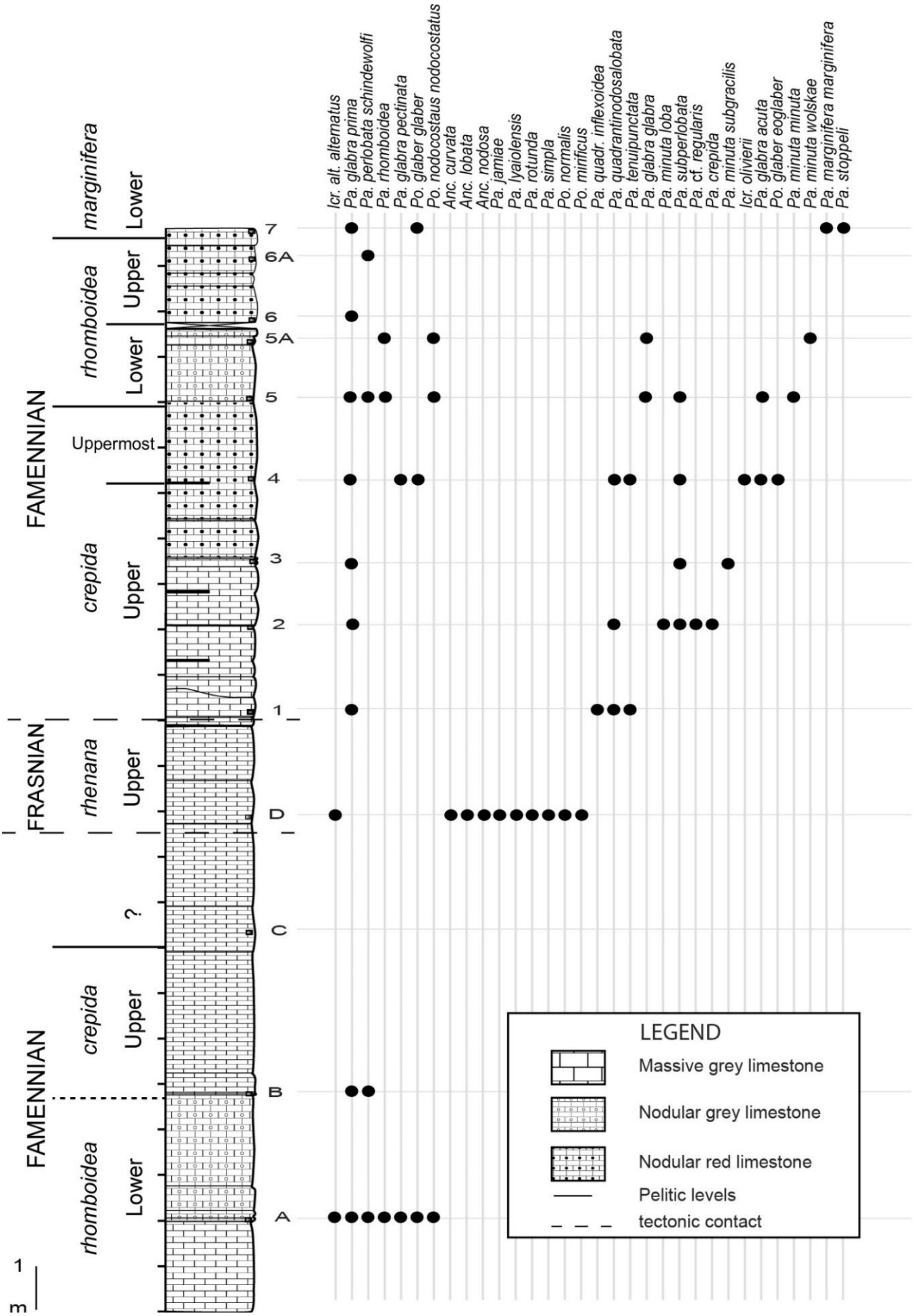

Figure 4.5. Stratigraphic log of the Pizzul West section and conodont distribution. Abbreviation: Anc. – Ancyrodella, Icr. – Icriodus, Pa. – Palmatolepis, Po. – Polygnathus.

	PIZZUL WEST														TOTAL
	Famennian		?	*Frasnian*	*Famennian*										
	Lower rhomboidea	Upper crepida		Upper rhenana	Upper crepida	Upper crepida	Upper crepida	Uppermost crepida	Lower rhomboidea	Lower rhomboidea	Upper rhomboidea	Upper rhomboidea	Lower marginifera	Lower expansa	
	A	B	C	D	1	2	3	4	5	5A	6	6A	7	Z	
Ancyrodella curvata				1											1
Ancyrodella lobata				4											4
Ancyrodella nodosa				4											4
Bispathodus stabilis														22	22
Icriodus alternatus alternatus	1			8											9
Icriodus olivierii								6							6
Palmatolepis crepida						1									1
Palmatolepis glabra acuta								2	3						5
Palmatolepis glabra glabra						1			23	5					29
Palmatolepis glabra pectinata	4							3							7
Palmatolepis glabra prima	4	3			1		1	23	26		1		4		63
Palmatolepis gracilis gracilis							1							20	21
Palmatolepis gracilis sigmoidalis														5	5
Palmatolepis jamiae				5											5
Palmatolepis lyaiolensis				4											4
Palmatolepis marginifera marginifera													1		1
Palmatolepis minuta minuta									7						7
Palmatolepis minuta loba						1									1
Palmatolepis minuta wolskae										2					2
Palmatolepis perlobata schindewolfi	4	1							3			2		26	36
Palmatolepis perlobata postera														2	2
Palmatolepis cf. *regularis*						1									1
Palmatolepis rhomboidea	3								3	5					11
Palmatolepis rotunda				1											1
Palmatolepis rugosa rugosa														2	2
Palmatolepis simpla				2											2
Palmatolepis stoppeli													1		1
Palmatolepis subperlobata						1	1	4	11						17
Palmatolepis tenuipunctata					3			2							5
Pseudopolygnathus controversus														5	5
Pseudopolygnathus irregularis														2	2
Pseudopolygnathus marburgensis marburgensis														2	2
Pseudopolygnathus micropunctatus														2	2
Polygnathus glaber eoglaber								2							2
Polygnathus glaber glaber	6							1	8				1		16
Polygnathus marginvolutus														8	8
Polygnathus mirificus				1											1
Polygnathus nodocostatus nodocostatus	3									1				4	8
Polygnathus normalis				1											1
Polygnathus obliquicostatus														7	7
Polygnathus styriacus														50	50
Ancyrodella sp.				5											5
Icriodus sp.				2	2	1		5							10
Palmatolepis sp.	18		1		12	1	1	1		15			5		54
Polygnathus sp.				7					1						8
Ramiforms		1		7	2			1	34	4	2	5		127	183
Unidentified	21			58			4	42	3	23		6	4	117	278
TOTAL	64	5	1	110	20	7	8	92	122	55	3	13	16	401	917
WEIGHT	1,9	1,8	1,7	1,9	2,2	1,7	1,4	1,2	1,2	2,1	2,4	1,9	1,9	2,6	25,9
ABUNDANCE	33,7	2,8	0,6	57,9	9,1	4,1	5,9	74,8	100,0	26,2	1,3	6,8	8,4	154,2	35,5

Table 4.1. Conodont distribution chart of the Pizzul West section. Sample PZW Z has been collected few meters from the section close to the limit with the Hochwipfel formation

Conodont data

Seven Biozones has been recognised in the PZW section (Tab 4.1):

The Upper *rhenana* Zone (sample PZW D) has been discriminated thanks to the joint occurrence of *Icriodus alternatus alternatus*, *Palmatolepis rotunda*, *Ancyrodella lobata*, *Palmatolepis jamiae* and *Palmatolepis lyaiolensis*. In fact, the first two taxa have their first occurrence, while the others became extinct within this zone (Ziegler & Sandberg 1990, Ji & Ziegler 1993, Ovnatanova & Kononova 2008).

The Upper *crepida* Zone has been discriminated in samples PZW 1-3, thanks of the first occurrence of the marker *Palmatolepis glabra prima*, and of *Palmatolepis glabra lepta* and *Palmatolepis minuta subgracilis*. The absence of taxa having a younger first occurrence suggests that also sample PZW B may belong to this biozone.

The Uppermost *crepida* Zone is recognized in sample PZW 4 by the joint occurrence of the marker *Palmatolepis glabra pectinata* and of *Palmatolepis tenuipunctata*, which has its last appearance datum within this zone (Ji & Ziegler 1993). In addition, *Icriodus olivierii* enters here at the base of its known range (Corradini 2008).

The Lower *rhomboidea* Zone is discriminated in samples PZW 5-5A by the presence of the marker *Palmatolepis rhomboidea*, and of *Palmatolepis minuta wolskae* and *Palmatolepis subperlobata*, which have their last occurrence within this Zone (Ji & Ziegler 1993). The Upper *rhomboidea* Zone (samples PZW 6, 6A) is here recognized by the extinction of *Palmatolepis minuta wolskae*.

The Lower *marginifera* Zone (sample PZW 7) is recognized by the first occurrence of the marker *Palmatolepis marginifera marginifera*. The presence of *Palmatolepis stoppeli*, which became extinct within this Zone (Ji & Ziegler 1993), confirms the attribution of PZW 7.

The Lower *expansa* Zone (Sample Z) is discriminated by the joint occurrence of *Palmatolepis rugosa rugosa*, *Polygnathus nodocostatus nodocostatus* and *Polygnathus styriacus*. The first one occurs for the first time in this zone, while the other two became extinct (Ji & Ziegler 1993).

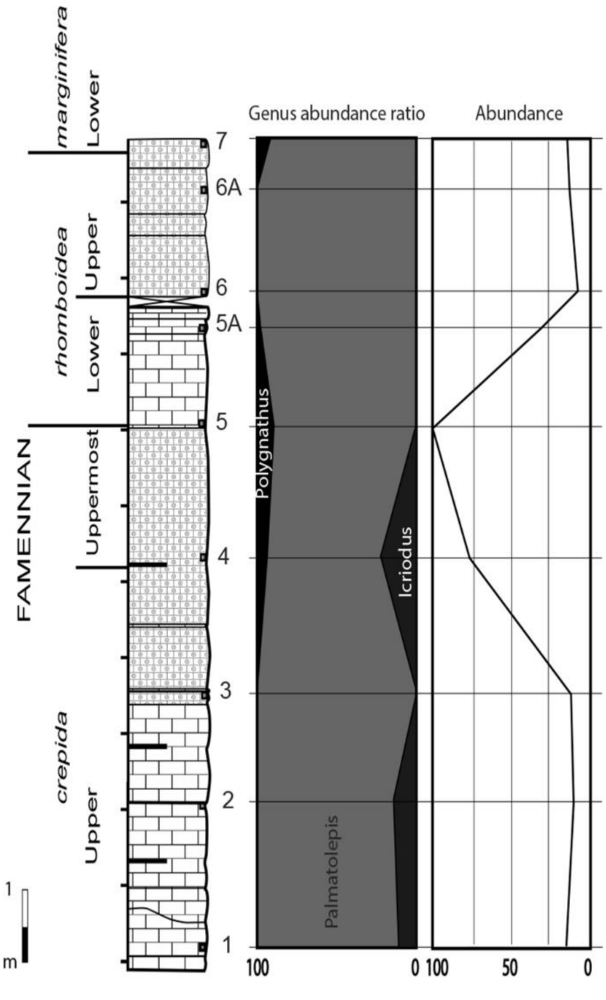

Figure 4.6.Genus abundance ratio and general conodont abundance for the PZW section.

Magnetic susceptibility data

The Pizzul West section has been sampled for the magnetic susceptibility analysis every ten cm in order to obtain a trend in which the presence of the Lower and Upper Condroz events (Becker et al. 1993a, 1993b) could be recognised. Ninety-five samples of limestone have been collected and cut from this section for the analysis of the low field magnetic susceptibility χ_{LF}. From these samples twenty-one have been measured to obtain the four hysteresis parameters: saturation magnetisation (Ms), saturation remanence (Mrs), coercive force (Hc), remanent coercive force (Hcr) and the high field magnetic susceptibility (χ_{HF}), useful to interpret the magnetic susceptibility signal. The high field susceptibility is obtained by subtracting the slope fitted to the reversible linear part of the hysteresis loop between 400 and 500 mT.

The mean χ_{LF} value of the section is about 9,97 × 10^{-8} m^3/kg. In the bottom part (1,5 m) of the section an increasing trend is observed with large fluctuations, where the limestone is massive. In contrast, throughout the rest of the section (1,5 – 11 m) the red nodular limestone occurs and the signal shows a decreasing trend.

There are two distinctive peaks seen (fig 4.8), one close to the sample PZW 3, within the Upper *crepida* Zone and one higher in the section in sample PZW 5, at the beginning of the Lower *rhomboidea* Zone and probably correspond to the Lower Condroz event.

The χ_{LF} has a good correlation with χ_{ferro} (r = 0.87), that is the ferromagnetic susceptibility ($\chi_{ferro} = \chi_{LF} - \chi_{HF}$), which suggests that the signal is mainly controlled by the ferromagnetic contribution. In contrast the correlation between χ_{LF} and χ_{HF} is very poor (r = 0.17). Therefore, the paramagnetic contribution does not affect the initial susceptibility signal.

It should be pointed out that all the signal (χ_{LF}, χ_{ferro} and χ_{HF}) show very low values, but this is common in carbonate rocks (between 1× 10-9 and 1× $10^{-7}m^3$/kg, Ellwood et al., 1999).

The values of Hc (mostly close to 20 mT) and Hcr (mostly <70 mT) are more or less constant in the lower part and are variable in the central and upper part of the section. The low values indicate the absence of high coercivity minerals, such as for instance haematite that is often associated with diagenetic processes causing a remagnetization of the natural remanent magnetisation (cf. Zwing et al. 2002, 2004). In the centre part, Hc and Hcr start to increase, probably due to the higher concentration of haematite in the red nodular facies.

The magnetic viscosity, which represents the superparamagnetic contribution (a small grain size that tend to lose the magnetization acquired in a short period of time) is rather low and therefore the susceptibility signal seems to be carried by particles with grain sizes beyond the superparamagnetic grain size range such as single domain (SD) or multidomain (MD) grains. In the Day Plot (fig 4.7), almost all samples plot inside of the pseudo-single domain (PSD) field.

However, two main clusters can be clearly distinguished (fig 4.7): the black one represents the central part of the section (from sample PZW 4 to PZW 6.7), while the green one is from lower part of the section plus the uppermost sample (PZW 7).

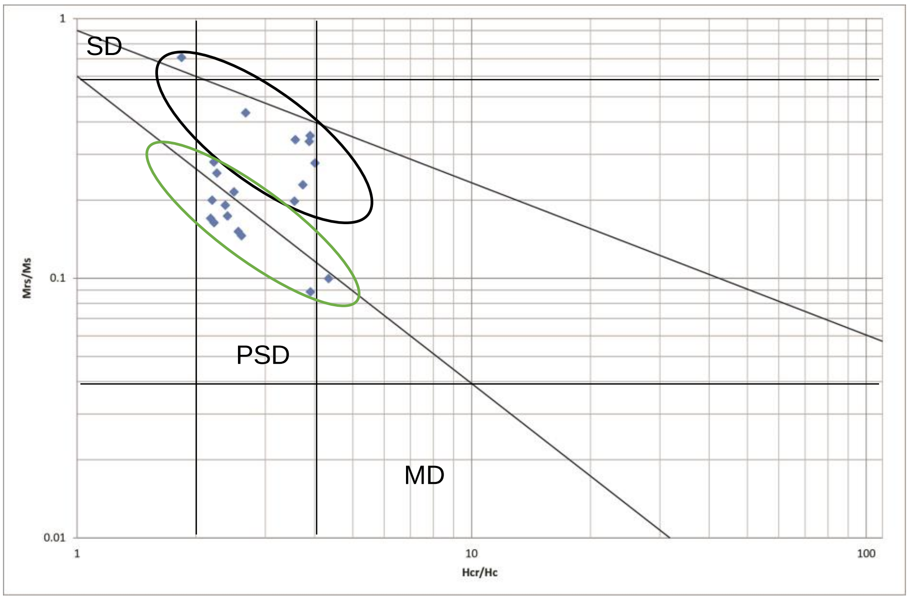

Figure 4.7. Day plot of the PZW section. The black cluster represent the samples PZW4-6. The green cluster is made up of samples PZW 1-3,7. SD=single domain; PSD= pseudosingle domain; MD=multi domain.

All geochemical parameters are more or less constant all along the section (fig 4.8). A correlation between χ_{LF} and the geochemical parameters is not given (AL_2O_3=0.07, SiO_2=0.12, TiO_2=0.12, K_2O=0.04). However, there is a good correlation between the χ_{HF} trend and geochemistry (AL_2O_3=0.84, SiO_2=0.81, TiO_2=0.85, K_2O=0.84), which means that the paramagnetic contributions are most likely of primary origin. Therefore, the ferrimagnetic signal as well as the haematite contributions may be of non-detrital origin and related to secondary processes. The transformation illite-smectite is a process that could be related to pressure solution (evident in the microfacies, fig 4.4) and the iron produced during this transformation could have been stayed in situ in clay aggregate minerals, enriching the ferromagnetic component of the signal.

The presence of two types of coercivity minerals (bimodal magnetic population) is reinforced by the fact that the hysteresis loop shows in many samples the wasp-waisted shape.

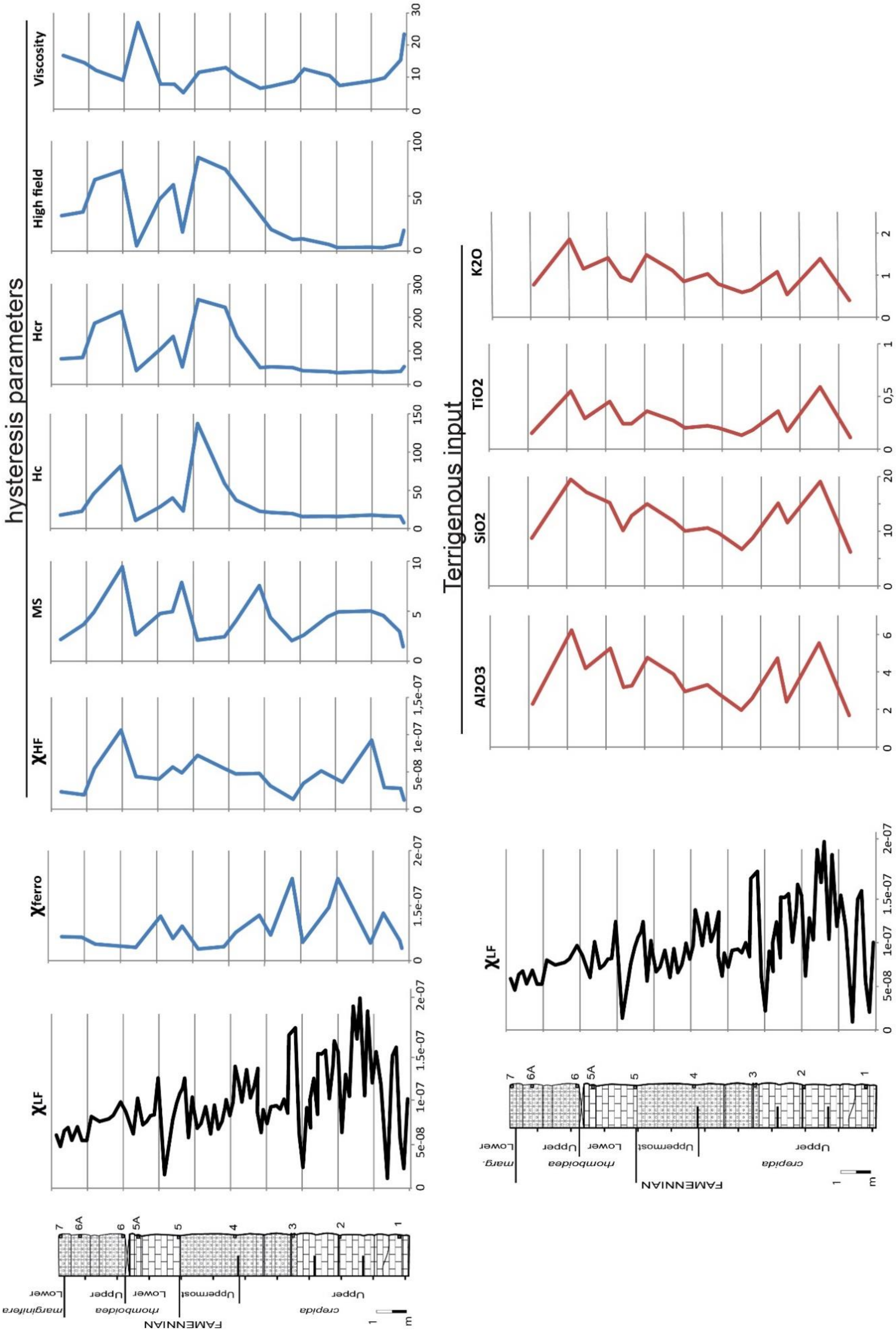

Figure 4.8. Low field magnetic susceptibility (χ_{LF}), ferromagnetic contribution (χ_{Ferro}), hysteresis parameters (high field magnetic susceptibility (χ_{HF}), saturation magnetization (Ms), coercive force (Hc), coercivity of remanence(Hcr), highfield remanence and viscosity decay) and geochemical data for the PZW section.

Pramosio Bassa section

The Pramosio Bassa section (PB) is located in the Pramosio Pass area. It expose almost 5 meters of well bedded, grey massive limestone (fig 4.9), in which a stratum that shows a microbialite and an ammonoid bed is clearly identifiable in the outcrop (PB 5a). The section shows a very faint imprint of tectonic, marked also in the Conodont color alteration index (CAI), which shows a value of 4-4.5. The section continue even after the sample PB 7, but unpublished data confirm the presence of an unconformity located probably after the sample 7, where the section is interrupted by some cover.

The microfacies is represented by a wackstone-packstone with a large amount of fossil remains: ammonoids, brachiopods, trilobites, crinoids, conodonts and vertebrate microremains (Perri et al. 1998).

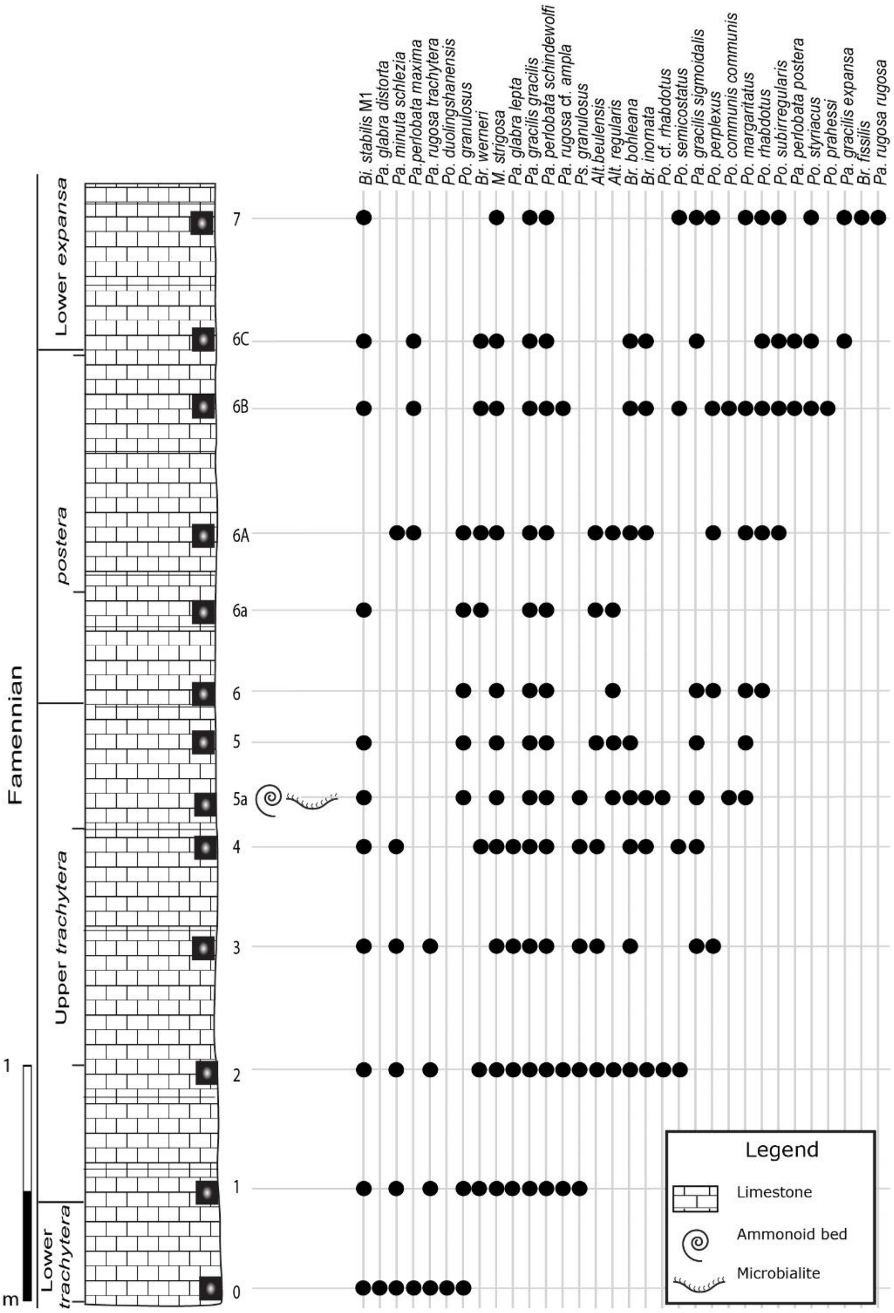

Figure 4.9. Stratigraphic log of the Pramosio Bassa section and conodont distribution. Abbreviation: Alt. – Alternognathus, Bi. – Bispathodus, Br. – Branmehla, M. – Mehlina, Pa. – Palmatolepis, Ps. – Pseudopolygnathus, Po. – Polygnathus.

Conodont data

Four Biozones has been recognized in the PB section (fig 4.9):

The conodont data of part of the section has been published by Perri et al. (1998), however new data are here provided. Sample PB 0 has been collected at the base of the section and the zonation of the section has been updated.

The Lower *trachytera* Zone (sample PB 0) is here recognized for the joint occurrence of *Palmatolepis glabra distorta* and *Palmatolepis rugosa trachytera*.

The Upper *trachytera* Zone (samples PB 1-5) has been discriminated by the joint occurrence of *Pseudopolygnathus granulosus*, *Palmatolepis rugosa trachytera* and *Polygnathus* cf. *rhabdotus*.

For the Lower *postera* Zone (sample PB 6), due to the upper occurrence in the section of *Polygnathus styriacus* and *Palmatolepis perlobata postera* (sample PB 6B), was considered crucial the presence of *Polygnathus rhabdotus*. The Upper *postera* Zone has not been discriminated in the PB section.

The Upper *expansa* Zone has been recognized by the presence of the marker *Palmatolepis gracilis expansa* that enter in sample PB 6C.

Thirty-one taxa belonging to seven genus discriminate four conodonts Zones, from the Lower *trachytera* to the Lower *postera* Zone (Tab 4.2). It should be remarked that this section show a peculiar abundance in samples PB 6B (*postera* Zone) and PB 6C (Lower *expansa* Zone): the first one gave 859 conodont/kg, while the abundance of the second reach 1870 conodont/kg. It is interesting to notice that the most abundant taxa in both samples is *Branmehla werneri* (Tab.4.2), in fact in sample PB 6B represent more than 30% of the fauna, whereas in sample PB 6C reach up to the 75% of the fauna.

Spathognathodids (*Bispathodus*, *Branmehla* and *Mehlina*) dominate the fauna of the Pramosio Bassa section.

	Pramosio Bassa													**TOTAL**
	Famennian													
	Lower trachytera	Upper trachytera	Upper trachytera	Upper trachytera	Upper trachytera	Upper trachytera	Upper trachytera	Lower postera	Lower postera	Lower postera	Lower postera	Lower expansa	Lower expansa	
	0	1	2	3	4	5a	5	6	6a	6A	6B	6C	7	
Altenognathus beulensis			28	4	4		15		4	35				90
Altenognathus regularis			10			13	6	1	8	18				56
Bispathodus stabilis M1	6	3	5	7	9	10	40		2		56	75	14	227
Branmehla bohlenana			6	1	3	3	1			1	7	5		27
Branmehla fissilis													11	11
Branmehla inornata			1		1	4				8	23	7		44
Branmehla werneri		25	19		5				2	228	640	2907		3826
Mehlina strigosa		1	5	5	3	2	3	1		13	88	105	3	229
Palmatolepis glabra distorta	2													2
Palmatolepis glabra lepta		1	1	1	1									4
Palmatolepis gracilis expansa												3	9	12
Palmatolepis gracilis gracilis		12	24	14	8	16	31	4	6	40	148	215	45	563
Palmatolepis gracilis sigmoidalis				8	7	4	24	4		24	3	21	20	115
Palmatolepis minuta schleizia	2	5	6	4	1									18
Palmatolepis perlobata maxima	2									1	2	1		6
Palmatolepis perlobata postera											5	1		6
Palmatolepis perlobata schindewolfi		22	33	12	20	15	36	6	12	65	247	214	110	792
Palmatolepis rugosa cf. *ampla*		1	3								4			8
Palmatolepis rugosa rugosa													1	1
Palmatolepis rugosa trachytera	2	34	15	8										59
Polygnathus communis communis						2					65			67
Polygnathus duolingshanensis	1													1
Polygnathus granulosus	4	2				4	18	1	14	137				180
Polygnathus margaritatus						3	9	2		2			1	17
Polygnathus perplexus				1				2		7	1		7	18
Polygnathus praehassi											1			1
Polygnathus rhabdotus								1		21	241	289	107	659
Polygnathus cf. *rhabdotus*			2			10								12
Polygnathus semicostatus			12		1						1		2	16
Polygnathus styriacus											128	146	68	342
Polygnathus subirregularis										1	13	37	2	53
Pseudopolygnathus granulosus		5	13	3	12	2								35
Altenognathus sp.										4				4
Icriodus n. sp. A											17	45	4	66
Palmatolepis sp.	6													6
Polygnathus sp.											111	39		150
Pb elements	3	2		1			2			1			1	10
Ramiforms	26													26
TOTAL	28	113	183	69	75	88	185	22	48	606	1801	4110	405	7733
WEIGHT	0,9	2,1	1,4	1,4	1,3	0,9	1,7	1,4	1,1	2,3	2,1	2,2	1,9	20,5
ABUNDANCE	31,1	54,1	134,1	48,4	60,0	96,1	109,1	16,3	44,2	266,4	859,3	1870,7	213,2	376,4

Table 4.2. Conodont distribution chart of the Pramosio Bassa section.

Magnetic susceptibility data

The Pramosio Bassa section has been sampled every ten cm for the magnetic susceptibility, the magnetic hysteresis and for the major element geochemistry analysis (fig 4.11). The aim was to verify if the "*Annulata* event" (Walliser 1984, House 1985) has been registered in the Pramosio Bassa section and to study the detrital evolution across this transgressive event.

Twenty-five samples for low field magnetic susceptibility (χ_{LF}) have been collected, and from seventeen of these the hysteresis loop has been measured.

The mean χ_{LF} value of the section is about 3,56 × $10^{-9}m^3/kg$, much more lower than in the other sections, this could be related to a scarce detrital input during the deposition of these limestones.

The χ_{LF} curve is very variable through the section and behave sequential. In the lower part of the section, the χ_{LF} increase, reaching the first peak in the lower part of the Upper *trachytera* Zone, then suddenly decrease reaching the zero (fig 4.11). A second peak within the Upper *trachytera* Zone, correspond to the ammonoid bed of the sample PB 5a. A third and last peak is marked in the upper part of the curve in the Lower *postera* Zone. The correlation of χ_{LF} with χ_{ferro} is high (r = 0.86), while the correlation with χ_{HF} is poor. Therefore, the χ_{LF} signal of the PB section is controlled by a small percentage of ferromagnetic contribution in a diamagnetic domain.

The high field susceptibility shows very low values in this section, in fact the paramagnetic contribution (χ_{HF}) is generally scarce in the section (fig 4.11) and totally absent in few samples (χ_{HF} <0).

The absence of heamatite in the section could be hypothesize because of the poor values of coercitive force (Hc) and coercivity of remanence (Hcr), which show respectively values lower than 10 mT for the Hc and values lower than 60 mT for the Hcr. In addition, there is no evidence of haematite in the microfacies. The viscosity decay, acquired measuring the relaxation time, show low values. This allow to exclude the presence of superparamagnetic particles in all the samples measured.

The measures plotted of the Day plot diagram represent a cluster of SD+MD particles (fig 4.10).

The correlation between χ_{LF} and the geochemical parameters is good (AL_2O_3=0.78, SiO_2=0.76, TiO_2=0.82, K_2O=0.80) while the correlation with the χ_{HF} is poor (AL_2O_3=0.30, SiO_2=0.23, TiO_2=0.39, K_2O=0.36). The absence of haematite in thin section and the given correlation with the geochemistry allow to hypothesize a detrital origin for the ferrimagnetic contribution that, as pointed out before, seems to control the low field magnetic susceptibility of this section.

The three peaks marked in the χ_{LF} are well expressed also in the major element curves, in particular the first two peaks in the Upper *trachytera* Zone could represent the “Upper Annulata event”.

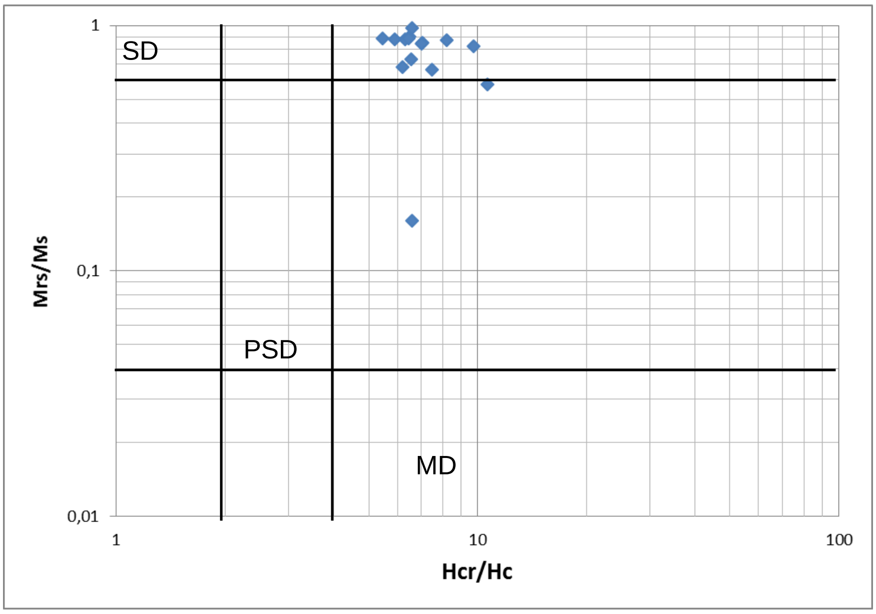

Figure 4.10. Day plot of the PB section. SD=single domain; PSD= pseudosingle domain; MD=multi domain.

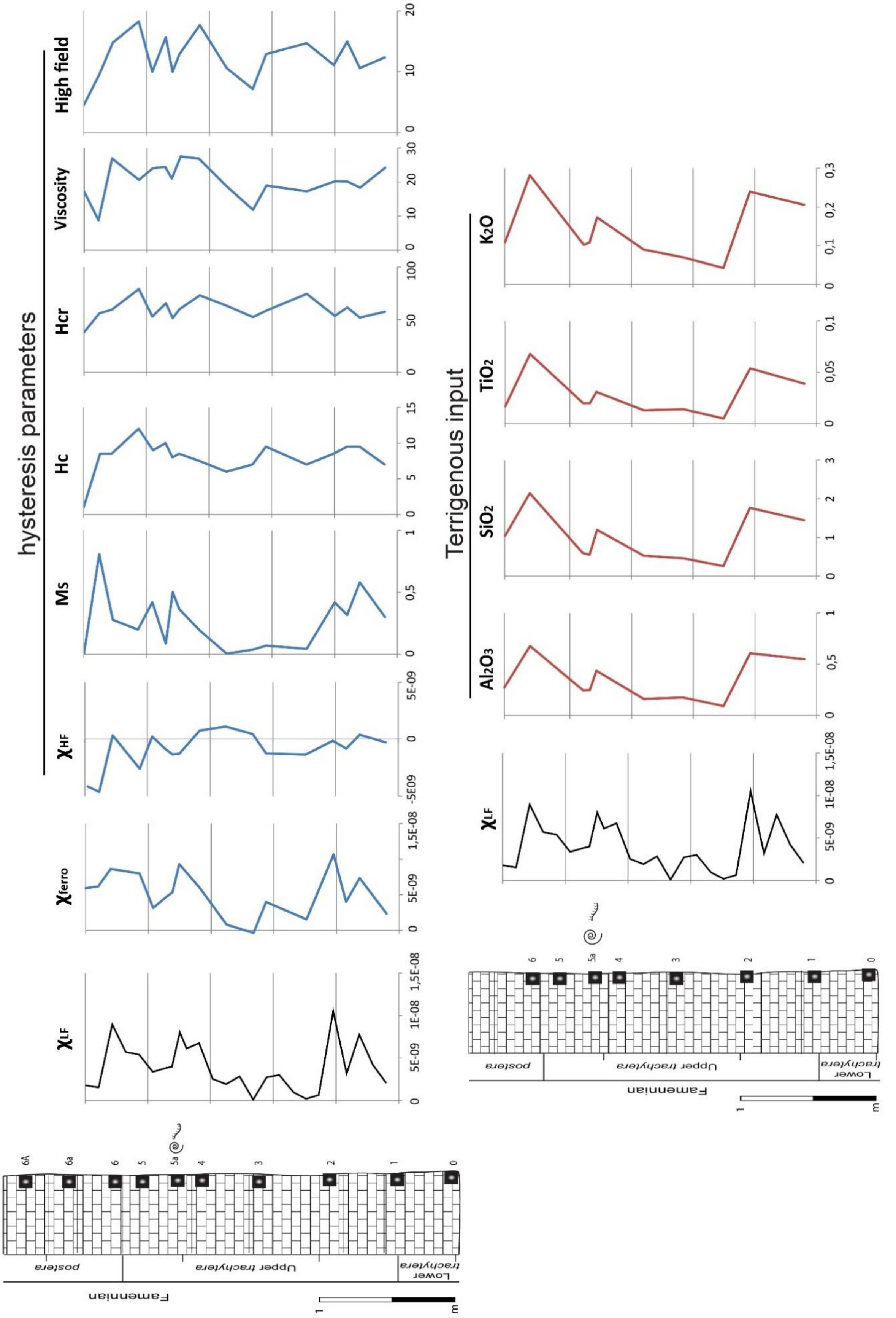

Figure 4.11. Low field magnetic susceptibility (χ_{LF}), ferromagnetic contribution (χ_{Ferro}), hysteresis parameters (high field magnetic susceptibility (χ_{HF}), saturation magnetization (Ms), coercitive force (Hc), coercivity of remanence(Hcr), highfield remanence, viscosity decay) and geochemical data for the PB section.

SARDINIA

Geographical setting

The area of work is located in the South-East of Sardinia, precisely in the Gerrei subregion, where the Devonian rocks extensively crops out (fig 4.12).

The area is included in the tablets of the IGM Topographic Map of Italy in a scale of 1: 25000 Goni (548-I), San Nicolò Gerrei (548-II), Ballao (549-I) and Villasalto (549-II). All the sections studied for this work are close to San Nicolò Gerrei and Villasalto.

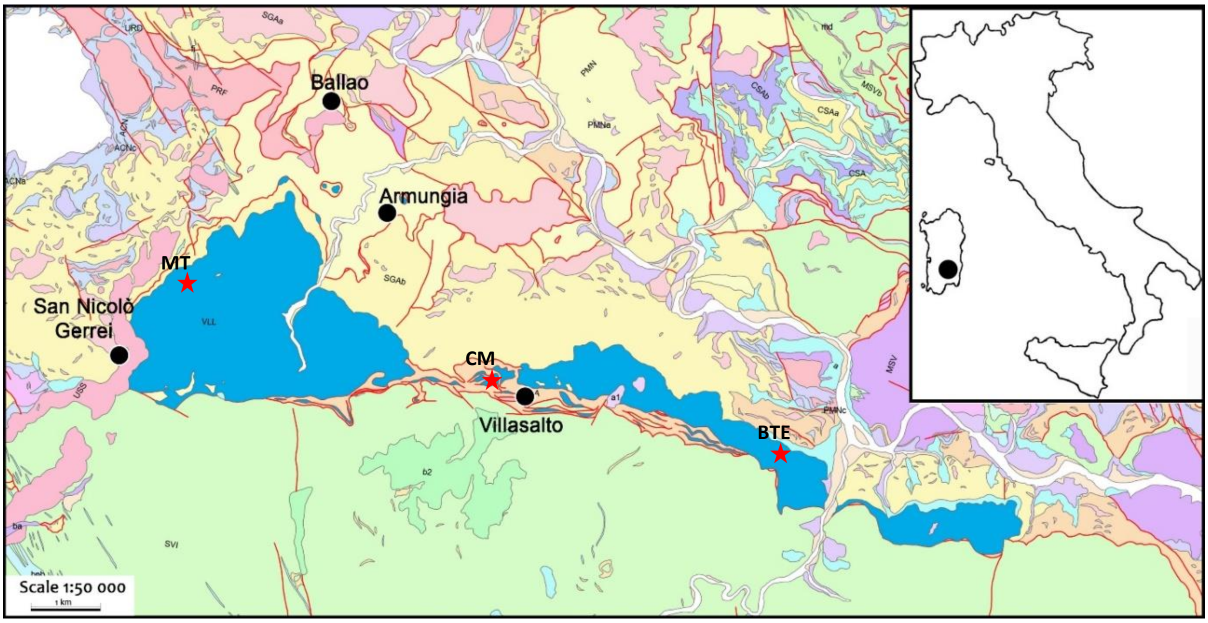

Figure 4.12. Geographical position of Sardinia and location of the studied area. The blue colour marks the Upper Devonian rocks. MT= Monte Taccu section; CM= Corona Mizziu sections; BTE= Bruncu Bullai section.

The structure of the Sardinian basement originated during the Variscan orogeny, about 300-250 years ago. It’s the result of a diacronous collision between two large continents: Laurussia and Gondwana, and from a variety of microplates including Armorica and Avalonia, which have become detached from the North Gondwana during the early stages of the orogeny (Ordovician).

Sardinia, as the rest of Southern Europe, underwent during the Miocene (Burdigalian) the Alpine Orogeny, due to the collision of the African and European plates. During this orogeny, the formation of a back-arc basin took place, causing the detachment of the Sardinia-Corsica block from the Provence (Southern France) and the opening of the Alghero-Provence basin. A subsequent drift of the island brought the latter to the actual position in the centre of the western Mediterranean Sea.

The main result of the Variscan orogeny in Sardinia is a tectono-metamorphic partition, three different zones have been distinguished from Northeast to Southwest (Inner, Nappe and Foreland Zones) (Carmignani et al. 1987) (fig 4.13). The Inner Zone crops out in the Northeast of the island, and expose metamorphic rocks up to anfibolitic facies. The Nappe Zone crops out widely in the Southeast of the island and expose mainly sedimentary rocks up to green schist metamorphic facies. The Foreland Zone crops out in the Southwest of Sardinia, and it is made up of sedimentary rocks affected by a very low grade of regional metamorphism (Funedda & Oggiano 2009).

The “Nappe Zone” (fig 4.13) is characterized by a series of units stacked on top of each other during the Variscan orogeny. This zone has been divided in two parts because of the different grade of metamorphism: the “Internal Nappe Zone” where the succession is affected by a medium-grade metamorphism, and the “External Nappe Zone”, in the central-southern Sardinia, where only low-grade metamorphic rocks crop out.

The Gerrei Tectonic Unit

The Gerrei Tectonic Unit (fig 4.14) is one of the units of the External Nappe Zone and it contains the most complete succession of the middle Paleozoic of Sardinia. It starts with the “San Vito Sandstones”, which represent a monotonous interbedding of gray micaceous sandstones, quarzites and shales. Based on acritarchs the San Vito sandstones, spans a time from the Middle Cambrian and the Lower Ordovician (Naud & Pittau Demelia 1987). An unconformity known as “Sarrabese’s Phase” and a polygenic conglomerate overlay the sandstones. The sequence continue with a volcano sedimentary succession originated by a volcanic arc during a subduction of oceanic crust underneath the Nord

Gondwanian margin. This unit, known as "Ordovician Volcanic Complex" contain different volcanic products from rhyolites to basalts and andesite (Carmignani et al. 1992).

After this volcanic succession, the Caradocian transgression took place and led the basin to a deep environment with the deposition of shales and limestones. Bryozoan, brachiopods, cistoids, trilobites, ostracods and conodonts are the fossil remains in the topmost calcareous beds. The conodont association has given an Upper Ordovician age (Hirnantian) (Ferretti et al. 1998, Ferretti & Serpagli 1999).

The classical "Thuringian Facies Triad" represents the Silurian and the Lower Devonian (Jaeger 1977). This unit starts with the "Lower Graptolitic shales", represented by black shales enriched in carbon and pyrite, interbedded with lydites and fosforites. A rich graptolitic fauna allow to date these shales to Llandovery-lower Ludlow (Meneghini 1857, Gortani 1923, Jaeger 1977, Barca & Jaeger, 1990, Storch & Piras 2009). The "Ockerkalk" represents a nodular shaley limestone with an ocraceous color. These limestones have been dated to the Ludlow-Pridoli (from the *hamata* to the *detortus* Zone) because of the rich conodont fauna (Barca et al. 1995, Corradini & Olivieri 1997, Corradini et al. 1998, 2000, Corradini & Ferretti 2009, Corriga et al. 2009). The "Thuringian facies Triad" ends in the Lower Devonian (Lochkovian) and the upper part of this facies is expresse

d by the "Upper Graptolitic shales", made up of alum shales. Pelagic graptolites, crinoids and rare brachiopods compose the fauna (Piras & Paschina 2009).

The succession continue with the "Tentaculitic shales and limestone" that represent an interbedding of thin pelites and limestones. Fossils contain is made up of tentaculitids and rare conodonts that allow to date this unit to the Lower-Middle Devonian. The Upper Devonian and the Lower Carboniferous is represented by the classical pelagic limestones, known as "*Clymeniae* Limestones" because of the presence of ammonoids in some levels (Lovisato 1894, Corradini 2007).

Several dozen meters of sandstones and polygenic conglomerates are present above the "*Clymeniae* Limestones" this represents the transaction to terrigenous sediments that end the pelagic sequence in South-East Sardinia. At the top of the Gerrei tectonic Unit at places crops out the "Conglomerate of Villasalto", interpreted as a syn-orogenic deposit accumulated in deep basins.

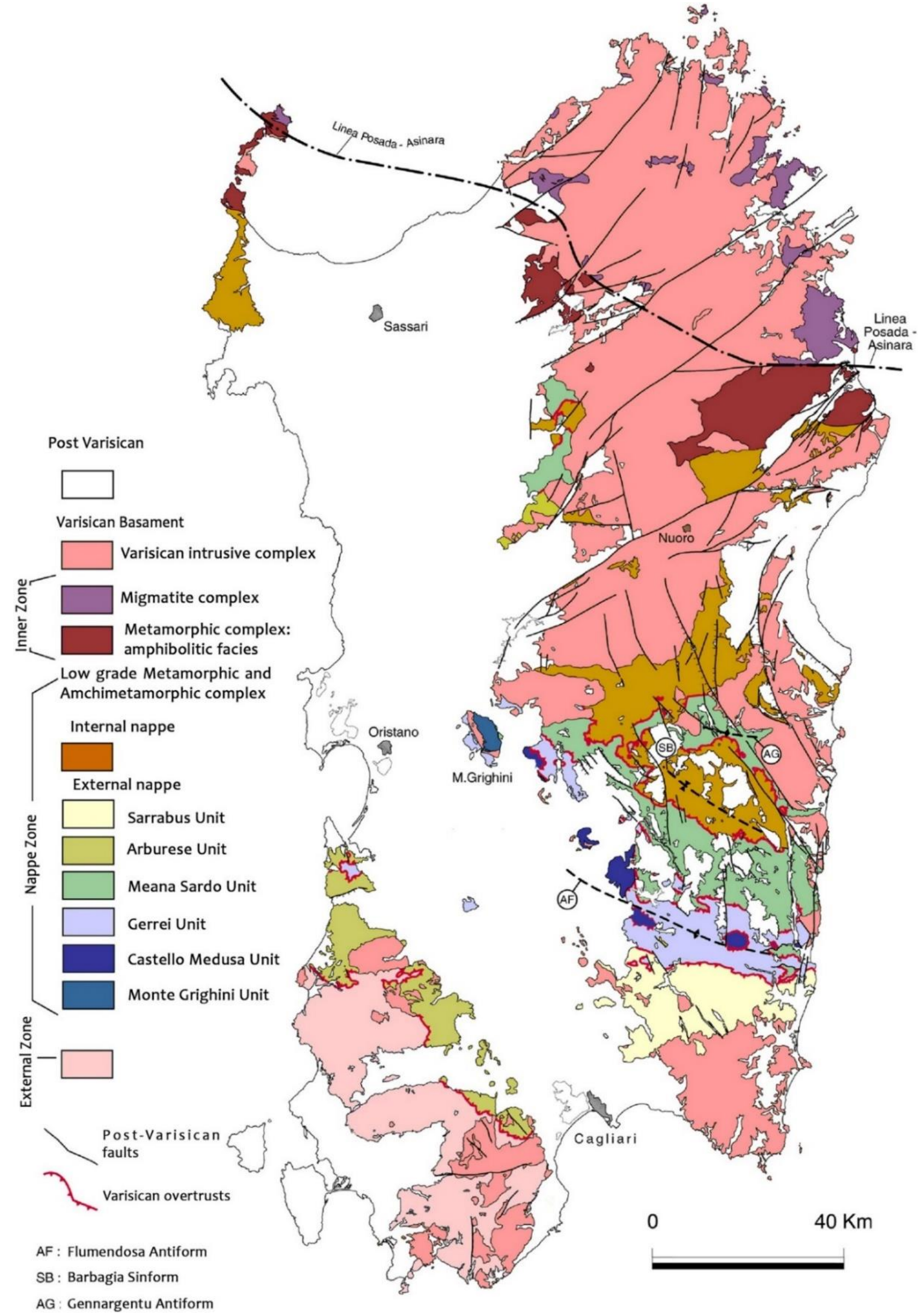

Figure 4.13. Geological scheme of Sardinia

The "Clymeniae Limestones"

The "*Clymeniae* Limestones" of Sardinia, also known as “Calcari di Villasalto”, crops out widely in the southeast of the island in the “External Nappe Zone”, but small outcrops are present also in the center, close to Ozieri. The origin of the name of this informal unit reflect the occurrence of levels with a very rich ammonoid fauna (Lovisato 1894). It is represented in the field mainly by grey massive limestones, with at places some levels of nodular limestones. The whole succession has been highly tectonized during the Varisican orogeny, and the true thickness of the unit has been hypothesized in about 50-70 m (Corradini 2008). The fossil contain is generally scarce, however some strata are very rich in crinoids steams and ammonoids. The microfossils fauna includes ostracodes, small shells (bivalves or brachiopods), fragments of echinoderms, gastropods, and rare trilobites. Conodonts are abundant; fish teeth and very rare brachiopods have been reported from acid-insoluble residues (Corradini 1998a, 1998c, Corradini et al. 2003, Derycke et al. 2008, and Mossoni et al. 2013b).

Ammonoids beds are concentrated in a few distinctive levels, mainly close to Famennian events like *Annulata* and *Dasberg*. Instead, the *Hangenberg* event is represented by a thin level of black shales (Corradini et al. 2003, Mossoni et al. 2013, 2015). Biofacies and microfacies suggest a deposition in a pelagic environment.

The age of these limestones have been provided from different studies during the last fifty years and spans from the Upper *hassi* Zone (Frasnian) to the Upper *duplicata* Zone (Carboniferous) (Pomesano Cherchi 1963, Olivieri 1970, 1985, Barca & Spalletta 1985, Corradini 2003, 2008, Corradini et al. 2001, 2003, Mossoni et al. 2013b, 2015).

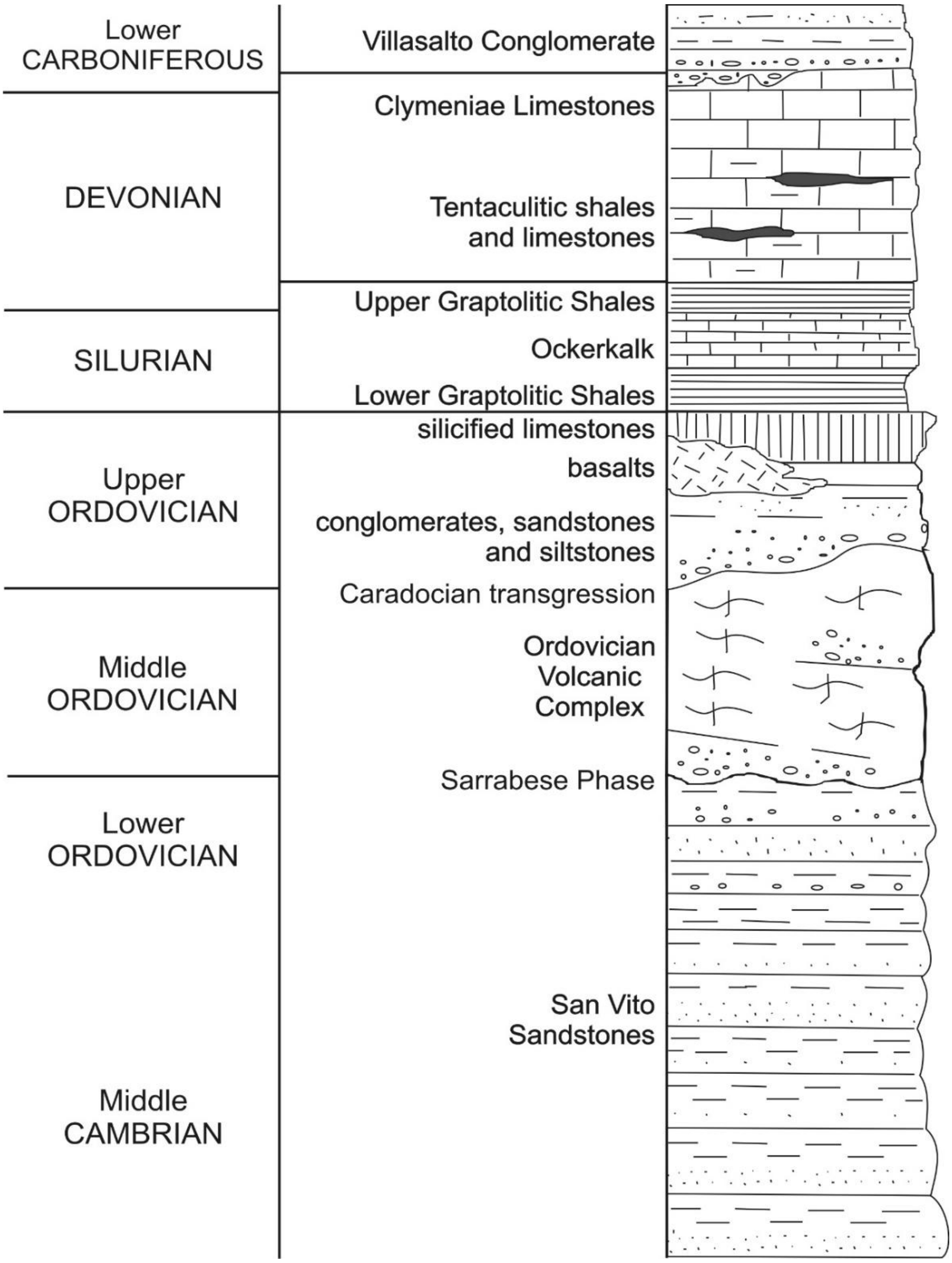

Figure 4.14. Scheme of the Gerrei Tectonic Unit (after Corradini et al. 2009)

Previous studies

Pomesano-Cherchi (1963) and few years later Olivieri (1965) reported conodonts Upper Devonian in age from the "Calcari a Clymenia" of the Gerrei subregion, in the southeast of Sardinia.

Few years later (1970) Oliveri in a monographic work provided the first biozonation for the Upper Devonian in Sardinia, identifing most of the Upper Devonian conodont Zones in the Corona Mizziu (CM) section close to Villasalto. Murru (1975), Spalletta & Vai (1982) and Barca & Spalletta (1985) reported, respectively, from the Monte Lora and from the Villasalto area, Upper Devonian conodonts. Corradini (1998a, 1998b, 1998c, 1998d, 2002, 2003) restudied and rearranged the CM section, and in the CM II reported sixteen conodonts Zones of the Famennian. Outcrops Tournaisian in age are rare in Sardinia, and until now only two section expose the Devonian/Carboniferous boundary: the Monte Taccu section (Corradini et al. 2001, 2003, Mossoni et al. 2013b), and the Bruncu Bullai section (Mossoni et al. 2015).

In addition, Pili & Saba (1975) described Upper Devonian conodonts from the Passo Correboi, on an Internal Nappe Zone, where there is a higher grade of metamorphism than the External Nappe Zone. Upper Devonian conodonts of south-western Sardinia have been reported in the valley of Cixerri by Leone (1973) and near Domusnovas by Olivieri (1985).

Bruncu Bullai section

The Bruncu Bullai (BTE) section is located few km SW of Villasalto in the northern slope of Bruncu Bullai hill at coordinates: 39°29'13.42"N; 9°26'15.25"E.

The section expose about eleven meters of massive gray limestone arranged in strata with a variable thickness from 20 cm up to 2 m (fig 4.15). A few limestone beds are present below the base of the section, but these have not been sampled because of the high tectonism. Fourteen biostratigraphic samples have been collected from this section.

Two distinctive levels of black shales are present in the upper part of the section (fig 4.15). The first level, between samples BTE 7 and BTE 8 is only a few centimeters thick and has a limited calcareous component evident in the field. The second shaley level (between samples BTE 10 and BTE 11) is about 50 cm thick, presents evident small lateral variations, and includes in its lower part a few chert nodules and a thin discontinuous calcareous level. A thrust, or a fault, follows this black shales level, evidenced in the field by a minor unconformity. Above, thick strata of limestones are present and the conodont data of the two samples (BTE 11-12) collected from these levels gave a Famennian age (Lover *marginifera* Zone).

According to conodont data (see below tab 4.3), the first shale level lies at the Devonian/Carboniferous boundary or just below, and can be considered as an equivalent of the Hangenberg Shales, whereas no data have been obtained from the second. However, according to its stratigraphical position it is likely Tournaisian in age and may represent a deeper sedimentation episode within the early phases of the Variscan orogeny (“Lower Alum Shale Event”, Becker 1993).

The microfacies (fig. 4.16) is a mudstone-wackestone all along the section. Fossil remains, mainly brachiopods and ammonoids, have been observed in thin section. The effect of the tectonic is constant in the section, calcite recrystallization and stylolite structures are present since sample BTE 4. It is evident an increase of the strain above sample BTE 7, but despite the faint metamorphic imprint, fossil remains are clearly recognizable. The sample BTE 10A shows tension gashes structures, due probably to the position inside the shaley level that absorbs the most the tectonic strain (fig 4.16D).

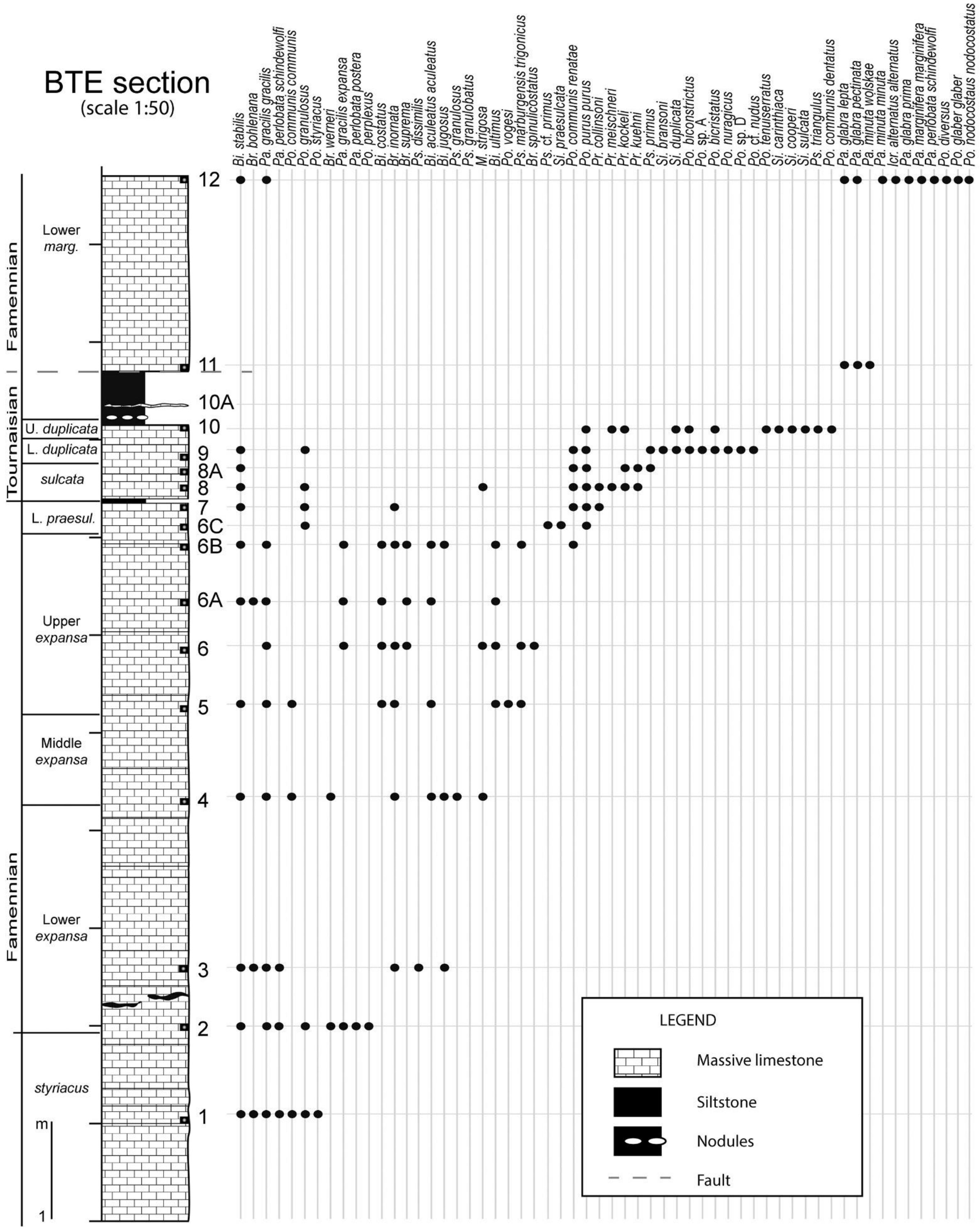

Figure 4.15. Stratigraphic log, biozonation and conodont occurrence of the Bruncu Bullai section. Abbreviation: Bi. – Bispathodus, Br. – Branmehla, Icr. – Icriodus, M. – Mehlina, Pa. – Palmatolepis, Ps. – Pseudopolygnathus, Pr. – Protognathodus, Po. – Polygnathus, Si. – Siphonodella.

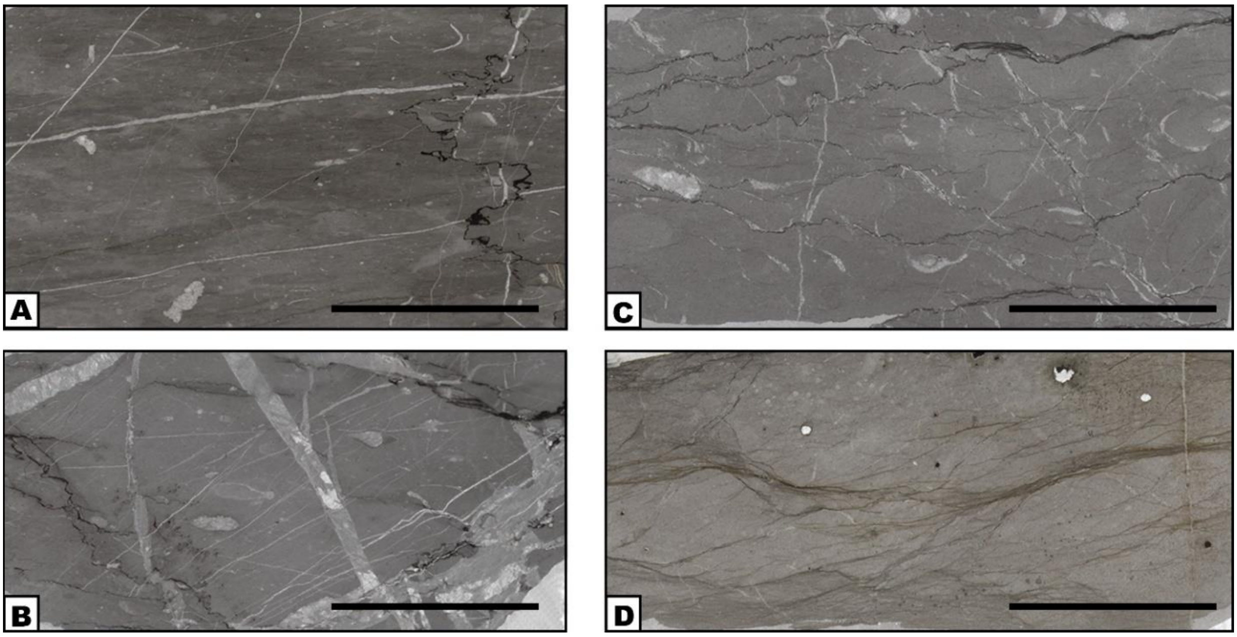

Figure 4.16. Microfacies of the Bruncu Bullai section. A – gray wackestone, sample BTE 5. B – gray wackestone with fossil remains and calcite ricristallization, in sample BTE 7. C – a gray wackestone with fossil remains and stylolite structures, in sample BTE 8. D – gray wackestone with tension gashes, sample BTE 10A. Scale bar 1 cm

Conodont data

Fifty-six taxa, between species and subspecies, belonging to genera *Branmehla*, *Bispathodus*, *Icriodus*, *Mehlina*, *Palmatolepis*, *Polygnathus*, *Protognathodus*, *Pseudopolygnathus*, and *Siphonodella* allow to recognize nine biozones, ranging from the Upper Famennian to the Lower Tournaisian. The Lower *marginifera* Zone is discriminated in the uppermost part of the section, above the tectonic duplication by the occurrence of the marker *Palmatolepis marginifera marginifera* in sample BTE 12. *Palmatolepis* dominate the association.

The *styriacus* Zone corresponds to an undifferentiated *postera* Zone of Ziegler & Sandberg (1990). It has been discriminated at the base of the section (sample BTE 1) by the presence of the marker, *Polygnathus styriacus*. *Palmatolepis gr. gracilis* and *Pa. perlobata schindewolfi* are the most abundant taxa.

It is worth to remark the high number of ramiform elements collected from this level, representing about one-half of the findings, even if their state of preservation is quite poor.

The Lower *expansa* Zone (samples 2-3) is recognized by the first occurrence of the marker*, Palmatolepis gracilis expansa*. *Palmatolepis perlobata postera* is here reported for the first time in Sardinia from this interval. This late entry of *Pa. perlobata postera* occurs also in the Carnic Alps (Perri & Spalletta 1998). *Pseudopolygnathus dissimilis* and *Branmehla werneri* are exclusive of this zone, whereas *Bispathodus jugosus* has its first occurrence. *Palmatolepis gracilis gracilis* is the most abundant species of this zone.

	Famennian										Tournaisian				?	Famennian		TOTAL
	styriacus	Lower expansa		Middle expansa	Upper expansa				Lower praesulcata		sulcata		Lower duplicata	Upper duplicata			Lower marginifera	
	1	2	3	4	5	6	6A	6B	6C	7	8	8A	9	10	10A	11	12	
Bispathodus aculeatus aculeatus				5	18		15	23										61
Bispathodus costatus			1		51	40	19	38										149
Bispathodus jugosus				1				3										4
Bispathodus spinulicostatus						16												16
Bispathodus stabilis	3	36	8	4	6		2	14		6	15	11	12				1	118
Bispathodus ultimus					49	27	7	18										101
Branmehla bohlenana	1		4				1											6
Branmehla inornata			9	5	6	25		7		1								53
Branmehla suprema						79	18	15										112
Branmehla werneri		3																3
Icriodus alternatus alternatus																	1	1
Mehlina strigosa				5		2					5							12
Palmatolepis glabra lepta																2	4	6
Palmatolepis glabra pectinata																2	17	19
Palmatolepis glabra prima																	14	14
Palmatolepis gracilis expansa		9				2	1	2										14
Palmatolepis gracilis gracilis	15	98	9	23	20	39	15	31									6	256
Palmatolepis marginifera marginifera																	28	28
Palmatolepis minuta minuta																	4	4
Palmatolepis minuta wolskae																1		1
Palmatolepis perlobata postera		4																4
Palmatolepis perlobata schindewolfi	11	29	1														19	60
Polygnathus biconstrictus													6	6				12
Polygnathus bicristatus													43	9				52
Polygnathus communis communis	1			1	5				8	5	44		1					65
Polygnathus communis dentatus														13				13
Polygnathus communis renatae								4		11	3	7	9					34
Polygnathus diversus																	1	1
Polygnathus glaber glaber																	9	9
Polygnathus granulosus	1	1																2
Polygnathus nodocostatus nodocostatus																	1	1
Polygnathus nuragicus													30					30
Polygnathus perplexus		1																1
Polygnathus purus purus									1	1	8	46	77	63				196
Polygnathus styriacus	6																	6
Polygnathus tenuiserratus													127	33				160
Polygnathus vogesi					1													1
Protognathodus collinsoni										4	8							12
Protognathodus kockeli											15	7		7				29
Protognathodus kuehni											7	3						10
Protognathodus meischneri											9			3				12
Pseudopolygnathus cf. *nudus*														6				6
Pseudopolygnathus dissimilis			16															16
Pseudopolygnathus granulobatus				12														12
Pseudopolygnathus granulosus				1														1
Pseudopolygnathus marburgensis trigonicus					2	5		1										8
Pseudopolygnathus primus									cf.			2	24					27
Pseudopolygnathus triangulus														20				20
Siphonodella bransoni													1					1
Siphonodella carinthiaca														1				1
Siphonodella cooperi M1														1				1
Siphonodella duplicata													4	2				6
Siphonodella praesulcata									2									2
Siphonodella sulcata														2				2
Polygnathus sp. A													11					11
Polygnathus sp. B													4					4
Bispathodus sp.						1		2										3
Branmehla sp.							7	8									1	16
Palmatolepis sp.	10															4	43	57
Polygnathus sp.	1				1			1	3	10	15	20	3	51		1	12	118
Pseudopolygnathus sp.				2	4	3	2	1	1	1		2		3				19
Ramiforms	53	20	4	10	23	46	27	40	6	26	36	20	38	22			30	401
Unidentified		82	14	7	18			9	6	1		7	15			13		172
TOTAL	102	283	66	76	204	285	114	217	28	66	165	125	405	242	0	23	191	2592
WEIGHT	1,3	2,0	1,7	2,1	2,3	1,4	0,8	2,3	2,9	1,2	1,8	1,3	1,5	2,2	0,4	1,0	3,0	29,2
ABUNDANCE	78,5	141,5	38,8	36,2	88,7	203,6	142,5	94,3	9,7	55,0	90,2	96,2	270,0	110,0	0,0	23,0	63,7	88,7

Table 4.3. Conodont distribution chart of the Bruncu Bullai section.

The Middle *expansa* Zone (sample 4) is discriminated by the entry of the marker *Bispathodus aculeatus aculeatus*. The abundance ratio shows an equity between the genus *Bispathodus*, *Pseudopolygnathus* and *Palmatolepis*.

The Upper *expansa* Zone (samples 5-6B) is recognized by the first occurrence of the marker *Bispathodus ultimus*. *Ps. marburgensis trigonicus* and *Polygnathus vogesi* are exclusive of this zone. Spathognathodids (mainly *Bispathodus* and *Branmehla*) are dominant, and *Branmehla suprema* is especially abundant in the upper part of the zone (fig 4.17).

The entry of *Siphonodella praesulcata* in sample BTE 6C allows the discrimination of the Lower *praesulcata* Zone. *Polygnathus communis renatae*, *Po. purus* and *Pr. collinsoni* enter, and *Branmehla inornata* has its last occurrence within this zone. Genus *Polygnathus*, relatively rare in the lower part of the section, becomes the dominant genus starting from this zone.The Upper *praesulcata* Zone have not been recognized in this section, as in other sections of the same age in Sardinia.

The occurrence of *Protognathodus kuehni* in sample BTE 8 allows to attribute the interval above the Hangenberg equivalent shales and below the first occurrence of *Siphonodella duplicata* to the *sulcata* Zone. Kaiser et al. (2009) used the same taxon to identify the base of the Carboniferous and named this zone *sulcata/kuehni* Zone. Subspecies of *Polygnathus communis* and Protognathodids are very abundant. *Pseudopolygnathus primus* has its first occurrence within this zone. The Lower *duplicata* Zone is documented by the entry of the marker *Siphonodella duplicata* in sample BTE 9. *Siphonodella bransoni*=(*Siphonodella duplicata* M1), *Polygnathus nuragicus* and *Polygnathus* sp.A have here their only occurrence in the section; *Po. teniuserratus*, *Polygnathus bicristatus* and *Po. biconstrictus* enter, whereas *Po. communis renatae* has its last occurrence. *Polygnathus* is the dominant genus. In this zone *Siphonodella* is present, whilst *Protognathodus* is absent.

The Upper *duplicata* Zone is discriminated in sample BTE 10 by the occurrence of Si. *cooperi* M1 and of Si. *carinthiaca*. *Pseudopolygnathus triangulus* and *Po. communis dentatus* have their only occurrence in the section.

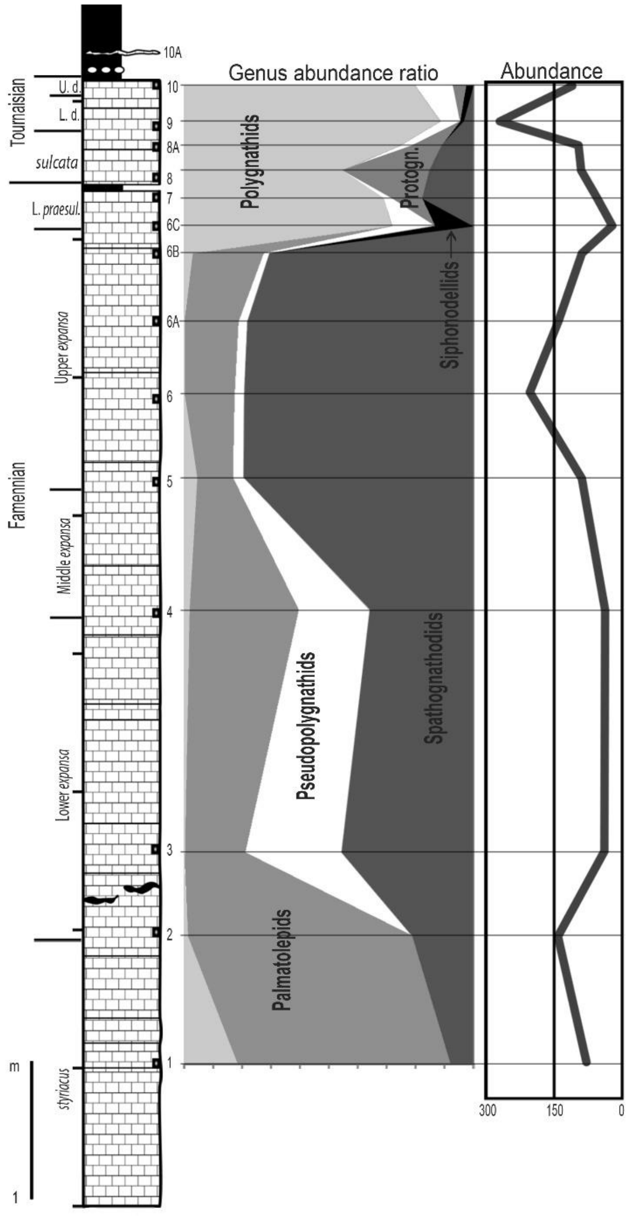

Figure 4.17. Genus abundance ratio and general conodont abundance for the BTE section. U.d =Upper duplicata; L.d = Lower duplicata; L.praesulc.= Lower praesulcata.

Magnetic susceptibility data

The Bruncu Bullai section has been sampled for the low field magnetic susceptibility (χ_{LF}) analysis every ten cm in order to obtain a curve (fig 4.19) and to identify the evolution of the magnetic susceptibility across the Hangenberg event. Seventeen samples of limestone have been collected across the Devonian/Carboniferous boundary from this section for the χ_{LF} analysis. As in the other sections, values of low field MS, high field MS and ferromagnetic MS show very low (χ_{LF}= 1,78x10^{-08}, χ_{HF}=1,70x10^{-08} and χ_{ferro}= 6,41x10^{-09}). From these samples, ten have been measured to obtain the hysteresis parameters (Ms, Mrs, Hc, Hcr). The χ_{LF} shows a good correlation with χ_{ferro} (r = 0,81). In contrast the correlation between χ_{LF} and χ_{HF} is very poor (r = 0,1), suggesting that the signal is not affected by the paramagnetic contribution and controlled only by the ferromagnetic. The average values of Hc and Hcr are lows (<20mT and <70mT respectively), this suggest a small concentration of high coercivity minerals. this hypothesis seems to be confirmed by the hysteresis loop, in fact all the samples show the classical shape for low coercivity minerals. The χ_{LF} curve is constant in the lower-centre part of the section (until BTE 7), while immediately after the Hangenberg event the curve become irregular and there are two distinctive peaks, one immediately after the black shales and the second 50 cm above. The other parameters are more or less constant all along the section (fig 4.19), however in the upper part of the section up to the last sample (BTE 10) there is an increase in the Hc and Hcr values, and this could be due to an increase in the heamatite percentage.

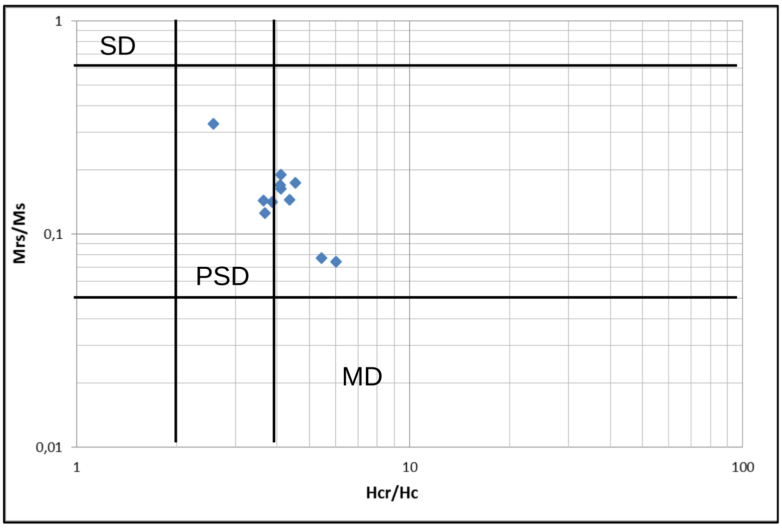

Figure 4.18. Day plot of the PZW section. The black cluster represent the samples PZW4-6. The green cluster is made up of samples PZW 1-3, 7. SD=single domain; PSD= pseudosingle domain; MD=multi domain.

The low values of magnetic viscosity indicate that there is no superparamagnetic contribution, and the Day Plot diagram shows that the grain size of all the samples form a cluster across the border between Pseudosingledomain and Multidomain (4.18). The detrital input, marked by the geochemical parameters, appears more or less constant all along the section. The correlation between the major elements and χ_{LF} is not so high (AL_2O_3=0.46, SiO_2=0.66, TiO_2=0.52, K_2O=0.35), while the correlation with χ_{HF} is not given (AL_2O_3=0.026, SiO_2=0.09, TiO_2=0.13, K_2O=0.05).

It is interesting to see that the increase of heamatite in the upper part of the section, registered in the hysteresis loop (Hc and Hcr) correlate with the increase of the TiO_2 , thus the presence of hematite in this section could probably have a detrital origin. In fig 4.19 it is possible to see that the peak in the first centimeters of the Carboniferous is expressed also in the geochemical measures.

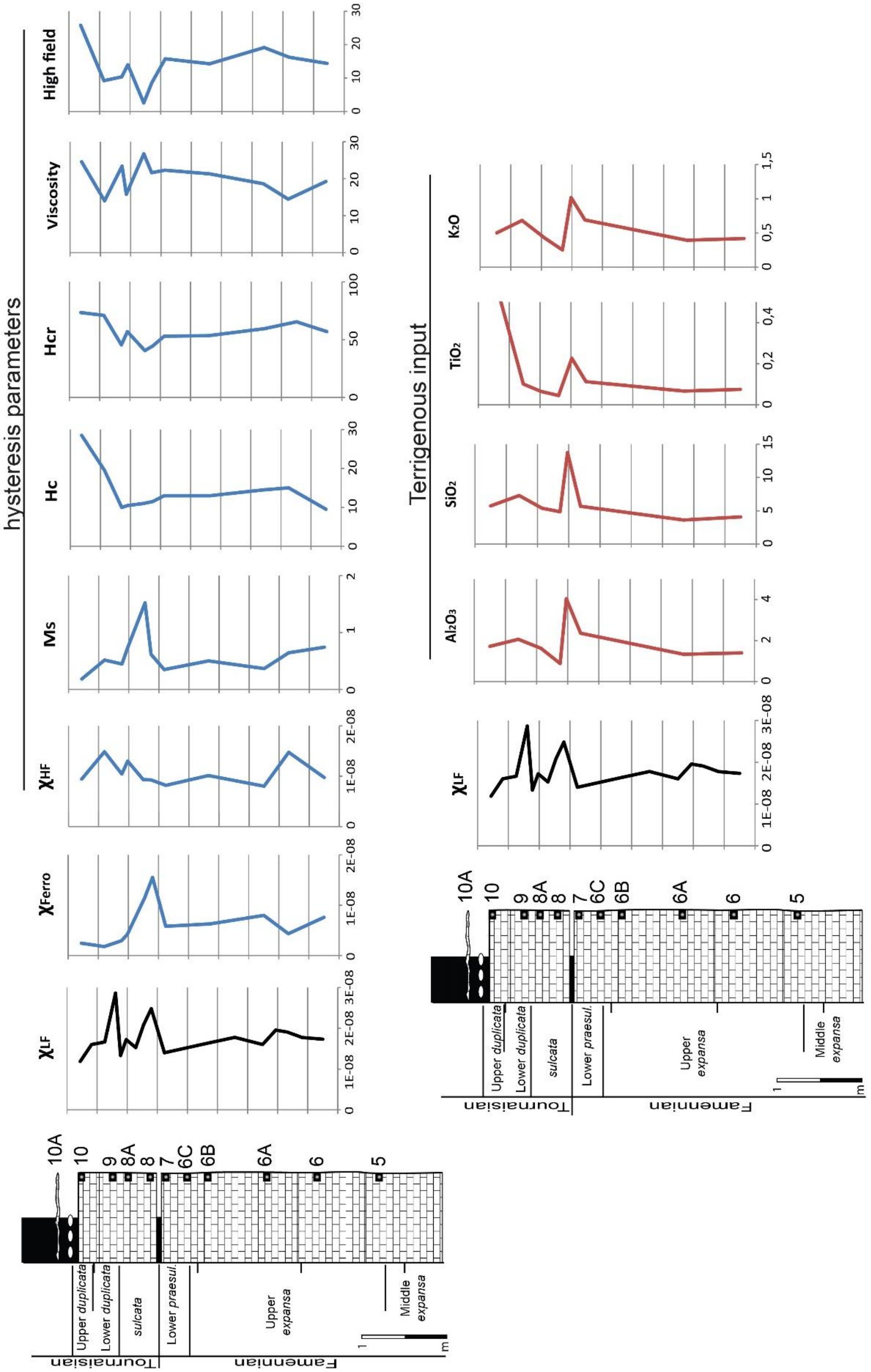

Figure 4.19. Low field magnetic susceptibility (χ_{LF}), ferromagnetic contribution (χ_{Ferro}), hysteresis parameters (high field magnetic susceptibility (χ_{HF}), magnetic saturation (MS), coercitive force (Hc), coercivity of remanence(Hcr), highfield remanence and viscosity decay) and geochemical data for the BTE section.

Monte Taccu section

The Monte Taccu (MT) section is located on the northern edge of Monte Taccu, a few km northeast of San Nicolò Gerrei village, at coordinates 39° 30' 38.953" N, 9° 19' 27.258" E.

It represent the only other section in Sardinia, beside the Bruncu Bullai section, where the Devonian/Carboniferous boundary is exposed. Corradini et al. (2003) studied part of the section.

The Monte Taccu section is overturned and exposes about 25 meters of "Clymeniae Limestone": a grey and rather massive limestone in strata up to 3 m thick (fig 4.20). The upper part of the section is more tectonically deformed than the lower part. At the Devonian/Carboniferous boundary an irregular thin level of dark shaley limestone is present, this level could be considered the equivalent of the Hangenberg event. The upper limit of the section is marked by a tectonic boundary with a highly deformed sandstone that bears silica nodules, this probably belong to the Ordovician San Vito Formation.

Considering also data from Corradini et al. (2003), twenty-three samples for conodont biostratigraphy have been collected from this section (fig 4.20).

The microfacies is a mudstone-wackestone, with evident calcite ricristallization. Fossil remains, mainly trilobites, brachiopods and ammonoids, have been observed in thin section. Bioclasts, mainly fragments of goniatites more frequent in the uppermost levels, are readily recognizable despite the lowgrade metamorphic overprint. Beside conodonts, the insoluble residues produced a few fish teeth (Corradini et al. 2003, Mossoni et al. 2013b).

Conodont data

The following ten biozones (fig 4.21) have been recognized in the Monte Taccu section (tab. 4.4):

The Upper *marginifera* Zone (samples 15-6A) has been discriminated from the base of the section by the occurrence of the index taxon *Palmatolepis marginifera utahensis*. *Palmatolepis* is the dominant genus, mainly represented by specimens of various subspecies of *Pa. glabra* and *Pa. marginifera.* The genus *Polygnathus* is less abundant than *Palmatolepis*, and the predominant species is *Polygnathus glaber glaber*. A few specimens of *Pa. glabra* are left in open nomenclature, because they do not fit in any of the subspecies already described.

The *velifer* Zone (sample 6C) is defined by the presence of the marker *Scaphignathus velifer velifer,* and by the first occurrence of *Alternognathus regularis.*

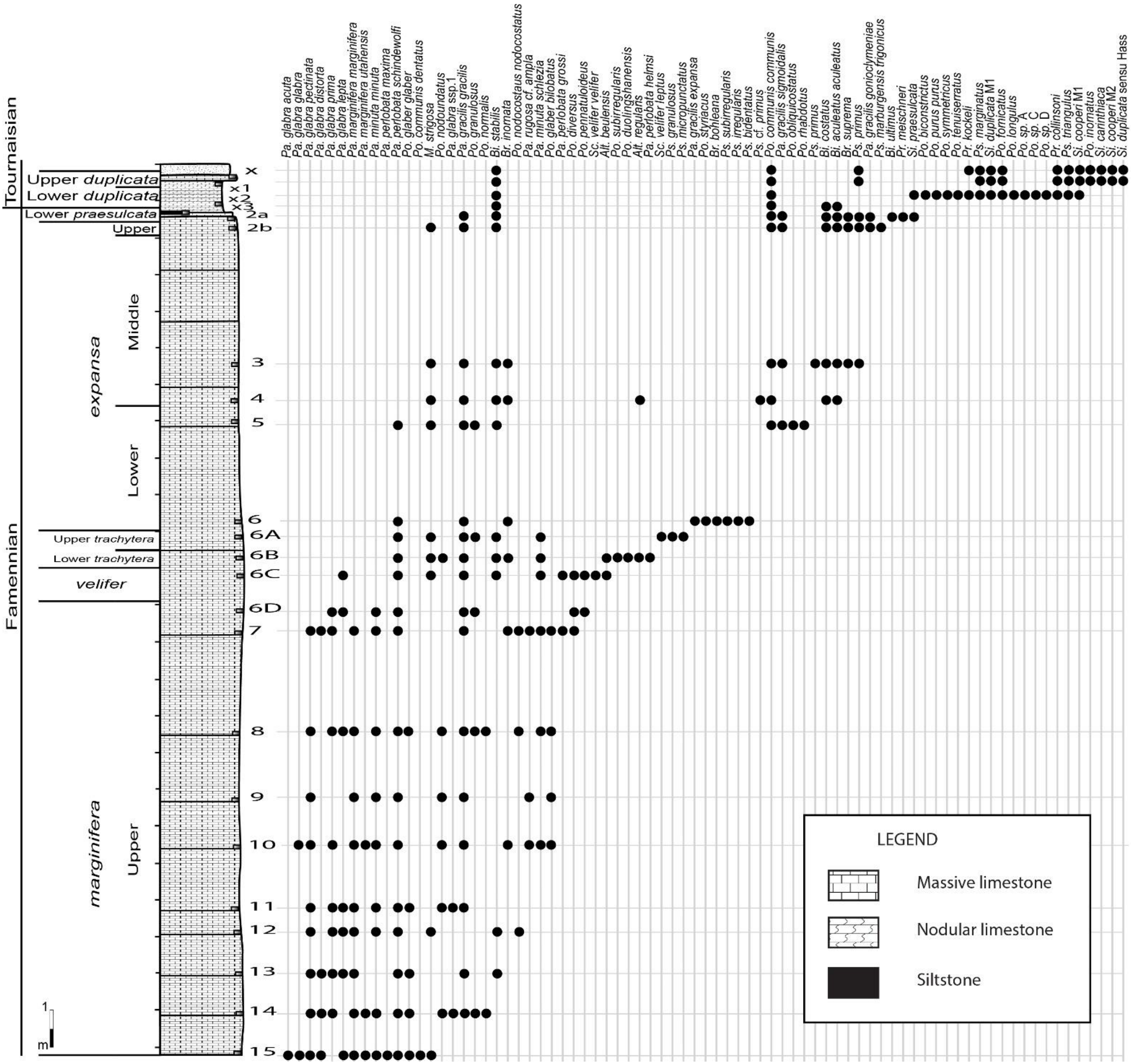

Figure 4.20. Stratigraphic log, biozonation and conodont occurrence of the Monte Taccu section. Abbreviation: Alt. – Alternognathus, Bi. – Bispathodus, Br. – Branmehla, Icr. – Icriodus, M. – Mehlina, Pa. – Palmatolepis, Ps. – Pseudopolygnathus, Pr. – Protognathodus, Po. – Polygnathus, Si. – Siphonodella.

The Lower *trachytera* Zone (sample 6B) is recognized based on the joint occurrence of *Palmatolepis perlobata helmsi*, *Polygnathus subirregularis*, *Palmatolepis glabra lepta,* and *Polygnathus glaber glaber*. The first two taxa have their first occurrence, while the others became extinct within this zone (Ji & Ziegler 1993).

The Upper *trachytera* Zone (sample 6A) is discriminated by the presence of the marker, *Pseudopolygnathus granulosus*, and by the occurrence of *Palmatolepis minuta schleizia* that has its last occurrence within this zone (Ji & Ziegler 1993).

	MONTE TACCU																							**TOTAL**
	Famennian																			*Tournaisian*				
	Upper marginifera									velifer	Lower trachytera	Upper trachytera	Lower expansa		Middle expansa		Upper expansa	Lower praesulcata		Lower duplicata	Upper duplicata			
	15	14	13	12	11	10	9	8	7	6D	6C	6B	6A	6	4	5	3	2B	2A	X3	X2	X1	X	
Alternognathus regularis											1	5				1								7
Bispathosus aculeatus aculeatus																	4	9	9	4		1		27
Bispathodus costatus																8	4	12	22	2				48
Bispathodus stabilis			1	1							1	2	23	30	2	12	6	3	1	3	1	16	3	105
Bispathus ultimus																			17					17
Branmehla bohlenana														6										6
Branmehla inornata						3			1			1		25		28	1							59
Branmehla suprema																	1	2	2					5
Mehlina strigosa		1		3							2	1	2		1	3	2	1						16
Palmatolepis glabra acuta	1																							1
Palmatolepis glabra distorta	14	1	6						8															29
Palmatolepis glabra glabra	52					2																		54
Palmatolepis glabra lepta	17		5	2	2			9		13	2													50
Palmatolepis glabra pectinata	10	12	7	14	21	4	2	17	23															110
Palmatolepis glabra prima		31	21	8	13	4		29	13	8														127
Palmatolepis glabra ssp.1		1			1																			2
Palmatolepis gracilis expansa														6					1					7
Palmatolepis gracilis gonioclymeniae																		1						1
Palmatolepis gracilis gracilis		3	7		6	4	5	13	12	2	3	23	6	43	37	40	42	16	7					269
Palmatolepis gracilis sigmoidalis															1		7	1	2					11
Palmatolepis marginifera marginifera	10	12	16	9	17	12	2	17	19															114
Palmatolepis marginifera utahensis	1	2				1																		4
Palmatolepis minuta minuta	22	9		7	1	3	9	15	13	12														91
Palmatolepis minuta schlezia								3	1		2	3	2											11
Palmatolepis perlobata grossi									2		1													3
Palmatolepis perlobata helmsi												2												2
Palmatolepis perlobata schindewolfi	10	13	6	3	3	10	6	20	13	25	4	16	3	26	9									167
Palmatolepis rugosa cf. *ampla*						1	2		1															4
Palmatolepis perlobata maxima	2																							2
Polygnathus biconstrictus																					3	197	16	216
Polygnathus communis communis															10	25	3	29	2	2	7	8		86
Polygnathus communis dentatus	2																							2
Polygnathus diversus									2	1	1													4
Polygnathus duolingshanensis												1												1
Polygnathus fornicatus																						1	1	2
Polygnathus glaber bilobatus						5	4	9	3															21
Polygnathus glaber glaber	23	5	10		7			3				1												49
Polygnathus granulosus		2						2		4			1		8									17
Polygnathus inornatus																							1	1
Polygnathus longulus																						18		18
Polygnathus nodocostatus nodocostatus				2				4	5															11
Polygnathus nodoundatus	3				1	1	1	2																8
Polygnathus normalis		5						17																22
Polygnathus obliquostatus															1									1
Polygnathus pennatuloideus										1														1
Polygnathus purus purus																					21	65	250	336
Polygnathus subirregularis												1												1
Polygnathus rhabdotus															14									14
Polygnathus styriacus														4										4
Polygnathus symmetricus																					1	4		5
Polygnathus tenuiserratus																					5	272		277
Protognathodus collinsoni																						6	12	18
Protognathodus kockeli																					1		15	16
Protognathodus meishneri																			1					1
Pseudopolygnathus bidentatus														1										1
Pseudopolygnathus cf. *primus*																8								8
Pseudopolygnathus granulosus		2											2											4
Pseudopolygnathus irregularis														5										5
Pseudopolygnathus marburgensis trigonicus																		1						1
Pseudopolygnathus marginatus																					1	1	4	6
Pseudopolygnathus micropunctatus													1											1
Pseudopolygnathus primus																	5				5	22	11	43
Pseudopolygnathus triangulus																						8	7	15
Scaphignathus velifer leptus													1											1
Scaphignathus velifer velifer											1													1
Siphonodella carinthiaca																							4	4
Siphonodella cooperi M1																						2	1	3
Siphonodella cooperi M2																							1	1
Siphonodella duplicata M1																					1	19	1	21
Siphonodella hassi																							3	3
Siphonodella praesulcata																			3					3
Siphonodella sulcata																					5	18		23
Bispathodus sp.																			2		2			4
Branmehla sp.	1																	1						2
Palmatolepis sp.	81	20	49	17	28	14	6	54	81	55	3	31		5					1					445
Polygnathus sp.	8	4	2	12	8	6	5	10	8	8		5		2					1		28	91	18	216
Protognathodus sp.																					1		1	2
Pseudopolygnathus sp.																		1					1	2
Siphonodella sp.														3							1	2		6
Ramiforms	91	17	33	11	18	22	18	110	67	19	9	25	32	93		22				3				590
Unidentified	153	17	17	12	25	36	24	71	44	63	34	70	23	134	13	53	9	17	2	5	12	134		968
TOTAL	501	157	180	101	151	128	84	405	316	211	64	187	96	383	96	200	84	94	73	19	95	885	350	4860
WEIGHT	2,1	2,8	2,2	3,2	2,1	2,5	2,4	2,3	2,6	1,8	2,3	3	2,5	2,1	6,1	1,9	6,3	3	2	1	1,2	1,8	3,1	60,3
ABUNDANCE	238,6	56,1	81,8	31,6	71,9	51,2	35,0	176,1	121,5	117,2	27,8	62,3	38,4	182,4	15,7	105,3	13,3	31,3	36,5	19,0	79,2	491,7	112,9	80,6

Table 4.4. Conodont distribution chart of the Monte Taccu section.

The *styriacus* Zone has not been documented and probably occurs in the thin interval between samples 6A and 6. In other Sardinian sections this biozone is very thin, and is less than one meter thick, like in the Corona Mizziu I section (Corradini 1998, 2003).

The Lower *expansa* Zone (samples 6-5) is recognized by the first occurrence of the marker, *Palmatolepis gracilis expansa*, and by the presence of *Polygnathus styriacus* and *Pseudopolygnathus irregularis* that have their last occurrence within this zone (Ji & Ziegler 1993, Hartenfels 2011).

The Middle *expansa* Zone (Sample 4-3) is here discriminated by the entry of *Bispathodus costatus*. *Pseudopolygnathus primus* first occurs.

The Upper *expansa* Zone (Sample 2B) is recognized by the first occurrence of *Pa. gracilis gonioclymeniae* and *Po. marburgensis trigonicus*, which make their entry within this zone (Ziegler & Sandberg 1984, Ji & Ziegler 1993).

The Lower *praesulcata* Zone (sample 2A-X3) is discriminated by the entry of the first representatives of the genus *Siphonodella*. The fauna includes several taxa whose range is restricted to the Devonian: *Bispathodus aculeatus, Bi. costatus, Bi. ultimus, Branmehla suprema, Mehlina strigosa, Palmatolepis gracilis*, and *Polygnathus vogesi*).The Upper *praesulcata* and the *sulcata* zones have not been recognized in the Monte Taccu section. The Lower *duplicata* Zone (sample X2) is documented by the entry of *Siphonodella duplicata* Morphotype 1. The Upper *duplicata* Zone (samples X1-X) has been recognized by the occurrence of *Si. cooperi* M1. In this biozone *Polygnathus* is the prevailing genus, especially *Po. purus purus*, *Po. biconstructus,* and *Po. tenuiserratus*.

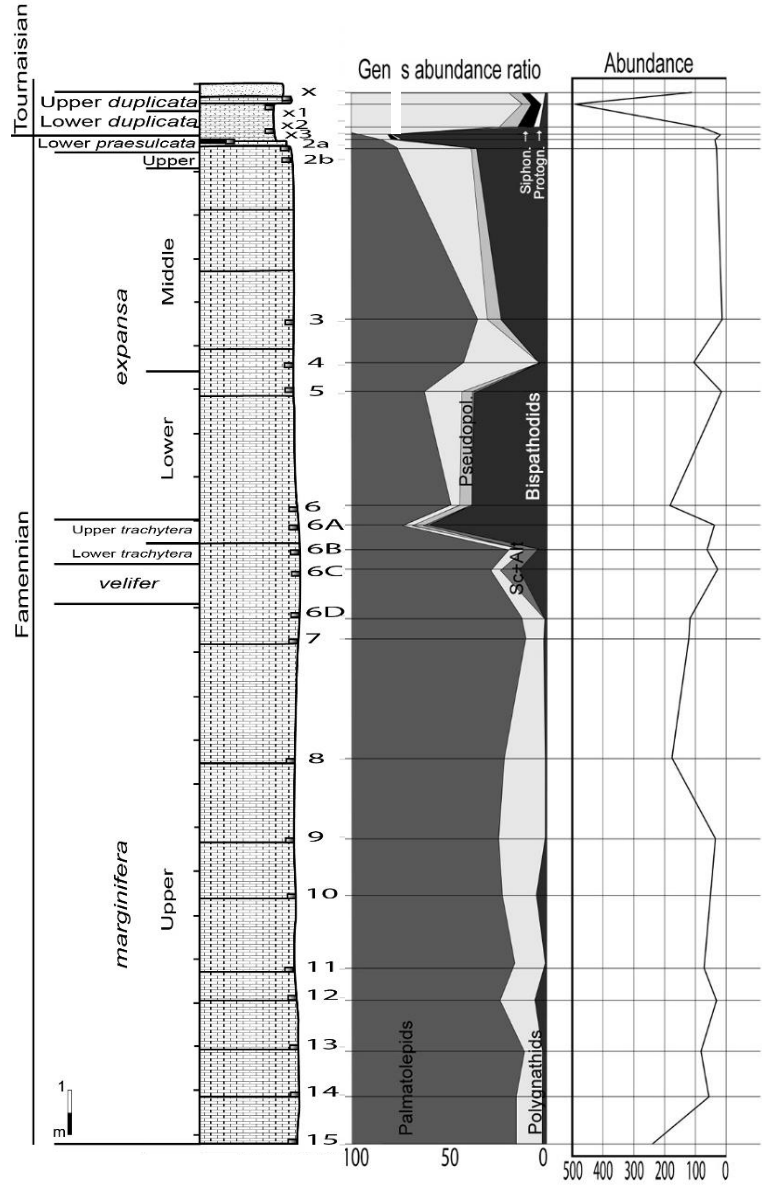

Figure 4.21.Genus abundance ratio and general conodont abundance for the BTE section

Magnetic susceptibility data

The Monte Taccu section has been sampled for the magnetic susceptibility analysis every ten cm from the upper part of the Middle *expansa* Zone to the Upper *duplicata* Zone (fig 4.22). The aim was to study the evolution of the detrital input across the Hangenberg event. Twenty samples of limestone have been collected across the Devonian/Carboniferous boundary from this section for the analysis of the low field magnetic susceptibility (χ_{LF}). The average values of MS and hysteresis measured in this section are comparable with those of the BTE section (χ_{LF}= 1,14x10^{-08}, χ_{ferro}= 3,83x10^{-09} and χ_{HF}=8,45x10^{-08}). Ten samples have been collected to obtain the hysteresis parameters (Ms, Mrs, Hc, Hcr). The χ_{LF} curve of this section is very similar to the curve of the Bruncu Bullai section (BTE), in fact both are quite constant in the lower part of the section with no significative fluctuations in the Famenian, then both show an increase in value and in the fluctuations startin from the Tournaisian (fig 4.22).

In the Monte Taccu section, after the sample MT 2b, the χ_{LF} tends to slightly increase and to become irregular. Two major peaks are distinguishable in the Carboniferous part of the section. The presence of negative values for ferromagnetic susceptibility (χ_{ferro}) is due to the high value of the high field magnetic susceptibility respect to the χ_{LF}, so the χ_{ferro} ($\chi_{ferro} = \chi_{LF} - \chi_{HF}$) shows negative values. This is an evidence that the paramagnetic contribution overcome the ferromagnetic, thus the low field magnetic susceptibility is controlled in the Monte Taccu section by the paramagnetic contribution.

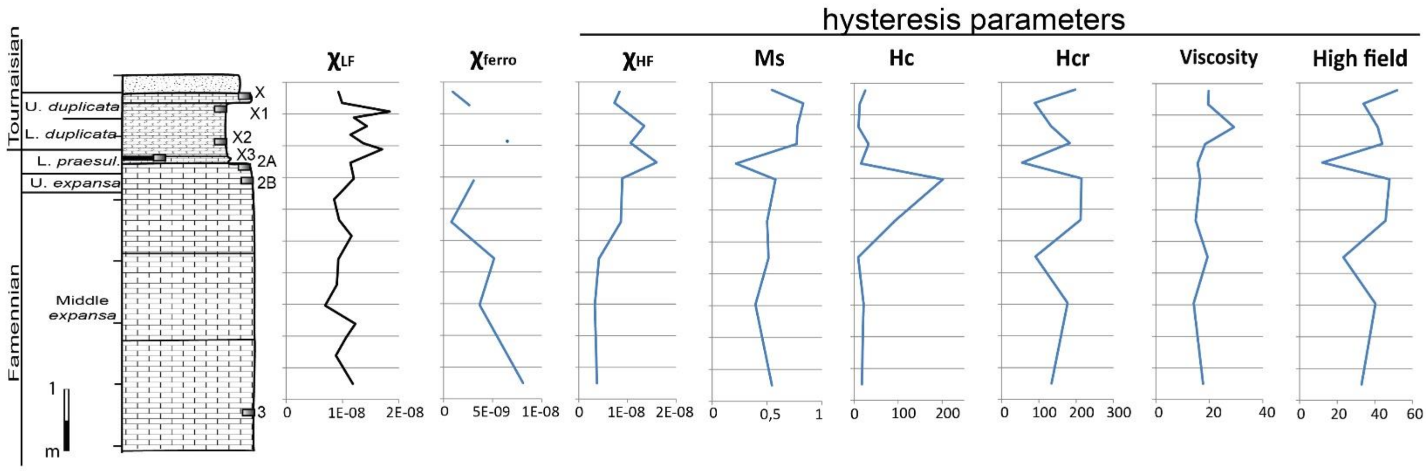

Figure 4.22. Low field magnetic susceptibility (χ_{LF}), hysteresis parameters (high field magnetic susceptibility (χ_{HF}), ferromagnetic contribution (χ_{Ferro}), magnetic saturation (MS), coercitive force (Hc), coercivity of remanence(Hcr), highfield remanence and viscosity decay) and geochemical data for the MT section

The values of coercitive force (Hc) and coercivity of remanence (Hcr) are peculiar in this section: while the Hc, excluding a peak close to sample MT 2b, show mainly low values (mean value= 43,80 mT, despite most of values show Hc <20 mT), the Hcr values are high (mean value= 148 mT). This is different from the other sections that shows either low values or high values for both parameters.

The low values of low field magnetic susceptibility (χ_{LF}= 1,14x10^{-08}) that generate a backfield curve close to the axis and the noise in the signal could explain this difference in values for Hc and Hcr.

The Day Plot diagram of this section show that the samples are scattered in the diagram (fig 4.23), while in the other sections there is one or two clusters and there are mixtures of PSD and MD.

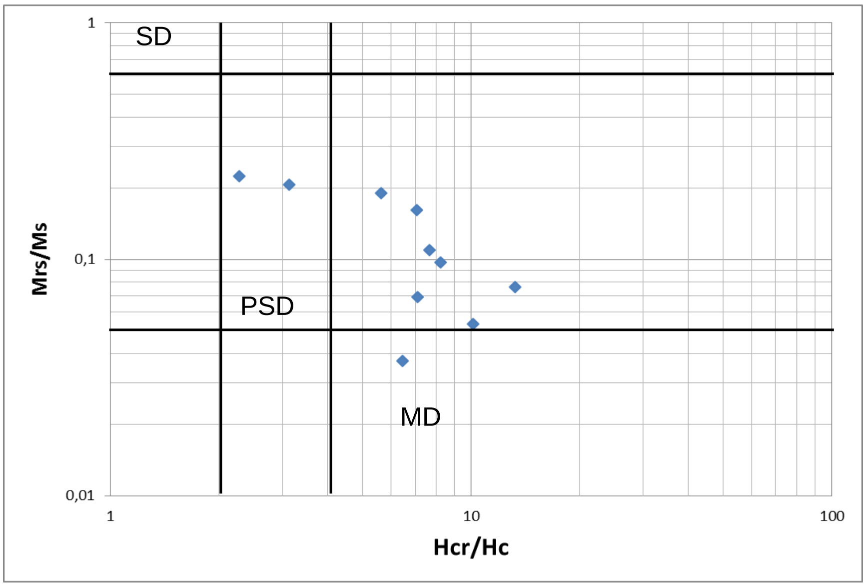

Figure 4.23. Day plot of the MT section. SD=single domain; PSD= pseudosingle domain; MD=multi domain

Corona Mizziu I and Corona Mizziu II sections

The Corona Mizziu sections are located about a km West of the Villasalto village, in which a calcareous hill crops out exposing the classical massive limestone of the Upper Devonian of Sardinia. The conodont biostratigraphy of the sections were studied by Corradini (2003). The conodont fauna of selected parts of the sections have been restudied for this work, and both sections have been sampled to study the detrital input across the selected events: the Annulata event in the Corona Mizziu I section and the Condroz event in the Corona Mizziu II section.

Corona Mizziu I

The Corona Mizziu I (CM I) section expose about 30 meters of well-bedded limestones (fig 4.24), with banks up to few meters in thickness. Generally, the strata tend to be thicker in the lower part of the section. The last few meters of the section (above sample CM I 26) lay on a disconformity immediately after the Lower *praesulcata* Zone and there is an overturned sequence caused by a fold visible only with the help of the biostratigraphy (Corradini 2003). Fossil remains are common in the central part of the section (CM I 18B-28) where ammonoid beds and rare crinoids are exposed.

The microfacies generally show a poorly fossiliferous micrite (mudstone), testifying a deposition in a pelagic environment. In the central part of the section fossil remains increase and the microfacies change from mudstone to wackestone-packstone. Ostracods, small shells, gastropods, fragments of echinoderms and trilobites are evident in thin section. The metamorphic imprint is observable only in the upper part of the section close to the fold.

The conodont data obtained from this section allow to discriminate twelve conodonts zones from the Lower *rhomboidea* to the Lower *praesulcata* Zones (for detail see Corradini 2003).

Corona Mizziu II

The Corona Mizziu II crops out a hundred meters far from the CM I section and expose 18 meters of grey massive limestones (fig 4.25), a short unexposed interval occurs in the upper part of the section between sample CM II 9 and CM II 10.

Despite the richness of some ammonoid beds of the CM I, the Corona Mizziu II section does not have such ammonoid beds. The section spans a time from the Lower *crepida* to the Lower *trachytera* Zones (Corradini 2003), the only conodonts zone missing is the *velifer* Zone.

The microfacies show a monotonous mudstone throughout the whole section with poor fossil remains. The tectonic imprint is marked by stylolite structures and calcite recrystallization.

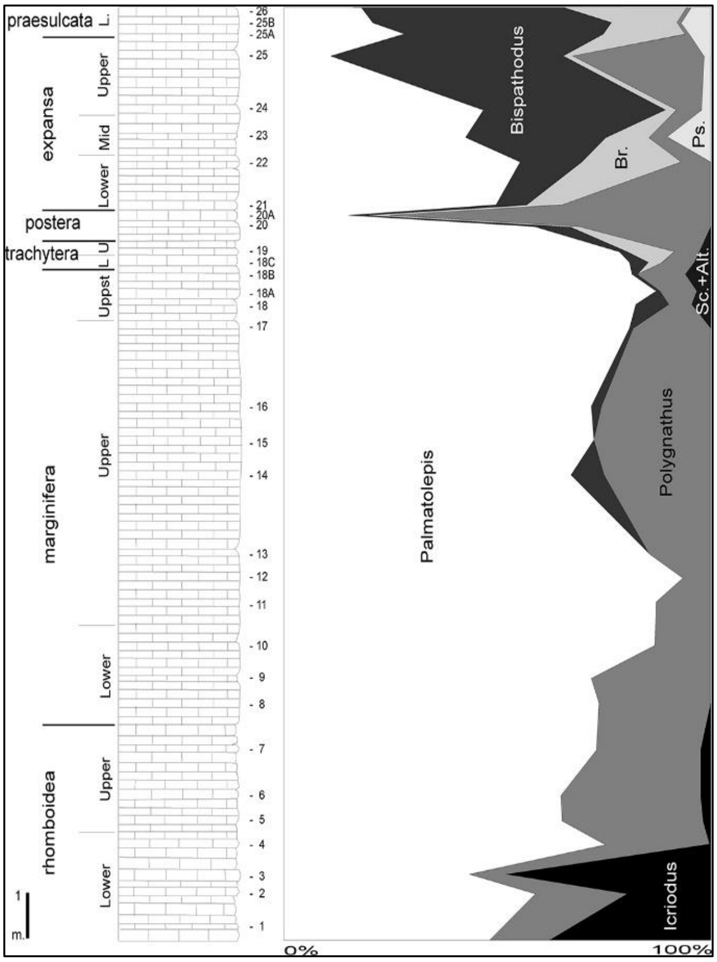

Figure 4.24. Genus abundance ratio for the CM I section

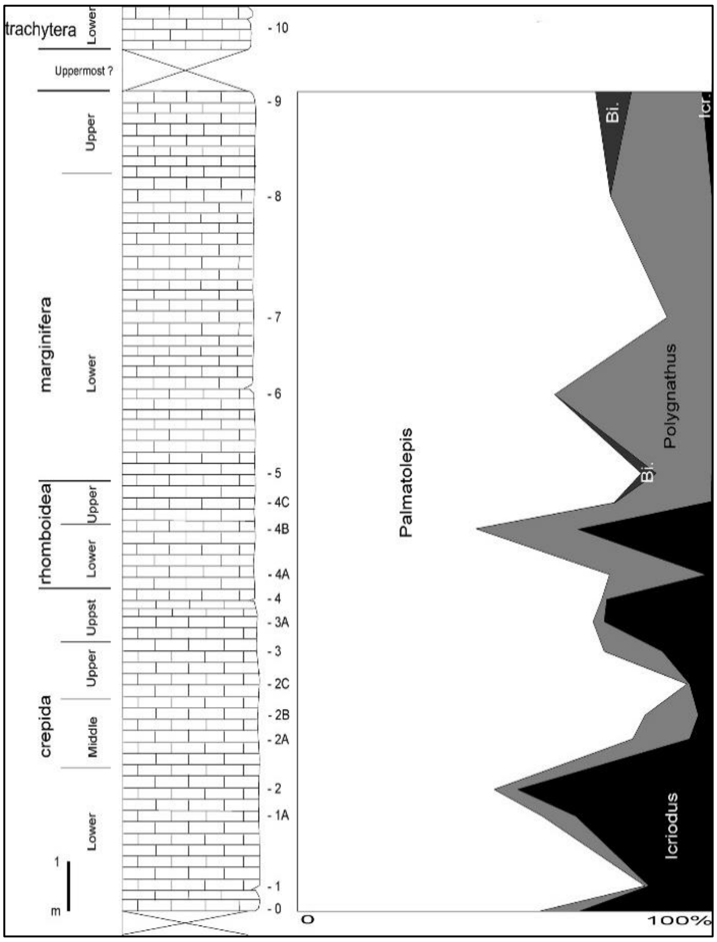

Figure 4.25. Genus abundance ratio for the CM II section.

Magnetic susceptibility data

Corona Mizziu I

The Corona Mizziu I section has been sampled for the low field magnetic susceptibility (χ_{LF}) measures and major element geochemistry from the *velifer* Zone up to the Upper *expansa* Zone (fig 4.27). The aim was to study the evolution of the detrital input across the "Upper and Lower *Annulata* events".

Fifty-three samples have been collected from the CM I section to measure the low field susceptibility. Among these samples, thirty-one have been chosen to perform the hysteresis loop and therefore to obtain the hysteresis parameters: Hc, Hcr, Ms and Mrs.

The mean χ_{LF} value of the section is about $9{,}05 \times 10^{-8}$ m^3/kg. In the bottom part (Uppermost *marginifera* Zone or *velifer* Zone) of the section, the magnetic curve can be considered constant even if some small fluctuations are visibles. Immediately after the sample CM I 19 there is a clear shift in the curve, marked also in the paramagnetic contribution (χ_{HF}) and less clearly in the ferromagnetic contribution. Above, in the upper part of the Upper *trachytera* Zone there is an increase in the low field magnetic susceptibility, marked by a clear shift in the curve.

The average value of the coercitive force (Hc) is low (<20 mT). The coercivity of remanence (Hcr) instead show high values in the bottom part of the section (up to sample CM I 19) and then tend to decrease to lower values (<70 mT). This suggest the presence of low coercivity minerals at least from the sample CM I 19. The high values of Hcr from sample CM I 17 to CM I 19 are expressed also by the viscosity decay. This is due probably to a faint diagenetic remagnetization of the natural remanent magnetisation, which led to the formation of superparamagnetic minerals. All of this data confirm the presence of an antiferromagnetic mineral such as haematite in the part of the section from sample CM I 17 to CM I 19.

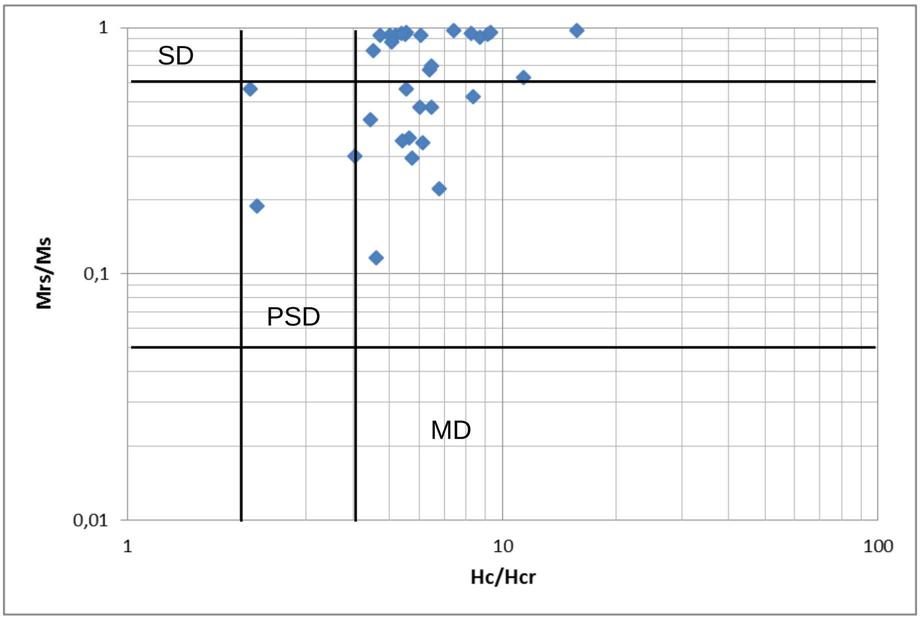

Figure 4.26. Day plot of the CM I section. SD=single domain; PSD= pseudosingle domain; MD=multi domain.

Considering that in the lower part of the section the high field susceptibility does not marks high values, it can be assumed that the haematite in this portion of the section could have a diagenetic origin.

The χ_{LF} / χ_{ferro} correlation (r = 0.69) is not higher as the χ_{LF} / χ_{HF} (r = 0.83), so the signal is controlled mainly by the paramagnetic contributions. The Day plot diagram show two cluster of values in the area of SD+MD domain, and in the PSD+MD domain (fig 4.26). However, these two cluster represent a mixture of samples from the whole section and not just from one particular part of it.

To study the terrigenous input, geochemical measure (major element geochemistry) were performed in thirteen selected samples of the CM I section (fig 4.27). The correlation between the terrigenous input and the low field magnetic susceptibility is good: AL_2O_3=0.68, SiO_2=0.51, TiO_2=0.70, K_2O=0.69.

The curve for the four oxides can be considered constant througout the section, however two peaks are visible respectively in the bottom and upper part. While the first peak is not expressed in the χ_{LF}, the second peak between the Lower and the Middle *expansa* Zone is expressed by the χ_{LF} and by the major elements (fig 4.27). This could probably be the evidence that the Dasberg crisis (House 2002) has been registered in the Corona Mizziu I section. Another peak expressed only in the SiO_2 coincide with the shift in the χ_{LF} curve and it is due probably to the presence of the upper *Annulata* event in the Upper *trachytera* Zone.

Titanium (Ti) and potassium (K) are considered proxies for detrital input flux in deep marine environment. Even considering the presence of heamatite in the bottom part of the section, the very good correlation between the low field magnetic susceptibility and the four oxides measured allow to give a general detrital origin input for the low field magnetic susceptibility of this section.

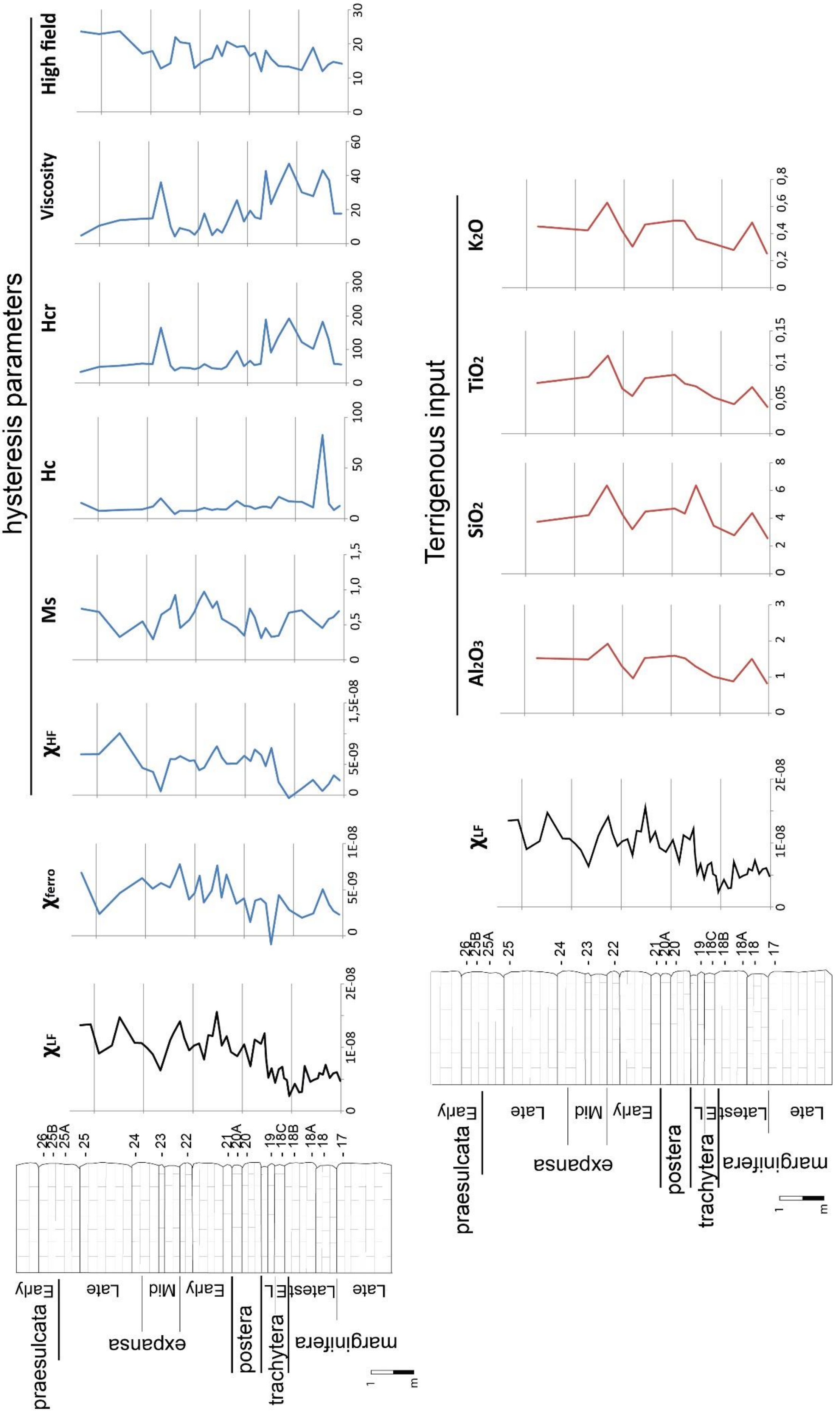

Figure 4.27. Low field magnetic susceptibility (χLF), ferromagnetic contribution (χFerro), hysteresis parameters (high field magnetic susceptibility (χHF), saturation magnatization (MS), coercitive force (Hc), coercivity of remanence(Hcr), highfield remanence and viscosity decay) and geochemical data for the CM I section

Corona Mizziu II

Ninety-four samples have been collected from the Corona Mizziu II section to measure the low field magnetic susceptibility, to acquire the hysteresis loop and to perform the major element analysis (fig 4.29). The aim was to acquire some magnetic and geochemical data across the Lower and Upper Condroz events respectively in the Lower and Upper *rhomboidea* Zone in order to study the detrital input across the event.

The mean low field magnetic susceptibility (χ_{LF}) values of the CM II section is about 2,47 × 10^{-8} m^3/kg. The χ_{LF} behaviour in this section and can be split into three parts (fig 4.29): the bottom part of the curve show a decreasing trend with large fluctuations from the Middle to the Uppermost *crepida* Zone, and then it starts to increase in the *rhomboidea* Zone with a sharp fluctuation in sample CM II 4B. After sample CM II 5, when the Lower *marginifera* Zone enter, the signal starts a general decrease with almost no fluctuations.

The χ_{LF} has a good correlation with χ_{ferro} (r = 0.85) and with χ_{HF} (r = 0.82). This suggests that the low field magnetic susceptibility of the Corona Mizziu II section is controlled by both the ferromagnetic and paramagnetic contributions.

The coercivity force (Hc) and the coercivity of remanence (Hcr) show low values (<10 mT and <70 mT) and both parameters appear to be constant from the bottom part of the section, up to the Upper *rhomboidea* Zone, then a slowly increase can be seen in both parameters. The increase of the coercivity remancence (Hcr) coincide with an increase of high field and viscosity decay. This could marks the presence of diagenesis or superparamagnetic (SP) particles. However, it seems that the grain size is beyond the range SP. The samples plotted in the Day plot diagram show that the grain size is made up of a cluster across the MD and PSD+MD domains (fig 4.28). The samples plotted in the MD domain come from the Lower *marginifera* Zone.

Major trace elements measures were performed on eleven selected samples, the general trend all along the section is constant with no significative peaks. The correlation with χ_{LF}, χ_{ferro} and χ_{HF} is not given, this because all oxides (AL_2O_3, SiO_2, TiO_2, K_2O) are constant throughout the section with no significative variation from the bottom to the upper part of the section.

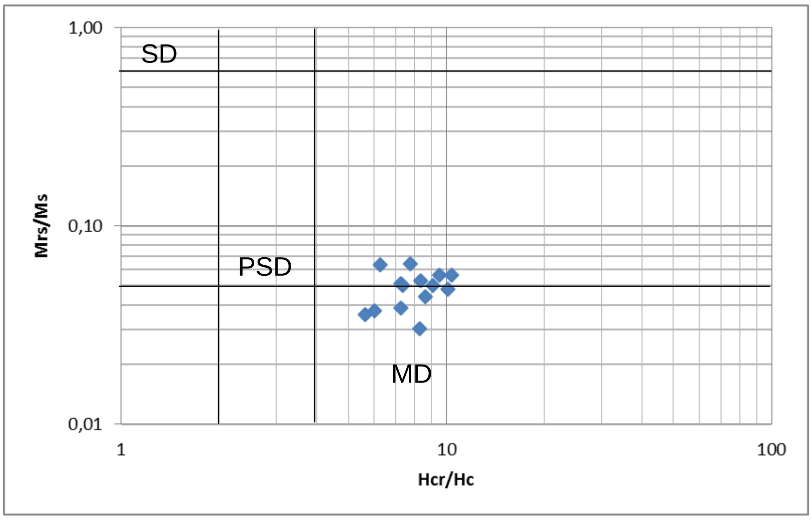

Figure 4.28. Day plot of the CM II section. SD=single domain; PSD= pseudosingle domain; MD=multi domain.

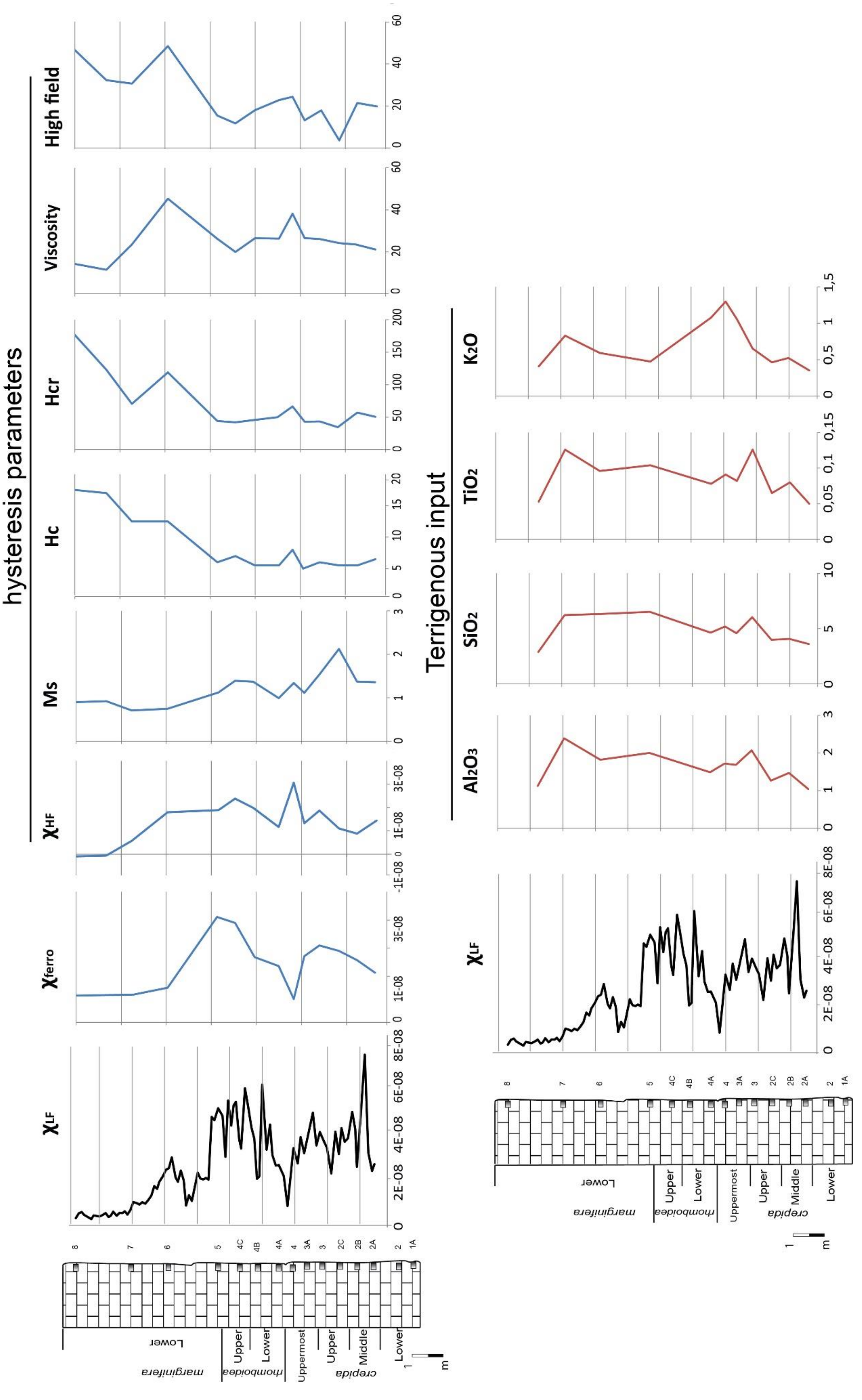

Figure 4.29. Low field magnetic susceptibility (χ_{LF}), ferromagnetic contribution (χ_{Ferro}), hysteresis parameters (high field magnetic susceptibility (χ_{HF}), saturation magnetization (MS), coercitive force (Hc), coercivity of remanence(Hcr), highfield remanence and viscosity decay) and geochemical data for the CM II section.

DISCUSSION AND CONCLUSIONS

Discussion

With the aim to investigate selected events in the Famennian in this work, six different sections from Sardinia and Carnic Alps have been studied for conodont biostratigraphy, low field magnetic susceptibility and major element geochemistry.

Some of these sections have been sampled and studied for the first time during this work (BTE, PZW), others have been updated (PB, MT), or partially restudied (CM I, CM II).

The conodont fauna shows a relative poor abundance in some sections (35.5 conodonts/Kg in the PZW section), while the average abundance is between 60 and 90 conodonts/Kg (BTE, MT, CM I and CM II), the PB section shows an higher average abundance (376.4 conodonts/Kg).

Generally, in the lower-middle part of the Famennian, *Palmatolepis* is the dominant genus in all the sections, after the *postera* Zone the spathognathodids (*Bispathodus*, *Branmehla* e *Mehlina*) become dominant. *Polygnathus* dominate the fauna from the latest Famennian to the lower Tournaisian.

The low field magnetic susceptibility (χ_{LF}) analysis reveals generally low values for all the six sections measured. This coincides with the mean value for carbonate rocks (between 1×10^{-9} and $1\times 10^{-7} m^3/kg$), proposed by Ellwood et al. (1999). The sections oldest in age (PZW and CM II) show higher values of low field magnetic susceptibility and large fluctuations in the magnetic curve (fig 5.1, 5.2).

The sections younger in age tend to show less fluctuations and a more constant curve (fig 5.1). Some peaks recognized in χ_{LF} curves coincides with the studied events, and will be analysed in the next paragraphs. Considering that saturation magnetization (Ms) do not depend on the grain size but rather on concentration (Devleeschouwer et al 2010), since that there is no correlation between ferromagnetic contribution (χ_{ferro}), Ms and the viscous decay (viscosity), it is possible to assume that the enhancement of ferromagnetic minerals is not due to the presence of superparamagnetic (SP) particles. Values of coercivity force (Hc) and coercivity of remanence (Hcr) are variables within the sections. Most of the samples plot in the range of the magnetite domain, which is under the 20mT for the coercivity force and under 70mT for the coercivity of remanence (figs 5.3, 5.4). The ferromagnetic component (χ_{ferro}) is dominated mainly by the presence of low coercivity minerals (such as magnetite). However, some samples plots in the range of the high coercivity minerals. Considering that the conodont Color Alteration Index (CAI) ranges between 4,5 - 5,5, the temperature which the rocks underneath is far beyond the temperature of the goethite-haematite transition. Thus, the high coercivity values measured are related to the presence of haematite, visible also in the microfacies. However, where high coercivity minerals control the χ_{LF}, the presence of hematite is here interpreted to be of detrital origin because the high field magnetic susceptibility (χ_{HF}) and viscous decay do not correlate.

The Day Plot diagram (fig 5.5) shows that the sections of the lower and upper Famennian (CM II, PZW, BTE and MT) show a mixture of Pseudosingledomain and Multidomain grains (PSD+MD), while the samples from the Middle Famennian (CM I and PB sections) plot in the Singledomain + Multidomain (SD+MD) area.

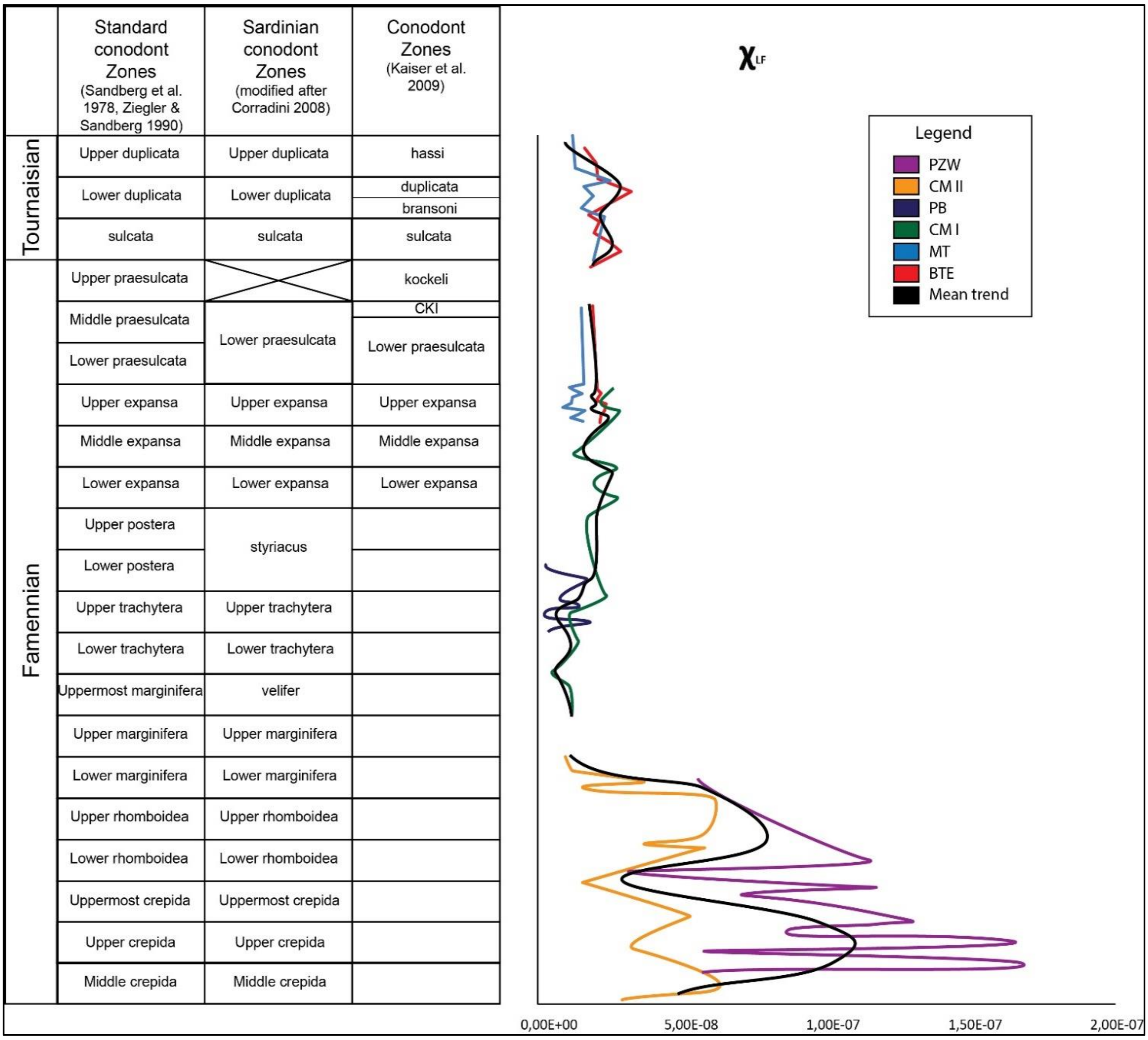

	Standard conodont Zones (Sandberg et al. 1978, Ziegler & Sandberg 1990)	Sardinian conodont Zones (modified after Corradini 2008)	Conodont Zones (Kaiser et al. 2009)
Tournaisian	Upper duplicata	Upper duplicata	hassi
	Lower duplicata	Lower duplicata	duplicata bransoni
	sulcata	sulcata	sulcata
Famennian	Upper praesulcata		kockeli
	Middle praesulcata	Lower praesulcata	CKI Lower praesulcata
	Lower praesulcata		
	Upper expansa	Upper expansa	Upper expansa
	Middle expansa	Middle expansa	Middle expansa
	Lower expansa	Lower expansa	Lower expansa
	Upper postera	styriacus	
	Lower postera		
	Upper trachytera	Upper trachytera	
	Lower trachytera	Lower trachytera	
	Uppermost marginifera	velifer	
	Upper marginifera	Upper marginifera	
	Lower marginifera	Lower marginifera	
	Upper rhomboidea	Upper rhomboidea	
	Lower rhomboidea	Lower rhomboidea	
	Uppermost crepida	Uppermost crepida	
	Upper crepida	Upper crepida	
	Middle crepida	Middle crepida	

Figure 5.1. Low field magnetic susceptibility curves of the studied section compared with the conodont zones. The black line represent a mean value considering all the magnetic signals. Orange line: CM II section. Purple line: PZW section. Dark blue line: PB section. Green line: CM I section. Light blue line MT section. Red line: BTE section.

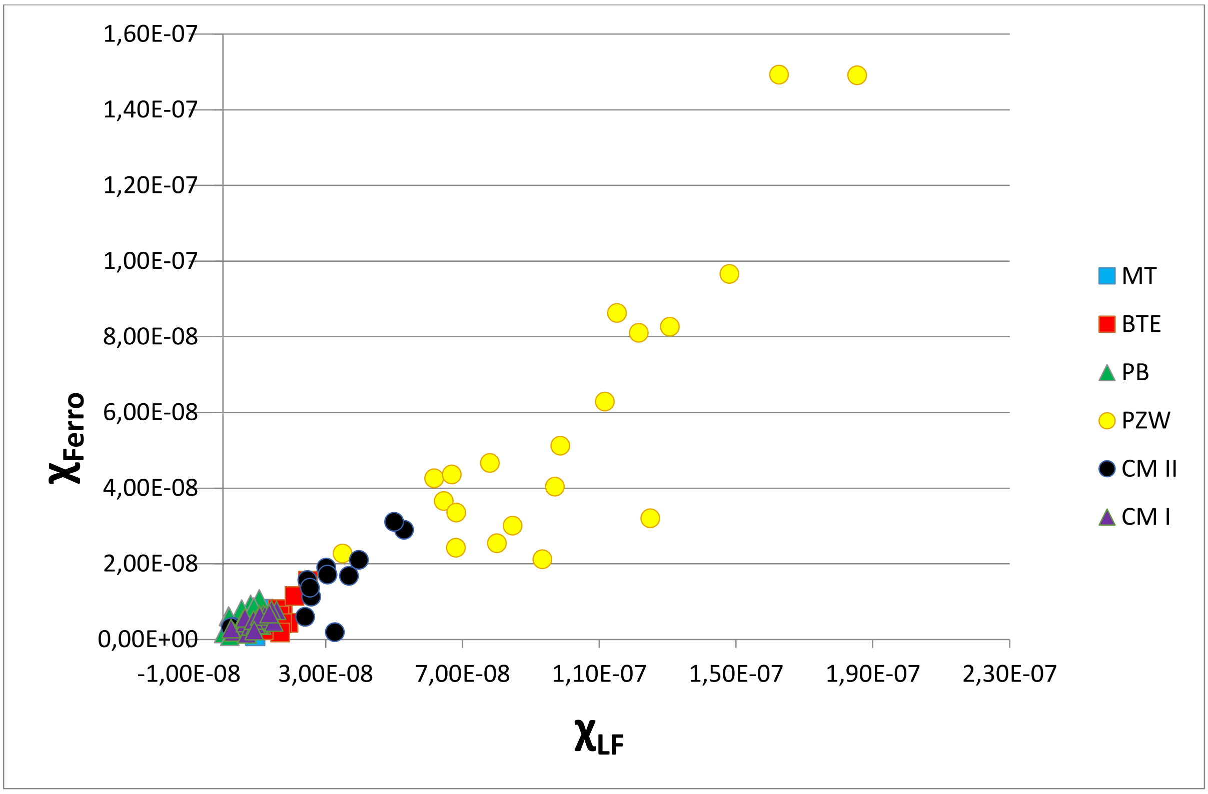

Figure 5.2. Relationship between χ_{LF} and χ_{ferro} in the studied sections.

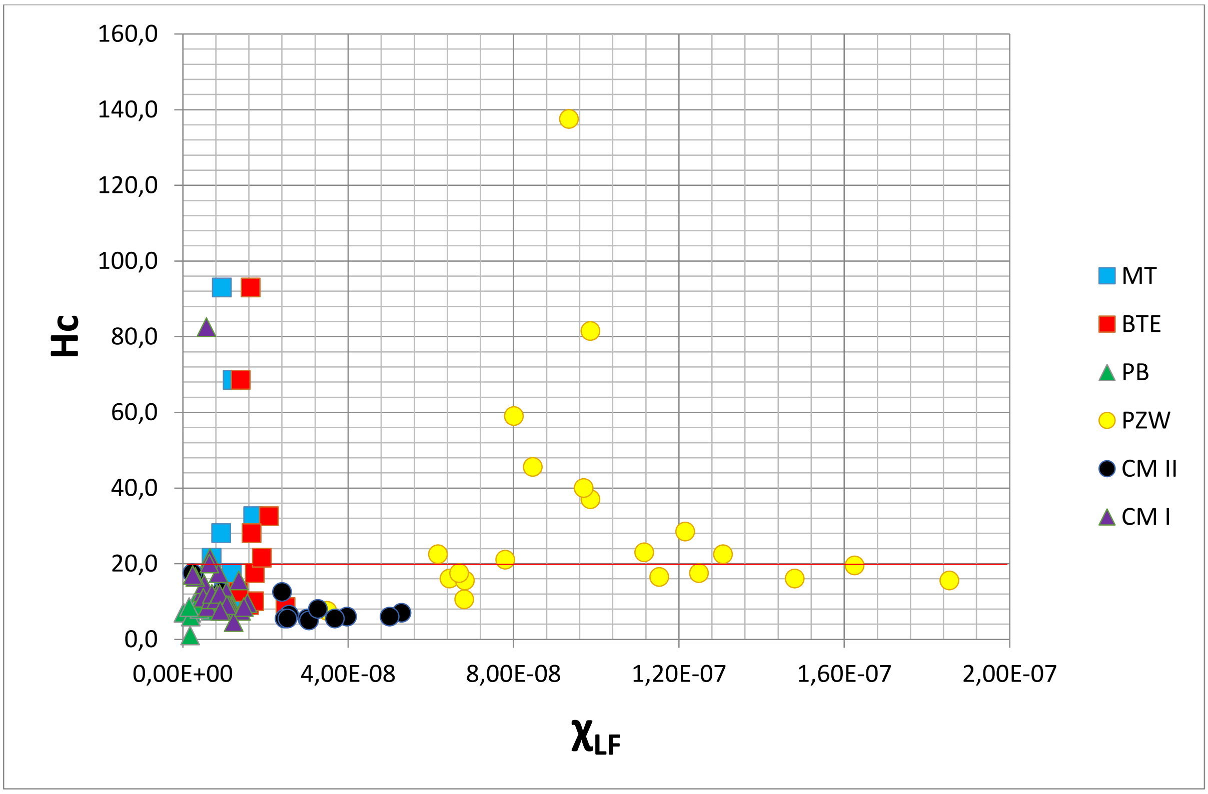

Figure 5.3. Crossplot reporting the low field magnetic susceptibility (χ_{LF}) and the coercivity force (Hc) in the studied sections: the values under the red line correspond to the domain of coercivity force values of magnetite

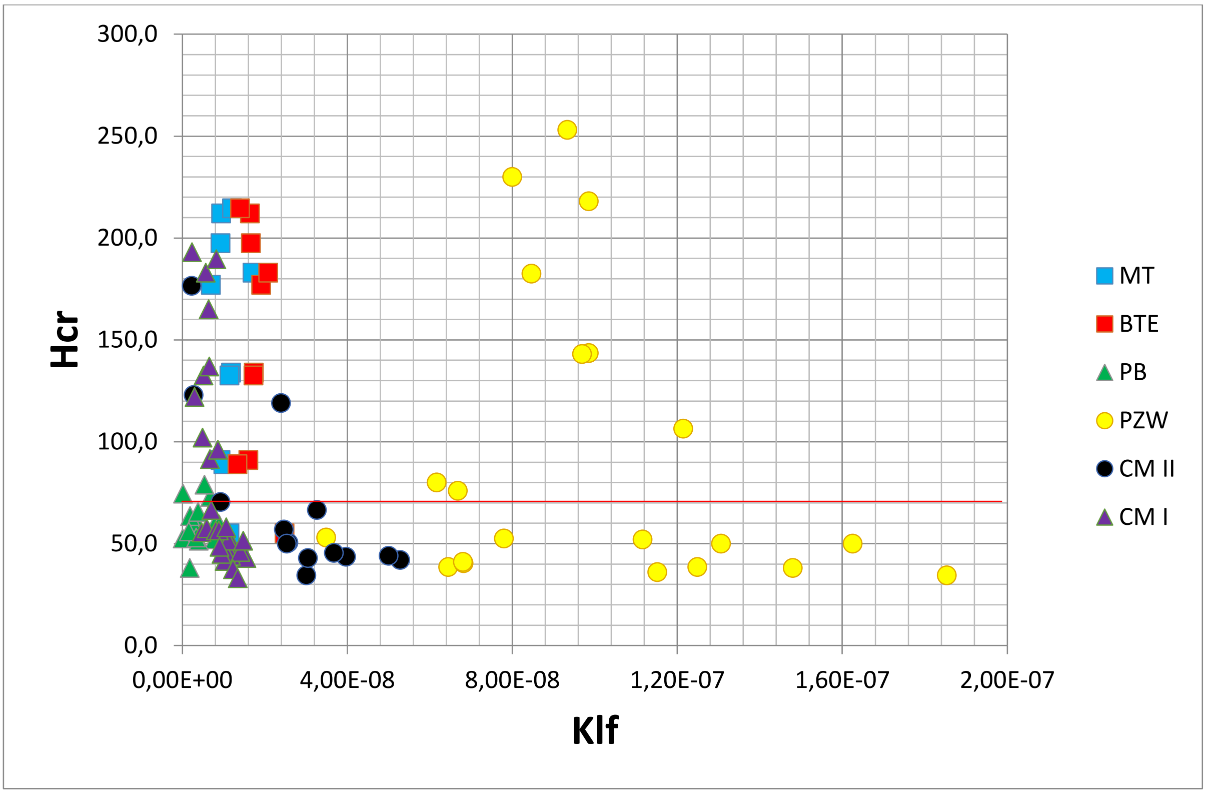

Figure 5.4. Crossplot reporting the low field magnetic susceptibility (χ_{LF}) and the coercivity of remanence (Hcr) in the studied sections: the values under the red line correspond to the domain of coercivity of remanence values of magnetite

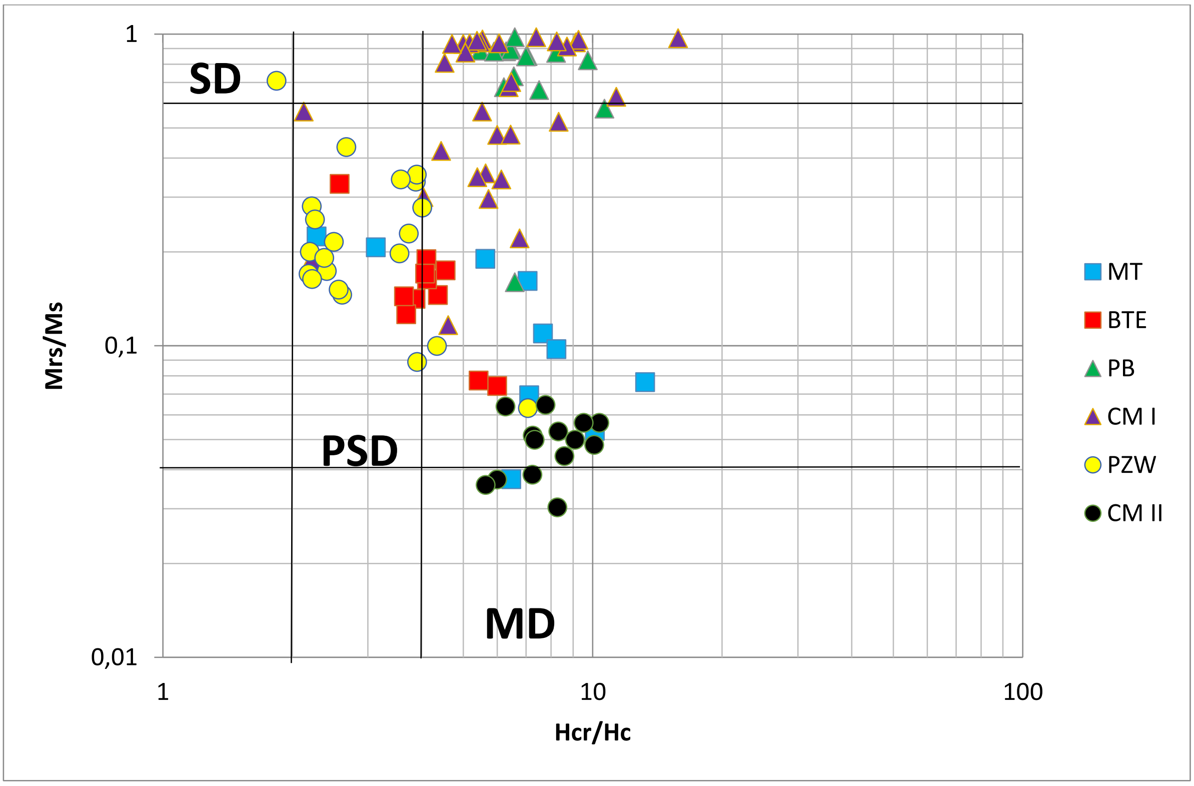

Figure 5.5. Day plot for the studied section.

Condroz Event – Comparation between PZW and CM II sections.

The Lower and Upper Condroz pulses have been investigated in two sections: the Pizzul West (PZW) in the Carnic Alps and the Corona Mizziu II (CM II) in Sardinia. Both show similarities in the low field magnetic susceptibility curve (χ_{LF}). The general trend is quite similar in the lower part of the sections showing a general decreasing trend from the Upper *crepida* toward the Uppermost *crepida* Zones. A distinctive peak can be identified in both sections at the boundary with the Lower *rhomboidea* Zone. As already pointed out in the introduction, the global eustatic curve presented by Johnson et al. (1985) show a general regressive trend in the Lower-Middle Famennian. During this general regression, events like Nehden and *Annulata* took place during transgressions, while the two Condroz pulses has been registered during sharp regressive pulses.

The PZW and the CM II are sections lithologically represented by nodular limestones, the PZW show three different facies while the CM II a single one, however both limestones were deposited in pelagic environments.

The mean χ_{LF} of these two sections is generally higher than the others are, mainly until the Upper *rhomboidea* Zone, while from the Lower *marginifera* Zone starts a general decrease to values close to the ones measured in the younger sections (fig 5.1).

The peak marked in both sections is time-equivalent to the Lower Condroz regressive pulse (LC), therefore it is evident that the LC has been registered in Sardinia and in the Carnic Alps. The χ_{LF} curve of the CM II section presents a major peak across the boundary between the Lower and Upper *rhomboidea* Zones, this peak can be identified as the Upper Condroz regressive pulse. In addition, the magnetic curve in the Upper *rhomboidea* Zone marks evident fluctuations, this could be related to a moment of oceanic instability after the sharp regression.

The PZW section show no peak time-equivalent to the Upper Condroz pulse, but a small interruption in the section could have obliterate the event, the χ_{LF} signal is quite regular and tend to continue in a general decrease up to the Lower *marginifera* Zone.

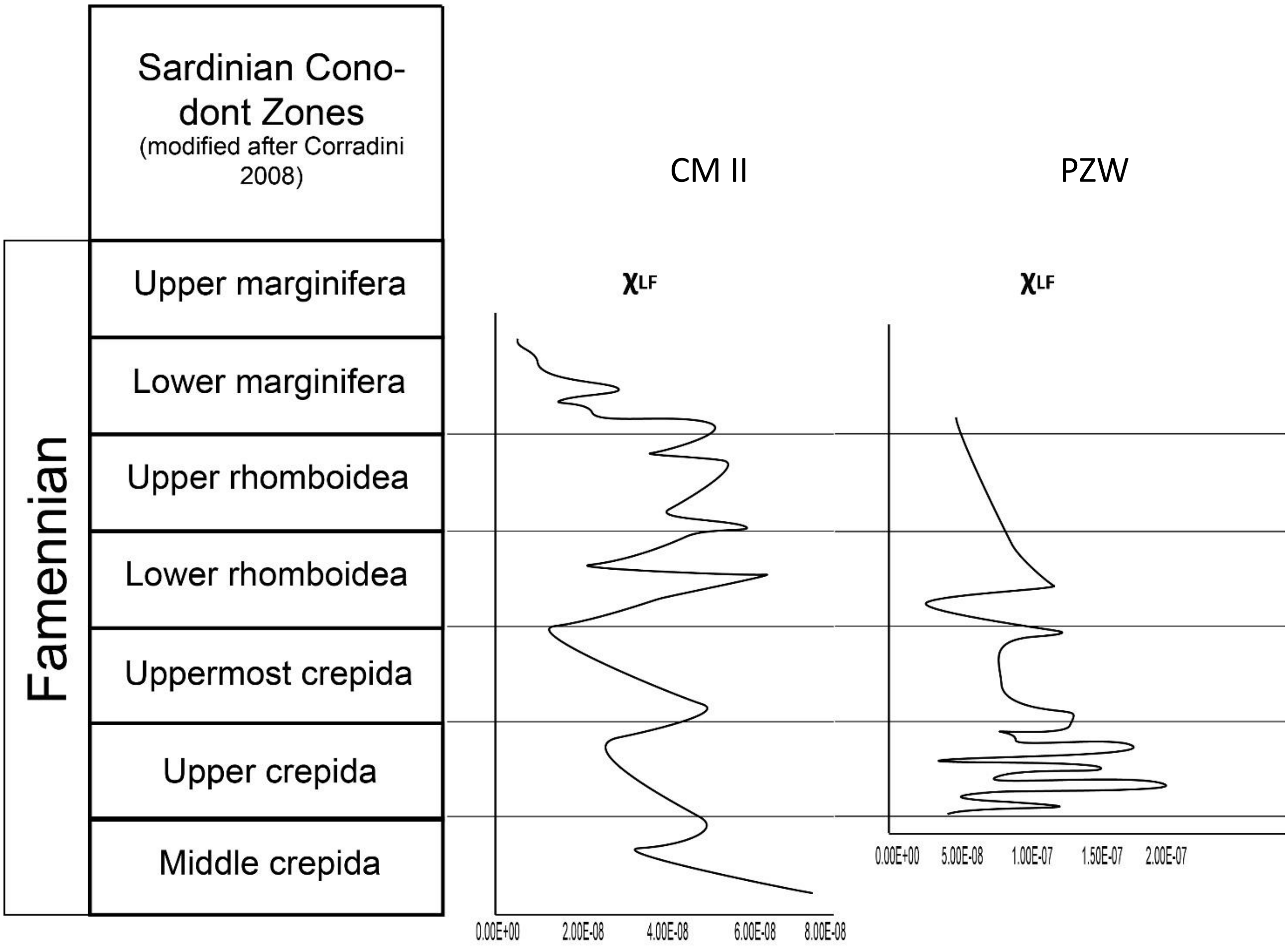

Figure 5.6. Comparison between the magnetic susceptibility curve of the Corona Mizziu II (CM II) and Pizzul West (PZW) sections. The curve represent the mean value of the original MS curve and due to the difference in thickness has been interpolated to fix the signal to the same biozone for both sections.

The palaeogeography of the areas involved in the Varisican orogeny during the Devonian has been widely studied using multydiscipinary approach by different authors. The Carnic Alps and the Sardinia-Corsica microplate are considered to be part of the Galatian Terrane detached from Nord Gondwana in the Lower Devonian (Von Raumer & Stampfli 2008). However, the relative position of the two areas during the Famennian has not yet been estabilished with certainty.

The paleogeography reconstructions of the Galatian terrane (fig 5.7) show a position for the Sardinia-Corsica microplate much closer to the land than the Carnic Alps. Thus, the percentage of terrigenous should be higher in the Sardinia than in the Carnic Alps. However, the low field magnetic susceptibility measured for this work shows higher values for the PZW section (and thus for the Carnic Alps) than that measured in the CM II section (Sardinia). The higher terrigenous percentage in the PZW section is marked also in the major elements geochemistry (tab 5.1).

	Al_2O_3	SiO_2	Fe_2O_3	TiO_2	K_2O
CM II	1.64	4.91	0.098	0.086	0.70
PZW	3.59	12.24	4.24	0.28	0.99

Table 5.1. Mean values of the major elements in the PZW and CM II sections.

In addition, while the Devonian of Sardinia is represented only by pelagic sediments, in the Carnic Alps the basin started to differentiate in the early Devonian, from proximal to pelagic domains.

The higher values of low field magnetic susceptibility and the general high values for Al, Si, Ti, K in the PZW section can be considered an index of a major sedimentary influx in the Carnic Alps. This could be explained by a minor distance from the source. This could lead to the hypothesis that during the Devonian the Carnic Alps were probably located geographically closer to the land than the Sardinia-Corsica microplate.

However, further analysis will be performed in the future to verify the grain size of the magnetic particles, an eventual bigger grain size for the PZW section could evaluate this hypothesis.

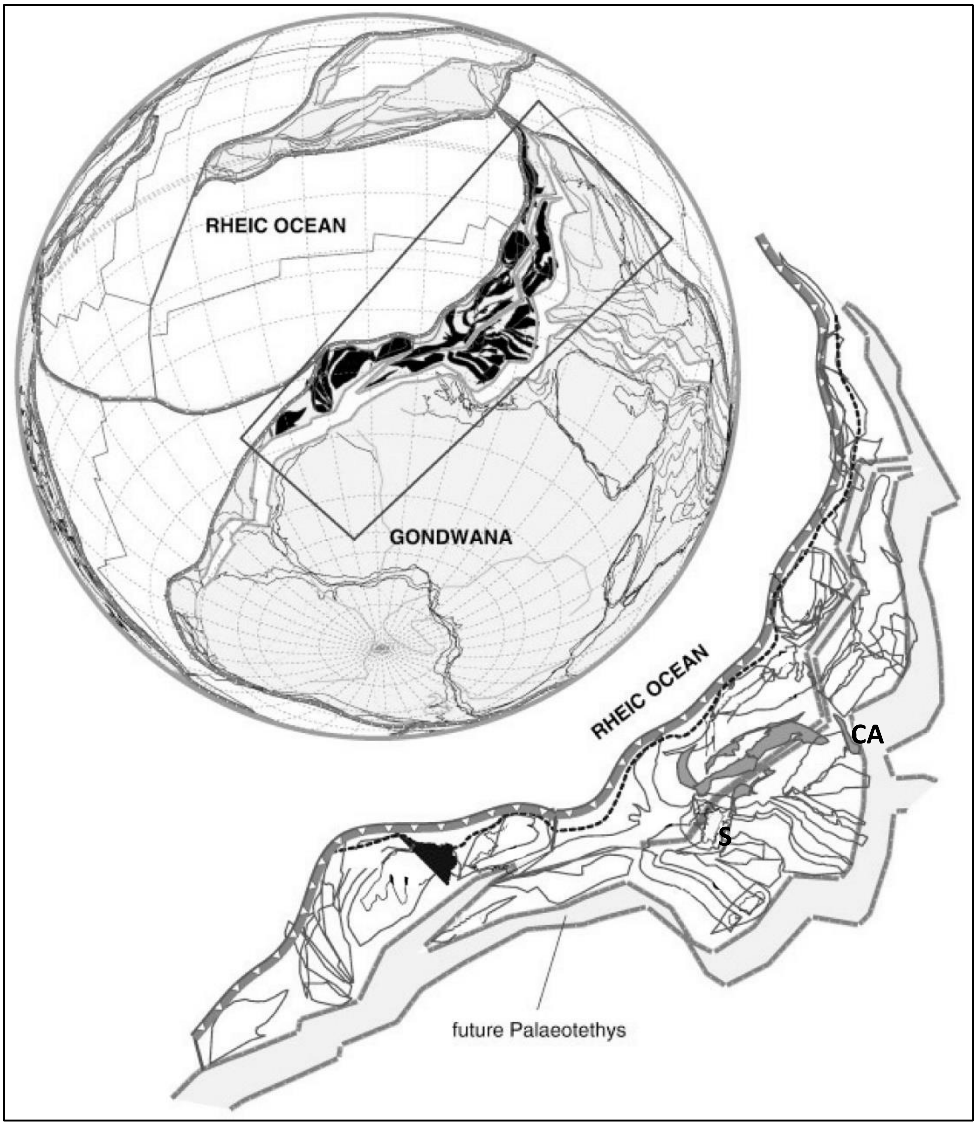

Figure 5.7.Global tectonic situation in the Lower Devonian. Detail of the Galatian Terrane assemblage. S=Sardinia. CA=Carnic Alps. (Von Raumer & Stampfli 2008, modified)

Annulata Event – Comparation between PB and CM I sections.

The Lower and Upper Annulata events (Becker 1993b) have been investigated in the Pramosio Bassa (PB) and Corona Mizziu I (CM I) sections. These two sections span a time from the Middle to the Upper Famennian.

The Annulata event has been described as a radiation event occurred in the Lower and Upper *trachytera* Zones (Middle Famennian)and sometimes evidenced by two levels of black shales.

This ammonoid radiation has been registered in the PB and in the CM I sections. The presence of a rich ammonoid bed in the Upper *trachytera* Zone, marking the Upper Annulata event has been recognized in the outcrops. Whereas, there is no sign of the Lower Annulata event in the field.

The Lower Annulata event (LA) has been described within the Lower *trachytera* Zone (Hartenfels 2011), and it is not here clearly represented as the Upper Annulata. In the CM I section the low field magnetic susceptibility (χ_{LF}) show a negative shift of the magnetic curve starting from the Uppermost *marginifera* Zone (*velifer*). This could probably be due to a poor detrital influx during the initial phase of the transgression that caused the Annulata event. The PB section does not contain the event, likely because the section starts in the upper part of the Lower *trachytera* Zone and part of the latter could be missing due to the presence of a tectonic contact.

The Upper Annulata event (UA) is marked in the CM I section by low values of χ_{LF} with a sharp shift in the magnetic signal within the upper part of the Upper *trachytera* Zone toward high values. The shift is marked also by the evolution of the major element geochemistry. This is probably due to a successive regression after the UA event. The PB section shows a signal controlled mainly by ferromagnetic minerals and the UA transgression is expressed between the first peak (Sample PB 2) and the second peak that coincides with the ammonoid radiation.

In the CM I section it is clearly expressed another peak, both in magnetic susceptibility and in the major elements. This peak, registered immediately before the Middle *expansa* Zone, could be related to the transgression that caused the Dasberg crisis.

The low field magnetic susceptibility data in the CM I section show a general increasing trend from the Uppermost *marginifera* Zone to the *expansa* Zone (fig 5.8), where tends to become more constant. However, the *trachytera* Zone is interested by a small, but evident, shift of the curve towards lower values. The PB section show an analogous pattern: in the lower part of the section, after a major peak the χ_{LF} decrease, then a small but constant increase in the upper part of the section, toward the *postera* Zone can be seen in the χ_{LF} curve.

The of low field magnetic susceptibility values are generally low for the whole *trachytera* Zone in both sections, thus a scarce sedimentary influx during the deposition of the limestones of this Zone can be assumed. This could be an evidence that the transgression considered as the cause of the Annulata event, has been registered both in Sardinia and in the Carnic Alps.

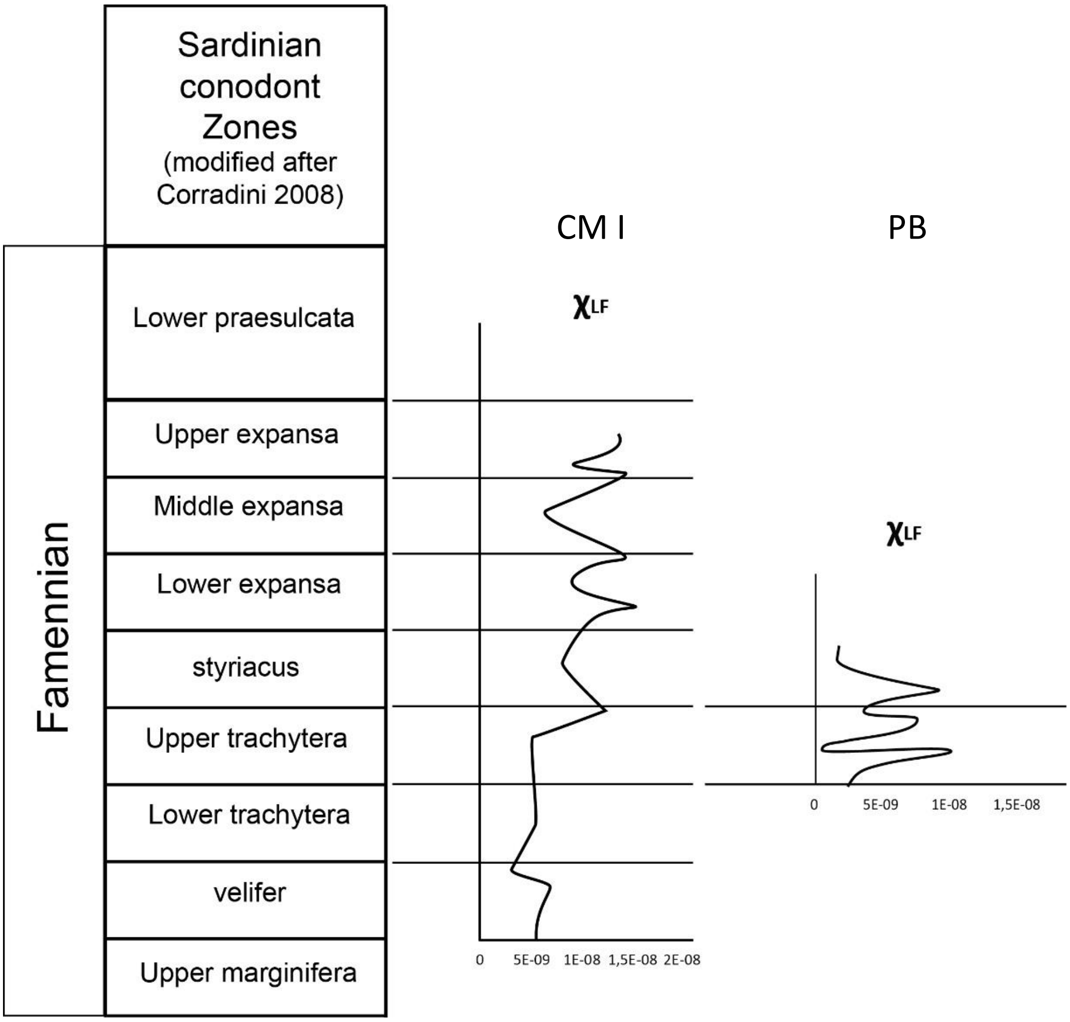

Figure 5.8. Comparison between the magnetic susceptibility curve of the Corona Mizziu I (CM I) and Pramosio Bassa (PB) sections. The curve represent the mean value of the original MS curve and due to the difference in thickness has been interpolated to fix the signal to the same biozone for both sections.

Hangenberg Event – Comparation between MT and BTE sections

The Hangenberg event have been investigated in the MT (Monte Taccu) and in the BTE (Bruncu Bullai) sections. The Devonian/Carboniferous boundary has been documented in Sardinia only in these two sections. The succession starts in the upper Famennian and is represented by a grey massive limestone followed by a thin level of black shales. The latter can be considered as time-equivalent to the Hangenberg event. The conodont fauna date the youngest Fammenian bed to the Lower *praesulcata* Zone. The Tournaisian, as the Famennian, is represented in both section by the same pelagic limestone, with a slightly increase in fossil remains in the younger strata. The differences start in the Tournaisian, in fact while in the BTE section the first stratum has been dated to the *sulcata* Zone (fig 4.12), the first Carboniferous bed for the MT belong to the Lower *duplicata* Zone, and the *sulcata* Zone is missing (fig 4.20). The Lower *duplicata* Zone has been recognized in the MT section for the presence of just one specimen of the marker *Siphonodella duplicata* (Corradini et al. 2003, Mossoni et al. 2013b).

The low field magnetic susceptibility (χ_{LF}) measures show a similar curve for the two sections, the comparison of the curves is good. During the Upper Famennian the curve is constant and no major fluctuations are present. During the Tournaisian instead, there is a change in the magnetic behaviour, in fact it is not constant and the values of magnetic susceptibility are higher than below the D/C boundary. In addition, the curves of the two sections show a similar pattern, made up of two major peaks with a minor one in-between. Geochemical data of the BTE section give a good correlation with the χ_{LF}.

It should be pointed out that the magnetic susceptibility is in slightly contrast with the eustatic cycle proposed to describe the Hangenberg crisis (Kaiser 2005). The lowstand system tract that led to the deposition of sandstones in several regions of North Gondwana and Germany in the latest Famennian, is not marked in the sections with an increase in the susceptibility values. However, the biostratigraphic data of the BTE section show a faunal turnover in an impoverished fauna within the deposition of the limestones of the Lower *praesulcata* Zone (samples BTE 6C-7). This could coincide with the widespread regression described in several regions by Kaiser (2005). Thus, the peculiar conodont data of the latest Famennian in Bruncu Bullai section could be the evidence that the "Hangenberg crisis" might already be started within the Lower *praesulcata* Zone.

The transgressive system track of the initial Tournaisian has been described as a time where the carbon platforms were not completely restored immediately after the Hangenberg event. The fluctuations in the low field magnetic susceptibility of both Sardinian sections could be an evidence of this instability in the oceanic domain during the lowermost Carboniferous.

As already pointed out by Corradini (2007) the Middle *praesulcata* Zone cannot be recognized in Sardinia, because the marker is missing and is considered rare in other European regions (Kaiser et al. 2008). The lack of the Upper *praesulcata* Zone is not marked in the field by the presence of a disconformity. Thus, it can be hypothesized a moment of non-deposition immediately after the transgressive system track that led to the deposition of the shales in the latest Famennian of Sardinia. As mentioned before in the text, the presence of the marker *Siphonodella duplicata* is scarce in the lower part of the Lower *duplicata* Zone of Sardinia. Considering this, and the given correlation of the low field magnetic susceptibility signal between the Monte Taccu and the Bruncu Bullai sections (fig 5.9), a slightly younger age for the first limestone bed above the Hangenberg shales equivalent could be hypothesized for the Bruncu Bullai section. It should be remarked also that the conodont fauna of sample BTE 8 could not exclude a Lower *duplicata* Zone. Thus, the range of the Lower *duplicata* Zone in the Bruncu Bullai section could be extended below, reaching the black shales, excluding the *sulcata* Zone.

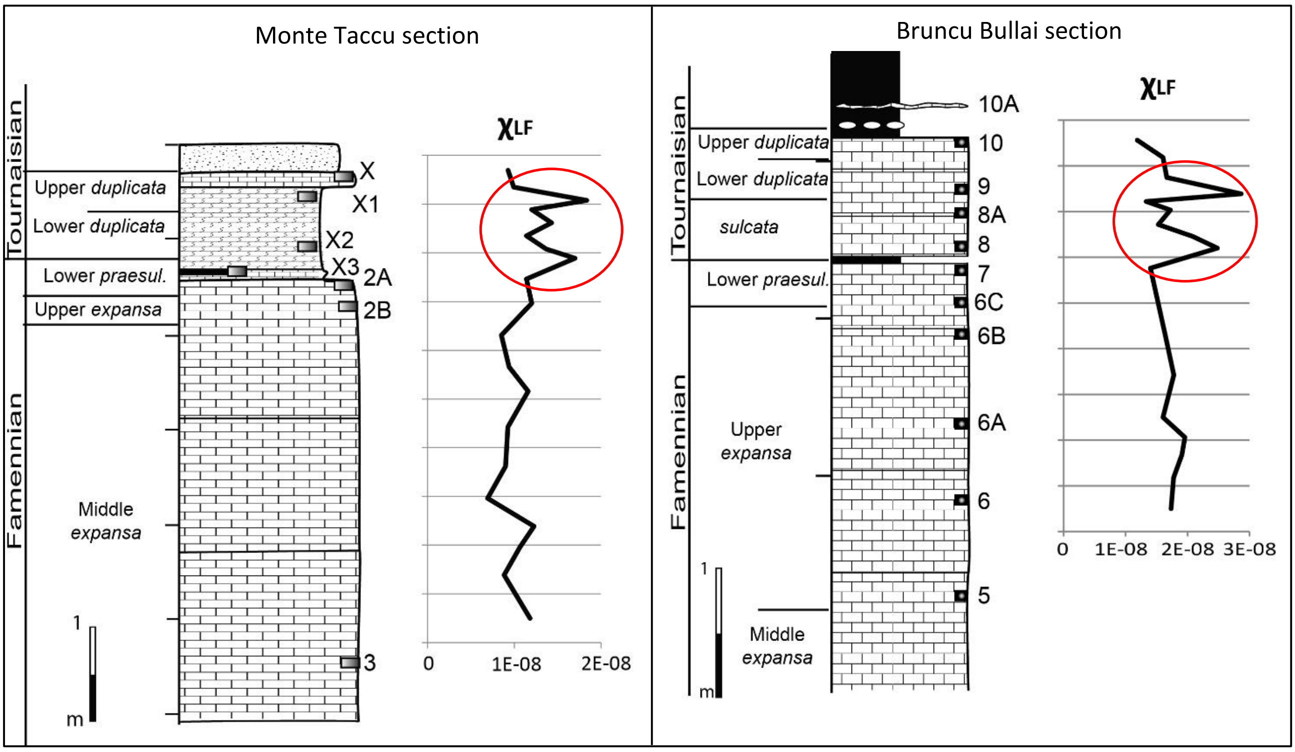

Figure 5.9. Correlation between the Low field magnetic susceptibility (χ_{LF}) of the Monte Taccu and the Bruncu Bullai sections.

Comments on the magnetic susceptibility

The low field magnetic susceptibility (χ_{LF}) has been considered by many authors a useful tool for the correlation of sedimentary strata (Crick et al. 1994, 1997, Ellewood et al. 2000).

One of the aim of this work was to verify the value of the MS as a tool to correlate section in pelagic domain. However, the magnetic susceptibility data provided here appear to be slightly in contrast with the literature.

The low field magnetic susceptibility curves from the Sardinian sections in which the D/C boundary is exposed (Monte Taccu and Bruncu Bullai) give a good correlation between the two sections. Both magnetic curves show a constant trend in the Famennian and a similar pattern in the Tournaisian: a small peak between two major peaks (fig 5.9).

The correlation between low field magnetic susceptibility data from pelagic limestone of the same age in Sardinia and in the Carnic Alps (CM I-PB and CM II-PZW) is not given. Even considering the differences in values that could be due to the influence of local factors, the resulting curve from sections of the same age does not give here a correlation (figs 5.6, 5.8).

Given the correlation in the two Sardinian sections, the use of the low field magnetic susceptibility as a tool to correlate pelagic section within the same basin seem to have been confirmed. However, the data provided by sections of the same age from different areas (Sardinia and Carnic Alps) show no correlation. Therefore, the use of the low field magnetic susceptibility in pelagic sections from different areas should be considered questionable.

Further analysis will be necessary to verify if the poor correlation is due to local differences between Sardinia and Carnic Alps or if the value of the method in domain with poor sedimentary influx is not valid.

The main results of this work can be resumed as follows:

- The biostratigraphic study in the six selected sections of Sardinia and Carnic Alps (Corona Mizziu I, Corona Mizziu II, Monte Taccu, Bruncu Bullai, Pizzul West, Pramosio Bassa) gave more than 28 000 conodonts belonging to 101 taxa between species and subspecies, included in twelve genera (*Ancyrodella*, *Alternognathus*, *Branmehla*, *Bispathodus*, *Icriodus*, *Mehlina*, *Palmatolepis*, *Polygnathus*, *Protognathodus*, *Pseudopolygnathus*, *Scaphignathus* and *Siphonodella*). All of these taxa have been studied and described in the systematic chapter.

  The conodont fauna recovered from the six sections allow to discriminate ten conodont Zones from the Upper *rhenana* Zone (Frasnian) to the Lower *expansa* Zone (Famennian) in the Carnic Alps, and nineteen conodont Zones from the Lower *crepida* Zone (Famennian) to the Upper *duplicata* Zone (Tournaisian) in Sardinia. In addition, the presence of the *sulcata* Zone have been reported for the first time in Sardinia (Bruncu Bullai section) and the Sardinia Conodont Zonation (Corradini 2007) have been updated.

  One new specimen of Pseudopolygnathus (*Ps. granulobathus,* Mossoni et al. 2015) and two specimens of *Polygnathus* (*Po. bicristatus* Mossoni et al. 2015, *Po. nuragicus* Mossoni et al. 2015) have been described and illustrated, while the range of *Polygnathus communis renatae* Corradini & Spalletta (in Corradini et al. 2003) has been extended up to the Lower *duplicata* Zone (Mossoni et al. 2015).

  The following specimens have been reported for the first time in the Carnic Alps (Pizzul West section): *Icriodus olivierii* Corradini 2003, *Palmatolepis lyaiolensis* Ji & Ziegler 1993, *Palmatolepis simpla* Ziegler & Sandberg 1990, *Pseudopolygnathus irregularis* Traghelen & Hartenfels 2011, *Polygnathus mirificus* Ji & Ziegler 1993.

- As for regional geology of Sardinia, the presence of black shales with siliceous nodules above the "Clymeniae Limestones" is documented from the Bruncu Bullai section. According to field observations, this level is tentatively considered as Tournaisian and related to the Lower Alum Shale event; however, more data are necessary for precisely date the strata. The presence of palynological data could confirm this hypothesis and a sample collected from the silica nodules layer is currently under investigation.

- The magnetic susceptibility data of six sections from the two areas gave values that are comparable with the standard value proposed for the carbonate rocks. A higher mean value of MS has been measured from the middle Famennian rocks, while a decrease of the mean value is observed in the sections younger in age. The presence of a general decrease of the sedimentary input, due probably to a climate cooling correlate to a glaciation in the southern hemisphere is here proposed to justify the difference in values of low field magnetic susceptibility. In addition, the correlation of the magnetic curve is given only in the sections of the same area (Monte Taccu and Bruncu Bullai). As for the other section, even considering that the investigated events have been recognized, the general magnetic curves of section from different areas (Corona Mizziu II-Pizzul West and CM I-Pramosio Bassa) are way too different to be considered correlable. Thus, while the use of the magnetic susceptibility as a tool to correlate sections for the Famennian-Tournaisian within the same basin is here confirmed, the use of it to correlate sections of the same age from different areas need further data in order to be considered valid.

- A new hypothesis for the relative palaeogeography of the areas of this work is here provided: the detrital input in the Carnic Alps is higher than the Sardinia, thus a close distance to the land is here hypothesize for the Carnic Alps.
- The “Lower Condroz regressive pulse” have been recognized in the two sections of Sardinia and Carnic Alps. A distinctive peak within the Lower *rhomboidea* Zone in The CM II and PZW magnetic curve could be related to the regressive event. The “Upper Condroz regressive pulse”(UC) has not been registered in the PZW section, while the MS in the Upper *rhomboidea* Zone of the CM II section shows high frequency fluctuation that could be related to the UC.
- The Annulata event has been recognized in the CM I (Sardinia) and in the PB sections (Carnic Alps). The Upper Annulata event is recognizable in the field because of the presence of a rich ammonoid bed .In addition, the low field magnetic susceptibility curve shows a distinctive peak within the Upper *trachytera* Zone. In general, a decrease in the MS value is evident during the whole *trachytera* Zone. The terrigenous percentage marked by the major element geochemistry shows low values in the same zone. A scarce detrital influx during the transgression of the "Annulata Event" is here proposed as a possible cause.
- The Hangenberg event has been investigated in the only two sections of Sardinia that expose the Devonian/Carboniferous boundary. However, the event has not been registered in the MT and BTE sections because the CKI (*costatus-kockeli* interregnum) and the Upper *praesulcata* Zone are missing. Since there is no evidence in the field of the effect of tectonism, this could be probably due to a sedimentary hiatus. The impoverished fauna of the Lower *praesulcata* Zone and an evident faunal tournover in samples BTE 6C-7 of the Bruncu Bullai section can be considered as a peculiarity for the upper part of the Famennian, this could be the evidence that the Hangenberg crisis was already started within the Lower *praesulcata* Zone.

SISTEMATIC

The conodont collection is housed in the Museum of Palaeontology "Domenico Lovisato" of Cagliari University (MDLCA), and in the Earth Sciences Department, University of Modena and Reggio Emilia (IPUM). The catalog numbers of figured elements can be obtained from the plate caption.
Taxonomy is focused on P1 element only. For suprageneric classification, a scheme proposed by Dzik (1988) modified is followed.

Phylum Chordata Bateson, 1886
Class Conodonta Pander, 1856
Order Ozarkodinida Dzik, 1976
Family Cavusgnathidae Austin & Rhodes, 1981

Type species: *Scaphignathus velifera* Helms, 1959.

Scaphignathus velifer velifer Helms, 1959
(Pl. 3, fig. 14)

1959	*Scaphignathus velifera* Ziegler - Helms, p. 655, pl. 2, figs. 19, pl. 5, figs. 20, 28.
1970	*Scaphignathus velifer* Helms *ex* Ziegler ms - Olivieri, p. 138, pl. 23, figs. 6-7.
1971	*Scaphignathus velifer* Helms - Beinert *et al*., p. 83, pl. 2, figs. 1-6, 8-9, 11 *(cum syn.*).
1984	*Scaphignathus velifer velifer* Helms - Ziegler & Sandberg, p. 188.
2003	*Scaphignathus velifer velifer* Helms - Corradini, pl. 10, fig. 7.
2013b	*Scaphignathus velifer velifer* Helms - Mossoni et al., fig. 3.14.

Remarks: According with Ziegler & Sandberg (1984), representatives of *Scaphignathus velifer velifer* have a predominantly right blade, but rare specimens may have a central blade. All the studied specimens have a right blade and a well developed trough in the anterior part of the platform. A few specimens are so narrow to resemble *Sc. vel. leptus*, but the presence of the trough allow to assign them to *Scaphignathus vel. velifer*.

Range: From the base of the Uppermost *marginifera* Zone to the Upper *trachytera* Zone (Ziegler & Sandberg, 1984).

Studied material: 27specimens from sections CM I, CM II and MT.

Scaphignathus velifer leptus Ziegler & Sandberg, 1984

(Pl. 5, figs. 10-11)

1984 *Scaphignathus velifer leptus* Ziegler & Sandberg p. 188, pl. 2, figs. 9-10 *(cum syn.*).

2003 *Scaphignathus velifer leptus* Ziegler & Sandberg - Corradini, pl. 10, fig. 8-9.

Remarks: According with Ziegler & Sandberg (1984), representatives of *Scaphignathus velifer leptus* have a very narrow platform ornamented with transverged ridges. The anterior blade is usually very high and located on the right side of the platform. It differs from *Scaphignathus velifer velifer* that present a broader platform and trough in the anterior part of the platform.

Range: From the base of the Uppermost *marginifera* Zone to the Upper *postera* Zone (Ziegler & Sandberg, 1984).

Studied material: 15 specimens from sections CM I.

Family Elictognathidae Austin & Rhodes, 1981

Genus *Alternognathus* Ziegler & Sandberg, 1984

Type species: *Alternognathus regularis* Ziegler & Sandberg, 1984.

Alternognathus regularis Ziegler & Sandberg, 1984

(Pl. 3, fig. 15)

1971 *Scaphignathus subserratus* (Branson & Mehl) - Beinert *et al*., p. 82, pl. 1, figs. 1-9, 11, 12.

1984 *Alternognathus regularis* n.sp. Ziegler & Sandberg, p. 188-189 *(cum syn*.).

2013b *Alternognathus regularis* Ziegler & Sandberg – Mossoni et al., fig. 3.15.

Remarks: This species of *Alternognathus* is characterized by a lanceolate symmetrical platform with a pronounced ornamentation made up of elongated nodes or ridges, sometimes there is a depression at the anterior end of the platform. The original diagnosis (Ziegler & Sandberg, 1984) discriminate

Alternognathus regularis from *Alt. beulensis* for the symmetry of the platform and because of the different ornamentation made up of nodes instead of ridges. However since the specimens in the synonymy of Ziegler & Sandberg (1984) shows a big variability in the ornamentation and is common to have some specimens with a symmetrical platform ornamented with ridges. It is consider diagnostic to discriminate the two subspecies of *Alternognathus* only the shape of the platform.
A. regularis differs from *A. beulensis* by the symmetrical shape of the platform with the anterior margins joining the blade in opposite position.

Range: From the *velifer* Zone to the Upper *postera* Zone (Ziegler & Sandberg, 1984).

Studied material: 97 elements from CM I, CM II and PB sections.

Alternognathus beulensis Ziegler & Sandberg, 1984

(Pl. 4, fig. 4)

1971 *Scaphignathus subserratus* (Branson & Mehl) - Beinert *et al*., p. 82, pl. 1, figs. 1-9, 11, 12.
1984 *Alternognathus beulensis* n.sp. Ziegler & Sandberg, p. 188-189, pl. 10, figs. 15-17.
1990 *Alternognathus beulensis* Ziegler & Sandberg – Perri & Spalletta, p. 59, pl. 1, fig. 1.
1991 *Alternognathus beulensis* Ziegler & Sandberg – Perri & Spalletta, p. 54, pl. 1, fig. 1.

Remarks: *Alternognathus beulensis* is characterized by a lanceolate platform tipped posteriorly, and ornamented with ridges. *Alt. beulensis* differs from *Alt. regularis* by the symmetrical shape of the platform and because of the ornamentation of the platform made up of ridges instead of nodes.

Range: From the *velifer* Zone to the Upper *postera* Zone (Ziegler & Sandberg, 1984).

Studied material: 63 elements from MT and PB sections.

Genus *Siphonodella* Branson & Mehl, 1944

1934b *Siphonognathus* Branson & Mehl (*non* Richardson 1858*, fide* Branson & Mehl 1948: 528).
1944 *Siphonodella* Branson & Mehl, in Shimer & Shrock: 245.

Type species: *Siphonognathus duplicata* Branson & Mehl 1934.

Siphonodella carinthiaca Schönlaub, 1969

(Pl. 7, fig. 18)

1969 *Siphonodella carinthiaca* n. sp. Schönlaub, p. 342-343; pl. 2, figs 1-3.

1973 *Siphonodella carinthiaca* Schönlaub – Klapper (*in* Ziegler), p. 453, pl. *Siphonodella*-1, fig. 1 (*cum syn.*).

1978 *Siphonodella carinthiaca* Schönlaub – Sandberg et al., p. 109, text-fig. 1.

1989 *Siphonodella carinthiaca* Schönlaub – Ji *et al*., p.95, pl. 15, figs 7-9.

1993 *Siphonodella carinthiaca* Schönlaub – Ji & Ziegler, pl. 41, figs 16-17.

2003 *Siphonodella carinthiaca* Schönlaub – Corradini et al., pl. 1, fig. 6.

2015 *Siphonodella carinthiaca* Schönlaub – Mossoni et al., fig. 7R

Remarks: Two main characteristics allow the discrimination of *Siphonodella carinthiaca* from all the other species of *Siphonodella*: the inner part of the platform is raised above the carina, and the transverse ridges of the outer platform that continues across the carina.

Range: From the Upper *duplicata* Zone to the top of the *sandbergi* Zone (Sandberg *et al*. 1978)

Studied material: 5 elements from BTE and MT sections.

Siphonodella cooperi Hass, 1959

(Pl. 7, fig. 19)

1959 *Siphonodella cooperi* n. sp. Hass, p. 392, Pl. 48, Fig. 35-36.

1975 *Siphonodella cooperi* Hass – Klapper (*in* Ziegler), p. 345-348, pl. *Siphonodella*-2, figs 4-5 (*cum syn*.).

1978 *Siphonodella cooperi* Hass, Morphotype 1 – Sandberg et al.: 107, fig. 1.

1978 *Siphonodella cooperi* Hass, Morphotype 2 – Sandberg et al.: 108, text-fig. 1.

1989 *Siphonodella cooperi* Hass, Morphotype 2 – Ji et al.: 95, pl. 15, figs 1-4.

1992 *Siphonodella cooperi* Hass, Morphotype 2 – Over, fig. 5.5.

1993 *Siphonodella cooperi* Hass, Morphotype 2 – Ji & Ziegler, pl. 42, figs 1-2.

2003 *Siphonodella cooperi* Hass, Morphotype 1 – Corradini et al., pl. 1, figs. 2-3.

2003 *Siphonodella cooperi* Hass, Morphotype 2 – Corradini et al., pl. 1, fig. 5.

2015 *Siphonodella cooperi* Hass – Mossoni et al., fig. 7R.

Remarks: Two morphotypes of *Siphonodella cooperi* were discriminated by Sandberg *et al.* (1978). M1 is characterized by transverse ridges on the outer side of the platform, and nodes on the inner side. The rostral ridges extend to the posterior tip as thickened rims along both platform margins. Nodes on the inner side and strong transverse ridges on the outer side of the platform characterize the ornamentation of *Siphonodella cooperi* M2. In this morphotype the inner rostral ridge ends in the anterior part of the platform; the outer one extends to the platform margin and may continue almost to the posterior tip as a raised margin. M2 includes elements showing a third rostral ridge on the inner side of the platform and an incipient rostral ridge on the inner side. The elements here assigned to M2 are mostly small. There are two rostral ridges, one ending a short distance within the anterior part of the inner part of the platform, the other reaching the outer anterior margin at about midlength of the platform.

Range: *Siphonodella cooperi* M1 ranges from the base of the Upper *duplicata* Zone to the *sandbergi* Zone; M2 from within the Upper *duplicata* Zone to the Upper *crenulata* Zone (Sandberg *et al*. 1978)

Studied material: M1-> 4 elements from BTE and MT sections; M2-> 1 elements from MT section.

Siphonodella bransoni Ji, 1985
(Pl. 4, fig. 15)

1934b *Siphonognathus duplicata* n. sp. Branson & Mehl, p. 296-297, pl. 24, figs 16-17.

1975 *Siphonodella duplicata* (Branson & Mehl) – Klapper (*in* Ziegler), p. 349-352, pl. *Siphonodella*-2, fig. 6 (*cum syn.*).

1978 *Siphonodella duplicata* (Branson & Mehl), Morphotype 1 – Sandberg et al.: 105, text-fig. 1.

1984 *Siphonodella duplicata* (Branson & Mehl), Morphotype 1 – Hou et al., pl. 3, figs. 1-2, 4.

1985 *Siphonodella bransoni* n. sp. Ji, p. 53, fig. 2.

1989 *Siphonodella duplicata* (Branson & Mehl), Morphotype 1 – Ji et al, p..87, pl. 10, figs. 1-7.

1993 *Siphonodella duplicata* (Branson & Mehl), Morphotype 1 – Ji & Ziegler*,* p 233, pl. 42, figs. 15-17.

2003 *Siphonodella duplicata* (Branson & Mehl), Morphotype 1 – Corradini et al., p 233, pl. 1, fig. 7.

<u>Remarks</u>: *Siphonodella bransoni* is characterized by an asymmetrical platform ornamented with strong transverse ridges on both sides of the platform. A well-developed rostrum is always present in the platform.The lower side presents a wide pseudokeel.

<u>Range</u>: From the lower part of the Lower *duplicata* Zone to the *sandbergi* Zone (Sandberg *et al*. 1978). *Siphonodella bransoni* is the index taxon for the *bransoni* Zone (Ji et al. 1987, Kaiser et al. 2009).

<u>Studied material</u>: 22 elements from BTE and MT sections.

Siphonodella duplicata (Branson & Mehl, 1934b)

(Pl. 7, figs. 16-17)

1934 *Siphonognathus duplicata* n. sp. Branson & Mehl, p. 296-297, pl. 24, figs. 16-17.
1975 *Siphonodella duplicata* (Branson & Mehl) – Klapper (*in* Ziegler), p. 349-352, pl. *Siphonodella*-2, fig. 6 (*cum syn.*).
1993 *Siphonodella duplicata* (Branson & Mehl), Morphotype 2 – Ji & Ziegler*,* p 233, pl. 42, figs. 13-14.
2015 *Siphonodella duplicata* (Branson & Mehl) – Mossoni et al., figs. 7P-7Q.

<u>Remarks</u>: This species of *Siphonodella* is characterized by a slightly asymmetrical platform, ornamented with ridges on both sides. Two rostral ridges usually form margins of a well-developed rostrum. *Siphonodella duplicata* is distinguished from *Siphonodella bransoni* because the lower surface has a keel instead of a pseudokeel. It differs from *Si. sulcata* because of the presence of the developed rostrum.

<u>Range</u>: From within the Lower *duplicata* Zone to the *sandbergi* Zone (Sandberg *et al*. 1978). *Siphonodella duplicata* is the index taxon for the *duplicata* Zone (Kaiser et al. 2009).

<u>Studied material</u>: 6 elements from BTE section.

Siphonodella hassi Ji, 1985

(Pl. 4, fig. 13)

1959 *Siphonodella duplicata* (Branson & Mehl) – Hass, pl. 49, figs 17-18 (only).

1978 *Siphonodella duplicata* sensu Hass – Sandberg et al., p. 107-108, text-fig. 1.

1985 *Siphonodella hassi* – Ji, p. 59, fig 14.

1993 *Siphonodella duplicata* sensu Hass – Ji & Ziegler, pl. 42, figs 6-9.

2003 *Siphonodella duplicata* sensu Hass – Corradini et al., pl. 1, fig. 4.

2009 *Siphonodella hassi* Ji – Kaiser et al., p. 127, pl. 2, fig. 6.

Remarks: According Sandberg *et al.* (1978), elements assigned to *Siphonodella hassi* are characterized by short and convergent rostral ridges. The ornamentation is made up of transverse ridges on the outer side of the platform and nodes on the inner side. It differs from *Si. duplicata* by having random nodes on the inner side and more convergent rostral ridges.

Range: *Siphonodella hassi* ranges from the base of the Upper *duplicata* Zone into the *crenulata* Zone (Sandberg *et al*. 1978).

Studied material: 3 elements from MT section.

Siphonodella praesulcata Sandberg, 1972
(Pl. 4, fig. 14, Pl. 5, figs. 19-21)

1972 *Siphonodella praesulcata* n. sp. Sandberg (*in* Sandberg *et al*.), p. 190, pl. 1, figs 1-17; pl. 2, figs. 10-19.

1975 *Siphonodella praesulcata* Sandberg – Klapper (*in* Ziegler), p. 355-356, pl. *Siphonodella*-2, fig. 1 (*cum syn*.).

1984 *Siphonodella praesulcata* Sandberg – Hou et al., pl. 1, figs. 1-10.

1987 *Siphonodella praesulcata* Sandberg – Kalvoda & Kukal, pl. 5, fig. 6.

1988 *Siphonodella praesulcata* Sandberg – Flajs & Feist, p. 68, pl. 5, figs 1-4, 8-14; pl. 6, figs. 1-12; pl. 7, figs 1-10.

1989 *Siphonodella praesulcata* Sandberg –Ji et al., p. 99-100, pl. 8, figs 4-9.

1992 *Siphonodella praesulcata* Sandberg – Over, fig. 7.1.

1993 *Siphonodella praesulcata* Sandberg – Ji & Ziegler, pl. 43, figs 8-10.

1998 *Siphonodella praesulcata* Sandberg – Corradini, pl. 1.4.2, fig. 5.

1998 *Siphonodella praesulcata* Sandberg – Spalletta, Perri & Pondrelli, pl. 2.4.1, fig. 4.

2003 *Siphonodella praesulcata* Sandberg – Corradini et al., pl. 1, figs. 8-10.
2009 *Siphonodella praesulcata* Sandberg – Kaiser et al., p. 128, pl. 1, figs. 12-13, 15-16; pl. 2, fig. 4.

Remarks: *Siphonodella praesulcata* differs from *Siphonodella sulcata* in the general shape of the platform: the former possessing a straight to slightly curved carina and pseudokeel; in the latter both are strongly curved. Transitional forms to *Siphonodella sulcata* are also known from the Upper *praesulcata* Zone.

Range: From the base of the Lower *praesulcata* Zone to the *sulcata* Zone (Sandberg *et al*. 1978).

Studied material: 18 elements from BTE, CM I and MT sections.

Siphonodella sulcata (Huddle, 1934)
(Pl. 7, fig. 20)

1934 *Polygnathus sulcata* n. sp. Huddle, pl. 8, figs. 22-23
1975 *Siphonodella sulcata* (Huddle) –Klapper (*in* Ziegler), p. 357-358, pl. *Siphonodella*-2, figs 2-3 (*cum syn*.).
1978 *Siphonodella sulcata* (Huddle) – Sandberg et al., p. 104-105, fig. 1.
1987 *Siphonodella sulcata* (Huddle) – Kalvoda & Kukal, pl. 5, figs. 1-2.
1988 *Siphonodella sulcata* (Huddle) – Flajs & Feist, p. 69, pl. 5, figs. 5-7; pl. 7, fig. 11; pl. 8, figs. 1-10; pl. 9, figs 1-3, 5.
1989 *Siphonodella sulcata* (Huddle) – Ji et al., p. 101-102, pl. 8, figs. 1-3; pl. 9, figs. 1-9; pl.10, fig. 8-9.
1992 *Siphonodella sulcata* (Huddle) – Over, figs. 7.2-7.3
1993 *Siphonodella sulcata* (Huddle) – Ji & Ziegler., pl. 43, figs 1-7.
2003 *Siphonodella sulcata* (Huddle) – Corradini et al., pl. 1, fig. 1.
2009 *Siphonodella sulcata* (Huddle) – Kaiser et al., p. 128, pl. 1, fig. 14; pl. 2, figs. 1-2, 5.
2015 *Siphonodella sulcata* (Huddle) – Mossoni et al., fig. 7T.

Remarks: *Siphonodella sulcata* is characterized by an asymmetrical platform ornamented on both sides by transverse ridges. A narrow groove separates the carina from the ridges. *Siphonodella sulcata* generally lacks a rostrum. In the inferior part of the element there is a characteristic pseudokeel. It is distinguished from *Siphonodella praesulcata* by having a curved carina and a curved pseudokeel. It differs from *Si. bransoni* because the latter has a complete rostrum comprising both sides of the platform.

Range: From the base of the *sulcata* Zone to the Lower *crenulata* Zone (Sandberg *et al*. 1978).

Studied Material: 25 elements from BTE and MT sections.

Family Gnathodontidae Sweet, 1988

Genus *Protognathodus* Ziegler, 1969

Type species*: Gnathodus kockeli* Bischoff, 1957

Protognathodus collinsoni Ziegler, 1969

(Pl. 7, fig. 25)

1969 *Protognathodus collinsoni* n.sp. Ziegler, p. 353-354, pl. 1, figs. 1-13.

1973 *Protognathodus collinsoni* Ziegler – Ziegler (*in* Ziegler), p. 415-416, pl. *Schmidtognathus*-2, fig. 4 (*cum syn*.).

1973 *Protognathodus collinsoni* Ziegler – Szulczewski, p.42-43, pl. 2, figs. 9-10.

1988 *Protognathodus collinsoni* Ziegler – Flajs & Feist, pl. 9, figs. 6-7.

1992 *Protognathodus collinsoni* Ziegler – Over, fig. 7.15.

2011 *Protognathodus collinsoni* Ziegler – Corradini et al., p. 18, pl. 1, figs. 4-8.

2015 *Protognathodus collinsoni* Ziegler – Mossoni et al., fig 7Y.

Remarks: *Protognathodus collinsoni* is characterized by a cup ornamented with few scattered nodes that can occur on both sides. It is distinguished from *Protognathodus meischneri* because the latter has a cup without ornamentation. It differs from *Protognathodus kockeli* because the nodes on the cup are not aligned in rows.

Range: Lower *preasulcata* Zone (Ziegler & Sandberg, 1984) to at least Upper *duplicata* Zone (Over, 1992).

Studied Material: 30 elements from BTE and MT sections.

Protognathodus kockeli (Bischoff, 1957)

(Pl. 7, fig. 24)

1957 *Gnathodus kockeli* n.sp. Bischoff: 25, pl. 3, figs 27-32.

1969 *Protognathodus kockeli* (Bischoff) – Ziegler, p. 354-355, pl. 1, figs 19-20, 23-25; pl. 2, figs 1-5.

1973 *Protognathodus kockeli* (Bischoff) – Szulczewski, p. 43-44, pl. 2, figs 11-13.

1973 *Protognathodus kockeli* (Bischoff) – Ziegler (*in* Ziegler), p. 417-418, pl. *Schmidtognathus*-2, fig. 5 (*cum syn*.).

1988 *Protognathodus kockeli* (Bischoff) – Flajs & Feist, pl. 9, figs 8-10.

1992 *Protognathodus kockeli* (Bischoff) – Over, fig 7.16.

2015 *Protognathodus kockeli* (Bischoff) – Mossoni et al., fig 7X.

Remarks: *Protognathodus kockeli* is characterized by a cup ornamented, on at least one side of the carina, by nodes arranged in a row sub parallel to the carina. When just one side of the carina bear a row of nodes the other half of the cup could bear scattered unarranged nodes. It differs from *Protognathodus collinsoni* because of the presence of the nodes aligned in rows.

Range: From the base of the Upper *praesulcata* Zone (Ziegler & Sandberg 1984) to the Early *crenulata* Zone (Lane *et al*. 1980).

Studied Material: 48 elements from BTE and MT sections.

Protognathodus kuehni Ziegler & Leuteritz, 1970

(Pl. 7, fig. 26)

1962 *Gnathodus* n. sp. B Collinson et al., text-fig. 3.

1969 *Protognathodus* n. sp. A Ziegler p.355, pl. 1, fig. 26.

1970 *Protognathodus kuehni* n.sp. Ziegler & Leuteritz (in Koch et al.), p.715, pl. 8, fig. 4.

1973 *Protognathodus kuehni* Ziegler & Leuteritz – Ziegler (in Ziegler), p. 419-420, *Schmidtognathus* Pl. 2, fig. 6.

1988 *Protognathodus kockeli-Prothognathodus kuehni* – Schönlaub et al., pl. 4, fig. 6.

1988 *Protognathodus praedelicatus* Lane et al. – Schönlaub et al., pl. 4, figs. 8-9.

2007 *Protognathodus kuehni* Ziegler & Leuteritz – Kaiser, pl. 2, figs. 2, 7.

2009 *Protognathodus kuehni* Ziegler & Leuteritz – Kaiser et al., pl. 2, fig. 15 (only).

2011 *Protognathodus kuehni* Ziegler & Leuteritz –Corradini et al., p. 19, pl. 1, figs. 20-22.

2014 *Protognathodus kuehni* Ziegler & Leuteritz – Mossoni et al., fig. 7Z.

Remarks**:** *Protognathodus kuehni* is characterized by an asymmetrical platform, ornamented with robust transverse ridges. In some specimen the carina tend to disappear in the cup. The occurrence of transverse ridges on the cup characterizes *Protognathodus kuehni* and distinguish it from other representatives of the genus. Transitional forms from *Protognathodus kockeli* are known: they bear both transverse ridges and nodes and have a more asymmetrical cup than *Protognathodus kuehni*. In lateral view the carina does not rise above the ornamentation and in some specimens can be suppressed in the posterior part of the cup.

Range: From the base of the *sulcata* Zone (Kaiser et al. 2009) or just below (Ziegler 1973) to within the *sandbergi* Zone (Lane et al. 1980).

Studied Material: 10 elements from the BTE section.

Protognathodus meischneri Ziegler, 1969

(Pl. 7, fig. 23)

1969 *Protognathodus meischneri* n.sp. – Ziegler, p. 353, pl. 1, figs. 14-18.

1973 *Protognathodus meischneri* Ziegler – Ziegler (*in* Ziegler), p. 421-422, pl. *Schmidtognathus*-2, fig. 3 (*cum syn*.).

1973 *Protognathodus meischneri* Ziegler – Szulczewski, p. 43, pl. 2, fig. 8.

1984 *Protognathodus meischneri* Ziegler – Hou *et al*., pl. 4, fig. 9.

1987 *Protognathodus meischneri* Ziegler – Webster *et al*., pl. 1, figs.5-7.

1988 *Protognathodus meischneri* Ziegler – Schönlaub, Feist & Korn, p. 155, pl. 4, figs. 1-2, 5.

1992 *Protognathodus meischneri* Ziegler – Over, fig. 7.14.

2015 *Protognathodus meischneri* Ziegler – Mossoni et al., fig 7W.

Remarks: *Protognathodus* meischneri differs from *Bispathodus stabilis* for the more posterior position and greater expansion of the basal cavity. It is distinguished from all other species of *Protognathodus* by the absence of ornamentation on the upper surface of the cup.

Range: From the base of the Lower *praesulcata* Zone (Ziegler & Sandberg 1984) to the *typicus* Zone (Webster *et al*. 1987).

Studied Material: 13 elements from BTE and MT sections.

Family Palmatolepididae Bassler, 1925

Genus *Palmatolepis* Ulrich & Bassler, 1926

Palmatolepis crepida Sannemann, 1955

(Pl. 1, fig. 18)

1955 *Palmatolepis crepida* n. sp. Sannemann, p.134, pl. 6, fig. 21.
1962 *Palmatolepis crepida crepida* Sannemann – Ziegler, p. 55, pl. 6, figs. 13-19 (no fig.12).
1993 *Palmatolepis crepida* Sannemann – Ji & Ziegler, p. 59, pl. 22, figs. 1-7; text-fig. 13, fig. 4.
2003 *Palmatolepis crepida* Sannemann – Corradini, pl. 3, figs. 7-8.
2013b *Palmatolepis crepida* Sannemann – Mossoni et al., p. 22, fig. 5.18.

Remarks: *Palmatolepis crepida* is characterized by having a drop-shape platform, with a shagreen surface. The inner anterior margin is convex, the outer margin is almost straight. The blade-carina is strongly curved, and the posterior carina is weakly pronounced. The central node is situated in the second half of the element. It is distinguished by *Palmatolepis tenuipunctata* by the lack of the outer lobe.

Range: From the Lower *crepida* Zone to the Lower *rhomboidea* Zone (Ji & Ziegler, 1993).

Studied material: 26 elements from CM I, CM II, PZW sections.

Palmatolepis glabra acuta Helms, 1963

(Pl. 5, fig. 2)

1963 *Palmatolepis (Panderolepis) serrata acuta* n. sp. Helms, p. 468, pl. 3, fig. 1-4,6.
1971 *Palmatolepis glabra acuta* Helms – Szulczewski, p. 33, pl. 14, figs. 6,7.
1990 *Palmatolepis glabra acuta* Helms – Perri & Spalletta, p. 60, pl. 1, figs. 4a-b.

1993 *Palmatolepis glabra acuta* Helms – Ji & Ziegler; pl. 16, figs 11, text-fig. 17, fig. 5.

Remarks: This subspecies of *Palmatolepis glabra* is characterized by a parapet in the inner anterior margin of the platform that ends with a thorn-like projection in the anterior end. The carina is slightly sigmoidal. It is distinguished by *Palmatolepis glabra glabra* by the presence of the thorn-like projection on the inner anterior margin, and by *Palmatolepis glabra distorta* by the lack of a pronounced parapet.

Range: From the upper part of the Lower *rhomboidea* Zone to the base of the Upper *marginifera* Zone (Ji & Ziegler, 1993).

Studied material: 60 elements from CM I, CM II, MT and PZW sections.

Palmatolepis glabra distorta Branson & Mehl, 1934a

(Pl. 4, fig. 6)

1934a *Palmatolepis distorta* Branson & Mehl, p. 237, pl. 18, figs. 13, 14.
1991 *Palmatolepis glabra distorta* Branson & Mehl – Perri & Spalletta, p. 60-61, pl. 1, figs. 5a-6b.
1993 *Palmatolepis glabra distorta* Branson & Mehl – Ji & Ziegler, p. 60, pl. 17, figs. 1-4; text-fig. 17, fig. 8.
2003 *Palmatolepis glabra distorta* Branson & Mehl – Corradini, p. 79, pl. 4, figs. 9-11.
2011 *Palmatolepis glabra distorta* Branson & Mehl – Hartenfels, p. 244-245, pl. 42, figs. 15-16.

Remarks: *Palmatolepis glabra distorta* is characterized by a sigmoidal platform. The inner anterior margin joins the blade at a right angle and has a long parapet that lies close and parallel to the carina. The presence of a boulge in the outer part of the platform distinguish *Palmatolepis glabra distorta* from *Palmatolepis glabra pectinata.*

Range: From the Lower *marginifera* Zone to the Lower *trachytera* Zone (Ji & Ziegler, 2003).

Studied material: 336 elements from CM I, CM II, MT and PB sections.

Palmatolepis glabra glabra Ulrich & Bassler, 1926

(Pl. 1, fig. 15)

1926 *Palmatolepis glabra* n. sp. Ulrich & Bassler, p. 51, pl. 9, fig. 20.

1993 *Palmatolepis glabra glabra* Ulrich & Bassler – Ji & Ziegler, p. 60-61, pl. 17, figs. 13-15; text-fig. 17, fig. 4.

2003 *Palmatolepis glabra glabra* Ulrich & Bassler – Corradini, p. 79, pl. 4, figs. 1-2.

2013b *Palmatolepis glabra glabra* Ulrich & Bassler – Mossoni et al., p. 22, fig. 5.15.

Remarks: *Palmatolepis glabra glabra* is characterized by a narrow and elongated platform. The inner anterior margin joins the blade at a right angle. The carina is slightly sigmoidal. It is distinguished from *Palmatolepis glabra prima* because of the angle of the insertion of the inner anterior margin into the blade, and by *Palmatolepis glabra distorta* by the lack of a pronounced parapet.

Range: From the Lower *rhomboidea* Zone to the Lower *marginifera* Zone (Ji & Ziegler, 2003).

Studied material: 87 elements from CM I, CM II, PZW and MT section.

Palmatolepis glabra lepta Ziegler & Huddle, 1969

(Pl. 4, fig. 16)

1969 *Palmatolepis glabra lepta* n.sub.sp. Ziegler, p. 380-381.

1977 *Palmatolepis glabra lepta* Ziegler & Huddle – Ziegler In Ziegler (ed.), p. 301-303, pl. Palmatolepis-7, figs. 1-3 (cum syn).

1991 *Palmatolepis glabra lepta* Ziegler & Huddle – Perri & Spalletta, p. 61, pl. 1, figs. 7a-8b.

1993 *Palmatolepis glabra lepta* Ziegler & Huddle – Ji & Ziegler, p.61, pl. 19, figs. 11-15; text-fig 17, fig. 3.

2003 *Palmatolepis glabra lepta* Ziegler & Huddle – Corradini et al., pl. 4, figs. 7-8.

Remarks: *Palmatolepis glabra lepta* is characterized by a slender and elongated platform. It has a triangular upwarded parapet in the anterior part of the inner platform. It is distinguished from all the other subspecies of *Palmatolepis glabra* by the inner part of the anterior platform.

Range: From the Upper *crepida* Zone to the Upper *trachytera* Zone (Ji & Ziegler, 1993).

Studied material: 112 elements from CM I, CM II, MT and PB sections.

Palmatolepis glabra pectinata Ziegler, 1962

(Pl. 1, fig. 19, Pl. 4, fig. 1)

1962 *Palmatolepis glabra pectinata* n.sub.sp. Ziegler, p. 398-399, pl. 2, figs.3-5.

1966 *Palmatolepis glabra pectinata* Ziegler – Glenister & Klapper, p. 814, pl. 89, figs. 1-3,5,9,10; pl. 10, figs. 4-5; pl. 91, figs 1,3,5.

1993 *Palmatolepis glabra pectinata* Ziegler – Ji & Ziegler, p.61, pl. 16, figs. 5-10, pl. 17, figs. 1-12; text-fig 17, fig. 7-8.

1998b *Palmatolepis glabra pectinata* Ziegler - Perri & Spalletta, p. 156, pl. 1.3.1, figs. 1-2.

2013b *Palmatolepis glabra pectinata* Ziegler – Mossoni et al., p. 22, fig. 5.19.

Remarks: This subpecies of *Palmatolepis glabra* is distinguished from *Pa. glabra prima* and *Palmatolepis glabra glabra* having a long parapet that lies close and parallel to the carina, and from *Palmatolepis glabra distorta* which is more sigmoidal and by the lack of the bulge in the posterior part of the outer platform. According to Ji & Ziegler (1993) there are two morphotypes of this specie that differs from the shape of the parapet.

Range: From the Uppermost *crepida* Zone to the Upper *marginifera* Zone (Ji & Ziegler, 1993).

Studied material: 253 elements from CM I, CM II, BTE MT and PZW sections.

Palmatolepis glabra prima Ziegler & Huddle, 1969

(Pl. 1, fig. 16)

1969 *Palmatolepis glabra prima* Ziegler & Huddle, p. 379, (cum syn).

1970 *Palmatolepis glabra prima* Ziegler & Huddle – Olivieri, p.100, pl.17, figs 1-4.

1977 *Palmatolepis glabra prima* Ziegler & Huddle – Ziegler In Ziegler (ed.), p. 309, pl. *Palmatolepis*-7, fig. 4-7 (*cum syn*).

1990 *Palmatolepis glabra prima* Ziegler & Huddle – Perri & Spalletta, p. 61, pl. 2, figs. 1a-b.

1993 *Palmatolepis glabra prima* Ziegler & Huddle – Ji & Ziegler, p.61, pl. 16, figs. 12-17, pl. 17, text-fig 17, fig. 2,9,17.

1998c *Palmatolepis glabra prima* Ziegler & Huddle - Perri & Spalletta, p. 156, pl. 1.3.1, figs. 3-4, 5.
2003 *Palmatolepis glabra prima* Ziegler & Huddle – Corradini, p. 79, pl. 4, figs. 3-6.
2013a *Palmatolepis glabra prima* Ziegler & Huddle – Mossoni et al., p. 22-23, fig. 5.16.

<u>Remarks</u>: *Palmatolepis glabra prima* is distinguished by the other subspecies of *Palmatolepis glabra* by the rounded, bulge-like parapet on the anterior inner platform and by *Palmatolepis tenuipunctata* by the lack of the outer lobe.

<u>Range</u>: From the Upper *crepida* Zone to the Upper *marginifera* Zone (Ji & Ziegler, 1993).

<u>Studied material</u>: 724 elements from BTE, CM I, CM II, MT and PZW sections.

Palmatolepis gracilis expansa Sandberg & Ziegler, 1979
(Pl.3, fig 9; Pl. 5, figs. 2a-2b; Pl. 7 fig. 3)

1979 *Palmatolepis gracilis expansa* Sandberg & Ziegler, p.178, pl.1 fig.6-8 *(cum syn*.).
1991 *Palmatolepis gracilis expansa* Sandberg & Ziegler - Perri & Spalletta, p.62, pl.4, fig.1.
1993 *Palmatolepis gracilis expansa* Sandberg & Ziegler – Ji & Ziegler (ed.), p.62, pl.6, fig.8-12; text-fig.14, fig.4.
2003 *Palmatolepis gracilis expansa* Sandberg & Ziegler - Corradini, pl. 6, fig.24.
2011 *Palmatolepis gracilis expansa* M1 Sandberg & Ziegler - Hartenfels, p. 251-252 pl. 45, figs. 6-8.
2011 *Palmatolepis gracilis expansa* M2 Sandberg & Ziegler - Hartenfels, p. 252-253 pl. 45, figs. 4-5.
2013b *Palmatolepis gracilis expansa* Sandberg & Ziegler – Mossoni et al., fig. 3.9.
2015 *Palmatolepis gracilis expansa* Sandberg & Ziegler – Mossoni et al., fig. 7C.

<u>Remarks</u>: *Palmatolepis gracilis expansa* is charcaterized by a broad platform, with a small lateral lobe. The blade-carina is generally short and slightly curved. It is distinguished from *Palmatolepis gracilis gracilis* by the wider platform and by the lack of raised marginal rims

<u>Range</u>: From the Lower *expansa* Zone to the Middle *praesulcata* Zone (Ji & Ziegler, 1993).

<u>Studied material</u>: 39 elements from BTE, CM I, MT and PB sections.

Palmatolepis gracilis gracilis Branson & Mehl, 1934a

(Pl. 2, figs. 15-16)

1934a *Palmatolepis gracilis* Branson & Mehl*,* p. 238, pl. 18, fig.8.

1969 *Palmatolepis gracilis gracilis* Branson & Mehl – Pölser, p. 399, pl. 6, fig 21.

1977 *Palmatolepis gracilis gracilis* Branson & Mehl – Ziegler In Ziegler (ed.), p. 315, pl. Palmatolepis-7, fig. 8-10 (cum syn).

1990 *Palmatolepis gracilis gracilis* Branson & Mehl - Perri & Spalletta, p.61, pl. 2, fig.2.

1991 *Palmatolepis gracilis gracilis* Branson & Mehl - Perri & Spalletta, p.62, pl. 4, fig.3-4.

1993 *Palmatolepis gracilis gracilis* Branson & Mehl – Ji & Ziegler, p.63, pl. 6, figs. 4-7; text-fig 14, fig. 2.

2013a *Palmatolepis gracilis gracilis* Branson & Mehl – Mossoni et al., p. 23, fig. 5.12-5.16.

Remarks: *Palmatolepis gracilis gracilis* is characterized by a small, narrow platform with a raised margin rim. The element is curved, in some species almost at a right angle. The keel underneath the central node is twisted around the small basal cavity. It is distinguished from *Palmatolepis minuta minuta* by the characteristic twisted keel.

Range: From the Upper *rhomboidea* Zone to the Upper *praesulcata* Zone (Ji & Ziegler, 1993).

Studied material: 1991 elements from all the sections.

Palmatolepis gracilis sigmoidalis Ziegler, 1962

(Pl. 2 fig. 11)

1962 *Palmatolepis deflectens sigmoidalis* n.subsp. Ziegler*,* p. 56 pl. 3, fig.24-28.

1969 *Palmatolepis gracilis sigmoidalis* Ziegler – Pölser, p. 399, pl. 6, fig 22.

1979 *Palmatolepis gracilis sigmoidalis* Ziegler – Sandberg & Ziegler; p. 178, pl. 1, fig 3-5.

1991 *Palmatolepis gracilis sigmoidalis* Ziegler – Perri & Spalletta, p. 64, pl. 4, fig 6.

1993 *Palmatolepis gracilis sigmoidalis* Ziegler – Ji & Ziegler, pl. 5, figs.1-3; text-fig 14, fig. 6.

2013a *Palmatolepis gracilis sigmoidalis* Ziegler – Mossoni et al., p. 23, fig. 5.11.

Remarks: *Palmatolepis gracilis sigmoidalis* is characterized by an extremely small platform consisting only of almost only raised rims, and with a strongly sigmoidal blade-carina. This subspecies differs from the other subspecies of *Pa. gracilis* by having a characteristic twisted platform and by the offset of the anterior carina.

Range: From within the Upper *trachytera* Zone to the Upper *praesulcata* Zone (Ji & Ziegler, 1993).

Studied material: 131 elements from CM I, MT and PZW sections.

Palmatolepis jamiae Ziegler & Sandberg, 1990

(Pl. 41, fig. 8)

1990 *Palmatolepis jamiae* Ziegler & Sandberg, p. 50-51, pl. 6, figs. 1-3,9,10 (only).
1993 *Palmatolepis jamiae* Ziegler & Sandberg – Ji & Ziegler, pl. 27, figs. 1-3.
2008 *Palmatolepis jamiae* Ziegler & Sandberg – Ovnatanova & Kononova, pl. 10, figs. 16-18; pl. 11, figs. 1-4, 5?, 6, 7?, 8, 9; pl. 14, fig. 10.
2013b *Palmatolepis jamiae* Ziegler & Sandberg – Mossoni et al., p. 23, fig. 5.8.

Remarks: *Palmatolepis jamiae* is characterized by a shagreen platform that tapers in the anterior part where the two margins join the blade more or less in the same position. A rounded well pronounced lobe is present just anteriorly of the central node. The inner posterior margin of the platform is concave. The carina is slightly sigmoidal, and well developed posterior of the central node where is composed of three or four nodes. This species differ from *Palmatolepis foliacea* by having a well-developed lobe with two sinuses.

Range: From the start of the *jamiae* Zone to the Upper *rhenana* Zone (Ziegler & Sandberg, 1990).

Studied material: 5 elements from PZW section.

Palmatolepis lyaiolensis Khrustcheva & Kuzmin, 1996

(Pl. 1, fig. 6)

1996 *Palmatolepis lyaiolensis* n.sp. Khrustcheva & Kuzmin, p.93, pl. 11, figs. 1-2.
2008 *Palmatolepis lyaiolensis* Khrustcheva & Kuzmin - Ovnatanova & Kononova, pl.13, figs. 4-11.
2013b *Palmatolepis lyaiolensis* Khrustcheva & Kuzmin – Mossoni et al., p. 23-24, fig. 5.6.

Remarks: This species is characterized by having a broad shagreen platform. The inner platform is rounded, while the outer platform is sub-triangular, because of the presence of a poorly differentiated lobe. The carina is slightly sigmoidal, and posterior of the central node is composed by one or two nodes. *Palmatolepis lyaiolensis* differs from *Palmatolepis hassi* in the poorly developed lobe, lacking well pronounced sinuses.

Range: From within the Lower *rhenana* Zone to the Upper *rhenana* Zone (Ovnatanova & Kononova, 2008).

Studied material: 4 elements from PZW section.

Palmatolepis marginifera marginifera Helms, 1959

(Pl. 2, fig. 18; Pl. 3, fig. 2)

1959 *Palmatolepis quadratinodosa marginifera* Ziegler (sic.) - Helms, p. 649, pl. 5, figs. 22-23.
1973 *Palmatolepis marginifera marginifera* Helms – Sandberg & Ziegler; p. 104, pl. 3, figs 13-14.
1977 *Palmatolepis marginifera marginifera* Helms – Ziegler In Ziegler (ed.), p. 328, pl. *Palmatolepis*-7, fig. 17-18; pl. *Palmatolepis*-8, figs. 1-2 (*cum syn*).
1990 *Palmatolepis marginifera marginifera* Helms - Perri & Spalletta, p.61, pl. 2, fig.3-4.
1993 *Palmatolepis marginifera marginifera* Helms – Ji & Ziegler, p.64, pl.13, fig.7-10; pl.14, fig.1-6; text-fig.17, fig.14.
1998b *Palmatolepis marginifera marginifera* Helms - Perri & Spalletta, p. 156, pl. 1.3.1, fig. 6.
1998 *Palmatolepis marginifera marginifera* Helms – Corradini, pl. 1.4.1, fig. 14.
2013a *Palmatolepis marginifera marginifera* Helms – Mossoni et al., p. 24, fig.6.18.
2013b *Palmatolepis marginifera marginifera* Helms – Mossoni et al., fig. 3.2.

Remarks: *Palmatolepis marginifera marginifera* is characterized by a rounded platform with a well-developed parapet parallel to the carina. The parapet starts in the inner anterior platform and it extend posterior the central node. It is distinguished from *Palmatolepis glabra distorta* by the length of the parapet and by the shape of the platform.

Range: From the base of the Lower *marginifera* Zone into the *velifer* Zone (Ji & Ziegler, 1993).

Studied material: 357 elements from BTE, CM I, CM II, MT and PZW sections.

Palmatolepis marginifera utahensis Ziegler & Sandberg, 1984

(Pl. 3, fig. 1)

1984 *Palmatolepis marginifera utahensis* Ziegler & Sandberg, p. 104, pl. 3, figs. 20, 20.

1990 *Palmatolepis marginifera utahensis* Ziegler & Sandberg - Perri & Spalletta, p.62, pl.2, figs.5-6.

1993 *Palmatolepis marginifera utahensis* Ziegler & Sandberg – Ji & Ziegler, p.64, pl.13, fig.6; text-fig. 17, figs.15.

2013b *Palmatolepis marginifera utahensis* Ziegler & Sandberg – Mossoni et al., fig. 3.1.

Remarks: *Palmatolepis marginifera utahensis* is characterized by a rounded platform with a well-developed parapet parallel to the carina. The inner anterior platform bear random but distinctive nodes. The inner anterior platform ornamentation distinguish *Palmatolepis marginifera utahensis* from *Palmatolepis marginifera marginifera*. It differs from *Palmatolepis rugosa trachytera* because the latter has an inner lobe.

Range: Upper *marginifera* Zone (Ji & Ziegler, 1993).

Studied material: 13 elements from CM I, CM II and MT sections.

Palmatolepis minuta minuta Branson & Mehl, 1934a

(Pl. 2, fig. 17)

1934a *Palmatolepis minuta* Branson & Mehl, p. 236, pl. 18, fig.1,6-7.

1962 *Palmatolepis minuta minuta* Branson & Mehl – Ziegler; pl. 3, figs 1-10, text fig. 5 b-n.

1990 *Palmatolepis minuta minuta* Branson & Mehl – Perri & Spalletta, p. 62, pl. 3, figs 1, 7.

1993 *Palmatolepis minuta minuta* Branson & Mehl – Ji & Ziegler, pl. 7, figs. 1-19; pl. 9, figs. 8-18; text-fig 13, figs. 9,15,16.

1998b *Palmatolepis minuta minuta* Branson & Mehl - Perri & Spalletta, p. 156, pl. 1.3.1, fig. 8.

2013a *Palmatolepis minuta minuta* Branson & Mehl – Mossoni et al., p. 24, fig.6.17.

Remarks: *Palmatolepis minuta minuta* is characterized by a lanceolate smooth platform. In some elements a weak outer lobe is present. The carina is straight or weakly curved. This species differ from *Palmatolepis rhomboidea* by the lacking of the bulge in the anterior part of the inner platform.

Range: From the Upper *triangularis* Zone to the Upper *trachytera* Zone (Ji & Ziegler, 1993).

Studied material: 585 elements from BTE, CM I, CM II, MT and PZW sections.

Palmatolepis minuta loba Helms, 1963

(Pl. 1, fig. 11)

1963 *Palmatolepis (Deflectolepis) minuta loba* Helms, p. 470, pl. 2, figs 13-14; pl. 3 fig. 12; text fig 2, fig. 39.
1970 *Palmatolepis minuta loba* Helms – Olivieri, p. 107, pl. 20, fig. 5.
1993 *Palmatolepis minuta loba* Helms – Ji & Ziegler, p.64, pl.10, fig,1-16, text-fig.13, fig.11-12.
2003 *Palmatolepis minuta loba* Helms – Corradini, p. 80, pl. 6, fig. 9.
2013a *Palmatolepis minuta loba* Helms – Mossoni et al., p. 24, fig. 5.11.

Remarks: This species is characterized by a lanceolate platform with a pronounced lobe in the outer side. The anterior carina is straight and the posterior carina is not well developed. It is distinguished from *Palmatolepis minuta minuta* by the presence of the lobe. It differs from *Pa. minuta schlezia* by the absence of the raised marginal rims of the platform and by *Pa. minuta woskae* by having a strong posterior carina.

Range: From the Lower *crepida* Zone to the Lower *rhomboidea* Zone (Ji & Ziegler, 1993).

Studied material: 27 elements from CM I, CM II and PZW sections.

Palmatolepis minuta schleizia Helms, 1963

(Pl. 4, fig. 3)

1963 *Palmatolepis (Deflectolepis) schleizia* Helms, p.471, pl. 3, fig.13 ; pl.4, fig.1-11.

1977 *Palmatolepis minuta schleizia* Helms - Ziegler in Ziegler (ed.), p.341, pl. *Palmatolepis*-9, fig.9-11 (*cum syn*)

1993 *Palmatolepis minuta schleizia* Helms - Ji & Ziegler, p.65, pl.9, fig.1-7; text fig.13, fig.10 ; text-fig.14, fig.1.

2003 *Palmatolepis minuta schleizia* Helms – Corradini, pl. 6, fig. 22.

<u>Remarks</u>: *Palmatolepis minuta schleizia* is characterized by a small subtriangular platform with a small outer lobe. The central node is well developed and there is an offset with the anterior blade-carina. The platform has raised marginal rims that allow to distinguish this subspecies of *Palmatolepis minuta* from all the other subspecies.

<u>Range</u>: From the Upper *rhomboidea* Zone to the Upper *postera* Zone (Ji & Ziegler, 1993).

<u>Studied material</u>: 212 elements from CM I, CM II, MT and PB sections

Palmatolepis minuta subgracilis Bishoff, 1956

(Pl. 5, fig. 36)

1956 *Palmatolepis subgracilis* Bishoff, p.130, pl. 9, figs 9-12; pl. 10, fig. 13.

1977 *Palmatolepis minuta subgracilis* Bishoff – Ziegler in Ziegler (ed.), p. 343, pl. *Palmatolepis*-9, fig 6 (*cum syn*).

2003 *Palmatolepis minuta subgracilis* Bishoff – Corradini; p. 80, pl. 6, fig. 21.

<u>Remarks</u>: *Palmatolepis minuta subgracilis* is characterized by a small and slender platform, with a small lobe. It is distinguished by the other subspecies of *Palmatolepis minuta* by the very small platform.

<u>Range</u>: From the Upper *crepida* Zone to the Lower *rhomboidea* Zone (Ziegler, 1977).

<u>Studied material</u>: 4 elements from CM I and PZW sections

Palmatolepis minuta wolskae Szulczewski, 1971

(Pl. 5, fig. 4)

1971 *Palmatolepis minuta wolskae* Szulczewski, p. 36, pl. 15, fig.2, 12-14.

1993 *Palmatolepis minuta wolskae* Szulczewski – Ji & Ziegler; p. 85 pl. 11, figs 1-11, text-fig. 13, figs 7-8.

2003 *Palmatolepis minuta wolskae* Szulczewski – Corradini; p. 80, pl.6, figs. 7-8.

Remarks: This species is characterized by a small ovoidal or subtriangular platform, with a small lobe in the outer platform. The posterior carina is absent. It is distinguished from *Palmatolepis minuta loba* by the absence of the posterior carina.

Range: From the Middle *crepida* Zone to the Lower *rhomboidea* Zone (Corradini, 2003).

Studied material: 30 elements from CM I, CM II and PZW sections.

Palmatolepis perlobata grossi Ziegler, 1960

(Pl. 5, fig. 8)

1960 *Palmatolepis rugosa grossi* Ziegler in Kronberg et al., p. 37, pl. 1, figs 1-2.

1979 *Palmatolepis perlobata grossi* Ziegler - Sandberg & Ziegler, p. 179.

1993 *Palmatolepis perlobata grossi* Ziegler - Ji & Ziegler, p. 66, pl. 13, fig. 12; text-fig. 15, fig. 7.

2003 *Palmatolepis perlobata grossi* Ziegler – Corradini, p. 81, pl. 7, fig. 8-9

Remarks: *Palmatolepis perlobata grossi* is characterised by a slender platform, with a well developed denticulated parapet in the outer anterior platform and a secondary carina that reaches the central node. The lateral lobe is well developed and slightly posteriorly directed. The posterior part of the platform is bent upward. Pa. perlobata grossi differs from all others subspecies of Pa. perlobata by having a well developed parapet on the outer anterior platform margin and a relatively narrow posterior platform.

Range: From the Upper *marginifera* Zone into the Upper *trachytera* Zone (Ji & Ziegler, 1993).

Studied material: 14 elements from CM I and MT section.

Palmatolepis perlobata helmsi Ziegler, 1962

(Pl. 5, fig. 7

1962 *Palmatolepis helmsi* Ziegler, p. 60, pl. 8, figs 16-17.
1979 *Palmatolepis perlobata helmsi* Ziegler - Sandberg & Ziegler, p. 179, pl. 1, figs 20-22.
1993 *Palmatolepis perlobata helmsi* Ziegler - Ji & Ziegler, p. 66, pl. 18, figs 7-10; text-fig. 15, fig. 9.
2003 *Palmatolepis perlobata helmsi* Ziegler – Corradini, p. 80, pl.7, figs. 6-7.

Remarks: *Palmatolepis perlobata helmsi* is characterized by a narrow and shagreen platform elongated posterior to the central node and widest anterior to the central node. The posterior tip is gently flexed upward. *Pa. perlobata helmsi* differs from *Pa. p. postera* by the slender platform and the weak ornamentation. It is different from *Pa. glabra lepta* because the latter has an evident triangular parapet.

Range: From the base of the Lower *trachytera* Zone into the Lower *expansa* Zone (Ji & Ziegler, 1993).

Studied material: 23 elements from CM I and MT sections.

Palmatolepis perlobata maxima Müller, 1956

(Pl. 4, fig. 20)

1956 *Palmatolepis maxima* Müller, p.29, tav.9, fig.37-40 (*only*).
1977 *Palmatolepis perlobata maxima* Müller - Ziegler in Ziegler (ed.), p.357, pl.*Palmatolepis*-12, fig.1-2 (*cum syn*.).
1979 *Palmatolepis perlobata maxima* Müller - Sandberg & Ziegler, p.179, pl.1, fig.19.
1990 *Palmatolepis perlobata maxima* Müller - Perri & Spalletta, p.62, pl.3, fig.6.
1993 *Palmatolepis perlobata maxima* Müller - Ji & Ziegler, p.66; text-fig.15, fig.6.
2011 *Palmatolepis perlobata maxima* Müller - Hartenfels, p.265-266; pl 47, fig.7-10.

Remarks: This subsperies of *Palmatolepis perlobata* is characterized by a slender platform with a sharp lobe in the outer platform. A secondary keel that extends into the outer lobe could be present. *Palmatolepis perlobata maxima* differs from *Palmatolepis perlobata schindewolfi* for the slimmer and elongated platform; and from *Palmatolepis perlobata* grossi for the absence of the inner parapet.

Range: From the Upper *marginifera* Zone to the Lower *expansa* Zone (Ji & Ziegler, 1993).

Studied material: 16 elements from CM I, CM II MT and PB.

Palmatolepis perlobata postera Ziegler, 1960

(Pl. 2, fig. 2; Pl. 7, fig 2)

1960 *Palmatolepis rugosa postera* n.subsp. Ziegler, p. 27, pl. 8, figs. 22-31; pl. 9, fig. 33.
1979 *Palmatolepis perlobata postera* Ziegler – Sandberg & Ziegler, p. 180, pl. 2, figs. 1-4.
1993 *Palmatolepis perlobata postera* Ziegler – Ji & Ziegler; text-fig 15, fig. 10.
2011 *Palmatolepis perlobata postera* Ziegler - Hartenfels, p.266-267; pl 48, fig.2.
2013a *Palmatolepis perlobata postera* Ziegler – Mossoni, p. 25, fig. 6.2.
2015 *Palmatolepis perlobata postera* Ziegler – Mossoni, fig. 7B.

Remarks: *Palmatolepis perlobata postera* is characterized by a broad curved platform with a shagreen surface. It is distinguished by the other subspecies of Palmatolepis perlobata by the absence of any lobe or by the occasional presence of a weak lobe on the outer part of the platform. This species was choosen as marker of the *postera* Zone by Ziegler & Sandberg (1984), however in North Gondwana is a very rare taxon (Corradini, 2008).

Range: From the Lower *postera* Zone to the Upper *expansa* Zone (Ji & Ziegler, 1993).

Studied material: 20 elements from BTE, CM I, CM II, PB and PZW sections.

Palmatolepis perlobata schindewolfi Müller, 1956

(Pl. 2, fig. 20; Pl. 5, fig. 1a-1b)

1956 *Palmatolepis perlobata schindewolfi* Müller, p. 27, pl. 8, figs. 22-31; pl. 9, fig. 33.
1969 *Palmatolepis perlobata schindewolfi* Müller – Pölser, p. 399, pl. 5, figs. 1-2, 9.
1970 *Palmatolepis perlobata schindewolfi* Müller – Olivieri, p. 109, pl. 20, figs. 11-14.
1977 *Palmatolepis perlobata schindewolfi* Müller – Ziegler In Ziegler (ed.), p. 361, pl. *Palmatolepis*-11, fig. 1-7 (*cum syn*).
1990 *Palmatolepis perlobata schindewolfi* Müller – Perri & Spalletta, fig. 63, pl. 3, figs. 4-5, 8.

1991 *Palmatolepis perlobata schindewolfi* Müller – Perri & Spalletta, fig. 66, pl. 4, fig. 7.

1993 *Palmatolepis perlobata schindewolfi* Müller – Ji & Ziegler; p.67, pl.18, figs.9-15; text-fig.15, fig.3.

2003 *Palmatolepis perlobata schindewolfi* Müller – Corradini, pl. 7, figs. 1-5.

2013a *Palmatolepis perlobata schindewolfi* Müller– Mossoni et al., p. 25, fig. 6.20.

Remarks: *Palmatolepis perlobata schindewolfi* is characterized by an arc-shaped and elongated platform. There is a small lobe on the outer platform, and generally the posterior end is pointed downward. The surface is smooth or weakly ornamented. This species is distinguished from *Palmatolepis perlobata perlobata* by its slender shape, the small lobe and the weak ornamentation.

Range: From the Upper *crepida* Zone to the Upper *expansa* Zone (Ji & Ziegler, 1993).

Studied material: 1543 elements from all the sections.

Palmatolepis quadrantinodosalobata Sannemann, 1955

(Pl. 1, fig. 14)

1955 *Palmatolepis quadrantinodosalobata* Sannemann, p. 328, pl.24, fig.6.

1969 *Palmatolepis quadrantinodosalobata* Sannemann – Pölser, p. 399, pl. 6, figs. 13-14.

1970 *Palmatolepis quadrantinodosalobata* Sannemann - Olivieri, p.112, pl.18, fig.9-11.

1973 *Palmatolepis quadrantinodosalobata* Sannemann - Ziegler In Ziegler (ed.), p.295, pl.*Palmatolepis*-4, fig.6-8 (*cum syn*.).

1993 *Palmatolepis quadrantinodosalobata* Sannemann - Ji & Ziegler, p.69, pl.23, fig.5-7; text-fig.12, fig.3,7-8.

2003 *Palmatolepis quadrantinodosalobata* Sannemann – Corradini, pl. 5, figs. 7-9.

2013a *Palmatolepis quadrantinodosalobata* Sannemann – Mossoni et al., p. 25-27, fig. 5.14.

Remarks: *Palmatolepis quadrantinodosalobata* is characterized by having a well-developed platform, rounded lobe in the outer part of the platform. The inner anterior part is covered with aligned or randomly disposed nodes (Ji & Ziegler 1993). A few specimens may have a few small nodes on the outer anterior part of the platform. *Palmatolepis quadrantinodosalobata* is distinguished from *Palmatolepis subperlobata* by the presence of the ornamentation, and by *Palmatolepis sandbergi* that has the whole inner platform covered by nodes

<u>Range</u>: From the base of the Lower *crepida* zone into the Lower *rhomboidea* Zone (Ji & Ziegler, 1993).

<u>Studied material</u>: 122 elements from CM I, CM II, and PZW sections

Palmatolepis regularis Cooper, 1931

(Pl. 1, fig. 12)

1931 *Palmatolepis regularis* n.sp. Cooper, p. 242, pl.28, fig. 36.
1962 *Palmatolepis* cf. *regularis* Cooper - Ziegler, p. 75-76, pl. 6, figs 20-24.
1969 *Palmatolepis* cf. *regularis* Cooper – Pölser, p. 399, pl. 5, figs. 3-4.
1993 *Palmatolepis* cf. *regularis* Cooper – Ji & Ziegler, pl. 21, figs. 6-10; text-fig. 16 figs. 7,9.
2013a *Palmatolepis regularis* Cooper – Mossoni et al., p. 27, fig. 5.12.

<u>Remarks</u>: This species is characterized by a shagreen, strongly sigmoidal platform lacking the outer lobe. Ji & Ziegler (1993) proposed two morphotypes that differ from the width of the platform. Morphotype 1 has a narrow and elongated platform, while morphotype 2 has a broader platform. The specimen from Pizzul West section belongs to morphotype 2. However, it should be pointed out that, since the range of the two morphotypes is the same and coincides with the range of the species, their utility is questionable. This species is distinguished by *Palmatolepis subperlobata* by the lack of the outer lobe.

<u>Range</u>: From the Upper *triangularis* Zone to the Lower *rhomboidea* Zone (Ji & Ziegler, 1993).

<u>Studied material</u>: 16 elements from CM I, CM II and PZW sections.

Palmatolepis rhomboidea Sannemann, 1955

(Pl. 1, fig. 9)

1955a *Palmatolepis rhomboidea* Sannemann, p. 329, pl. 24, fig. 14.
1970 *Palmatolepis rhomboidea* Sannemann – Olivieri, p. 114, pl. 16, figs. 11-14.
1985 *Palmatolepis rhomboidea* Sannemann – Ziegler in Ziegler (ed.), p. 299, pl. *Palmatolepis*-1, fig. 6-7 (*cum syn*).

2003 *Palmatolepis rhomboidea* Sannemann – Corradini, p. 83, pl. 3, figs. 19-21.
2013a *Palmatolepis rhomboidea* Sannemann – Mossoni, p. 27-28, fig. 5.9.

Remarks: *Palmatolepis rhomboidea* is characterized by a small rhomboidal platform with an evident bulge in the outer anterior part. It is distinguished by *Palmatolepis minuta minuta* and *Palmatolepis delicatula delicatula* by the bulge or low parapet in the outer anterior platform and the shorter free blade.

Range: From the Lower *rhomboidea* Zone to the lower part of the Upper *marginifera* Zone (Corradini, 2003).

Studied material: 144 elements from CM I, CM II and PZW sections.

Palmatolepis rotunda Ziegler, 1990

(Pl. 1, fig. 7)

1990 *Palmatolepis rotunda* n.sp. Ziegler & Sandberg, p.62, pl. 10, figs. 1-5.
1998e *Palmatolepis rotunda* Ziegler & Sandberg – Perri & Spalletta, p. 204, pl. 2.2.1, figs. 12.
2013a *Palmatolepis rotunda* Ziegler & Sandberg – Mossoni, p. 28, fig. 5.7.

Remarks: *Palmatolepis rotunda* is characterized by a broad rounded inner posterior platform. There is a well developed rounded lobe in the outer platform, with two evident sinuses. The anterior carina is strongly curved, while the posterior carina is not well pronounced.

Range: From the start of the Upper *rhenana* Zone to the top of the *linguiformis* Zone (Ziegler & Sandberg, 1990).

Studied material: 1 element from PZW section.

Palmatolepis rugosa rugosa Branson & Mehl, 1934a

(Pl. 2 fig. 1)

1934a *Palmatolepis rugosa* n.sp. Branson & Mehl, p. 236, pl. 18, figs. 15,16,18,19.

1979 *Palmatolepis rugosa rugosa* Branson & Mehl – Sandberg & Ziegler, p. 180, pl. 2, figs. 1-4.

1991 *Palmatolepis rugosa rugosa* Branson & Mehl – Perri & Spalletta, p. 66, pl. 4, figs. 8-9.

1993 *Palmatolepis rugosa rugosa* Branson & Mehl – Ji & Ziegler; text-fig 15, fig. 12.

2013a *Palmatolepis rugosa rugosa* Branson & Mehl – Mossoni et al., p. 28, fig. 6.1.

<u>Remarks</u>: This species is characterized by a broad strongly ornamented platform, with a very pronounced outer lobe. The carina is strongly curved anterior the central node. It is distinguished from the other subspecies of *Palmatolepis rugosa* by the pattern of the ornamentation, that shows ridge-type nodes in the inner parapet and a series of coarse nodes in the anterior part of the outer platform.

<u>Range</u>: From the Lower *expansa* Zone to the Upper *expansa* Zone (Ji & Ziegler, 1993).

<u>Studied material</u>: 3 elements from PB and PZW sections.

Palmatolepis rugosa cf. *ampla* Müller, 1956 (*sensu* Ziegler, 1960)

(Pl. 3, fig. 5)

1960 *Palmatolepis rugosa ampla* Müller - Ziegler *in* Kronberg *et al*., p. 38, pl. 1, figs 3-4.

1962 *Palmatolepis rugosa ampla* Müller - Ziegler, pl. 8, fig. 6.

1977 *Palmatolepis rugosa* cf*. ampla* Müller - Ziegler in Ziegler (ed.) in *Pa. rugosa ampla* Müller, p. 401, pl. *Palmatolepis*-14, figs 1-3 (*cum syn.).*

1993 *Palmatolepis rugosa* cf. *ampla* Müller – Ji & Ziegler, pl. 13, fig. 11, pl. 18 fig. 16., text-fig 15, fig. 5.

2003 *Palmatolepis rugosa* cf. *ampla* Müller – Corradini, p. 53, pl. 5, figs 17-18.

2013b *Palmatolepis rugosa* cf. *ampla* Müller – Mossoni et al., fig. 3.5.

<u>Remarks</u>: This species is characterized by a broad sigmoidal platform, with a weak ornamentation made up of random nodes, sometimes the platform is unornamented. It is distinguished from *Palmatolepis rugosa ampla* (which has a younger range) because the latter has a strong ornamentation in the inner anterior platform.

<u>Range</u>: From the Upper *marginifera* Zone to the Lower *trachytera* Zone (Ji & Ziegler, 1993).

Studied material: 21 elements from CM I, CM II, MT, PB and PZW sections.

Palmatolepis rugosa trachytera Ziegler, 1960

(Pl. 5, fig. 3)

1960 *Palmatolepis rugosa trachytera* Ziegler *in* Kronberg *et al.*, p. 38, pl. 1, fig. 6; pl. 2, figs 1-9.
1970 *Palmatolepis rugosa trachytera* Ziegler - Olivieri, p. 114, pl. 18, figs 13-14.
1977 *Palmatolepis rugosa trachytera* Ziegler - Ziegler *in* Ziegler (ed.), p. 405, pl. *Palmatolepis*-14, figs 6-11 (*cum syn*.)
1984 *Palmatolepis rugosa trachytera* Ziegler - Ziegler & Sandberg, p. 187, pl. 1, figs 1-5, 12.
1998b *Palmatolepis rugosa trachytera* Ziegler - Corradini, pl. 1.4.2, fig. 19.

Remarks: *Palmatolepis rugosa trachytera* is characterized by having a narrow outer platform with a well developed long parapet and a wide posterior part of the inner platform. The inner anterior platform bears trasversally elongated nodes. Some specimens bear few small nodes, irregularly disposed on the platform. *Pa. rugosa trachytera* differs from *Pa. rugosa ampla* by the occurrence of the parapet, the reduced lobe and the wide posterior platform.

Range: From the Lower *trachytera* Zone to the Upper *trachytera* Zone (Ji & Ziegler, 1993).

Studied material: 210 elements from CM I, CM II, and PB sections.

Palmatolepis simpla Ziegler & Sandberg, 1990

(Pl. 1, fig. 4)

1990 *Palmatolepis simpla* n.sp. Ziegler & Sandberg, p.47-48, pl. 4, figs. 9-12.
2013a *Palmatolepis simpla* Ziegler & Sandberg – Mossoni et al., p. 28, fig. 5.4.

Remarks: *Palmatolepis simpla* is characterized by a broad platform, almost rounded in the posterior part, while in the anterior part became narrow. There is a rounded lobe in the outer part of the anterior platform. The anterior outer platform margin is concave. It is distinguished from *Palmatolepis proversa* by the weaker marginal fortification and for the less pronounced lobe.

<u>Range</u>: From the Upper *hassi* Zone to the Upper *rhenana* Zone (Ziegler & Sandberg, 1990).

<u>Studied material</u>: 2 elements from PZW section.

Palmatolepis stoppeli Ziegler, 1960

(Pl. 2, fig. 19)

1960 *Palmatolepis* sp. Ziegler, Ziegler pl. 7 figs. 12-13
1977 *Palmatolepis stoppeli* n.sp. Sandberg & Ziegler; p. 106-107, pl. 3 figs. 1-11, pl. 5, fig. 13.
1993 *Palmatolepis stoppeli* Ziegler – Ji & Ziegler, p.71, pl. 14, figs. 7-12;text-fig. 17, fig. 12..
2013b *Palmatolepis stoppeli* Ziegler – Mossoni et al., p. 28, fig. 6.19.

<u>Remarks</u>: This species is characterized by a broad sub-ovoidal platform with an evident ramp in the upper part of the outer platform. It is distinguished from *Palmatolepis quadrantinodosa inflexa* by the broad platform and by the lack of ornamentation on the surface and from *Palmatolepis rhomboidea* because the latter have in the inner platform a small bulge instead of an evident ramp.

<u>Range</u>: Upper *rhomboidea* Zone to Lower *marginifera* Zone (Ji & Ziegler, 1993).

<u>Studied material</u>: 1 element from PZW section.

Palmatolepis subperlobata Branson & Mehl, 1934a

(Pl. 1, fig. 17)

1934a *Palmatolepis subperlobata* n.sp. Branson & Mehl, p. 235, pl. 18, figs. 11,21.
1971 *Palmatolepis subperlobata* Branson & Mehl – Szulczewski, p. 40-41, pl. 13, fig. 12.
1993 *Palmatolepis subperlobata* Branson & Mehl – Ji & Ziegler, pl.20, figs. 3-9; pl. 21, figs. 11-12;text-fig. 16, figs. 5,6,8.
2003 *Palmatolepis subperlobata* Branson & Mehl – Corradini, pl. 3, figs. 1-4.
2013a *Palmatolepis subperlobata* Branson & Mehl – Mossoni et al., p. 28-29, fig. 5.17.

<u>Remarks</u>: *Palmatolepis subperlobata* is characterized by a shagreen platform with a well-developed lobe on the outer platform. The carina is strongly sigmoidal and is only weakly developed posterior of the

node. This species is distinguished from *Palmatolepis tenuipunctata* which has a relatively narrow, elongated platform and a small outer lobe. Ji & Ziegler (1993) describe three morphotypes of *Pa. subperlobata*.

Range: From the base of the Lower *triangularis* Zone to the Upper *marginifera* Zone (Corradini, 2003).

Studied material: 214 elements from CM I, CM II and PZW sections.

Palmatolepis tenuipunctata Sannemann, 1955
(Pl. 1, fig. 13)

1955b *Palmatolepis tenuipunctata* Sannemann, p. 136, pl. 6, fig. 22.
1969 *Palmatolepis tenuipunctata* Sannemann – Pölser, p. 399, pl. 5, fig. 21.
1970 *Palmatolepis tenuipunctata* Sannemann – Olivieri, p. 117, pl. 18, figs. 1-2.
1993 *Palmatolepis tenuipunctata* Sannemann – Ji & Ziegler , p.72, pl.19, fig.1-6; text-fig.16, fig.2.
2003 *Palmatolepis tenuipunctata* Sannemann – Corradini, pl. 3, figs. 11-13.
2013a *Palmatolepis tenuipunctata* Sannemann – Mossoni et al., p. 29, fig. 5.13.

Remarks: *Palmatolepis tenuipunctata* is characterized by an elongated platform, with a small lobe in the outer part. The blade-carina is moderatly sigmoidal. Underneath the element there is a thin keel that goes all along the platform. It is distinguished from *Palmatolepis subperlobata* by the less developed lobe and from *Palmatolepis glabra prima* by the presence of the lobe.

Range: From the Upper *triangularis* Zone to the Uppermost *crepida* Zone (Ji & Ziegler, 1993).

Studied material: 61 elements from CM I and PZW sections.

Family Polygnathidae Bassler, 1925

Genus *Ancyrodella* Ulrich & Bassler, 1926

Ancyrodella curvata Branson & Mehl, 1934a
(Pl. 1, fig. 3)

1934a *Ancyrodella curvata* n.sp. Branson & Mehl, p. 241, pl. 19, figs. 6, 11.
1966 *Ancyrodella curvata* Branson & Mehl – Glenister & Klapper, p.798, pl. 86, figs. 13-15.
1993 *Ancyrodella curvata* Branson & Mehl – Ji & Ziegler, p. 96, pl. 2, figs. 4-5.
1998d *Ancyrodella curvata* Branson & Mehl – Perri & Spalletta, p. 204, pl. 2.2.1, fig. 1.
2013a *Ancyrodella curvata* Branson & Mehl – Mossoni et al., p. 19, fig. 5.3.

Remarks: *Ancyrodella curvata* is characterized by a strongly pronounced latero-posterior lobe which can bear a secondary carina and a secondary keel. The anterior lobes are well developed. The carina goes all along the element and is bounded by two rows of nodes, one on each side of the carina. The platform is covered by nodes. It is distinguished from *Ancyrodella lobata* by a secondary carina on the latero-posterior lobe and a secondary keel.

Range: From within the Lower *hassi* zone to the end of the *linguiformis* zone (Ji & Ziegler, 1993).

Studied material: 61 elements from PZW section.

Ancyrodella lobata Branson & Mehl, 1934a

(Pl. 1, fig. 2)

1934a *Ancyrodella lobata* n.sp. Branson & Mehl, p. 239-240, pl. 19, fig.14, pl. 21, figs. 22-23.
1971 *Ancyrodella lobata* Branson & Mehl – Szulczewski, p.13, pl. 3, figs. 1-4 only.
1985 *Ancyrodella lobata* Branson & Mehl – Klapper & Lane, p. 923-924, pl. 14, fig. 12,13,16,17.
1989 *Ancyrodella lobata* Branson & Mehl – Ji, pl. 3, fig. 3.
1993 *Ancyrodella lobata* (Branson & Mehl) – Ji & Ziegler, p. 96, pl. 2, figs. 6-10.
2013a *Ancyrodella lobata* (Branson & Mehl) – Mossoni et al., p. 19, fig. 5.2.

Remarks: *Ancyrodella lobata* is characterized by an ornamented platform, with two rows of big nodes on each side. The platform is bilaterally asymmetrical with a well-developed lobe-like protrusion on the outer side. The lobe is covered with random nodes and underneath is evident a secondary keel.
It is distinguished from *Ancyrodella curvata* by a lobe-like protrusion, rather than a distinct latero-posterior lobe on the outer platform, and by the lack of the secondary carina on this lobe-like protrusion.

Range: Nearly from the start of the Lower *hassi* Zone into the Upper *rhenana* Zone (Ji & Ziegler, 1993).

Studied material: 4 elements from PZW section.

Ancyrodella nodosa Ulrich & Bassler, 1926

(Pl. 1, fig. 1)

1926 *Ancyrodella nodosa* n. sp. Ulrich & Bassler, p.48, pl. 1, figs. 1-13.

1958 *Ancyrodella nodosa* Ulrich & Bassler – Ziegler, p. 44, pl. 11, fig. 1.

1966 *Ancyrodella nodosa* Ulrich & Bassler – Glenister & Klapper, p.798-799, pl.86, figs. 5-12.

1993 *Ancyrodella nodosa* Ulrich & Bassler – Ji & Ziegler, p. 96, pl. 2, figs. 11-12; text-fig. 8, figs 8-9.

2008 *Ancyrodella nodosa* Ulrich & Bassler - Ovnatanova & Kononova, p.1080-1081, pl.26, figs. 11-16.

2013b *Ancyrodella nodosa* Ulrich & Bassler – Mossoni et al., p. 19-21, fig. 5.1.

Remarks: *Ancyrodella nodosa* is characterized by an alate platform ornamented with random nodes. The carina extends beyond the platform in the posterior part of the element, due to the constriction of the posterior margins of the platform. It is distinguished from *Ancyrodella lobata* and *Ancyrodella curvata* by the absence of the lobe-like protrusion on the outer platform.

Range: Nearly from the start of the Upper *hassi* Zone to the end of the *linguiformis* Zone (Ji & Ziegler, 1993).

Studied material: 4 elements from PZW section.

Genus *Bispathodus* Müller, 1962

Type species: *Spathodus spinulicostatus* E.R.Branson, 1934, pl. 27, fig. 19.

Bispathodus aculeatus aculeatus (Branson & Mehl, 1934a)

(Pl. 3, fig. 20)

1934a *Spathodus aculeatus* Branson & Mehl, p. 186, pl. 17, figs 11, 14.

1970 *Spathognathodus aculeatus* (Branson & Mehl) - Olivieri, p. 142, pl. 12, fig. 1; pl. 26, fig. 1.

1974 *Bispathodus aculeatus aculeatus* (Branson & Mehl) - Ziegler, Sandberg & Austin, p. 101, pl. 1, fig. 5; pl. 2, figs. 1-8 (*cum syn*.).

1975 *Bispathodus aculeatus aculeatus* (Branson & Mehl) - Ziegler *in* Ziegler (ed.), p. 19, pl. *Bispathodus*-1, figs. 1-4.

2003 *Bispathodus aculeatus aculeatus* (Branson & Mehl) - Corradini, p.84-85, pl. 1, figs 3-5.

2013b *Bispathodus aculeatus aculeatus* (Branson & Mehl) – Mossoni et al., fig. 3.20.

Remarks: *Bispathodus aculeatus aculeatusis* is a pectiniform element characterized by a partially fused blade denticles. The basal cavity is small, more or less in central position. Above the basal cavity, on the right side of the blade, a few accessory denticles are present. In the studied material the number of these accessory denticles is variable from one to three, and in some specimens they are connected to the blade by thin ridges.

The occurrence of these accessory denticles in central position allow to distinguish *Bi. aculeatus* from the other species of *Bispathodus*. *Bi. aculeatus aculeatus* differs from *Bi. aculeatus anteposicornis* because the latter has one more accessory denticle on the right side of the blade anterior the basal cavity.

Range: From the base of the Middle *expansa* Zone into the Lower Carboniferous (Ziegler & Sandberg, 1984).

Studied material: 213 elements from BTE, CM I and MT sections.

Bispathodus costatus (E.R.Branson, 1934)
Morphotype 1 Ziegler, Sandberg & Austin, 1974

(Pl. 3, fig. 19; Pl. 7, fig. 5)

1962 *Spathognathodus costatus costatus* (E.R.Branson) - Ziegler, p. 107, pl. 14, figs 1-2, 4-6, 9-10.

1970 *Spathognathodus costatus costatus* (E.R.Branson) - Olivieri, p. 143, pl. 12, fig. 4; pl. 26, fig. 7.

1974 *Bispathodus costatus* (E.R.Branson) M1- Ziegler, Sandberg & Austin, p. 102, pl. 2, fig. 13.

1975 *Bispathodus costatus* (E.R.Branson) M1- Ziegler *in* Ziegler (ed.), p. 33, pl. *Bispathodus*-2, fig. 8.

2003 *Bispathodus costatus* (E.R.Branson) M1- Corradini, p. 85, pl. 1, fig. 6.

2013b *Bispathodus costatus* (E.R.Branson) – Mossoni et al., fig. 3.19.

2015 *Bispathodus costatus* (E.R.Branson) – Mossoni et al., fig. 7E.

Remarks: *Bispathodus costatus* is characterized by denticles completely fused to form a blade. On the right side, a second row of denticles is parallel to the main blade and almost reaches the posterior end. In a few specimens, the denticles of the secondary row can be connected to the main blade by weak ridges. The basal cavity is wide open and is developed below the posterior half of the element.

Bi. costatus differs from *Bi. spinulicostatus* and *Bi. ultimus* by the lack of nodes or ridges on the left side of the blade; It is different from *Bi. aculeatus* in having denticles on the right side of the blade up to the posterior end. The wide basal cavity distinguish *Bi. costatus* M1 from *Bi. costatus* M2.

Range: From the Middle *expansa* Zone to the Middle *praesulcata* Zone (Ziegler & Sandberg, 1984).

Studied material: 213 elements from BTE, CM I and MT sections.

Bispathodus jugosus (Branson & Mehl, 1934a)

(Pl. 7, fig. 4)

1934a *Spathodus jugosus* Branson & Mehl, p. 190, pl. 17, figs. 12, 22.

1962 *Spathognathodus jugosus* (Branson & Mehl) - Ziegler, p. 110, pl. 13, figs. 17-19 (*cum syn*.).

1974 *Bispathodus jugosus* (Branson & Mehl) - Ziegler, Sandberg & Austin, p. 103, pl. 1, figs. 3-4; pl. 3, figs. 12, 23, 26 (*cum syn*.).

1975 *Bispathodus jugosus* (Branson & Mehl) - Ziegler *in* Ziegler (ed.), p. 37, pl. *Bispathodus*-3, figs. 1-4.

2003 *Bispathodus jugosus* (Branson & Mehl) - Corradini, p. 85, pl. 1, fig. 9.

2015 *Bispathodus jugosus* (Branson & Mehl) – Mossoni et al., fig. 7D.

Remarks: *Bispathodus jugosus* is a pectiniform element with the denticles of the main blade almost completely fused. A second row of denticles parallel to the main blade occur on the right side of the element. In the posterior part, a few, very small denticles (“germ denticles”) occur between the main and the secondary blade. The basal cavity is wide and positioned under the posterior two thirds of the element, up to the posterior end. *Bi. jugosus* is distinguished from all the other species of *Bispathodus* by the occurrence of the “germ denticles”.

Range: From the Lower *expansa* Zone into the Upper *expansa* Zone (Ziegler & Sandberg, 1984).

Studied material: 10 elements from BTE, and CM I sections.

Bispathodus spinulicostatus (E.R. Branson, 1934)

(Pl. 7, fig. 6)

1934 *Spathodus spinulicostatus* E.R.Branson, p. 305, pl. 27, fig. 19.

1970 *Spathognathodus costatus spinulicostatus* (E.R.Branson) - Olivieri, p. 145, pl. 12, fig. 7; pl. 26, figs 9-10

1974 *Bispathodus spinulicostatus* (E.R.Branson) - Ziegler, Sandberg & Austin, p. 103, pl. 1, fig. 6-8; pl. 3, figs 20, 22 (*cum syn*.).

1975 *Bispathodus spinulicostatus* (E.R.Branson) - Ziegler *in* Ziegler (ed.), p. 43, pl. *Bispathodus*-3, figs 5-8.

2003 *Bispathodus spinulicostatus* (E.R.Branson) - Corradini, p. 85, pl. 1, figs. 10-11.

2015 *Bispathodus spinulicostatus* (E.R.Branson) – Mossoni et al., fig. 7F.

Remarks: This species of *Bispathodus* is characterized by a row of nodes on the right side of the main blade, which almost reaches the posterior end. On the left side of the main blade one or a few nodes are present on the basal cavity, these nodes can be connected to the main blade by ridges. The basal cavity is small and located in central position. *Bi. spinulicostatus* is distinguished from *Bi. ultimus* by having nodes, instead of ridges on the left side of the blade.

Range: From the Middle *expansa* Zone into the Lower Carboniferous (Ziegler & Sandberg, 1984).

Studied material: 126 elements from BTE and CM I sections.

Bispathodus stabilis (Branson & Mehl, 1934a)

Morphotype 1, Ziegler, Sandberg & Austin, 1974

(Pl. 2, fig. 8)

1934a *Spathodus stabilis* Branson & Mehl, p. 188, pl. 17, fig. 20.

1962 *Spathognathodus stabilis* (Branson & Mehl) - Ziegler, p. 110, pl. 13, figs 4-5, 9-10.

1974 *Bispathodus stabilis* (Branson & Mehl) M1 - Ziegler, Sandberg & Austin, p. 103, pl. 3, figs 1-3.

1975 *Bispathodus stabilis* (Branson & Mehl) M1 - Ziegler *in* Ziegler (ed.), p. 47, pl.*Bispathodus*-2, figs 9-11.

1985 *Bispathodus stabilis* (Branson & Mehl) M1 - Barca & Spalletta, fig. 6.7.

1985 *Bispathodus stabilis* (Branson & Mehl) - Olivieri, pl. 9, figs. 12-13.

1992 *Bispathodus stabilis* (Branson & Mehl) M1 of Ziegler *et al*. (1974)- Over, p. 307, figs. 6.1-6.16, 6.21, 6.26, 6.28.

2003 *Bispathodus stabilis* (Branson & Mehl) – Corradini, pl. 1, fig. 1.

2013a *Bispathodus stabilis* (Branson & Mehl) – Mossoni et al., fig. 6.8.

Remarks: *Bispathodus stabilis* is a pectinifom element with a thin and nearly straight blade, bearing discrete denticles. Close to the posterior end, the denticles are shorter. The basal cavity is small, more or less symmetrical, and localized beneath the posterior half of the element, but do not reaches the posterior end.

Range: *From* the Upper marginifera Zone through the Lower Carboniferous (Ziegler & Sandberg, 1984).

Studied material: 632 elements from BTE, CM I, MT, PB and PZW sections.

Bispathodus stabilis (Branson & Mehl, 1934a)
Morphotype 2, Ziegler, Sandberg & Austin, 1974

1962 *Spathognathodus stabilis* (Branson & Mehl) - Ziegler, pl. 13, figs 1-3, 6-8.

1970 *Spathognathodus stabilis* (Branson & Mehl) - Olivieri, p. 145, pl. 12, fig. 3; pl. 26, figs 3-6.

1974 *Bispathodus stabilis* (Branson & Mehl) M1 - Ziegler, Sandberg & Austin, p. 103, pl. 3, fig. 2.

1975 *Bispathodus stabilis* (Branson & Mehl) M1 - Ziegler *in* Ziegler (ed.), p. 47, pl.*Bispathodus*-2, fig. 12.

2003 *Bispathodus stabilis* (Branson & Mehl) – Corradini, pl. 1, fig. 2.

Remarks: *Bispathodus stabilis* M2 is similar to *Bi. stabilis* M1, from which differs by the shape of the basal cavity. The latter is wide, slightly asymmetrical, and reaches the posterior end of the element.

Range: From the Lower *expansa* Zone into the Lower Carboniferous (Ziegler & Sandberg, 1984).

Studied material: 135 elements from CM I section.

Bispathodus ultimus (Bischoff, 1957)
Morphotype 1, Ziegler & Sandberg, 1984
(Pl. 7, fig. 7)

1957 *Spathognathodus spinulicostatus ultimus* Bischoff - Ziegler *in* Flügel & Ziegler pl. 1, figs 10, 16, 17.
1974 *Bispathodus ultimus* (Bischoff) - Ziegler, Sandberg & Austin, p. 104, pl. 2, fig.12.
1984 *Bispathodus ultimus* (Bischoff) M1 - Ziegler & Sandberg, p. 186 (*cum syn*.).
2003 *Bispathodus ultimus* (Bischoff) – Corradini, pl. 1, fig. 12-13.
2015 *Bispathodus ultimus* (Bischoff) – Mossoni et al., fig. 7G.

Remarks: *Bispathodus ultimus* is a pectiniform element characterized by having a row of lateral ridges, perpendicular to the blade on the right side of the blade all along the element. A second row of transversal ridges occurs in the posterior half of the left side of the element. A wide-open basal cavity is located beneath the posterior half of the element, up to the posterior end. *Bi. ultimus* differs from *Bi. spinulicostatus* by having transversal ridges, instead of nodes, on the left side of the element. *Bi. ultimus* M1 is distinguished from *Bi. ultimus* M2 by the wide basal cavity.

Range: From the base of the Upper *expansa* Zone to the Middle *praesulcata* Zone (Ziegler & Sandberg, 1984).

Studied material: 156 elements from BTE, CM I and MT sections.

Bispathodus ultimus (Bischoff, 1957)
Morphotype 2, Ziegler & Sandberg, 1984

1957 *Spathognathodus ultimus* Bischoff, p. 57, pl. 4, figs. 24-26.
1969 *Spathognathodus ziegleri* Rhodes, Austin & Druce, p. 238, pl. 4, figs. 5-8.
1979 *Bispathodus ziegleri* (Rhodes, Austin & Druce) - Nicoll & Druce, p. 22, pl. 26, fig. 6.
1984 *Bispathodus ziegleri ziegleri* (Rhodes, Austin & Druce) - Luppold *in* Luppold *et al*., p. 100, pl. 4, fig. 10.
1984 *Bispathodus ultimus* (Bischoff) M2 - Ziegler & Sandberg, p. 186, tav. 2, figs. 3-5, 7 (only) (*cum syn*.).
2003 *Bispathodus ultimus* (Bischoff) M2 – Corradini, pl. 1, figs. 13-14.

Remarks: *Bispathodus ultimus* M2 differs from *Bi*. *ultimus* M1 by the relatively small basal cavity, localized more or less in central position. In addition, in *Bi*. *ultimus* M2 the ridges on the left side of the blade are somehow weaker than these on the right side.

Range: From the Upper *expansa* Zone to the Middle *praesulcata* Zone (Ziegler & Sandberg, 1984).

Studied material: 50 elements from CM I section.

Genus *Branmehla* Hass, 1959

Type species: *Spathodus inornatus* Branson & Mehl, 1934a.

Branmehla bohlenana (Helms, 1959)

(Pl. 5, figs. 12-13)

1959 *Spathognathodus bohlenanus* Helms, p. 658, pl. 6, figs 5-8.
1970 *Spathognathodus bohlenanus* Helms - Olivieri, p. 81, pl. 12, fig. 2; pl. 26, fig. 2 (*cum syn*.).
1985 *Spathognathodus bohlenanus* Helms - Barca & Spalletta, fig. 6.6.
1991 *Branmehla bohlenana* (Helms, 1959) – Perri & Spalletta, p. 59-60, pl. 3, fig. 1.
2003 *Branmehla bohlenana* (Helms, 1959) – Corradini, pl. 2, figs. 1-2.

Remarks: *Branmehla. bohlenana* is a pectiniform element characterized by a blade slightly curved in the posterior third of the element. A small, slightly asymmetrical, basal cavity is located in the posterior third of the element. It is distinguished by the other species of *Branmehla* by the asymmetrical basal cavity.

Range: From the Uppermost *marginifera* Zone to the Upper *expansa* Zone (Corradini, 2003)

Studied material: 114 elements from the BTE, CM I, MT and PB sections.

Branmehla inornata (Branson & Mehl, 1934a)

(Pl. 4, fig. 19)

1934a *Spathodus inornatus* Branson & Mehl, p. 187, pl. 17, fig. 23.
1959 *Branmehla inornata* (Branson & Mehl) - Hass, p. 381, pl. 50, fig. 3.
1962 *Spathognathodus inornatus* (Branson & Mehl) - Ziegler, p. 111, pl. 12, fig. 24.
1992 *Branmehla inornata* (Branson & Mehl) - Over, p. 308, pl. 6, fig. 31.
2003 *Branmehla inornata* (Branson & Mehl) – Corradini, pl. 2, figs. 7-8.

Remarks: *Branmehla inornata* is a pectiniform element with a straight blade. The posterior part of the blade decreases in height toward the end, while denticles are higher in the central part of the element. The cusp is only slightly highest than the adjacent denticles, and in some specimens is difficult to distinguish.
Br. inornata differs from *Br. bohlenana* by the low posterior part of the blade.

Range: From the Upper *marginifera* Zone to the Upper *praesulcata* Zone (Ziegler & Sandberg, 1984).

Studied material: 182 elements from the BTE, CM I, MT and PB sections.

Branmehla suprema (Ziegler, 1962)
(Pl. 7, fig. 10)

1962 *Spathognathodus supremus* Ziegler, p. 114, pl. 13, figs 20-26.
1991 *Branmehla suprema* (Ziegler) – Perri & Spalletta, p. 60, pl. 3, figs. 4-5.
2003 *Branmehla suprema* (Ziegler) - Corradini, p. 86-87, pl. 2, figs. 4-5.
2015 *Branmehla suprema* (Ziegler) – Mossoni et al., fig. 7J.

Remarks: *Branmehla suprema* is characterized by having a curved blade in the posterior part of the element and a strongly asymmetrical basal cavity. These peculiar characteristics allow to distinguish *Br. suprema* from all the representatives of the genus. In the studied material there is a high abundance of *Br. suprema* in the Upper *expansa* Zone.

Range: From the Upper *expansa* Zone to the Middle *praesulcata* Zone (Ziegler & Sandberg, 1984).

Studied material: 322 elements from the BTE, CM I and MT sections.

Branmehla werneri (Ziegler, 1962)

(Pl. 7, figs. 8-9)

1962 *Spathognathodus werneri* Ziegler, p. 115, pl. 13, figs 11-16.
2003 *Branmehla werneri* (Ziegler) – Corradini, pl. 2, fig. 3.
2011 *Branmehla werneri* (Ziegler) – Hartenfels, p. 231-232, pl. 36, figs. 1-3.
2015 *Branmehla werneri* (Ziegler) – Mossoni et al., figs. 7H-7I.

Remarks: A very low blade in the posterior third characterizes this species of *Branmehla*. A small cusp occur in correspondence with the variation in height of the blade. Basal cavity thin and slightly asymmetrical is developed under the all posterior third of the element. The evident difference in the height of the blade allow to distinguish *Br. werneri* from all the other species of *Branmehla*. In the studied material there is a high abundance of *Br. werneri* in the Lower *expansa* Zone.

Range: From the Lower *marginifera* Zone into the Lower *expansa* Zone (Ziegler & Sandberg, 1984).

Studied material: 3883 elements from the BTE, CM I and PB sections.

Genus *Mehlina* Youngquist, 1945

Type species: *Mehlina gradata = Mehlina irregularis* Youngquist, 1945.

Mehlina strigosa (Branson & Mehl, 1934a)

(Pl. 5, fig. 16)

1934a *Spathodus strigosus* Branson & Mehl, p. 187, pl. 17, fig. 17.
1962 *Spathognathodus strigosus* (Branson & Mehl) - Ziegler, p. 111, pl. 12, figs 21-23 (*cum syn*.).
1991 *Mehlina strigosa* Branson & Mehl- Perri & Spalletta, p. 60, pl.3, fig. 6.
2003 *Mehlina strigosa* Branson & Mehl- Corradini, p. 73, pl.2, fig. 6.

Remarks: *Mehlina strigosa* is a pectiniform element with small denticles decreasing in height in the central part of the blade. The lower margin of the anterior and posterior part of the element form an angle of about 150-160°. The edges of the basal cavity are reduced to lips.

<u>Range</u>*:* From the base of the Lower *marginifera* Zone to the Middle *praesulcata* Zone (Ziegler & Sandberg, 1984).

<u>Studied material:</u> 283 elements from the BTE, CM I, CM II and PB sections.

Family Polygnathidae Bassler, 1925

Genus *Polygnathus*, Hinde, 1879

Type species. - *Polygnathus dubius* Hinde, 1879.

Polygnathus biconstrictus Gedik, 1969

(Pl. 4, fig. 12)

1969 *Polygnathus biconstrictus* n. sp. Gedik, p. 236, pl. 4, figs. 1,2, 4-7.
1969 *Polygnathus biconstrictus* Gedik – Schönlaub, p. 332-333, pl. 1, fig. 9 (only).
1970 *Polygnathus flexomarginatus* n. sp. Olivieri,p. 122, pl. 8, figs 9-10, pl. 21, figs. 8-11.
1974 *Polygnathus biconstrictus* Gedik – Gedik, p. 18, pl. 4, figs. 1, 2, 4-7.
2003 *Polygnathus biconstrictus* Gedik - Corradini & Spalletta, p. 236, pl. 4 figs. 6-7.

<u>Remarks</u>: *Polygnathus biconstrictus* is characterized by a slender platform, slightly curved in the posterior tip. In the anterior third of the platform there is a characteristic constriction of the margins in both sides of the platform. Most of the studied material falls within the variability reported in literature, with the exception of some elements from sample MT X1 that are less ornamented than those illustrated. They show both anterior margins strongly folded toward the carina (typical of the species), but the platform is almost smooth as in *Po. communis communis*. Other elements from the same sample show anterior margins of the platform less folded than in typical elements and a generally less sturdy platform.

<u>Range</u>: From the Lower *duplicata* Zone to the *sandbergi* Zone (Schönlaub, 1969).

<u>Studied Material</u>: 214 elements from BTE and MT sections.

Polygnathus bicristatus Mossoni et al. 2015

(Pl. 6, figs. 1-7)

2005 *Polygnathus* sp. Kaiser, pl. 2, figs. 3-4.
2009 *Polygnathus* sp. B Kaiser et al., pl. 2, figs. 7-8.
2015 *Polygnathus bicristatus* Mossoni et al., pag 10-11, figs 6A-G.

Remarks: *Polygnathus bicristatus* have a subtriangular, elongated and slightly asymmetrical platform. Distinctive transversal ridges, that in their inner part almost reach the carina, constitute the ornamentation. In some elements the ridges on the posterior part of the platform are weak and look to be constituted by narrowly arranged nodes. The size of the anterior rows of nodes can be slightly different on the two sides, being one more developed that the other. *Polygnathus bicristatus* is distinguished from the other species of *Polygnathus* because of the characteristic ornamentation and the thin and elongated basal cavity. It differs from *Polygnathus* sp. B because the latter has a somewhat larger platform bearing randomly arranged nodes, instead of ridges, on its posterior part.

Studied material: 52 elements from BTE section.

Range: From the Lower *duplicata* Zone to the Upper *duplicata* Zone (Mossoni et al. 2015 in press).

Polygnathus communis communis Branson & Mehl 1934b

(Pl. 4, fig. 11)

1934b *Polygnathus communis* n.sp. Branson & Mehl, p. 293, pl. 24, figs 1-4.
1969 *Polygnathus communis communis* Branson & Mehl – Schönlaub, p. 333, pl. 1, figs 11-13.
1970 *Polygnathus communis* Branson & Mehl – Olivieri, p.121, pl. 24, figs 1-2.
1991 *Polygnathus communis communis* Branson & Mehl – Perri & Spalletta, p. 70, pl. 5, figs. 1-2.
1993 *Polygnathus communis communis* Branson & Mehl – Ji & Ziegler, p.76, pl.35, figs 4-6, text-fig. 21, figs 2, 5.
2003 *Polygnathus communis communis* Branson & Mehl – Corradini et. al., p. 236, pl. 2, figs. 6-7.

Remarks: This species of *Polygnathus* is characterized by a smooth and nearly oval platform. The basal cavity is small and is followed by a depression. From the depression starts a keel that reach the posterior end of the platform.

Range: From within the Middle *crepida* Zone into the *anchoralis-latus* Zone (Ji & Ziegler 1993).

Studied Material: 331 elements from BTE, CM I, CM II, MT and PB sections.

Polygnathus communis dentatus Druce, 1969

(Pl. 7, fig. 14)

1969 *Polygnathus communis dentatus* n.sp. Druce p. 95-96, pl. 18, figs. 13-14.

1993 *Polygnathus communis dentatus* Druce – Ji & Ziegler, p.76, pl.35, figs 7-12, text-fig. 21, fig 3.

2015 *Polygnathus communis dentatus* Druce – Mossoni et al., fig. 7P.

Remarks: *Polygnathus communis renatae* is characterized by the presence of denticulate lateral margin on each side of the anterior platform, that distinguish from all other subspecies of *Polygnathus communis*.

Studied material: 36 elements from BTE and MT sections.

Range: From the *velifer* Zone to the Lower *crenulata* Zone (Ji & Ziegler 1993).

Polygnathus communis renatae Corradini & Spalletta (in Corradini et al.), 2003

(Pl. 3, fig. 6; Pl. 7, fig. 21)

2003 *Polygnathus communis renatae* n.sp. Corradini & Spalletta (in Corradini et al.), p. 236, pl. 2, figs. 1-5.

2013b *Polygnathus communis renatae* Corradini & Spalletta – Mossoni et al., fig. 3.6.

2015 *Polygnathus communis renatae* Corradini & Spalletta – Mossoni et al., fig. 7U.

Remarks: *Polygnathus communis renatae* is characterized by the presence of a single node on the anterior lateral margin on each side of the platform, that distinguish from all other subspecies of *Polygnathus communis*. The taxon is up to now known only in Sardinia.

Studied material: 36 elements from BTE and MT sections.

<u>Range</u>: From the Lower *praesulcata* Zone to the Lower *duplicata* Zone (Mossoni et al. 2015).

Polygnathus duolingshanensis Ji & Ziegler, 1993

(Pl. 3, fig. 13)

1993 *Polygnathus duolingshanensis* n.sp. Ji & Ziegler, p. 75-76, pl. 35, figs. 13-18.

2013b *Polygnathus duolingshanensis* Ji & Ziegler - Mossoni et al., fig. 3.13.

<u>Remarks</u>: *Polygnathus duolingshanensis* is characterized by a small, symmetrical, triangular and flat platform, ornamented with short marginal ridges. The basal cavity is large and elliptical, located in the anterior end of the platform. It is distinguished from all *Polygnathus* of the "*nodocostatus*-group" for the small triangular platform with marginal short ridges.

<u>Range</u>: From the *velifer* Zone to the Lower *trachytera* Zone (Ji & Ziegler, 1993).

<u>Studied material</u>: 4 elements from BTE and MT sections.

Polygnathus diversus Helms, 1959

(Pl. 3, fig. 8)

1959 *Polygnathus diversa* n. sp. Helms, p. 650, pl. 5, figs. 5-8; text-fig. 2.

1984 *Polygnathus diversus* Helms - Olivieri, pl. 7, figs. 2-5.

2003 *Polygnathus diversus* Helms – Corradini, p. 76-77, pl. 9, figs. 8-9.

2013b *Polygnathus diversus* Helms - Mossoni et al., fig. 3.8.

<u>Remarks</u>: *Polygnathus diversus* is characterized by having a small platform, ornamented with nodes or spike-like denticles. The blade has an evident offset from the carina. It is distinguished from all *Polygnathus* of the "*nodocostatus*-group" by the distinctive offset of the carina.

<u>Range</u>: From the Lower *rhomboidea* Zone to the Lower *postera* Zone (Corradini, 2003).

<u>Studied material</u>: 39 elements from BTE, CM I and MT sections.

Polygnathus fornicatus Ji, Xiong & Wu, 1985

(Pl. 4, fig. 17)

1985 *Polygnathus fornicatus* n.sp. Ji, Xiong & Wu, p. 114, pl. 34, fig. 17.
1989 *Polygnathus fornicatus* Ji, Xiong & Wu – Ji et al., p. 87, pl. 21, figs. 1-3.
1999 *Polygnathus fornicatus* Ji, Xiong & Wu – Mawson & Talent, pl. 6, figs. 1-3, 5, 8.
2003 *Polygnathus fornicatus* Ji, Xiong & Wu – Corradini & Spalletta, p. 236, pl. 4 fig. 11.

Remarks: Only two elements have been assigned to this species. One, from sample MT X, is broken, but has the very broad platform typical of the species. The other is a very large element with a wide platform ornamented with transverse ridges, and with an upturned inner margin.

Range: From the Upper *duplicata* to the Lower *crenulata* zones (Ji et al. 1989).

Studied Material: 2 elements from MT section.

Polygnathus glaber bilobatus Ziegler, 1962

(Pl. 3, fig. 3)

1962 *Polygnathus glabra bilobata* Ziegler, p. 89, pl. 10, figs. 4-5, 16-17, 21.
1975 *Polygnathus glaber bilobatus* Ziegler - Klapper in Ziegler (ed.), p. 285, pl. *Polygnathus*-5, fig. 2 *(cum syn.*).
1984 *Polygnathus glaber bilobatus* Ziegler - Olivieri, pl. 8, fig. 4.
2003 *Polygnathus glaber bilobatus* Ziegler - Corradini, p. 80, pl. 8, fig. 7.
2013b *Polygnathus glaber bilobatus* Ziegler – Mossoni et al., fig. 3.3.

Remarks: *Polygnathus glaber bilobatus* is a subspecies of *Polygnathus glaber* characterized by having a lanceolate platform with distinctive outer lobe. It differs from the other subspecies of *Polygnathus glaber* by the occurrence of a wide lobe-like enlargement of the anterior part of the platform.

Range: From the Lower *marginifera* Zone to the Lower *trachytera* Zone (Ji & Ziegler, 1993).

Studied material: 97 elements from CM I and MT sections.

Polygnathus glaber eoglaber Ji & Ziegler, 1993

(Pl. 5, fig. 14)

1993 *Polygnathus eoglaber* Ji & Ziegler, p. 78, pl. 36, figs. 10-15; text-fig 21, fig.10.
2003 *Polygnathus glaber eoglaber* Ji & Ziegler – Corradini, p. 82, pl. 8, fig. 2.

Remarks: *Polygnathus glaber eoglaber* is characterized by a small smooth platform and by the prolongation of the carina slightly after the posterior end of the platform, almost to form a small free blade. It differ from all the subspecies of *Polygnathus glaber* by having a posterior blade.

Range: From the Upper *triangularis* Zone to the Upper *rhomboidea* Zone (Ji & Ziegler, 1993).

Studied material: 16 elements from CM I and PZW sections.

Polygnathus glaber glaber Ulrich & Bassler, 1926

(Pl. 2, fig. 13)

1926 *Polygnathus glaber* Ulrich & Bassler; p.46, pl. 7, fig.13.
1969 *Polygnathus glabra glabra* Ulrich & Bassler – Schönlaub, p. 295, pl.2, fig 14.
2003 *Polygnathus glaber glaber* Ulrich & Bassler – Corradini, p. 79-80, pl. 8, figs. 3-5.
2013a *Polygnathus glaber glaber* Ulrich & Bassler – Mossoni et al., p. 29-30, fig. 6.13.

Remarks: *Polygnathus glaber glaber* is characterized by a small, ovate shagreen platform. Few specimens present slightly raised lateral margins. It is different from *Polygnathus glaber eoglaber* by the lack of the posterior free blade.

Range: From the base of the Lower *rhomboidea* Zone into the Lower *trachytera* Zone (Corradini, 2003).

Studied material: 366 elements from BTE, CM I, CM II and PZW sections.

Polygnathus granulosus Branson & Mehl, 1934a

(Pl. 4, fig. 18)

1934a *Polygnathus granulosus* Branson & Mehl, p. 246, pl.20, fig.21, 23.

1973 *Polygnathus granulosus* Branson & Mehl - Ziegler in Ziegler (ed.), p.361, pl.Polygnathus-3, fig.6-7 (cum syn.).

1993 *Polygnathus granulosus* Branson & Mehl - Ji & Ziegler, p.80, pl.34, fig.11; text-fig.20, fig.11.

2003 *Polygnathus granulosus* Branson & Mehl – Corradini, p. 83-84, pl. 9, figs. 4-5.

Remarks: This species of *Polygnathus* is characterized by having a broad platform with a highly variable outline, from heart-shape to rounded. The surface is covered with random nodes. It is distinguished by *Polygnathus nodocostatus nodocostatus* because the latter has an ornamentation made up of aligned nodes.

Range: From the Upper *marginifera* Zone into the Lower *expansa* Zone (Corradini, 2003).

Studied material: 242 elements from all the sections.

Polygnathus longulus Corradini & Spalletta (in Corradini et al.), 2003

2003 *Polygnathus longulus* n. sp. Corradini & Spalletta, p. 237, pl. 3 figs. 13-15.

Remarks: A species of *Polygnathus* with a very slender, symmetrical and elongated platform with strongly upturned margins, denticulated anteriorly. The ornamentation consists of very faint transverse ridges. It differs from all other species of latest Devonian and Early Carboniferous polygnathids for its extremely elongate and narrow platform.

Range: Upper duplicata Zone (Corradini et al. 2003).

Material: 19 elements from the MT section.

Polygnathus marginvolutus Gedik, 1969

(Pl. 2, fig. 9)

1969 *Polygnathus marginvolutus* n. sp. Gedik, p. 237, pl. 5, figs. 2-8.
1991 *Polygnathus marginvolutus* Gedik – Perri & Spalletta, p. 71, pl. 6, figs. 1-2.
1998d *Polygnathus marginvolutus* Gedik – Perri & Spalletta, p. 179, pl. 1.5.2, fig. 7.
2013a *Polygnathus marginvolutus* Gedik – Mossoni et al., p. 30, fig. 6.9.

Remarks: This species is characterized by a subtriangular or heart-shape platform with upturned margins. The anterior margins are often scalloped. The posterior part of the platform bear weak ridges that do not reach the carina, while the anterior part is smooth.

Range: From within the Upper *trachytera* Zone to the Upper *expansa* Zone (Perri & Spalletta, 1991).

Studied material: 8 elements from PZW section.

Polygnathus mirificus Ji & Ziegler, 1993

1993 *Polygnathus mirificus* n.sp. Ji & Ziegler, pl. 37, figs. 16-21.
2013b *Polygnathus mirificus* Ji & Ziegler – Mossoni et al., p. 30.

Remarks: *Polygnathus mirificus* is characterized by an asymmetrical and lanceolate platform ornamented with transverse ridges. The anterior margin of the plat- form bears small denticles. The carina, generally extended to the posterior tip of the platform, is low and composed of fused denticles. *Polygnathus mirificus* is distinguished from *Polygnathus alatus*, *Polygnathus webbi* and *Polygnathus normalis* by having an asymmetrical platform with strong denticulate outer margin.

Range: From within the Upper *rhenana* Zone to the *linguiformis* Zone (Ji & Ziegler, 1993).

Studied material: 1 elements from PZW section.

Polygnathus nodocostatus nodocostatus Branson & Mehl, 1934a

(Pl. 2, fig. 3,14)

1934a *Polygnathus nodocostata* Branson & Mehl, p. 246, pl. 20, figs. 9-13; pl. 21, fig. 15.
1969 *Polygnathus nodocostata nodocostata* Branson & Mehl – Schönlaub, p. 295, pl. 2, fig. 12.
1970 *Polygnathus nodocostatus nodocostatus* Branson & Mehl – Olivieri, p. 125, pl. 22, fig. 1-5.
1993 *Polygnathus nodocostata nodocostata* Branson & Mehl – Ji & Ziegler, pl. 34, figs. 13-15; text-fig. 20, fig. 1.
2003 *Polygnathus nodocostatus nodocostatus* Branson & Mehl – Corradini, p. 84-85, pl. 9, figs. 1-2.
2013a *Polygnathus nodocostatus nodocostatus* Branson & Mehl – Mossoni et al., p. 30, figs. 6.3, 6.14.

Remarks: *Polygnathus nodocostatus nodocostatus* is characterized by a large platform, with a very variable outline. The platform is entirely covered by rows of nodes parallel to the carina. It is distinguished by *Polygnathus perplexus* by the lack of the collar formed by two asymmetrically developed rostral ridges, and by *Polygnathus granulosus* because the latter has a randomly disposition of the nodes in the upper surface.

Range: From the Lower *crepida* Zone to the Lower *expansa* Zone (Ji & Ziegler, 1993).

Studied material: 156 elements from BTE, CM I, CM II, MT and PZW sections.

Polygnathus nodoundatus Helms, 1961

(Pl. 3, fig. 17)

1961 *Polygnathus nodoundata* Helms, p. 690-691, pl. 1, figs. 9-11, 20; pl. 2, figs. 7, 11-14; text-fig. 8.
1990 *Polygnathus nodoundatus* Helms – Perri & Spalletta, p.66, pl. 5, figs. 7a-8b.
2003 *Polygnathus nodoundatus* Helms – Corradini, p.86, pl. 9, fig. 3.
2013b *Polygnathus nodoundatus* Helms – Mossoni et al., fig. 3.17.

Remarks: *Polygnathus nodoundatus* is characterized by having an asymmetrical platform. The inner margin is straight, and the outer is concave in the anterior part and convex posteriorly. The platform bears random nodes, which in juvenile specimens can be aligned in parallel rows. The rows are present only in the anterior part of the platform, where they form a collar beside the carina. The platform shape *Po. nodoundatus* is distinctive respect all the other representatives of the "*nodocostatus* group".

Range: From the Upper *marginifera* Zone to the Lower *trachytera* Zone (Perri & Spalletta, 1990).

Studied material: 27 elements from CM I and MT sections.

Polygnathus normalis Miller & Youngquist, 1947
(Pl. 4, fig. 5)

1947 *Polygnathus normalis* n. sp. Miller & Youngquist, p. 515, pl. 74, figs. 4-5.

1966 *Polygnathus normalis* Miller & Youngquist – Glenister & Klapper, p. 829-830, pl. 95,fig. 6,21-22.

1993 *Polygnathus normalis* Miller & Youngquist – Ji & Ziegler, pl. 39, figs. 9-15; text-fig. 18, fig.14.

Remarks: *Polygnathus normalis* is characterized by having an asymmetric platform with a posterior margin incurved and a slightly constricted anterior margin. The platform is covered by transversal ridges. Some authors consider *Polygnathus normalis* as young synonym of *Polygnathus webbi*. However I believe that the two forms are different species because *Polygnathus webbi* has a strongly constricted anterior platform and a more expanded posterior outer platform.

Range: From within the Upper *rhenana* Zone to the Lower *postera* Zone (Ji & Ziegler, 1993).

Studied material: 136 elements from CM I, CM II and PZW section.

Polygnathus nuragicus Mossoni et al., 2015
(Pl. 6, figs. 13-19)

2015 *Polygnathus nuragicus* Mossoni et al. n.sp., p. 11-12, figs.7M-7S.

Remarks: *Polygnathus nuragicus* is distinguished from representatives of *Po. communis* group because of the lack of the well evident depression just posterior of the basal cavity, and because the keel starts from the basal cavity. It differs from *Po. tenuiserratus* for the shape of the platform and because the latter has the ornamentation limited to the external margins; it is different from *Po. biconstrictus* because the latter has a constricted anterior part of the platform with margins folded upward.

<u>Range</u>: Lower *duplicata* Zone (Mossoni et al. 2014).

<u>Studied material</u>: 30 elements from BTE section.

Polygnathus obliquicostatus Ziegler, 1962

(Pl. 2, fig. 12)

1962 *Polygnathus obliquicostatus* n.sp. Ziegler, p. 92, pl. 11, figs 8-12.

1970 *Polygnathus obliquicostatus* Ziegler - Olivieri, p. 128, pl. 23, figs 4-5.

1993 *Polygnathus obliquicostatus* Ziegler – Ji & Ziegler, text-fig. 19, fig.5.

1998c *Polygnathus obliquicostatus* Ziegler - Perri & Spalletta, p. 166, pl. 1.4.2, figs. 10a-b.

2003 *Polygnathus obliquicostatus* Ziegler – Corradini & Spalletta, p. 237, pl. 4 fig. 9.

2003 *Polygnathus obliquicostatus* Ziegler - Corradini, p. 112, pl.10, figs. 3-5.

2013a *Polygnathus obliquicostatus* Ziegler – Mossoni et al., p. 30-31, fig. 6.12.

<u>Remarks</u>: *Polygnathus obliquicostatus* is characterized by a thin and elongated platform, with the posterior part turned downward. The platform bears oblique transverse ridges that forms an angle of about 45° with the carina, more evident posterior of the carina, where occupy the whole platform. It is distinguished by *Polygnathus semicostatus* because the latter has on the inner platform ridges perpendicular to the carina, and a generally more developed tongue. It differs from *Polygnathus extralobatus* in the more thinly and symmetrical platform.

<u>Range</u>: From the Lower *styriacus* Zone to the Lower *praesulcata* Zone (Corradini et al., 2003).

<u>Studied material</u>: 96 elements from BTE, CM I and MT sections.

Polygnathus pennatuloideus Holmes, 1928

(Pl. 3, fig. 16)

1928 *Polygnathus pennatuloidea* n.sp. Holmes, p. 32-33, pl. 11, fig. 14.

1966 *Polygnathus pennatuloidea* Holmes – Glenister & Klapper, p. 830, pl. 94, figs. 12-13.

1993 *Polygnathus pennatuloidea* Holmes – Ji & Ziegler, p. 83, pl. 34, fig.12; text. fig. 20, fig. 10.

2013b *Polygnathus pennatuloideus* Holmes - Mossoni, fig. 3.16.

Remarks: *Polygnathus pennatuloideus* is characterized by having an asymmetrical platform in which the inner part is widest anteriorly and the outer is widest posteriorly, giving almost a sigmoidal shape. The basal cavity is small and elongated, there is a keel that is continuous throughout the length of the inferior platform. It is distinguished from *Polygnathus nodocostatus nodocostatus* mainly in the outline and the ornamentation of the platform.

Range: From the Upper *marginifera* Zone to the Lower *expansa* Zone (Ji & Ziegler, 1993).

Studied material: 1 element from the MT section.

Polyngathus perplexus Thomas, 1949

(Pl. 5, fig. 5)

1949 *Polygnathus perplexa?* Thomas, p. 418, pl. 2, fig. 23.
1961 *Polygnathus perplexa* Thomas - Helms, p. 692, pl. 1, figs 18-19; pl. 4, figs 1-3, 5; text-fig. 10.
1970 *Polygnathus perplexus* Thomas - Olivieri, p. 129, pl. 22, figs 6-7.
2003 *Polygnathus perplexus* Thomas - Corradini, pl. 9, fig 15.

Remarks: *Polygnathus perplexus* has a slender and slightly asymmetrical platform, covered by nodes arranged in longitudinal rows. The anterior part of the platform bears two unequal collar ridges parallel to the carina. *Polygnathus* perplexus differs from *Polygnathus nodocostatus nodocostatus* by having a collar ridges in the anterior platform; it is distinguished by *Polygnathus margaritatus* by having an asymmetrical platform and the unequal collar ridges in the anterior platform.

Range: From the Upper *marginifera* Zone to the Middle *expansa* Zone (Ji & Ziegler, 1993).

Studied material: 48 elements from BTE, CM I & PB sections.

Polygnathus purus purus Voges, 1959

(Pl. 7, fig. 15)

1959 *Polygnathus purus purus* n.sp. Voges: , p. 291-292, pl. 34, figs 21-26.
1969 *Polygnathus purus purus* Voges – Schönlaub, p. 336, pl. 1, fig. 16.
1970 *Polygnathus purus purus* Voges – Olivieri, pl. 11, figs 9-11; pl.25, figs 1-5.
1973 *Polygnathus purus purus* Voges – Szulczewski, p. 40-41, pl. 3, fig 7.
1974 *Polygnathus purus purus* Voges – Gedik, p. 20-21, pl. 4, figs 20-21.
2003 *Polygnathus purus purus* Voges – Corradini & Spalletta, p. 19, pl. 2 figs 8-10.
2015 *Polygnathus purus purus* Voges – Mossoni, fig 7O.

Remarks: Elements attributed to this species display a wide range of minor variations in outline of the platform; the inner and outer side may be more or less symmetrical. In several elements the platform is strongly asymmetrical, with one of the anterior margins not rounded, but sloping from the blade towards the middle part of the platform, where the unit is widest. The anterior right and left margins of the platform may be opposite each other or may meet the blade at different points.

Range: From the Upper *expansa* Zone to the Lower *crenulata* Zone (Ji & Ziegler 1993).

Studied Material: 531 element from BTE, CM I and MT sections.

Polygnathus rhabdotus Schäfer, 1976

(Pl. 5, figs. 17-18)

1957 *Polygnathus rhabdotus* Schäfer, p. 146, pl. 1, figs 18-22.
2003 *Polygnathus rhabdotus* Schäfer – Corradini, p. 19, pl. 2 figs 8-10.

Remarks: *Polygnathus rhabdotus* is characterized by a slightly asymmetrical, elongated, subtriangular platform, tipped posteriorly. The ornamentation is made up of transversal ridges in the anterior part of the platform, and by small, randomly arranged nodes in the posterior part. The particular ornamentation allow to distinguish *Polygnathus rhabdotus* from all the other species of *Polygnathus*.

Range: From the Lower *postera* Zone to the Middle *expansa* Zone (Schäfer 1976, Corradini 2003).

Studied material: 692 elements from CM I and PB sections.

Polygnathus cf. *rhabdotus* Schäfer, 1976

2011 *Polygnathus* cf. *rhabdotus* Schäfer – Hartenfels, p. 299, pl. 58 fig 5.

Remarks: *Polygnathus* cf. *rhabdotus* is characterized by a slightly asymmetrical subtriangular platform, tipped posteriorly. The inner platform surface is smooth and the ornamentation is restricted to few nodes on the platform margin. The ornamentation made up of just few nodes distinguish *Polygnathus* cf. *rhabdotus* from *Polygnathus rhabdotus.*

Range: Upper *trachytera* Zone (Hartenfels 2011).

Studied material: 692 elements from CM I and PB sections.

Polygnathus pusillus Corradini & Spalletta (in Corradini et al.), 2003

(Pl. 4, figs. 8a-8b)

2003 *Polygnathus pusillus* n. sp. Corradini & Spalletta, p. 238, pl. 2 figs 12-15

Remarks: *Polygnathus pusillus* is characterized by a small, narrow, pointed platform and relatively long free blade. The platform is smooth, flat to slightly concave differs from all the other Early Carboniferous species in having a very small, unornamented platform and a basal cavity followed by a high keel.

Range: Upper *duplicata* Zone (Corradini & Spalletta, 2003).

Studied Material: 62 elements from MT section.

Polygnathus sp. A

(Pl. 6, figs. 8-11)

2015 *Polygnathus* sp. A. Mossoni et al., fig. 6H-K.

Remarks: The elements assigned to this species are slender and have a lanceolate platform tipped in the posterior part. The anterior margins of the platform reach the carina with a sharp angle. The platform is ornamented with weak ridges and has reinforced edges at its point of maximum width. Posterior end of the platform tipped.

Po. sp. A is distinguished from the *Po*. *nuragicus* because the latter has thickened margins in the anterior part of the platform. The lanceolate elongated platform of the platform distinguish *Po*. sp. A from *Po*. *tenuiserratus*.

Studied material: 9 elements from BTE section.

Range: Lower *duplicata* Zone (Mossoni et al. 2015).

Polygnathus sp. B

(Pl. 6, fig. 12)

2015 *Polygnathus* sp. B. Mossoni et al., fig. 6L.

Remarks: *Polygnathus* sp. B is distinguished from *Polygnathus bicristatus* by the generally wider platform and the ornamentation constituted by randomly arranged nodes on the posterior part of the platform.

Studied material: 4 elements from BTE section.

Range: Lower *duplicata* Zone (Mossoni et al. 2015).

Polygnathus styriacus Ziegler, 1957

(Pl. 2, fig. 7; Pl. 7, fig 1)

1957 *Polygnathus styriacus* Ziegler, p. 47, pl. 1, figs. 12-13.
1993 *Polygnathus styriacus* Ziegler – Ji & Ziegler, p. 84, pl.34, fig.6-10; text-fig.20, fig.12.
1998d *Polygnathus styriacus* Ziegler – Perri & Spalletta, p. 179, pl. 1.5.2, fig. 8.
1998g *Polygnathus styriacus* Ziegler – Perri & Spalletta, p. 226, pl. 2.5.1, fig. 8.
2003 *Polygnathus styriacus* Ziegler – Corradini, p. 110, pl. 9, fig. 10.
2011 *Polygnathus styriacus* Ziegler - Tragelehn & Hartenfels, p. 12, pl. 1, figs. 10-19.
2011 *Polygnathus styriacus* Ziegler - Hartenfels, p. 303-305, pl. 55, figs 2-4.
2013a *Polygnathus styriacus* Ziegler - Mossoni et al., p. 31, Fig. 6.7.
2015 *Polygnathus styriacus* Ziegler - Mossoni et al., fig. 7A.

Remarks: *Polygnathus styriacus* is characterized by a small sub-triangular platform covered by weak nodes irregularly arranged in the posterior part. The anterior part of the platform is not ornamented, and is strongly deflected downward. *Polygnathus styriacus* differs from *Polygnathus vogesi* by the ornamentation pattern. It is distinguished from *Polygnathus granulosus* by the sub-triangular platform and the downward deflection of the anterior part of the platform.

Range: From the base of the Lower *styriacus* Zone (Lower *postera* Zone) to the Lower *expansa* Zone (Ji & Ziegler, 1993)

Studied material: 389 elements from BTE, CM I, MT, PB and PZW sections.

Polygnathus subirregularis Sandberg & Ziegler, 1979

(Pl. 4, fig. 9)

1979 *Polygnathus subirregularis* n.sp. Sandberg & Ziegler, p. 186, pl. 4, figs. 9-13.
1993 *Polygnathus subirregularis* Sandberg & Ziegler – Ji & Ziegler, text-fig.20, fig.8.

Remarks: *Polygnathus subirregularis* is characterized by an elongate, ovate platform.The platform is ornamented with row of nodes parallel to the carina, separated from it by adcarinal grooves. The outer adcarinal groove extend to the posterior tip and is generally shallower than the inner groove. The carina is sharply deflected outward at midlenght of the platform.

<u>Range</u>: From the base of the Lower *trachytera* Zone to the Lower *expansa* Zone (Ji & Ziegler, 1993)

<u>Studied material</u>: 343 elements from MT and PB sections.

Polygnathus tenuiserratus Corradini & Spalletta (in Corradini et al.), 2003

(Pl. 7, fig. 12)

2003 *Polygnathus tenuiserratus* n. sp. Corradini & Spalletta, p. 239, pl. 3 fig. 1-10.
2015 *Polygnathus tenuiserratus* Corradini & Spalletta- Mossoni et al., fig. 7L.

<u>Remarks</u>: *Polygnathus tenuiserratus* has a nearly symmetrical, flat platform, lanceolate to ovate in outline. The basal cavity is small with raised margins. It is located in the anterior part of the platform and is followed by a keel that reach the posterior tip. It differs from *Polygnathus biconstrictus* because the latter show the tipical constriction in the anterior part of the platform.

<u>Range</u>: Lower and Upper *duplicata* Zones, Corradini & Spalletta (in Corradini et al. 2003)

<u>Studied Material</u>: 437 elements from BTE and MT, sections.

Genus *Pseudopolygnathus*, Branson & Mehl, 1934b

Pseudopolygnathus bidentatus Traghelen & Hartenfels, 2011

(Pl. 3, fig. 11)

2011 *Pseudopolygnathus bidentatus* n.sp – Traghelen & Hartenfels, p. 7-8, pl. 2, figs. 4-6.
2013b *Pseudopolygnathus bidentatus* Traghelen & Hartenfels – Mossoni et al., fig. 3.11.

<u>Remarks</u>: *Pseudopolygnathus bidentatus* is characterized by having a slightly asymmetrical, slender platform that bear a distinctive node on each side. The basal cavity is wide in the anterior part and extends to the rear-end. It is distinguished from the other species of *Pseudopolygnathus* by the presence of the single node on each side of the platform.

<u>Range</u>: From the Upper *styriacus* Zone to the Lower *expansa* Zone (Traghelen & Hartenfels, 2011).

<u>Studied material</u>: 1 element from MT section.

Pseudopolygnathus controversus Sandberg & Ziegler, 1979

(Pl. 2, fig. 6)

1979 *Pseudopolygnathus controversus* n.sp. Sandberg & Ziegler, p. 182, pl.3, figs. 12-17.

1998f *Pseudopolygnathus controversus* Sandberg & Ziegler – Perri & Spalletta, p. 226, pl. 2.5.1, fig. 10.

2011 *Pseudopolygnathus controversus* Sandberg & Ziegler – Hartenfels, p. 510, pl. 62, figs. 10-11.

2013a *Pseudopolygnathus controversus* Sandberg & Ziegler – Mossoni et al., p.31, fig. 6.6.

<u>Remarks</u>: *Pseudopolygnathus controversus* is characterized by an asymmetrical lanceolate platform with an ornamented surface. The length of the right side of the platform extends much farther anteriorly than the left side as a row of transverse ridges or nodes. It is distinguished from *Pseudopolygnathus brevipennatus* by the asymmetrical platform.

<u>Range</u>: From the Upper *styriacus* Zone to the Lower *expansa* Zone (Sandberg & Ziegler, 1979).

<u>Studied material</u>: 5 elements from the PZW section.

Pseudopolygnathus dissimilis (Helms & Wolska, 1967)

(Pl. 5, fig. 9)

1967 *Polygnathus dissimilis* Helms & Wolska, p. 229, fig. 2.

2003 *Pseudopolygnathus dissimilis* (Helms & Wolska) – Corradini, p. 91, pl. 10, fig. 10-11.

<u>Remarks</u>: *Pseudopolygnathus dissimilis* has a strongly asymmetrical platform, wider on the outer side. Adcarinal throughts are normally present at both sides of the carina. The ornamentation is made up of nodes on the anterior part, more developed close to the margins of the platform. It is distinguished from all the other species of pseudopolygnathus because of the asymmetrical platform.

Range*: From the upper part of the Lower expansa* Zone into the Middle *expansa* Zone*.*

Studied Material: 40 elements from CM I and MT section.

Pseudopolygnathus granulosus Ziegler, 1962

(Pl. 3, fig. 7)

1956 *Pseudopolygnathus* n.sp. Bishoff & Ziegler, p. 164, pl. 11, figs. 1-2.

1962 *Pseudopolygnathus granulosa* n.sp Ziegler, p. 99-100, pl. 11, figs. 25-30.

2011 *Pseudopolygnathus granulosus* Ziegler – Hartenfels, p. 311-312, pl. 62, figs. 2-4.

2013b *Pseudopolygnathus granulosus* Ziegler – Mossoni et al., fig. 3.7.

Remarks: This species of *Pseudopolygnathus* is characterized by a platform that tapers posteriorly. The surface bear strong nodes that are generally aligned in longitudinal rows. The basal cavity is in the anterior part of the lower side and is wide. It is distinguished from *Ps. marburgensis marburgensis* and *Ps. granulobatus* because *Ps. granulosus* has less distinct lobes, if developed at all.

Range: From the Upper *trachytera* Zone into the Upper *postera* Zone (Hartenfels, 2011)*.*

Studied Material: 51 elements from BTE, MT and PB sections.

Pseudopolygnathus granulobatus Mossoni et al., 2015

(Pl. 6, figs. 21-24)

2015 *Pseudopolygnathus granulobatus* n.sp. Mossoni et al., fig. 6U-Z.

Remarks: A species of *Pseudopolygnathus* characterized by an asymmetrical, strongly heart-shaped, ornamented platform, with a distinctive lateral lobe. The platform is large in the anterior part and narrow posteriorly. The basal cavity is large and extends below the whole element. *Ps. granulobatus* is distinguished from *Ps. granulosus* by the pronounced lobe in one side of the platform and from *Ps. marb. trigonicus* because the latter shows a row of distinctive nodes in the anterior part of the platform and has a distinctive basal cavity. The ornamentation is more pronounced in the large elements, than in the small ones.

Studied material: 12 elements from BTE section.

Range: Middle *expansa* Zone (Mossoni et al 2015).

Pseudopolygnathus irregularis Traghelen & Hartenfels, 2011

(Pl. 3, fig. 10)

2011 *Pseudopolygnathus irregularis* n. sp. Traghelen & Hartenfels; p. 8, pl. 2, fig. 16-23.

2013a *Pseudopolygnathus irregularis* Traghelen & Hartenfels – Mossoni et al., p. 31-32, fig. 6.4.

2013b *Pseudopolygnathus irregularis* Traghelen & Hartenfels – Mossoni et al., fig. 3.10.

Remarks: This species of *Pseudopolygnathus* has an asymmetrical platform, which extends to the posterior tip of the element. The outline of the platform is irregular and the edges are slightly raised. The surface is ornamented with distinctive and irregular nodes. It is distinguished from the others species of *Pseudopolygnathus* by the irregular outline of the platform and by the ornamentation.

Range: From the Upper *styriacus* Zone to the Lower *expansa* Zone (Traghelen & Hartenfels, 2011).

Studied material: 7 elements from MT and PZW sections.

Pseudopolygnathus marburgensis marburgensis Bishoff & Ziegler, 1956

(Pl. 2, fig. 10)

1956 *Pseudopolygnathus marburgensis* n. sp. Bishoff & Ziegler, p. 162-163, pl. 11, figs 9, 11-13.

1979 *Pseudopolygnathus marburgensis marburgensis* Bishoff & Ziegler - Sandberg & Ziegler, p. 182, pl.3, figs.1-4.

2011 *Pseudopolygnathus marburgensis marburgensis* Bishoff & Ziegler – Hartenfels, p. 512, pl. 64, fig. 5.

2013a *Pseudopolygnathus marburgensis marburgensis* Bishoff & Ziegler– Mossoni et al., p. 32, fig. 6.10.

Remarks: This subspecies of *Pseudopolygnathus marburgensis* is characterized by a trilobate platform and a trilobate basal cavity. The upper surface of the platform is strongly ornamented, with some distinctive nodes in the anterior part of the platform. The outer lobe has a secondary carina that forms nearly a right angle with the main carina, the inner lobe bear large crowded nodes or a bifurcate pattern. This subspecies of *Pseudopolygnathus marburgensis marburgensis* differs from *Pseudopolygnathus marburgensis trigonicus* because the latter has a cross-shape basal cavity.

Range: From the Upper *styriacus* Zone to the Middle *expansa* Zone (Ziegler & Sandberg, 1984).

Studied material: 2 elements from the PZW section.

Pseudopolygnathus marburgensis trigonicus Ziegler, 1962
(Pl. 7, fig. 11)

1962 *Pseudopolygnathus trigonica* Ziegler, p. 101, pl. 12, figs. 8-13.
1970 *Pseudopolygnathus trigonicus* Ziegler – Olivieri, p. 137, pl. 25, figs. 9-10.
1979 *Pseudopolygnathus marburgensis trigonicus* Ziegler - Sandberg & Ziegler, p. 182.
2003 *Pseudopolygnathus marburgensis trigonicus* Ziegler – Corradini, p. 99-100, pl. 10, figs. 12-13.
2015 *Pseudopolygnathus marburgensis trigonicus* Ziegler – Mossoni, fig. 7K.

Remarks: *Pseudopolygnathus marburgensis trigonicus* is similar to *Ps. m. marburgensis* for the general shape of the platform. Nevertheless, it differs from the latter by the asymmetry of lateral lobes and the weak ornamentation on the platform. The basal cavity has restricted lobes that form a pseudokeel on the posterior lobe.

Range: From the Upper *expansa* Zone to the Middle *praesulcata* Zone (Ziegler & Sandberg, 1984).

Studied material: 50 elements from BTE, CM I and MT sections.

Pseudopolygnathus marginatus (Branson & Mehl, 1934b)
(Pl. 4, fig. 10)

1934b *Polygnathus marginata* n.sp. Branson & Mehl, p. 294-295, pl. 23, figs 25-27.

1981 *Pseudopolygnathus marginatus* (Branson & Mehl) – Klapper (*in* Ziegler), p. 387-389, pl. *Pseudopolygnathus*-3, figs. 4-5 (*cum syn*.).

2003 *Pseudopolygnathus marginatus* (Branson & Mehl) – Corradini & Spalletta, p.239, pl. 5, fig. 3.

Remarks: *Pseudopolygnathus marginatus* has a symmetrical lanceolate platform. The ornamentation is made up of transverse ridges that extends from the margins to near the carina. It can be distinguished from *Pseudopolygnathus fusiformis* because the latter has a thinner and elongate platform.

Range: From the Lower *duplicata* Zone to the *isosticha*-Upper *crenulata* Zone (Corradini & Spalletta 2003).

Studied Material: 6 elements from and MT section.

Pseudopolygnathus micropunctatus Bischoff & Ziegler, 1956

(Pl. 2, fig 5; Pl. 3, fig. 12)

1956 *Pseudopolygnathus micropunctata* Bischoff & Ziegler, p. 163, pl. 11, figs 7-8, 10.

1979 *Pseudopolygnathus* cf. *micropunctatus* Bischoff & Ziegler - Sandberg & Ziegler, p. 183, pl. 3, figs. 5-7.

1998f *Pseudopolygnathus micropunctatus* Bischoff & Ziegler – Perri & Spalletta, p. 226, pl. 2.5.1, fig. 12.

2003 *Pseudopolygnathus micropunctatus* Bischoff & Ziegler - Corradini, p. 112, pl. 10, fig. 14.

2011 *Pseudopolygnathus micropunctatus* Bischoff & Ziegler – Hartenfels, p. 510, pl. 63, figs. 1-6, 8-10.

2013a *Pseudopolygnathus micropunctatus* Bischoff & Ziegler – Mossoni et al., p. 32, fig. 6.5.

2013b *Pseudopolygnathus micropunctatus* Bischoff & Ziegler – Mossoni et al., fig. 3.12.

Remarks: This species is characterized by a lanceolate platform with a shagreen surface. Some specimens show a weak lobe in the inner part of the platform, but it is not a distinctive character. The weak ornamentation distinguish *Pseudopolygnathus micropunctatus* among all the other representative of genus *Pseudopolygnathus*.

Range: From the Upper *trachytera* Zone to the Upper *expansa* Zone (Corradini, 2003).

Studied material: 12 elements from CM I, MT and PZW sections.

Pseudopolygnathus primus Branson & Mehl, 1934b

(Pl. 3, fig. 18)

1934b *Pseudopolygnathus prima* n.sp. Branson & Mehl, 298, pl. 24, fig. 24-25.

1970 *Pseudopolygnathus dentilineatus* E.R. Branson – Olivieri, p. 135, pl. 24, fig. 7.

1993 *Pseudopolygnathus dentilineatus* E.R. Branson – Ji & Ziegler, pl. 43, fig. 18.

1993 *Pseudopolygnathus primus* Branson & Mehl – Ji & Ziegler, pl. 43, fig. 19.

2003 *Pseudopolygnathus primus* Branson & Mehl – Corradini & Spalletta, p.239, pl. 5 figs. 5-6.

2013b *Pseudopolygnathus primus* Branson & Mehl – Mossoni et al., fig. 3.18.

Remarks: *Pseudopolygnathus primus* is characterized by a variable outline of the platform. Some elements present a pointed, restricted platform and others a wider platform more rounded anteriorly. In some elements the denticulation extends further anteriorly on the right side of the platform. The ornamentation also is variable; there are elements ornamented with strong transverse ridges running along the whole width of the platform and others bearing transverse ridges, and/or very large nodes, on the platform margins.

Range: From the highest part of the Lower *expansa* Zone (Klapper *in* Ziegler 1981) to the Lower *crenulata* Zone (Sandberg *et al*. 1978).

Studied Material: 35 elements from BTE and MT sections.

Pseudopolygnathus rapiformis Corradini & Spalletta (in Corradini et al.), 2003

(Pl. 4, figs. 7a-b)

1959 *Pseudopolygnathus* cf. *fusiformis* Branson & Mehl – Voges, p. 295, pl. 34, figs. 42-44.

1969 *Pseudopolygnathus fusiformis* Branson & Mehl – Schönlaub, p. 339, pl. 1, fig. 14.

1974 *Pseudopolygnathus fusiformis* Branson & Mehl – Gedik, p. 22, pl. 5, fig. 22 (only).

2003 *Pseudopolygnathus rapiformis* Corradini & Spalletta, p.240, pl. 5 figs. 1-2

Remarks: A species of *Pseudopolygnathus* characterized by a narrow, almost smooth, and symmetrical platform, tapering distinctively towards the pointed posterior end. The carina is more or less curved near the posterior end. The basal cavity is drop-like, continuing to the tip as a sharp keel.

Pseudopolygnathus rapiformis differs from *Pseudopolygnathus fusiformis* bacause the platform margins are not denticulate, and because the latter is characteristically straight, whereas forms attributed to *Pseudopolygnathus rapiformis* are curved near the posterior end.

Range: From the Upper *duplicata* Zone to the *sandbergi* Zone (Voges 1959).

Studied Material: 16 elements from BTE section.

Pseudopolygnathus triangulus triangulus Voges, 1959

(Pl. 7, fig. 22)

1959 *Pseudopolygnathus triangula triangula* n.ssp*.* Voges, p. 304-305, pl. 35, figs. 7-13, text-fig. 5.

1989 *Pseudopolygnathus triangulus triangulus* Voges – Ji et al., p. 94, pl. 23, figs. 3-5.

1993 *Pseudopolygnathus triangulus triangulus* Voges – Ji & Ziegler, pl. 43, fig. 15.

2003 *Pseudopolygnathus triangulus triangulus* Voges - Corradini et al., p.241, pl. 5 fig. 4.

2015 *Pseudopolygnathus triangulus triangulus* Voges – Mossoni et al., fig 7V.

Remarks: *Pseudopolygnathus triangulus triangulus* is characterized by having a triangular platform. The upper surface is ornamented with transverse ridges. On the lower side a wide basal cavity is located at the beginning of the platform and it is followed by a keel that reach the posterior tip. It is distinguished by the other species of *Pseudopolygnathus* for the triangular platform.

Range: From the Upper *duplicata* Zone (Ji & Ziegler 1993) to the *isosticha*-Upper *crenulata* Zone (Sandberg *et al*. 1978).

Studied Material: 35 elements from BTE and MT section.

Genus *Icriodus* Branson & Mehl, 1938

Icriodus alternatus alternatus Branson & Mehl, 1934a

(Pl. 1, fig. 5)

1934a *Icriodus alternatus alternatus* n.sp. Branson & Mehl, p. 225-226, pl. 13, figs. 4-6.

1984 *Icriodus alternatus alternatus* Branson & Mehl – Sandberg & Dreesen, pl. 2, figs. 5.11.

1993 *Icriodus alternatus alternatus* Branson & Mehl – Ji & Ziegler, p.55, pl. 5, figs. 5-8;text-fig. 6, fig 2.

1998d *Icriodus alternatus alternatus* Branson & Mehl – Perri & Spalletta, p. 204, pl. 2.2.1, figs. 4-5.

2003 *Icriodus alternatus alternatus* Branson & Mehl – Corradini, p. 92, pl.2, figs. 9-12.

2013a *Icriodus alternatus alternatus* Branson & Mehl – Mossoni et al., p. 21, fig. 5.5.

Remarks : *Icriodus alternatus alternatus* is characterized by a thin and elongated platform. It has three rows of longitudinal nodes that covered the platform. The central row is located anterior to those of the lateral rows. The central raw has a cusp at the posterior end. The basal cavity is deep and narrow in the anterior half of the platform, wider in the posterior third. It is distinguished from *Icriodus alternatus helmsi,* which has the posterior cusp aligned with one of the lateral rows.

Range: From the Upper *rhenana* Zone to the Uppermost *crepida* Zone (Schülke, 1999).

Studied material: 197 elements from BTE, CM II and PZW sections.

Icriodus olivierii Corradini, 1998

(Pl. 1, fig. 10)

1970 *Icriodus symmetricus* Branson & Mehl – Olivieri, pl.14, fig 9.

1998 *Icriodus olivierii* Corradini – Corradini, pl. 1.4.1, fig. 8.

2003 *Icriodus olivierii* Corradini – Corradini, p. 92-93, pl. 2, figs. 14-21 (cum syn.).

2013b Corradini – Mossoni et al., p. 21-22, fig. 5.10.

Remarks: *Icriodus olivierii* is characterized by having a thin and elongated platform, with the longitudinal axis straight or slightly curved. There are three rows of longitudinal nodes. The nodes of the middle row laterally compressed and longitudinally elongated, in some cases are almost joined together. The basal cavity is deep and narrow in the anterior half of the platform, wider posteriorly.

Range: From the Upper *rhenana* Zone to the Uppermost *crepida* Zone (Corradini, 2003).

Studied material: 237 elements from CM I, CM II and PZW sections.

ACKNOWLEDGMENTS

The first thanks goes to Prof. Carlo Corradini that introduced me to the biostratigraphy and taught me all that I know about conodonts and palaeontology. All the advices and the help during the lasts three years have been the base of this work. Thank you Carlo!

Claudia, Luca e Monica thanks for all the advices and the time spent in the Carnic Alps. I have learnt a lot from you during the time spent together! I will never forget the lunches and the dinners..amazing!

Dr Anne Christine Da Silva and Dr Simo Spassov thanks for your help with the issues of the magnetic susceptibility and for allowing me to work in your laboratories.

Nicola Carta thanks for the help during the time spent in the field in Sardinia.

Thanks to Elena Spano that taught me how to process the samples for the geochemical analysis and for the help during the measures!

I am grate to Prof. Alfredo Loi and to Prof. Hanna Matyja that helped me with the thesis, giving me great advices to improve my work.

Major thanks to my family that gave me all the support during the nine years spent studying geology and palaeontology. It because of your sacrifices that I have been able to go this far. Thank you Mama, Thank you Dad! A special thanks to my sister, my grandmothers, all my uncles and friends..

Last but not least, Maria Giovanna..always by my side no matter what..always supporting me when I needed the most and pushing me to go forward..Thanks..I love you!

I gratefully acknowledges Sardinia Regional Government for the financial support of my PhD scholarship (P.O.R. Sardegna F.S.E. "Operational Programme of the Autonomous Region of Sardinia, European Social Fund 2007–2013" – Axis IV Human Resources, Objective l.3, Line of Activity l.3.1.).

REFERENCES

1. Austin R.L. & Rhodes F. H. T. 1981 Cavusgnathidae. Treatise on Invertebrate Paleontology, Part W, Miscellanea, Supplement 2, Conodonta, Geological Society of America and the University of Kansas 158-160.
2. Bagnoli G., Ferretti A., Serpagli E., Vai G.B. 1998. Late Ordovician conodonts from the Valbertad Section (Carnic Alps). In: Perri MC, Spalletta C (eds) Southern Alps Field Trip Guidebook. In: Seventh international conodont symposium held in Europe, 1998. *Giornale di Geologia*, Special Issue, vol 60, pp 138–149.
3. Bandel K. 1972. Palökologie und Paläogeographie im Devon und Unterkarbon der zentralen Karnischen Alpen. *Palaeontographica Abhandlunghen A* 141(1–4): 1–117.
4. Bandel K. 1974. Deep-water limestones from the Devonian-Carboniferous of the Carnic Alps, Austria. In: Hsu KJ, Jenkyns HC (eds) Pelagic sediments: on land and under the Sea. *IAS Spec Publ*, vol 1. Wiley, New York, pp 93–116.
5. Barca S. & Spalletta C. 1985. Nuove osservazioni sul conglomerato di Villasalto (Carbonifero inferiore-medio, Sardegna). *Giornale di Geologia S3 46*, 25-32.
6. Barca S. & Jaeger H. 1990. New geological and biostratigraphical data on the Silurian in SE Sardinia. Close affinity with Thuringia. *Bollettino della Società Geologica Italiana*, 108 (1989): 565-580.
7. Barca S., Corradini C., Ferretti A., Olivieri R. & Serpagli E. 1995. Conodont biostratigraphy of the "Ockerkalk" (Silurian) from Southeastern Sardinia. *Rivista Italiana di Paleontologia e Stratigrafia*, 100, 459-476.
8. Bassler R. 1925. Classification and stratigraphic use of the conodonts. *Bulletin. Geological Society of America*, 36, 218-220.
9. Bateson W. 1885. The later stages in the development of Balanoglossus kowalevskii, with a suggestion as to the affinities of the Enteropneusta. *Quarterly Journal of Microscopical Science* 25: 81-122.
10. Becker H. & Fassbinder J.W.E 1999. Magnetometry of a Scythian settlement in Siberia near Cicahin the Baraba Steppe 1999. In "3rd International Conference on Archaeological Prospection" (J. W. E. Fassbinder, and W. E. Irlinger, eds.), pp. 168-172.
11. Becker R.T. 1992a. Zur Kenntnis von Hemberg-Stufe und Annulata-Schiefer im Nordsauerland (Oberdevon, Rheinisches Schiefergebirge, GK 4611 Hohenlimberg). *Berlinen Geowissen Abhandlungen* 3, 3-41.
12. Becker R.T. 1992b. Analysis of ammonoid palaeobiogeography in relation to the global Hangenberg (terminal Devonian) and Lower Alum Shale (Middle Tournaisian) events. *Annales de la Société géologique de Belgique* 115, 459-473.
13. Becker R.T. 1993a. Stratigraphische Gliederung und Ammonoideen– Faunen im Nehdenium (Oberdevon II) von Europa und Nord- Afrika. *Courier Forschungsinstitut Senckenberg* 155:1–405.
14. Becker R.T. 1993b. Anoxia, eustatic changes, and Upper Devonian to lowermost Carboniferous global ammonoid diversity. In: House MR (ed) *The ammonoidea: Environment, ecology, and evolutionary change. Systematics Association*, Special Volume 47. Clarendon Press, Oxford, pp115–163.
15. Becker R.T. 1996. New faunal records and holostratigraphic correlation of the Hasselbachtal D/C-boundary auxiliary stratotype (Germany). *Annales de la Société géologique de Belgique* 117 (1): 19-45.
16. Becker R. T. & House M. R. 1994. Kellwasser Events and goniatite successions in the Montagne Noire with comments on possible causations. *Courier Forschungsinstitut Senckenberg* 169, 45–77.
17. Becker R. T. & House M. R. 1997. Sea-level changes in the Upper Devonian of the Canning Basin. *Courier Forschungsinstitut Senckenberg* 199, 129–146.
18. Beinert R.J., Klapper G., Sandberg C.A & Ziegler W. 1971. Revision of Scaphignathus and description of Clydagnathus? ormistoni n.sp. (Conodonta, Upper Devonian). *Geologica et Palaeontologica* 5, 81-91; Marburg.
19. Bischoff G. 1956. Oberdevonische Conodonten (toI) aus dem Rheinischen Schiefergebirge. *Notizblatt des Hessisches Landesamt für Bodenforschung* 84, 115-137.
20. Bischoff G. 1957. Die Conodonten-Stratigraphie des rhenoherzynischen Unterkarbons mit Berücksichtigung der Wocklumeria-Stufe und der Devon/Karbon-Grenze. *Abhandlungen des Hessisches Landesamt für Bodenforschung* 19, 1-64; Wiesbaden.

21. Bischoff G. & Ziegler W. 1956. Das Alter der "Urfer Schishten" im Marburger Hinterland nach Conodonten. *Notizblatt des Hessisches Landesamt für Bodenforschung* 84, 138-169.
22. Bless J.M., Becker R.T., Higgs K., Paproth E. & Streel M. 1993. Eustatic cycles around the Devonian-Carboniferous boundary and the sedimentary and fossil record in Sauerland (Federal Republic of Germany). – *Annales de la Societé géologiqué Belge* 115 (2), 689-702.
23. Boulila S., Galbrun B., Hinnov L.A., & Collin P.Y. 2008. Orbital calibration of the Early Kimmeridgian (southeastern France): implications for geochronology and sequence stratigraphy. *Terra Nova*. 20, p. 455-462.
24. Branson E.B. & Mehl M.G. 1934a. Conodonts from the Grassy Creek shale of Missouri. *Missouri University Studies* 8, 3: 171-259.
25. Branson E.B. & Mehl, M.G. 1934b. Conodonts from the Bushberg sandstone and equivalent formations of Missouri. *Missouri University Studies* 8, 4: 265-300.
26. Branson E.B. & Mehl, M.G 1938. Conodonts from the lower Mississippian of Missouri. In E.B. Branson et al. (eds.), Stratigraphy and palaeontology of the lower Mississippian of Missouri. *Missouri University Studies* 13: 128-148.
27. Branson E.B. & Mehl M.G. 1944. Conodonts; In Shimer, H.W & Shrock, R.R. (Eds.): Index fossils of North America. John Wiley & sons; 235-246; New York.
28. Branson E.R. 1934. Conodonts from the Hannibal Formation of Missouri. *Missouri University Studies* 8 (4), 301-343.
29. Buggisch W. 1991. The global Frasnian^Famennian 'Kellwasser'- Event. *Geology Rundschau*. 80, 49^72.
30. Carmignani L., Gattiglio M., Maxia M., Oggiano G., Pertusati P.C. 1986. The geology of Gerrei. *In* Carmignani, L., Cocozza T., Ghezzo C., Pertusati P.C. & Ricci C.A. (Eds.), *Guide-book to the excursion on the Paleozoic Basement of Sardinia*, IGCP No.5, *Newsletter special issue*, 61-72.
31. Carmignani L., Barca S., Carosi R., Di Pisa A., Gattiglio M., Oggiano G. & Pertusati P. C. 1992. Schema del basamento sardo; in Carmignani L., Pertusati P.C., Barca S., Carosi R., Di Pisa A., Gattiglio M. Musumeci G. & Oggiano G. (Eds.): Struttura della Catena Ercinica in Sardegna - guida all'escursione: 11-38; Siena.
32. Carta, N. 2011. Caratterizzazione Biostratigrafica delle Unità Litologiche affioranti nell'area di Monte Pizzul, Passo del Cason di Lanza (Alpi Carniche). Master Thesis, University of Cagliari: 130 pp.
33. Collinson C., Scott A.J. & Rexroad C.B. 1962. Six charts showing biostratigraphic zones and correlations based on conodonts from the Devonian and Mississippian rocks of the upper Mississippi valley. *Illinois Geological Survey Circular* 328, 32 p.
34. Cooper C.L. 1931. New conodonts from the Woodford Formation of Oklahoma. *Journal of. Paleontology* 5 (3), 230-243.
35. Corradini C., 1998a. *Conodonti del Devoniano Superiore nei "Calcari a Clymeniae" di Villasalto (Sardegna Sud-Orientale): Tassonomia e Biostratigrafia*. 139 pp. PhD Thesis, Università di Modena, Italy.
36. Corradini C. 1998b, New Devonian (Famennian) taxa of Polygnathids and Icriodids (Conodonts) from Sardinia. *Giornale di Geologia 60*, Spec. Issue, 89-92.
37. Corradini C. 1998c. Famennian conodonts from two sections near Villasalto. *Giornale di Geologia 60*, Spec. Issue, 122-135.
38. Corradini C. 1998d. The middle-late Devonian of Su Nuargi, East of Domusnovas. *Giornale di Geologia*, 60, Spec. Issue, 188-193
39. Corradini C. 2002. The Clymeniae limestone in the Corona Mizziu Sections (SE Sardinia, Italy). *Rendiconti della Società Paleontologica Italiana 1*, 261-264.
40. Corradini C. 2003. Late Devonian (Famennian) conodonts from the Corona Mizziu sections near Villasalto (Sardinia, Italy). *Palaeontographia Italica 98*, 65–116.
41. Corradini, C. 2007. Calcari a Clymenie. In Carta Geologica d'Italia 1:50000 – Catalogo delle Formazioni; fascicolo VI – Unità tradizionali e/o storiche. Quaderni, s. III, 7: 298-301.
42. Corradini C. 2008. Revision of Famennian-Tournaisian (Late Devonian-Early Carboniferous) conodont biostratigraphy of Sardinia, Italy. *Revue de micropaléontologie* 51: 123-132.
43. Corradini C. & Olivieri R. 1997. Conodont biostratigraphy of some supplementary sections in the Sardinian "Ockerkalk" (Upper Silurian). *Bollettino del Museo regionale di Scienze Naturali di Torino*, 15: 89- 100.

44. Corradini C. & Ferretti A. 2009. The Silurian of the External Nappes (southeastern Sardinia). *Rendiconti della Società Paleontologica Italiana 3*, 43-49.

45. Corradini C. & Corriga M.G. 2010. Silurian and lowermost Devonian conodonts from the Passo Volaia area (Carnic Alps, Italy). *Bollettino della Società Paleontologica Italiana* 49(3):237–253.

46. Corradini C. & Corriga M.G. 2012. A Prídolí-Lochkovian conodont zonation in Sardinia and the Carnic Alps: implications for a global zonation scheme. *Bulletin of Geoscience* 87(4):635–650. doi:10.3140/bull.geosci.1340.

47. Corradini C., Ferretti A. & Serpagli E. 2000. Correlazioni biostratigrafiche negli “Ockerkalk” (Siluriano sup.) della Sardegna sud-orientale. In Cherchi A. & Corradini C. (Eds), Crisi biologiche, radiazioni adattative e dinamica delle piattaforme carbonatiche. *Accademia Nazionale di Scienze Lettere Arti di Modena*, Collana di Studi 21: 87-92.

48. Corradini C., Barca S. & Spalletta C. 2003. Late Devonian-Early Carboniferous conodonts from the “Clymeniae limestones” of SE Sardinia (Italy). *Courier Forschungs-Institut Senckenberg* 245: 227-253.

49. Corradini C., Leone F., Loi A. & Serpagli E. 2001. Conodont Stratigraphy of a highly tectonised Siluro-devonian Section in the San Basilio area (SE Sardinia). *Bollettino della Società Paleontologica Italiana 40*, 315-323.

50. Corradini C., Simonetto L., Serventi P., Calligaris C. & Rigo R. 2005. Loboliti (Crinoidea) del Devoniano basale di Monte Zermula (Alpi Carniche, Italia). *Rendiconti della Società Paleontologica Italiana* 2: 27-34.

51. Corradini C., Kaiser S.I., Perri M.C. & Spalletta C. 2011. *Protognathodus* (Conodonta) and its potential as a tool for defining the Devonian/Carboniferous boundary. *Rivista Italiana di Paleontologia e Stratigrafia 116*, 15-28.

52. Corradini C., Pondrelli M., Corriga M.G., Simonetto L., Kido E., Suttner T.J., Spalletta C. & Carta, N. 2012. Geology and stratigraphy of the Cason di Lanza area (Mount Zermula, Carnic Alps, Italy). Berichte des Institutes für Erdwissenschaften, Karl-Franzens-Universität Graz, Band 17: 83-103.

53. Corradini C., Corriga M.G., Kido E., Muscio G., Pondrelli M., Suttner T.J., Simonetto L. & Spalletta C., 2013. Cason di Lanza - leggere il passato nelle rocce. *Le guide del Geoparco della Carnia*, 1-48.

54. Corriga M.G, Corradini C. & Ferretti A. 2009. Silurian conodonts from Sardinia: an overview. *Rendiconti della Società Paleontologica Italiana* 3: 95-107.

55. Corriga M.G. 2011. *Biostratigrafia a conodonti attorno al limite Siluriano–Devoniano in alcune aree del NordGondwana*. PhD Thesis, University of Cagliari: 152 pp.

56. Corriga M.G & Corradini C. (2009) Upper Silurian and lower Devonian conodonts from the Monte Cocco II Section (Carnic Alps, Italy). *Bulletin of Geoscience* 84(1):155–168. doi:10.3140/bull.geosci.1112

57. Corriga M.G., Suttner T.J., Kido E., Corradini C., Pondrelli M., Simonetto L. 2011. The age of the La Valute limestone-Findenig limestone transition in the La Valute Section (Lower Devonian, Carnic Alps, Italy). *Gortania Geologia, Paleotologia, Paletnologia* 32:5–12.

58. Crick R.E., Ellwood B. & El Hassani A., 1994. Integration Of Biostratigraphy, Magnetic Susceptibility And Relative Sea-Level Change: A New Look At High Resolution Correlation. *Subcommission On Devonian Stratigraphy, Newsletter* 11: 59-66.

59. Crick R.E., Ellwood B.B., Hassani A.E., Feist R. & Hladil J., 1997. MagnetoSusceptibility Event and Cyclostratigraphy (MSEC) of the Eifelian - Givetian GSSP and associated boundary sequences in north Africa and Europe. Episodes 20 (3), 167- 175.

60. Da Silva A.C., Mabille C. & Boulvain F. 2009. Influence of sedimentary setting on the use of magnetic susceptibility: examples from the Devonian of Belgium. *Sedimentology* 56, 1292-1306.

61. Da Silva A.C., Yans J. & Boulvain F. 2010. Sedimentology and magnetic susceptibility during the “punctata” event of the Ardenne area (Belgium): identification of severe and rapid sea level fluctuations. In: Da Silva, AC. and Boulvain, F. (eds): magnetic susceptibility, correlations and Palaeozoic environments. *Geologica Belgica*, 13/4, 319-332.

62. Da Silva A.C., Dekkers M., Mabille C. and Boulvain F. 2012. Magnetic signal an its relationship with paleoenvironments and diagenesis - examples from the Devonian carbonates of Belgium. *Studia Geophysica & Geodaedica* 56, 677−704, DOI: 10.1007/s11200-011-9005-9

63. De Vleeschouwer D., Whalen M.T., Day J.E. & Claeys P. 2012. Cyclostratigraphic calibration of the Frasnian (Late Devonian) time scale (western Alberta, Canada). *Geological Society of America Bulletin* 124, 5-6, p. 928-942

64. Day R., Fuller M. & Schmidt V.A., 1977. Hysteresis properties of titanomagnetics: grain-size and compositional dependence. *Phys.Earth Planet.Inter.*13, 206–267.

65. Derycke C., Spalletta C., Perri M.C. & Corradini C. 2008. Famennian Chondrichthyan Microremains From Morocco And Sardinia. *Journal of Paleontology* 82 (5): 984-995.

66. Devleeschouwer X., Petitclerc E., Spassov S. and Préat A., 2010. The Givetian-Frasnian boundary at Nismes parastratotype (Belgium): the magnetic susceptibility signal controlled by ferromagnetic minerals. In: Da Silva A.C. and Boulvain F. (Eds.), Magnetic Susceptibility, Correlations and Palaeozoic Environments. *Geologica Belgica* 13, 351–366.

67. Devuyst F. X. & Kalvoda J. 2007. Early evolution of the genus Eoparastaffella (Foraminifera) in Eurasia: the interiecta group and related forms, late Tournaisian to early Viséan (Mississippian). *Journal of Foraminiferal Research*, roč. 37, č.1, s.69-89. ISSN 0096-1191

68. Dopieralska J. 2003. *Neodymium isotopic composition of conodonts as a palaeoceanographic proxy in the Variscan oceanic system*. Ph.D. Dissertation University of Giessen, 111 pp, Giessener elektr Bibl, URL: http://geb.uni-giessen.de/geb/volltexte/2003/1168/, URN: urn:nbn:de:hebis:26-opus-11682

69. Dreesen R., 1989. The « Cheiloceras Limestone » a Famennian (Upper Devonian) event-stratigraphical marker in Hercynian Europe and Northwestern Africa? Bulletin Societè Belgique Géologié, 98-2: 127-133.

70. Druce 1969. Devonian and Carboniferous from the Bonaparte Gulf Basin, Northwest Australia and their use in international correlation. *Commonwealth of Australia, Department of National Development, Bureau of Mineral Resources, Geology and Geophysics, Bulletin* 98, 33-78.

71. Dunlop D.J., 2002. Theory and application of the Dayplot (Mrs/Ms versus Hcr/Hc) 1. Theoretical curves and tests using titanomagnetite data. *Journal of Geophysics Research* 107, 2056 doi: 0.1029/2001JB000486.

72. Dzik J. 1976. Remarks on the evolution of Ordovician conodonts. *Acta Palaeontologica Polonica 21*, 395-455.

73. Ellwood B.B., Crick R.E., El Hassani A., 1999. The MagnetoSusceptibility Event and Cyclostratigraphy (MSEC) method used in geological correlations of Devonian rocks from Anti-Atlas Morocco. *American Association Petrology Geological Bulletin* 83, 1119-1134.

74. Ellwood B.B., Crick R.E., El Hassani A., Benoist S. & Young, R.2000. MagnetoSusceptibility Event and Cyclostratigraphy (MSEC) in Marine Rocks and the Question of Detrital Input Versus Carbonate Productivity. *Geology* 28, 1135 - 1138.

75. Ellwood B.B., Garcia-Alcalde J.L., El Hassani A., Hladil J., Soto, F.M., Truyols-Massoni, M., Weddige, K. & Koptikova, L. 2006. Stratigraphy of the Middle Devonian Boundary: Formal Definition of the Susceptibility Magnetostratotype in Germany with comparisons to Sections in the Czech Republic, Morocco and Spain. *Tectonophysics* 418, 31-49.

76. Ellwood B.B., Tomkin J., Richards B., Benoist S.L. & Lambert L.L. 2007. MSEC Data Sets Record Glacially Driven Cyclicity: Examples from the Arrow Canyon Mississippian-Pennsylvanian GSSP and Associated Sections. *Palaeogeography, Palaeoclimatology, Palaeoecology* 255, 377-390. doi: 10.1016/j.palaeo.2007.08.006.

77. Ellwood B.B., Tomkin J.H., Ratcliffe K.T., Wright M. & Kafafy A.M. 2008. High-resolution magnetic susceptibility and geochemistry for the Cenomanian/Turonian boundary GSSP with correlation to time equivalent core. *Palaeogeography, Palaeoclimatology, Palaeoecology* 261, 105-126.

78. Feist R. 2002. The Palaeozoic of the Montagne Noire, Southern France, Montpellier. In North Gondwana midPalaeozoic Biodynamics and ECOS VIII. *Guidebook of the Field Trip Excursion*, pp 1–82. Montpellier. Subcommission on Devonian Stratigraphy

79. Ferrari A., Vai G.B. 1966. Ricerche stratigrafiche e paleoecologiche al M. Zermula. *Giornale di Geologia* 33, 389–416.

80. Ferretti A., Serpagli E. & Leone F. 1998. Late Ordovician conodonts from umbrabrutta between Donigala and Lago Mulargia. In Serpagli E. (ed.), Sardinia Field-trip Guide-book, ECOS VII. *Giornale di Geologia*, 60, Spec. Issue: 202-208.

81. Ferretti A. & Serpagli E. 1999. Late Ordovician conodont faunas from southern Sardinia, Italy: biostratigraphic and paleogeographic implications. *Bollettino della Società Paleontologica Italiana*, 37(2-3): 215-236.

82. Ferretti A., Schonlaub H.P. 2001. New conodont faunas from the Late Ordovician of the Central Carnic Alps, Austria. *Bollettino della Società Paleontologica Italiana* 40(1), 3–15.

83. Flajs G. & Feist R. 1988. Index conodonts, trilobites and environment of the Devonian-Carboniferous Boundary beds at La Serre (Montaigne Noire, France); in Flajs G, Feist R. & Ziegler W. (eds.): Devonian- Carboniferous Boundary- Results of recent studies *Courier Forschungs-Institut Senckenberg* 100: 53-107, 11 pls.

84. Flanders P. J. 1994. Collection, measurement and analysis of airborne magnetic particulates from pollution in the environment. *Journal of Applied Physics* 75, 5931-5936.

85. Funedda A. & Oggiano G. 2009. Outline of the Varisican basement of Sardinia. *Rendiconti della Società Paleontologica Italiana 3*, 23-35.

86. Gedik I. 1969. Karnik Alpler'den Alt Karbonifere ait conodontlar. *The Mineral Research and Exploration Institut of Turkey, Bulletin* 70, 229-242.

87. Gedik I. 1974. Conodonten aus dem Unterkarbon der Karnischen Alpen. *Abhandlungen Der Geologischen Bundesanstalt* 31, 1-29.

88. Gephart J.W. 1990. FMSI: a fortran program for inverting fault/slickenside and earthquake focal mechanism data to obtain the regional stress tensor. *Computer Geoscience* 16(7), 953–989.

89. Gephart J.W. & Forsyth D.W. 1984. An improved method for determining the regional stress tensor using earthquake focal mechanism data: application to the San Fernando earthquake sequence. *Journal of Geophysics Research* 89(B11): 9305–9320. doi: 10.1029/JB089iB11p09305

90. Girard C., Cornée J.-J., Corradini C., Fravalo A. & Feist R. 2014. Paleoenvironmental changes at Col des Tribes (Montagne Noire, France), a reference section for the Famennian of north Gondwana-related areas. *Geological Magazine*, 151: 864-884. doi: 10.1017/S0016756813000927

91. Glenister B.F. & Klapper G. 1966. Upper Devonian conodonts from the Canning Basin, Western Australia. – *Journal of Paleontolgy* 40 (4), 777-842.

92. Gortani M. 1923a. Faune Paleozoiche della Sardegna - parte I le graptoliti di Goni. *Paleontographia Italica*, 28: 1-69.

93. Gortani M. 1923b. Faune Paleozoiche della Sardegna - parte II Graptoliti della Sardegna Orientale. *Paleontographia Italica*, 28: 85-112.

94. Hartenfels S. 2011. Die globalen Annulata-Events und die Dasberg-Krise (Famennium, Oberdevon) in Europa and Nord Afrika – hochaösende Conodonten-Stratigraphie, Karbonat – *Mikrofazies, Paläodiversität. Münstersche Forschungen zur Geologie and Paläontologie* 105: 17-527.

95. Hartenfels S. & Becker R.T. 2009. Timing of the global Dasberg crisis – implications for Famennian eustasy and chronostratigraphy. In Over J. (ed): Studies in Devonian Stratigraphy: Proceedings of the 2007 International Meeting of the Subcommission on Devonian Stratigraphy and IGCP 499, *Palaeontographica Americana* 63, 71-97.

96. Hass W.H. 1959. Conodonts from the Chappel Limestone of Texas. *U.S. Geological Survey Professional Paper* **294**, 365-399, pls.46-50; Washington.

97. Helms J. 1959. Conodonten aus dem Saalfelder Oberdevon (Thuringen). *Geologie*, 8 (6): 634-677.

98. Helms J. 1961. Die “nodocostata-Gruppe” der Gattung Polygnathus (Oberdevonische Conodonten). *Geologie* 10, 674-711.

99. Helms J. 1963. Zur "Phylogenese" und Taxionomie von Palmatolepis (Conodontida, Oberdevon). *Geologie* 12 (4), 449-485.

100. Helms J. & Wolska Z. 1967. New Upper Devonian conodonts from Poland and Germany. *Acta Paleontogica Polonica* 12 (2), 227-238; Warszawa.

101. Higgs K.T. & Streel M., 1994. Palynological age for the lower part of the Hangenberg Shales in Sauerland, Germany *Annales de la Societé géologiqué Belge* 116, 243–247.

102. Hinde G. J. 1879. On conodonts from the Chazy and Cincinnati group of the Cambro-Silurian and from the Hamilton and Genesee shale divisions of the Devonian in Canada and the United States. *Geological Society of London Quarterly Journal* 35 (3), 351-369.

103. Hladil J., 2002. Geophysical records of dispersed weathering products on the Frasnian carbonate platform and early Famennian ramps in Moravia, Czech Republic: proxies for eustasy and palaeoclimate. *Palaeogeography Palaeoclimatology Palaeoecology* 181, 213−250.

104. Hladil J., Vondra M., Cejchan P., Vich R., Koptíková L. and Slavík L., 2010. The dynamic timewarping approach to comparison of magnetic-susceptibility logs and application to Lower Devonian calciturbidites (Prague Synform, Bohemian Massif). In: Da Silva A.C. and Boulvain F. (Eds.), *Magnetic Susceptibility, Correlations and Palaeozoic Environments. Geologica Belgica 1*3, 385–406.

105. Holmes G.B. 1928. A bibliography of the conodonts with descriptions of early Mississippian species. *U. S. Natural Museum Proa* 72, pp. 1-38, pis. 1-11.

106. Hou H., Ji Q., Xiong J. & Wu X. 1984. A possible stratotype of Devonian-Carboniferous boundary in Guizhou provincve, south China. *Courier Forschungsinstitut Senckenberg* 67, 193-205.

107. House M. R. 1985. Correlation of mid-Palaeozoic ammonoid evolutionary events with global sedimentary perturbations. *Nature*, 313, 17–22.

108. House M. R. 1996. Juvenile Goniatite Survival Strategies following Devonian Extinction Events. *Geological Society*, Special Publications, 102, 163–185.

109. House M.R. 2002. Strength, timing, setting and cause of Mid-Palaeozoic extinctions. *Palaeogeography, Palaeoclimatology, Palaeoecology* 181, 5–25.

110. Huddle, J.W. 1934. Conodonts from the New Albany Shale of Indiana. *Bulletins of American Paleontology* 21 (72), 1-136; Ithaca, N.Y.

111. Husson D., Galbrun B., Laskar J, Hinnov L.A, Thibault N., Gardin S. & Locklair R.E, 2011. Astronomical calibration of the Maastrichtian (Late Cretaceous). *Earth and Planetary Science Letters* 305, Issues 3–4, 15 P. 328-340, ISSN 0012-821X, http://dx.doi.org/10.1016/j.epsl.2011.03.008

112. Isaacson P.E., Díaz-Martínez E., Grader G.W., Kalvoda J., Babek O. & Devuyst F.X. 2008. Late Devonian–earliest Mississippian glaciation in Gondwanaland and its biogeographic consequences. *Palaeogeography, Palaeoclimatology, Palaeoecology* 268, 126–142.

113. Jaeger H. 1977. The Silurian-Devonian boundary on Thuringia and Sardinia. In Martinsson, A. (ED.): The Silurian-Devonian boundary. IUGS, s.A : 117-125.

114. JI Q. 1985. Study on the phylogeny, taxonomy, zonation and biofacies of Siphonodella (conodonta). *Bulletin Institute of Geology* 11, 51-75.

115. Ji Q. & Ziegler, W. 1993. The Lali Section: an excellent Reference Section for Upper Devonian in South China. - *Courier Forschungs-Institut Senckenberg*, 157: 1-183.

116. Ji Q., Xiong J. & Wu S. 1985. Systematics Palaeontology 5: Conodonts.- In: Hou H., Ji, Q., Xiong J., Wu S., Gao I., Sheng H., Wei J. & Turner S. (Eds): Guizhou-Mujua Nipen-Shiten Xi jexian [Muhua sections of Devonian-Carboniferous boundary beds], 226 pp. Geological Publishing House, Beijing.

117. Ji Q., Wang Z., Sheng H., Hou J., Feng R., Wei J., Wang S., Wang H., Xiang L. & Fu G. 1989. The Dapushang section: An excellent section for the Devonian-Carboniferous boundary stratotype in China. *Science Press*, 1-165; Beijing.

118. Johnson J.G., Klapper G., Sandberg C.A., 1985. Devonian eustatic fuctuations in Euramerica. *Geological Society of America Bulletin* 96, 567-587.

119. Joachimski M.M., Buggisch W., 1993. Anoxic events in the late Frasnian - causes of the Frasnian-Famennian faunal crisis? *Geology* 21, 675-678.

120. Kaiser S. I. 2005. *Mass Extinctions, Climatic and Oceanographic Changes at the Devonian/Carboniferous Boundary*. Ph.D. Dissertation, Ruhr-Universität, Bochum, Germany, 156 pp.

121. Kaiser S.I. 2007. Conodontenstratigraphie und Geochemie (δ13Ccarb, δ13Corg, δ18Ophosph) aus dem Devon/Karbon-Grenzbereich der Karnischen Alpen. *Jahrbuch der Geologischen Bundesalstalt* 147, 301-314.

122. Kaiser S.I., Steuber T., Becker R.T., 2008. Environmental change during the Late Famennian and Early Tournaisian (Late Devonian–Early Carboniferous) — implications from stable isotopes and conodont biofacies in southern Europe. In: Aretz, M., Herbig, H.-G., Somerville, I.D. (Eds.), Carboniferous Platforms and Basins: *Geological Journal* Spec. Issue, 43 (2–3), 241–260.

123. Kaiser S.I., Becker R.T., Spalletta C. & Steuber T., 2009. High-resolution conodont stratigraphy, biofacies, and extinctions around the Hangenberg Event in pelagic successions from Austria, Italy, and France. *Palaeontolographica Americana* 63, 97–139.

124. Kaiser S. I., Becker R.T., Steuber T., Aboussalam S.Z. 2011. Climate-controlled mass extinctions, facies, and sea-level changes around the Devonian–Carboniferous boundary in the eastern Anti-Atlas (SE Morocco). *Palaeogeography Palaeoclimatology Palaeoecology* 310(3), 340-364.
125. Kalvoda J. & Kukal Z. 1987. Devonian-Cerboniferous Boundary in the Moravian Karst at Lesní Lom Quarry, Brno-Líszn, Czechoslovakia. – In: Brenckle, P.L., Lane, H.R. & Manger, W.L. (Eds): Selected Studies in Carboniferous Paleontology and Biostratigraphy. *Courier Forschungs-Institut Senckenberg* 98, 95-117.
126. Katz B., Elmore D., Cogoini M., Engel M.H. & Ferry S. 2000. Association between burial diagenesis of smectite, chemical remagnetization, and magnetite authigenesis in the the Vocontian trough, SE France. *Journal of Geophysics Research* 105:851–868
127. Kent D.V. 1982. Apparent correlation of palaeomagnetic intensity and climatic records in deep-sea sediments. *Nature* 299, 538-539.
128. Khrusheva E.N. & Kuzmin A.V. 1996. New late Frasnian conodonts of the Genus Palmatolepis from the Lyaiol'skaya Formation of southern Timan" *Palaeontologicheskyi Zhurnal* 3, 90-93.
129. Klapper G. & Lane H.R. 1985. Frasnian (Upper Devonian) Conodont sequence at Luscar Mountain and Mount Haultain, Alberta Rocky Mountains". *Canadian Society of Petroleum Geology* 3, 469-478.
130. Korn D. 2004. The mid-Famennian ammonoid succession in the Rhenish Mountains: the "annulata Event" reconsidered. *Geological Quarterly*, 48(3), 245-252.
131. Kreutzer L. 1990. Mikrofazies, Stratigraphie und Palaogeographie des Zentralkarnischen Hauptkammes zwischen Seewarte und Cellon. *Jahrbuch der Geologischen Bundesanstalt* 133(2):275–343.
132. Kreutzer L. 1992. Palinspastische Entzerrung und Neugliederung des Devons in den Zentralkarnischen Alpen aufgrund von neuen Untersuchungen. *Jahrbuch der Geologischen Bundesanstalt* 135(1):261–272.
133. Lane H.R., Sandberg C.A., & Ziegler W. 1980. Taxonomy and phylogeny of some lower Carboniferous conodonts and preliminary standard post-Siphonodella zonation. *Geologica et Palaeontologica* 14, 117-168.
134. Läufer A.L. 1996. Variscan and Alpine tectonometamorphic evolution of the Carnic Alps (Southern Alps)-structural analysis, illite cristallinity, K-Ar and Ar-Ar geochronology. *Tübinger Geowisseschaften Arbeiten*, A26, 40 pp.
135. Leone F. 1973. La serie paleozoica del settore di Orbai-Monte Maiori (Valle del Cixerri – Sardegna Sud-Occidentale). *Bollettino della Società Geologica Italiana* 92, 621-633.
136. Lovisato D. 1894. Il Devoniano nel Gerrei (Sardegna). *Atti della Reale Accademia dei Lincei, Rendiconti Classe Scienze Fisiche Matematiche Naturali* 3: 460-470.
137. Luppold F.W., Hanh G. & Korn D. 1984. Trilobiten-, Ammonoideen- und Conodonten-stratigraphie des Devon/ Karbon-Grenzprofiles auf dem Müssenberg (Rheinisches Schiefergebirge); in: Paproth E. & Streel M. (eds.): The Devonian-Carboniferous boundary. *Courier Forschungs-Institut Senckenberg* 67, 91-121
138. Manzoni M. 1965. Faune a conodonti del Siluriano e Devoniano delle Alpi Carniche (Nota 1: M. Cocco, M. Lodin, M. Zermula, Val Bombaso, alta valle del Degano). *Giornale di Geologia*, s. 2, 33: 179-206.
139. Manzoni M. 1966. Conodonti neodevonici ed eocarboniferi al Monte Zermula (Alpi Carniche). *Giornale di Geologia*, s. 2, 33 (1965): 461-488.
140. Mawson R. & Talent J.A. 1999. Early Carboniferous (mid-Tournaisian) conodonts from north-eastern Queensland (Ruxton and Teddy Mountain Formations): age implication and stratigraphic alignments. – In: Serpagli E. (Ed.): Studies on conodonts - Proceedings of the Seventh European Conodont Symposium: *Bollettino della Società Paleontologica Italiana* 37 (2-3), 407-425.
141. Mead A.G. & Tauxe L. 1986. Oligocene Paleoceanography of the South Atlantic: paleoclimatic implications of sediment accumulation rates and magnetic susceptibility measurements. *Paleoceanology* 1, 273-284.
142. Meneghini G. 1857. Palèontologie de l'Ile de Sardaigne. In La Marmora A., Voyage en Sardaigne: 53-144.
143. Mossoni A., Corradini C. & Pondrelli M., 2013a. Famennian (Late Devonian) conodonts from the Pizzul West section (Carnic Alps, Italy). *Gortania Geologia, Paleotologia, Paletnologia* 34: 13-34.
144. Mossoni, A., Corradini, C. & Spalletta, C. 2013b. Conodonts from the Monte Taccu section (Famennian-Tournaisian, Sardinia, Italy). *Asociación Paleontológica Argentina, Publicación Especial 13*, 85-90.
145. Mossoni A., Carta N., Corradini C. & Spalletta C. 2015. Conodonts across the Devonian/Carboniferous boundary in SE Sardinia (Italy). *Bulletin of Geosciences* 90(2), 371–388.

146. Müller K.J. 1956. Zur Kenntnis der Conodonten-Fauna des europaischen Devons, 1; Die Gattung Palmatolepis. *Abhandlunghen and Senckenbergischen Naturforschenden Gesellschaft* 494, 1-70.
147. Müller K.J. 1962. Zur systematischen Einteilung der Conodontoporida. *Palaontologische Zeitschrift*, 36, 109-107.
148. Murru, M. 1975. Primi risultati biostratigrafici sul Siluriano–Devoniano del M. Lora (Sardegna sud-orientale). *Rendiconti del Seminario della Facoltà di Scienze dell'Università di Cagliari 45*, 325-331.
149. Naud G. & Pittau Demelia P. 1987. Prémiere decuverte d'acritarches du Cambrien moyen à superieure basal et du Tremadoc - Arenigien dans la basse vallée du Flumendosa: mise an evidence d'un nouveau temoin de la Phase Sarde en Sardaigne orientale. I.G.C.P. n.5 Newsletter 7, 85-86.
150. Nicoll R.S. & Druce E.C. 1979. Conodonts from the Fairfield Group, Canning Basin, Western Australia. *Bureau of Mineral Resources Bulletins* 190, 1-134; Canberra.
151. Olivieri, R. 1965. L'aspetto della fauna a Conodonti del Devoniano superiore del Gerrei (Sardegna). *Bollettino della Società Paleontologica Italiana 4*, 28-63.
152. Olivieri R. 1970, Conodonti e zonatura del Devoniano superiore e riconoscimento del Carbonifero inferiore nei calcari di Corona Mizziu (Gerrei, Sardegna). *Bollettino della Società Paleontologica Italiana 8*, 63-152.
153. Olivieri R. 1985. Middle and Late Devonian conodonts from Southwestern Sardinia. *Bollettino della Società Paleontologica Italiana 23* (1984), 269-210.
154. Over D.J. 1992. Conodonts and the Devonian-Carboniferous boundary in the Upper Woodford Shale, Arbuckle Mountains, South-Central Oklahoma. *Journal of Palaeontology* 66, 293-311.
155. Ovnatanova N.S. & Kononova L.I. 2008. Frasnian conodonts from the Eastern Russian Platform. *Palaeontological Journal* 42, n 10: 997-1166.
156. Pander C. H. 1856. Monographie der Fossilen Fische de Silurischen Systems der Russian-Baltischen *Gouvernements, Akademie der Wissenschaften*, 91.
157. Pas D, Da Silva A-C, Suttner T, Kido E, Bultynck P, Pondrelli M, Corradini C, De Vleeschouwer D, Dojen C, Boulvain F. 2014. Insight into the development of a carbonate platform through a multi-disciplinary approach: a case study from the Upper Devonian slope deposits of Mount Freikofel (Carnic Alps, Austria/Italy). *International journal of Earth Science* 103:519–553. doi:10.1007/ s00531-013-0969-2
158. Pili P. & Saba O. 1975. Presenza di Devoniano a conodonti nelle assise carbonatiche di Correboi (Sardegna centro-orientale). *Bollettino Società Sarda di Scienze Naturali 5*, 1-8; Cagliari.
159. Piras S. & Paschina F. 2009. The Lower Devonian Upper Graptolitic Shales in the Sa Ruinosa Section (SE Sardinia). *Rendiconti della Società Paleontologica Italiana*, 3 (2): 191-194.
160. Perri M.C., and Spalletta C., 1981a. Conodonti e biozonatura del Frasniano (Devoniano sup.) di Pramosio, Alpi Carniche. *Bollettino della Società Paleontologica Italiana* 19 (1980), 2, 281-310.
161. Perri M.C., and Spalletta C., 1981b. "*Ancyrodella pramosica"* n. sp. from the Lower Frasnian of the Carnic Alps. *Bollettino della Società Paleontologica Italiana* 20(1981), 1, 93-98.
162. Perri M.C. & Spalletta, C. 1990. Famennian conodonts from climenid pelagic limestone, Carnia Alps, Italy. - *Palaeontographia Italica*, 77: 55-83.
163. Perri, M.C. & Spalletta C. 1991. Famennian conodonts from Cava Cantoniera and Malpasso sections, Carnic Alps, Italy. – *Bollettino della Società Paleontologica Italiana*, 30(1): 47-78.
164. Perri M.C. & Spalletta C 1998a. Updating of the conodont biostratigraphy in the Carnic Alps (Italy). 116-119. *Giornale di Geologia*, s. 3, 60, Spec. Issue.
165. Perri M.C. & Spalletta C. 1998b. The Upper *marginifera* Zone (Late Devonian) in the Casera Collinetta di Sotto C section (Carnic Alps, Italy). 150-157. *Giornale di Geologia*, s. 3, 60, Spec. Issue.
166. Perri M.C. & Spalletta C. 1998c. Late Famennian conodonts from the Casera Collinetta di Sotto B section (Carnic Alps, Italy). 158-167. *Giornale di Geologia*, s. 3, 60, Spec. Issue.
167. Perri M.C. & Spalletta C 1998d. Latest Devonian and Early Carboniferous conodonts from the Casera Collinetta di Sotto A section (Carnic Alps, Italy). 168-181. *Giornale di Geologia*, s. 3, 60, Spec. Issue.
168. Perri M.C. & Spalletta C. 1998e. The Frasnian-Famennian boundary at the Pramosio A section (Carnic Alps, Italy). 198-205. *Giornale di Geologia*, s. 3, 60, Spec. Issue.
169. Perri M.C. & Spalletta C. 1998f. Middle Famennian conodonts of the Elios section (Carnic Alps, Italy). 206-213. *Giornale di Geologia*, s. 3, 60, Spec. Issue.

170. Perri M.C. & Spalletta C. 1998g. Late Famennian conodonts of the Malpasso section (Carnic Alps, Italy). 220-227. *Giornale di Geologia*, s. 3, 60, Special Issue.

171. Perri M.C., Spalletta C., and Pondrelli M., 1998. Late Famennian conodonts from the Pramosio Bassa section (Carnic Alps, Italy). In: M.C. Perri, and C. Spalletta (Eds), *Southern Alps Field Trip Guidebook, ECOS VII. Giornale di Geologia,* 60, Special Issue, 228-233.

172. Pölser, P. 1969. Conodonten aus dem Devon der Karnischen Alpen (Findenigkofel, Österreich). *Jahrbuch der Geologischen Bundesanstalt*, 112: 399-440.

173. Pondrelli M. 1998. *Evoluzione deformativa del nucleo ercinico carnico centro-orientale*. Università di Bologna (Ph.D. Thesis), 178 pp.

174. Pondrelli M., Corradini C., Corriga M.G., Kido E., Mossoni A., Simonetto L., Spalletta C., Suttner T. J., Carta N. 2015. Depositional evolution of a lower Paleozoic portion of the Southalpine domain: the Mt. Pizzul area (Carnic Alps, Italy). *International journal of Earth Science* (Geol Rundsch) 104, 147-178. (doi:10.1007/s00531-014-1069-7)

175. Pomesano Cherchi, A. 1963. I primi conodonti della Sardegna nei calcari neodevonici del Gerrei. *Istituto di Geologia e Paleontologia dell'Università di Cagliari 2*, 1-11.

176. Rhodes F.H.T., Austin R.T & Druce E.C. 1969. British Avonian (Carboniferous) conodont faunas, and their value in local and intercontinental correlation. *Bulletin of the British Museum (Natural History),* Geol. Suppl. 5: 1-363.

177. Riquier L., Averbuch O., Devleeschouwer X. and Tribovillard N., 2010. Diagenetic versus detrital origin of the magnetic susceptibility variations in some carbonate Frasnian-Famennian boundary sections from Northern Africa and Western Europe: implications for paleoenvironmental reconstructions. *International journal of Earth Science* 99, S57–S73.

178. Sandberg, C.A. & Ziegler, W. 1979. Taxonomy and biofacies of important conodonts of Late Devonian *styriacus*-Zone, United States and Germany. *Geologica et Palaeontologica 13*, 173-212.

179. Sandberg, C.A., Streel, M. & Scott, R.A. 1972. Comparison between conodont zonation and spore assemblages in the Devonian-Carboniferous boundart in the western and central United States and in Europe. Septième Congrès Internat. Stratigraphie Géologie di Carbonifère, Krefeld, 23-28 august 1971, Compte Rendu, 1: 179-203, 4 pls.; Krefeld.

180. Sandberg, C.A., Ziegler, W., Leuteritz, K. & Brill, S.M. 1978. Phylogeny, speciation and zonation of *Siphonodella* (Conodonta, Upper Devonian and Lower Carboniferous). *Newsletters on Stratigraphy 7*, 102-120.

181. Sandberg C. A. & Dreesen R. 1984. Late Devonian icriodontid biofacies models and alternate shallow-water conodont zonation; in Clark, D.L. (ed.), *Conodont biofacies and provincialism. Geological Society of America*. Special Paper, 196, 143-178.

182. Sandberg C.A., Ziegler W, Dreesen R. & Butler J. 1988. Late Frasnian mass extinction: conodont event stratigraphy, global changes, and possible causes. *Courier Forschungsinstitut Senckenberg* 102:263– 307.

183. Sannemann, D. 1955a. Beitrag zur Untergliederung des Oberdevons nach Conodonten. *Nues Jahrbuch fur Geologie und Paläontologie Abhandlungen* 100, 3: 324-331.

184. Sannemann, D. 1955b. Oberdevonische Conodonten (to IIa). *Senckenbergiana Lethaea* 26, 1/2: 123-156.

185. Schäfer W. 1976. Einige neue Conodonten aus dem höheren Oberdevon des Sauerlandes (Rheinisches Schiefergebirge). *Geologica et Palaeontologica* 10, 141-152.

186. Schönlaub, H.P. 1969a. Das Paläozoikum zwischen Bishofalm und Hoem Trieb (Zentrale Karnischen Alpen). *Jahrbuch der Geologischen Bundesanstalt*, 112, 265-320; Wien.

187. Schönlaub, H.P. 1969b. Conodonten aus dem Oberdevon und Unterkarbon des Kronhofgrabens (Karnischen Alpen, Österreich): *Jahrbuch der Geologischen Bundesanstalt* 112, 321-354; Wien.

188. Schönlaub, H.P. 1979. Das Paläozoikum in Österreich. *Abhandlunghen der Geologischen Bundesanstalt* 33, 1–24

189. Schönlaub, H.P. 1985. Das Paläozoikum der Karnischen Alpen. *Arbeitstag Geologischen Bundesanstalt*, 34–52

190. Schönlaub H.P. 1988. The Ordovician-Silurian boundary in the Carnic Alps of Austria. In: Cocks LRM, Rickards RB (eds) A global analysis of the Ordovician–Silurian Boundary. British Museum (Natural History), London, vol 43, pp 107–115

191. Schönlaub, H.P. 1992. Stratigraphy, Biogeography and Paleoclimatology of the Alpine Paleozoic and its implications for Plate movements. *Jahrbuch der Geologischen Bundesanstalt* 135, 381-418.

192. Schönlaub, H.P., Feist, R. & Korn, D. 1988. The Devonian-Carboniferous Boundary at the section "Grüne Schneid" (Carnic Alps, Austria): A preliminary report. – In: Flajs, G, Feist, R. & Ziegler, W. (eds): Devonian- Carboniferous Boundary- Results of recent studies. *Courier Forschungsinstitut Senckenberg* 100, 149-167.
193. Schönlaub, H.P., Attrepp, M, Boeckelmann, K., Dreesen, R., Feist, R., Fenninger, A., Hahn, G., Klein, P., Korn, D., Kratz, R., Magarizt, M., Orth, C.J. & Schramm, J.-M. 1992. The Devonian/Carboniferous Boundary in the Carnic Alps (Austria) – A multidisciplinary approach. *Jahrbuch der Geologischen Bundesanstalt* 135, 57-98; Wien.
194. Schülke I. & Popp A. 2005. Microfacies development, sea-level change, and conodont stratigraphy of Famennian mid- to deep platform deposits of the Beringhauser Tunnel section (Rheinisches Schiefergebirge, Germany). *Facies*50, 647–664, DOI 10.1007/s10347-004-0041-6
195. Selli, R. 1963. Schema geologico delle Alpi Carniche e Giulie occidentali. *Giornale di Geologia* 30(2):1–121.
196. Sepkoski J.J., JR. 1996. Patterns of Phanerozoic extinction: a perspective from global data bases. – In: Walliser, O.H. (ed.): Global events and event stratigraphy in the Phanerozoic, pp. 35-51. Springer, Berlin.
197. Shackleton N.J., 1999. Will Oxygen isotope stratigraphy survive to the next Millenium. EOS Trans. AGU, Abstract Annual Meeting (San Francisco) 80 (46), F505.
198. Simakov K.V. 1993. The dynamics and biochronological structure of the Hangenbergian bioevent. *Palaeogeography, Palaeoclimatology, Palaeoecology* 104: 127-137.
199. Spalletta C., Vai G., Venturini C. 1980. Il flysch ercinico nella geologia dei Monti Paularo e Dimon (Alpi Carniche). *Memorie della Società Geologica italiana* 20(1979):143–265.
200. Spalletta, C. & Vai, G.B. 1982. Contatto Devoniano pelagico-flysch ercinico a Villasalto (Gerrei). In: Carmignani, L., Cocozza, T., Ghezzo, C., Pertusati, P.C., Ricci, C.A. (Eds): Guida alla Geologia del Paleozoico sardo. *Guide Geologiche Regionali - Società Geologica. Italiana*, 117-118.
201. Spalletta C., and Perri M.C., 1998. The Lower expansa Zone (Late Devonian) in the Pramosio section (Carnic Alps, Italy). In: M.C. Perri, and C. Spalletta (Eds), *Southern Alps Field Trip Guidebook, ECOS VII. Giornale di Geologia* s. 3, 60, Special Issue, 234-241.
202. Spassov S. & Valet J.P. 2012. Detrital magnetizations from redeposition experiments of different natural sediments. *Earth and Planetary Science Letters* 351-352(2012), 147–157.
203. Storch P. & Piras S. 2009. Silurian graptolites of Sardinia: assemblages and biostratigraphy. *Rendiconti della Società Paleontologica Italiana*, 3 (1): 77-93.
204. Storch P. & Schonlaub H.P. 2012. Ordovician-Silurian boundary graptolites of the Southern Alps, Austria. *Bulletin of Geoscience* 87(3):755–766.
205. Streel M. 2000. Global Famennian climates based on palynomorph quantitative analysis. - In: Rodrigues, M.A.C. & Pereira, E. (eds.): *Ordovician – Devonian palynostratigraphy in western Gondwana: Update, Problems and Perspectives,* pp. 77-103
206. Streel M., Caputo M.V., Loboziak S. & Melo J.H.G., 2000. Late Frasnian^Famennian climates based on palynomorph analysis and the question of the Late Devonian glaciations*. Earth-Science Reviews* 52, 121-173.
207. Sweet W.C. 1988. The Conodonta: Morphology, taxonomy, Paleoecology and Evolutionary History of a Long-Extinct Animal Phylum. *Oxford University Press*, 1-212; New York.
208. Szulczewski, M. 1973. Famennian-Tournaisian neptunian dykes and their conodont fauna from Dalnia in the Holy Cross Mts. *Acta Geologica Polonica* 23 (1): 15-59; Warszawa.
209. Tauxe L., Steindorf J.L. & Harris A. 2006. Depositional remanent magnetization: toward an improved theoretical and experimental foundation. *Earth Planetary Science Letters* 244, 515–529.
210. Traghelen H. & Hartenfels S. 2002. *Kostenhof quarry (Frankwald, Bavaria) – A potential reference section for the Early/Middle and Missle/Late Famennian boundary*. Document Subcommission Devonian Stratigraphy. Annual Meeting Toulouse 2002, 7 pp.
211. Traghelen H. & Hartenfels S. 2011. Neue Conodont taxa aus dem höheren Famennium (Oberdevon) des Frankenwaldes. *Münstersche Forschungen zur Geologie and Paläontologie 105*, 1-15.
212. Tribovillard N., Algeo T.J., Lyons T. & Riboulleau A., 2006. Trace metals as paleoredox and paleoproductivity proxies: An update. *Chemical Geology* 232, 12−32.
213. Ulrich E.O. & Bassler R.S. 1926. A classification of the toothlike fossils, conodonts, with descriptions of American Devonian and Mississippian species. *Proceedings of U.S. Natural History Museum* 68, 1-63.

214. Vai G.B. 1976. Stratigrafia e paleogeografia ercinica delle Alpi. *Memorie della Società Geologica Italiana* 13(1), 7–37.

215. Vai G.B. 1980. Sedimentary environment of Devonian pelagic limestones in the Southern Alps. *Lethaia* 13(1):79–91

216. Venturini C. 1990. Field workshop on Carboniferous to Permian sequence of the Pramollo-Nassfeld Basin (Carnic Alps) (September2–8, 1990). Guidebook.

217. Venturini C., Spalletta C., Vai G.B., Pondrelli M., Del Zotto, S., Fontana, C., Longo Salvador, G. & Carulli, G.B. 2009. Note Illustrative al Foglio 031 Ampezzo, Carta geologica d'Italia alla scala 1:50.000. ISPRA, Servizio Geologico Italiano, 232 pp.

218. Voges A. 1959. Conodonten aus dem Unterkarbon I and II (Gattendorfiaund Pericyclus-Stufe) des Sauerlandes. *Paläontologische Zeitschrift* 3, 266-314.

219. Von Raumer J. & Stampfli G. M. 2008. The birth of the Rheic Ocean – Early Palaeozoic subsidence patterns and tectonic plate scenarios. *Tectonophysics* 461, 9-20

220. Walden J., Oldfield F., & Smith J. 1999. Environmental magnetism: a practical guide. *Technical Guide vol 6. Quaternary Research Association*, London.

221. Walliser O.H. 1964. Conodonten des Silurs. *Abhandlunghen des Hessisches Landesamt für Bodenforschung* 41:106.

222. Walliser, O. H. 1984a. Geologic processes and global events. *Terra Cognita*, 4: 17-20.

223. Walliser O.H., 1984b. Pleading for a natural D/C boundary. *Courier Forschungs-Institut Senckenberg*. 67, 241-246.

224. Walliser O. H. 1996. Global events in the Devonian and Carboniferous. Pp 225-250, in: *Global Events and Event Stratigraphy*, O. H. Walliser (ed.), Springer Verlag, Berlin, Germany.

225. Webster G.D., Davis L.E. & Wickwire D.W. 1987. Lithostratigraphy and biostratigraphy of Early Mississippian strata of southeastern Idaho and northeastern Utah, U.S.A. - In: Brenckle, P.L., Lane, H.R. & Manger, W.L. (Eds): Selected Studies in Carboniferous Paleontology and Biostratigraphy. *Courier Forschungs-Institut Senckenberg* 98: 179-191.

226. Wylde P. & Berry W.B.N. 1984. Destabilisation of the oceanic density structure and its significance to marine “extinction” events. *Palaeogeography Palaeoclimatology Palaeoecology* 48, 143-162.

227. Youngquist W.L. 1945. Upper Devonian conodonts from the Independence (?) shale of Iowa. *Journal of Paleontology* 19 (4): 355-367; Tulsa.

228. Zegers T.E., Dekkers M.J. & Bailly S. 2003. Late Carboniferous to Permian remagnetization of Devonian limestones in the Ardennes: role of temperature, fluids and deformation. *Journal of Geophysics Research* 108:2357. doi:10.1029/2002JB002213.

229. Ziegler W. 1957. Die Gliederung des Oberdevons und unterkarbons am Steinberg westlich von Graz mit Conodonten. In H. Flugel and W. Ziegler, *Mitteilungen des naturwissenschaftlichen Vereins der Steiermark* 87, 25-60.

230. Ziegler W. 1960. Conodonten aus dem Rheinischen Untedevon (Gedinnium) des Remscheider sattels (Rheinisches Schiefergebirge). *Palaontologische Zeitschrift*, 34, 169-201.

231. Ziegler W. 1962. Taxionomie und Phylogenie Oberdevonischer Conodonten und ihre stratigraphische Bedeutung. *Abhandlunghen des Hessisches Landesamt für Bodenforschung*, 38: 166.

232. Ziegler W. 1969. Eine neue Conodontenfauna aus dem höchsten Oberdevon. *Fortschritte in der Geologie der Rheinland und Westfalen* 17, 343-360; Krefeld.

233. Ziegler W. (ed.) 1971. Catalogue of conodonts, v. 1. - E. Schweizerbart'sche Verlagsbuchhandlung: 1-504.

234. Ziegler W. (ed.). 1973. Catalogue of Conodonts, v. 2. - E. Schweizerbart'sche Verlagsbuchhandlung: 1-404.

235. Ziegler W. (ed.) 1977. Catalogue of conodonts, v. 3. - E. Schweizerbart'sche Verlagsbuchhandlung: 1-569.

236. Ziegler W. (ed.). 1981. Catalogue of Conodonts, v. 4. - E. Schweizerbart'sche Verlagsbuchhandlung: 1-445.

237. Ziegler W. & Huddle J.W. 1969. Die Palmatolepis glabra-Gruppe (Conodonta) nach der Revision der Typen von Ulrich & Bassler durch J. W. Huddle. *Fortschritte in der Geologie der Rheinland und Westfalen* 16, 377-386.

238. Ziegler W. & Leuteritz, K. 1970. Die Grenze Devon/Karbon in Koch V. M., Leuteritz K. & Ziegler W.: Alter, Fazies und Palaogeographie der Oberdevon/Unterkarbon-Schichtenfolge an der Seiler bei iIserlohn. *Fortschritte in der Geologie der Rheinland und* Westfalen 17, 679-372.

239. Ziegler W. & Sandberg, C. A. 1984. Palmatolepis-based revision of upper part of standard Late Devonian conodont zonation; in CLARK, D.L. (ed.), Conodont biofacies and provincialism. *Geological Society of America*, *special paper*, 196: 179-194, 2 pls.

240. Ziegler, W. & Sandberg, C.A. 1990. The Late Devonian Standard Conodont Zonation. *Courier Forschungs-Institut Senckenberg*, 121: 1-115.

241. Ziegler W., Sandberg C.A. & Austin R.L. 1974. Revision of Bispathodus group (Conodonta) in the Upper Devonian and Lower Carboniferous. *Geologica et Palaeontologica* 8: 97-112.

242. Zwing, A., Bachtadse, V. & H.C. Soffel 2002. Late Carboniferous remagnetisation of Palaeozoic rocks in the NE Rhenish Massif, Germany. *Physics and Chemistry of the Earth* 27, 1179–1188.

243. Zwing, A., Matzka, J., Bachtadse, V. & H.C. Soffel 2004. Rock magnetic properties of remagnetized Palaeozoic clastic and carbonate rocks from the NE Rhenish massif, Germany. *Geophysical Journal International* 160, 477–486.

PLATES

Pl 1. **1**. *Ancyrodella nodosa* Ulrich & Bassler, 1926 MDLCA 30225, upper view, sample PZW D (Upper *rhenana* Zone); **2**. *Ancyrodella lobata* Branson & Mehl, 1934, MDLCA 30226, upper view, sample PZW D (Upper *rhenana* Zone); **3**. *Ancyrodella curvata* Branson & Mehl, 1934, MDLCA 30227, upper view, sample PZW D (Upper *rhenana* Zone); **4** *Palmatolepis simpla* Ziegler & Sandberg, 1990, MDLCA 30228, upper view, sample PZW D (Upper *rhenana* Zone); **5**. *Icriodus alternatus alternatus* Branson & Mehl, 1934, MDLCA 30229, upper view, sample PZW D (Upper *rhenana* Zone); **6**. *Palmatolepis lyaiolensis* Khrustcheva & Kuzmin, 1996, MDLCA 30230, upper view, sample PZW D (Upper *rhenana* Zone); **7**. *Palmatolepis rotunda* Ziegler & Sandberg, 1990, MDLCA 30231, upper view, sample PZW D (Upper *rhenana* Zone); **8**. *Palmatolepis jamiae* Ziegler & Sandberg, 1990, MDLCA 30232, upper view, sample PZW D (Upper *rhenana* Zone); **9**. *Palmatolepis rhomboidea* Sannemann, 1955, MDLCA 30233, upper view, sample PZW 5 (Lower *rhomboidea* Zone); **10**. *Icriodus olivierii* Corradini, 1998, MDLCA 30234, upper view, sample PZW 4 (Uppermost *crepida* Zone). **11**. *Palmatolepis minuta loba* Helms, 1963, MDLCA 30235, upper view, sample PZW 2 (Upper *crepida* Zone); **12**. *Palmatolepis* cf. *regularis* Cooper, 1931, MDLCA 30236, upper view, sample PZW 2 (Upper *crepida* Zone); **13**. *Palmatolepis tenuipunctata* Sannemann, 1955, MDLCA 30237, upper view, sample PZW 1 (Upper *crepida* Zone); **14**. *Palmatolepis quadrantinodosalobata* Sannemann, 1955, MDLCA 30238, upper view, sample PZW 4 (Uppermost *crepida* Zone); **15**. *Palmatolepis glabra glabra* Ulrich & Bassler, 1926, MDLCA 30239, upper view, sample PZW 5 (Lower *rhomboidea* Zone); **16**. *Palmatolepis glabra prima* Ziegler & Huddle, 1969, MDLCA 30240, upper view, sample PZW 5 (Lower *rhomboidea* Zone); **17**. *Palmatolepis subperlobata* Branson & Mehl, 1934, MDLCA 30241, upper view, sample PZW 4 (Uppermost *crepida* Zone); **18**.*Palmatolepis crepida* Sannemann, 1955, MDLCA 30242, upper view, sample PZW 2 (Upper *crepida* Zone); **19**. *Palmatolepis glabra pectinata* Ziegler, 1962, MDLCA 30243, upper view, sample PZW 4 (Uppermost *crepida* Zone).

Plate 1

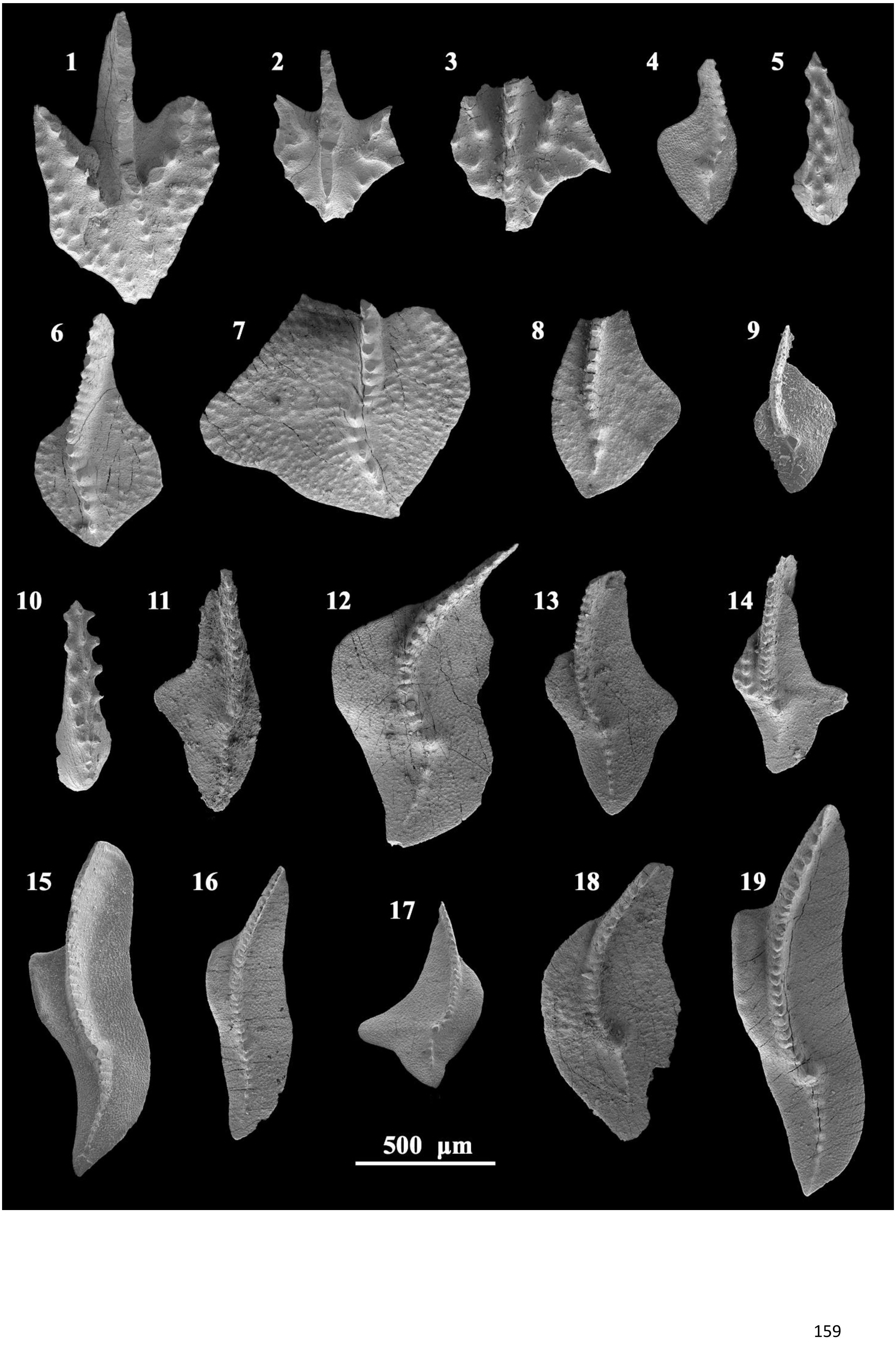

Pl 2. **1**. *Palmatolepis rugosa rugosa* Branson & Mehl, 1934, MDLCA 30244, upper view, sample PZW Z (Upper *expansa* Zone); **2**. *Palmatolepis perlobata postera* Ziegler, 1960, MDLCA 30245, upper view, sample PZW Z (Upper *expansa* Zone); **3**. *Polygnathus* cf. *nodocostatus* Branson & Mehl, 1934, MDLCA 30246, upper view, sample PZW Z (Upper *expansa* Zone); **4**. *Pseudopolygnathus irregularis* Traghelen & Hartenfels, 2011, MDLCA 30247, upper view, sample PZW Z (Upper *expansa* Zone); **5**. *Pseudopolygnathus micropunctatus* Bishoff & Ziegler, 1956, MDLCA 30248, upper view, sample PZW Z (Upper *expansa* Zone); **6**. *Pseudopolygnathus controversus* Sandberg & Ziegler, 1979, MDLCA 30249, upper view, sample PZW Z (Upper *expansa* Zone); **7**. *Polygnathus styriacus* Ziegler, 1957, MDLCA 30250, upper view, sample PZW Z (Upper *expansa* Zone); **8**. *Bispathodus stabilis* (Branson & Mehl, 1934), MDLCA 30251, upper view, sample PZW Z (Upper *expansa* Zone); **9**. *Polygnathus marginvolutus* Gedik, 1969, MDLCA 30252, upper view, sample PZW Z (Upper *expansa* Zone); **10**. *Pseudopolygnathus marburgensis marburgensis* Bishoff & Ziegler, 1956, MDLCA 30253, upper view, sample PZW Z (Upper *expansa* Zone (Upper *expansa* Zone); **11**. *Palmatolepis gracilis sigmoidalis* Ziegler, 1962, MDLCA 30254, upper view, sample PZW Z (Upper *expansa* Zone); **12**. *Polygnathus obliquostatus* Ziegler, 1962, MDLCA 30255, upper view, sample PZW Z (Upper *expansa* Zone); **13**. *Polygnathus glaber glaber* Ulrich & Bassler, 1926, MDLCA 30256, upper view, sample PZW 5 (Lower *rhomboidea* Zone); **14**. *Polygnathus nodocostatus nodocostatus* Branson & Mehl, 1934, MDLCA 30257, upper view, sample PZW 5 (Lower *rhomboidea* Zone); **15**. *Palmatolepis gracilis gracilis* Branson & Mehl, 1934b, MDLCA 30258, lower view, sample PZW Z (Upper *expansa* Zone); **16**. *Palmatolepis gracilis gracilis* Branson & Mehl, 1934b, MDLCA 30259, upper-lateral view, sample PZW Z (Upper *expansa* Zone); **17**.*Palmatolepis minuta minuta* Branson & Mehl, 1934, MDLCA 30260, upper view, sample PZW 5A (Lower *rhomboidea* Zone); **18**. *Palmatolepis marginifera marginifera* Helms, 1959, MDLCA 30261, upper view, sample PZW 7 (Lower *marginifera* Zone); **19**. *Palmatolepis stoppeli* Sandberg & Ziegler, 1973, MDLCA 30262, upper view, sample PZW 7 (Lower *marginifera* Zone); **20**. *Palmatolepis perlobata schindewolfi* Muller, 1956, MDLCA 30263, upper view, sample PZW 5 (Lower *rhomboidea* Zone).

Plate 2

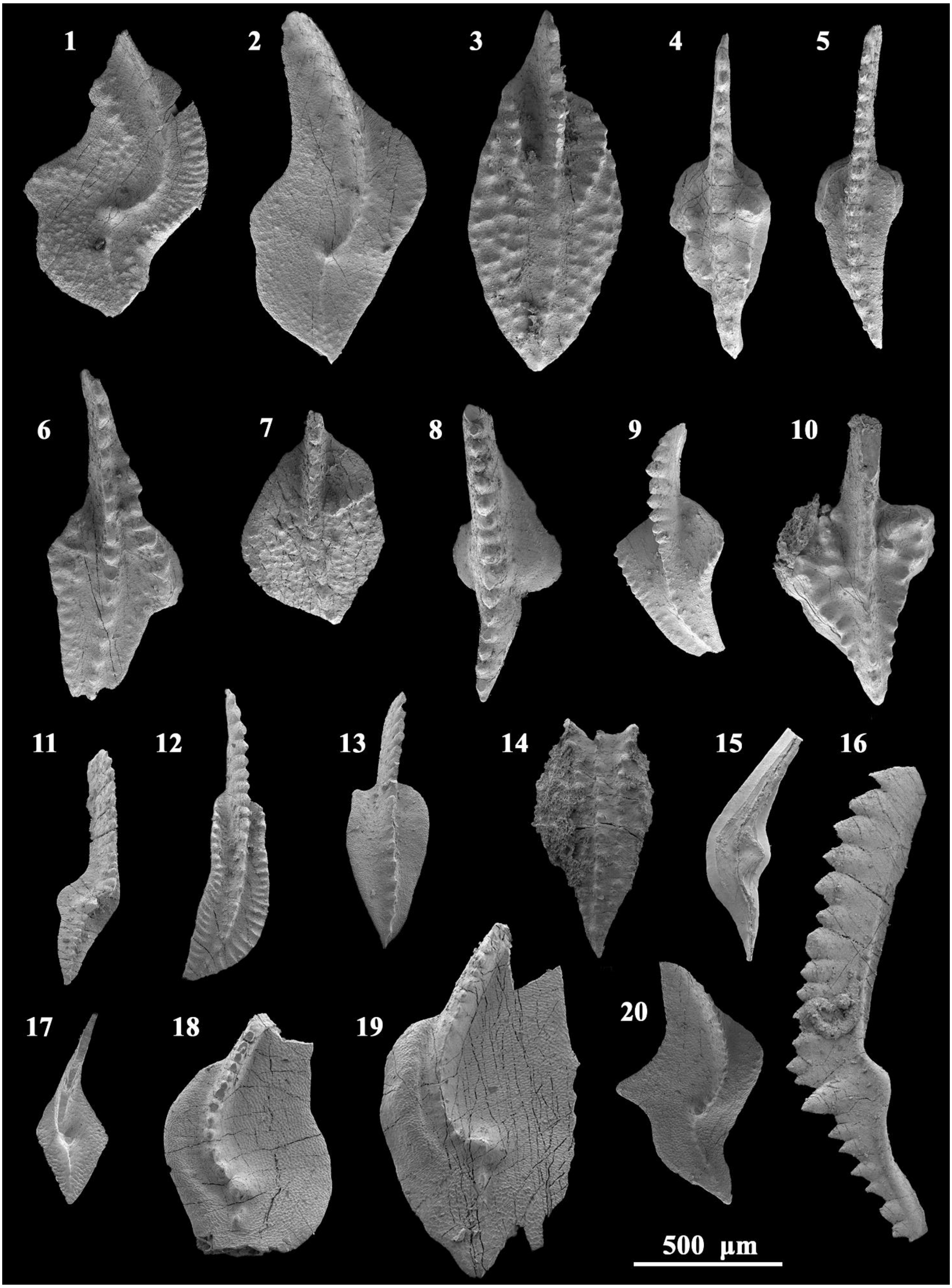

Pl 3. 1. *Palmatolepis marginifera utahensis* Ziegler & Sandberg, 1984, MDLCA 30201, upper view, sample MT 15 (Upper *marginifera* Zone); **2.** *Palmatolepis marginifera marginifera* Helms, 1961, MDLCA 30202, upper view, sample MT 10 (Upper *marginifera* Zone); **3.** *Polygnathus glaber bilobatus* Ziegler, 1962, MDLCA 30203, upper view, sample MT 10 (Upper *marginifera* Zone); **4.** *Palmatolepis glabra* ssp., MDLCA 30204, upper view, sample MT 14 (Upper *marginifera* Zone); **5.** *Palmatolepis rugosa* cf. *ampla* Müller, 1956, MDLCA 30205, upper view, sample MT 9 (Upper *marginifera* Zone); **6.** *Polygnathus communis renatae* Corradini & Spalletta, 2003 (in Corradini et al., 2003), MDLCA 30206, upper view, sample MT 9 (Upper *marginifera* Zone); **7.** *Pseudopolygnathus granulosus* Branson & Mehl, 1934a, MDLCA 30207, upper view, sample MT 6A (Upper *trachytera* Zone); **8.** *Polygnathus diversus* Helms, 1959, MDLCA 30208, upper view, sample MT 7 (Upper *marginifera* Zone); **9**. *Palmatolepis gracilis expansa* Sandberg & Ziegler, 1979, MDLCA 30209, upper view, sample MT 6 (Lower *expansa* Zone); **10.** *Pseudopolygnathus irregularis* Traghelen & Hartenfels, 2011, MDLCA 30210, upper view, sample MT 6 (Lower *expansa* Zone); **11.** *Pseudopolgnathus bidentatus* Hartenfels, 2011, MDLCA 30211, upper view, sample MT 6 (Lower *expansa* Zone); **12.** *Pseudopolygnathus micropunctatus* Bishoff & Ziegler, 1956, MDLCA 30212, upper view, sample MT 6A (Upper *trachytera* Zone); **13.** *Polygnathus duolingshanensis* Ji & Ziegler, 1993, MDLCA 30213, upper view, sample MT 6B (Lower *trachytera* Zone); **14.** *Scaphignathus velifer velifer* Helms, 1959, MDLCA 30214, upper view, sample MT 6C (*velifer* Zone); **15.** *Alternognathus regularis* Ziegler & Sandberg, 1984, MDLCA 30215, upper view, sample MT 5 (Lower *expansa* Zone); **16.** *Polygnathus pennatuloideus* Holmes, 1928, MDLCA 30216, upper view, sample MT 6C (*velifer* Zone); **17.** *Polygnathus nodoundatus* Helms, 1961, MDLCA 30217, upper view, sample MT 15 (Upper *marginifera* Zone); **18.** *Pseudopolygnathus primus* Branson & Mehl, 1934b, MDLCA 30218, upper view, sample MT 4 (Middle *expansa* Zone); **19.** *Bispathodus costatus* (Branson, 1934), MDLCA 30219, upper view, sample MT 4 (Middle *expansa* Zone); **20.** *Bispathodus aculeatus aculeatus* (Branson & Mehl, 1934a), MDLCA 30220, lateral view, sample MT X3 (Lower *praesulcata* Zone).

Plate 3

1

2

3

4

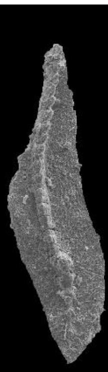

5

6

7

8

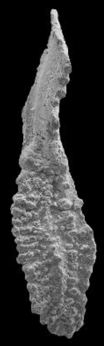

9

10

11

12

13

14

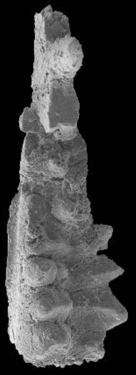

15

16

17

18

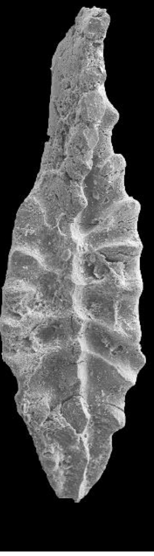

19

20

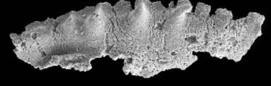

Pl 4. 1. *Palmatolepis glabra pectinata* Ziegler, 1962, MDLCA 30321, upper view, sample MT 7 (Upper *marginifera* Zone); **2.** *Palmatolepis glabra acuta* Helms, 1963, MDLCA 30322, upper view, sample MT 15 (Upper *marginifera* Zone); **3.** *Polygnathus minuta schleizia* Helms, 1963, MDLCA 30323, upper view, sample MT 6A (Upper *trachytera* Zone); **4.** *Alternognathus beulensis* Ziegler & Sandberg, 1984, MDLCA 30324, upper view, sample MT 6B (Lower *trachytera* Zone); **5**. *Polygnathus normalis* Miller & Youngquist, 1947, MDLCA 30325, upper view, sample MT 8 (Upper *marginifera* Zone); **6.** *Palmatolepis glabra distorta* Branson & Mehl, 1934a, MDLCA 30326, upper view, sample MT 7 (Upper *marginifera* Zone); **7a-b.** *Pseudopolygnathus rapiformis* Corradini & Spalletta, 2003 (in Corradini et al., 2003), IPUM 27639, upper and lower views, (Upper *duplicata* Zone); **8a-b.** *Polygnathus pusillus* Corradini & Spalletta, 2003 (in Corradini et al., 2003), IPUM 27611, upper and lower views, (Upper *duplicata* Zone); **9**. *Polygnathus subirregularis* Sandberg & Ziegler, 1979, MDLCA 30327, upper view, sample MT 6B (Lower *expansa* Zone); **10.** *Pseudopolygnathus marginatus* Branson & Mehl, 1934b, IPUM 27641, upper view, sample MT X2 (Upper *duplicata* Zone); **11.** *Polgnathus communis communis* Branson & Mehl, 1934b, IPUM 27606, upper view, (Upper *duplicata* Zone); **12.** *Polgnathus biconstrictus* Gedik, 1969, IPUM 27628, upper view, sample MT X1 (Upper *duplicata* Zone); **13.** *Siphonodella hassi* Ji, 1985, IPUM 27594, upper view, sample MT X (Upper *duplicata* Zone); **14.** *Siphonodella praesulcata* Sandberg, 1972, IPUM 27597, upper view, (Lower *praesulcata* Zone); **15.** *Siphonodella bransoni* Ji, 1985, IPUM 27596, upper view, (Upper *duplicata* Zone); **16.** *Palmatolepis glabra lepta* Ziegler & Huddle, 1969, MDLCA 30332, upper view, sample MT 6C (*velifer* Zone); **17.** *Polygnathus fornicatus* Ji, Xiong & Wu, 1928, IPUM 27631, upper view, sample MT X1 (Upper *duplicata* Zone); **18.** *Polygnathus granulosus* Branson & Mehl, 1934a, MDLCA 30329, upper view, sample MT 6A (Upper *trachytera* Zone); **19.** *Branmehla inornata* (Branson & Mehl, 1934a), MDLCA 30330, upper view, sample MT 10 (Upper *marginifera* Zone); **20.** *Palmatolepis perlobata maxima* (Branson & Mehl, 1934a), MDLCA 30331, upper view, sample MT 15 (Upper *marginifera* Zone).

Plate 4

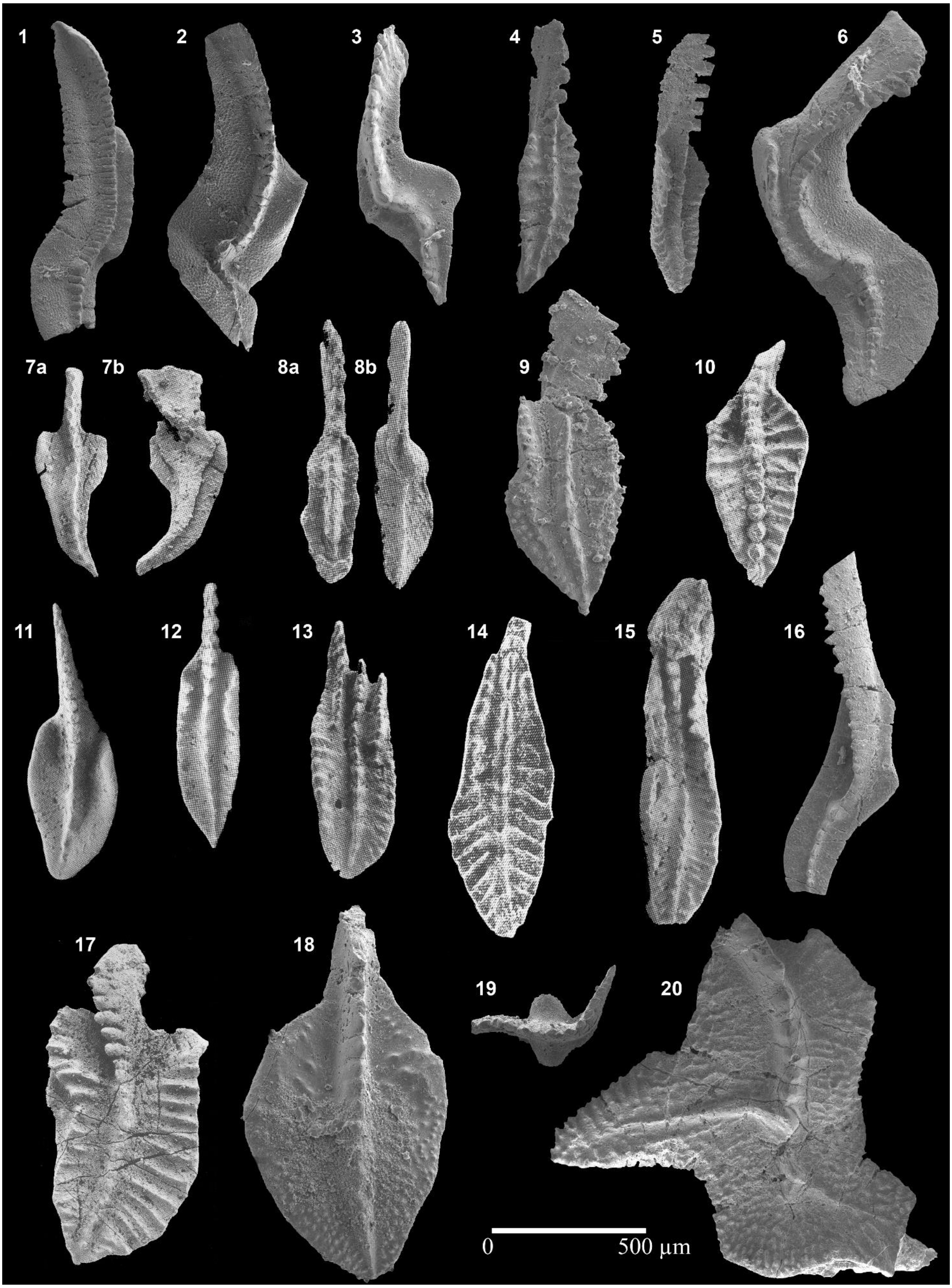

Pl 5. 1a-b. *Palmatolepis perlobata schindewolfi* Müller, 1956, upper view, PB section (Upper *trachytera* Zone); **2a-b.** *Palmatolepis gracilis expansa* Sandberg & Ziegler, 1979, upper and lower views, PB section (Lower *expansa* Zone); **3**. *Palmatolepis rugosa trachytera* Ziegler, 1960, IPUM 26020, upper view, sample CM I 19 (Upper *trachytera* Zone); **4**. *Palmatolepis minuta wolskae* Szulczewski, 1971, IPUM 27762, upper view, sample CM I 2 (Lower *rhomboidea* Zone); **5**. *Polygnathus perplexus* Thomas, 1949, IPUM 27809, upper view, sample CM I 19 (Upper *trachytera* Zone); **6**. *Palmatolepis minuta subgracilis* Bishoff, 1956, IPUM 26073, upper view, sample CM I 2 (Lower *rhomboidea* Zone); **7**. *Palmatolepis perlobata helmsi* Ziegler, 1962, IPUM 27780, upper view, sample CM I 19 (Upper *trachytera* Zone); **8.** *Palmatolepis perlobata grossi* Ziegler 1960, IPUM 27782, Upper view, sample CM I 17 (Upper *marginifera* Zone); **9.** *Pseudopolygnathus dissimilis* (Helms & Wolska, 1967), IPUM 26012, Upper view, sample CM I 23 (Middle *expansa* Zone); **10.** *Scaphignathus velifer leptus* Sandberg & Ziegler, 1984, IPUM 26015, upper view, sample CM I 18A (*velifer* Zone); **11.** *Scaphignathus velifer leptus* Sandberg & Ziegler, 1984, IPUM 27818, lateral view, sample CM I 18C (Lower *trachytera* Zone); **12.** *Branmehla bohlenana* Helms, 1959, IPUM 27698, upper view, sample CM I 18C (Lower *trachytera* Zone); **13.** *Branmehla bohlenana* Helms, 1959, IPUM 27699, lateral view, sample CM I 19 (Upper *trachytera* Zone); **14**. *Polygnathus eoglaber* Ji & Ziegler, 1993, IPUM 25982, upper view, sample CM II 2A (Lower *crepida* Zone); **16.** *Mehlina strigosa* (Branson & Mehl, 1934a), MDLCA 30332, Lateral view, sample MT 14 (Upper *marginifera* Zone). **17.** *Polygnathus rhabdotus* Schäfer, 1976, IPUM 26013, Upper view, sample CM I 21 (Lower *expansa* Zone); **18.** *Polygnathus rhabdotus* Schäfer, 1976, IPUM 27810, Upper view, sample CM I 21 (Lower *expansa* Zone); **19.** *Siphonodella praesulcata* Sandberg, 1972, IPUM 26006, upper view, sample CM I 26 (Lower *praesulcata* Zone); **20.** *Siphonodella praesulcata* Sandberg, 1972, IPUM 27823, lateral view, sample CM I 26 (Lower *praesulcata* Zone); **21.** *Siphonodella praesulcata* Sandberg, 1972, IPUM 27824, lower view, sample CM I 25B (Lower *praesulcata* Zone).

Plate 5

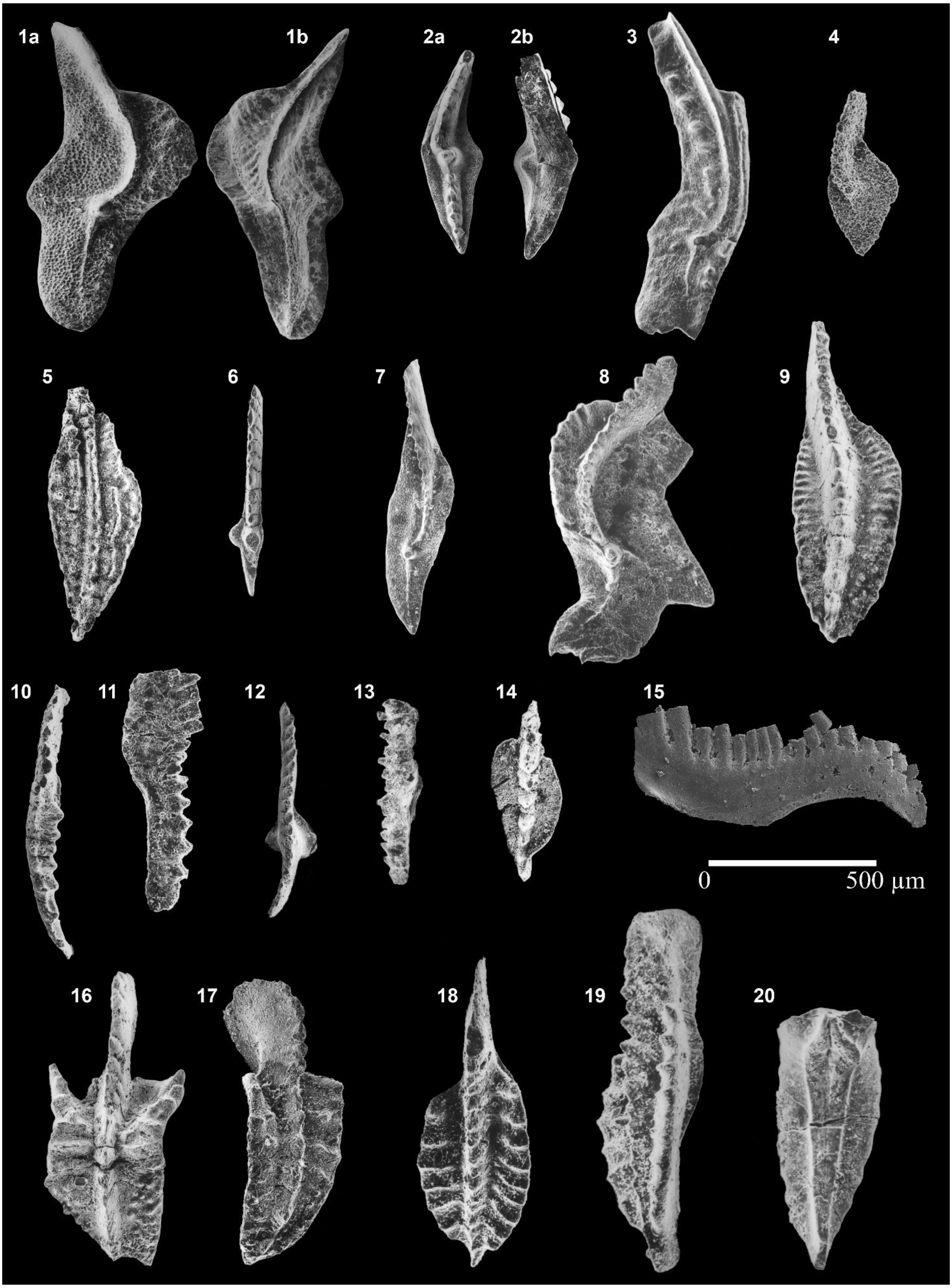

Pl 6. 1–2. *Polygnathus bicristatus,* upper and lower views of MDLCA 30279, sample BTE 9 (Lower *duplicata* Zone). **3-4.** *Polygnathus bicristatus*, upper and lower views of the holotype MDLCA 30280, sample BTE 9 (Lower *duplicata* Zone); **5.** *Polygnathus bicristatus*, upper view of MDLCA 30281, sample BTE 9 (Lower *duplicata* Zone); **6.** *Polygnathus bicristatus*, upper view of MDLCA 30282, sample BTE 9 (Lower *duplicata* Zone); **7.** *Polygnathus bicristatus*, upper view of MDLCA 30283, sample BTE 9 (Lower *duplicata* Zone); **8.** *Polygnathus* sp. A, upper-lateral view of MDLCA 30284, sample BTE 9 (Lower *duplicata* Zone); **9.** *Polygnathus* sp. A, upper-lateral view of MDLCA 30285, sample BTE 9 (Lower *duplicata* Zone); **10.** *Polygnathus* sp. A, upper view of MDLCA 30286, sample BTE 9 (Lower *duplicata* Zone); **11.** *Polygnathus* sp. A, lower view of MDLCA 30287, sample BTE 9 (Lower *duplicata* Zone); **12.** *Polygnathus* sp. B, upper view of MDLCA 30288, sample BTE 9 (Lower *duplicata* Zone); **13-14.** *Polygnathus nuragicus*, upper and lower views of MDLCA 30289, sample BTE 9 (Lower *duplicata* Zone); **15-16.** *Polygnathus nuragicus*, upper-lateral and lower views of MDLCA 30290, sample BTE 9 (Lower *duplicata* Zone); **17-18.** *Polygnathus nuragicus*, lateral and lower views of MDLCA 30291, sample BTE 9 (Lower *duplicata* Zone); **19.** *Polygnathus nuragicus*, upper view of MDLCA 30292, sample BTE 9 (Lower *duplicata* Zone); **20.** *Pseudopolygnathus* sp. A, upper view of MDLCA 30293, sample BTE 10 (Upper *duplicata* Zone); **21-22.** *Pseudopolygnathus granulobatus*, upper and lower views, MDLCA 30294, sample BTE 4 (Middle *expansa* Zone); **23-24.** *Pseudopolygnathus granulobatus,* upper view of MDLCA 30295, sample BTE 4 (Middle *expansa* Zone).

Plate 6

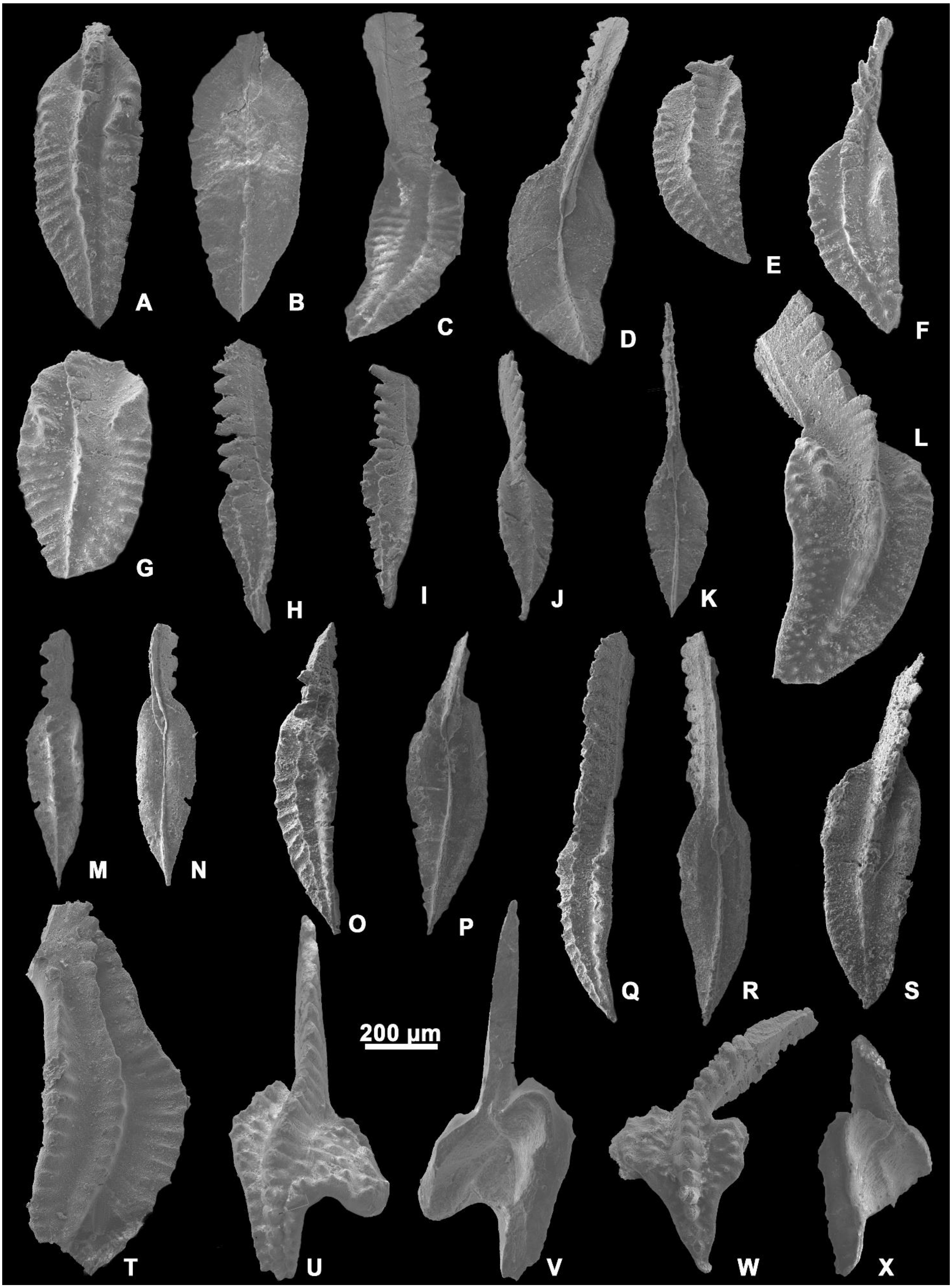

Pl 7. 1. *Polygnathus styriacus* Ziegler, 1957, upper view of MDLCA 30296, sample BTE 1 (*styriacus* Zone); **2.** *Palmatolepis perlobata postera* Ziegler, 1960, upper view of MDLCA 30297, sample BTE 2 (Lower *expansa* Zone); **3.** *Palmatolepis gracilis expansa* Sandberg & Ziegler, 1979, upper view of MDLCA 30298, sample BTE 2 (Lower *expansa* Zone); **4.** *Bispathodus jugosus* (Branson & Mehl 1934a), upper view of MDLCA 30299, sample BTE 4 (Middle *expansa* Zone); **5.** *Bispathodus costatus* (Branson, 1934), upper view of MDLCA 30300, sample BTE 5 (Upper *expansa* Zone); **6.** *Bispathodus spinulicostatus* (Branson, 1934), upper view of MDLCA 30301, sample BTE 6 (Upper *expansa* Zone); **7.** *Bispathodus ultimus* (Bischoff, 1957), upper view of MDLCA 30302, sample BTE 5 (Upper *expansa* Zone); **8–9.** *Branmehla werneri* (Ziegler, 1957), lateral and upper views of MDLCA 30303, sample BTE 2 (Lower *expansa* Zone); **10.** *Branmehla suprema* (Ziegler, 1962), upper view of MDLCA 30304, sample BTE 6 (Upper *expansa* Zone); **11.** *Pseudopolygnathus marburgensis trigonicus* Ziegler, 1962, upper view of MDLCA 30305, sample BTE 5 (Upper *expansa* Zone); **12.** *Polygnathus tenuiserratus* Corradini & Spalletta (in Corradini et al.), 2003, upper view of MDLCA 30306, sample BTE 10 (Upper *duplicata* Zone); **13.** *Pseudopolygnathus* cf. *nudus* Pierce & Langenheim 1974, upper view of MDLCA 30307, sample BTE 10 (Upper *duplicata* Zone); **14.** *Polygnathus communis dentatus* Druce, 1969, upper view of MDLCA 30308, sample BTE 10 (Upper *duplicata* Zone); **15.** *Polygnathus purus purus* Voges, 1959, upper view of MDLCA 30309, sample BTE 8A (*sulcata* Zone); **16.** *Siphonodella duplicata* (Branson & Mehl 1934b), upper view of MDLCA 30310, sample BTE 10 (Upper *duplicata* Zone); **17.** *Siphonodella duplicata* (Branson & Mehl 1934b), upper view of MDLCA 303111, sample BTE 10 (Upper *duplicata* Zone); **18.** *Siphonodella carinthiaca* Schönlaub, 1969, upper view of MDLCA 30312, sample BTE 10 (Upper *duplicata* Zone); **19.** *Siphonodella cooperi* Hass, 1959, upper view of MDLCA 303113, sample BTE 10 (Upper *duplicata* Zone); **20.** *Siphonodella sulcata* Huddle, 1934, upper view of MDLCA 303114, sample BTE 10 (Upper *duplicata* Zone); **21.** *Polygnathus communis renatae* Corradini & Spalletta (in Corradini et al.), 2003, upper view of MDLCA 30315, sample BTE 8 (*sulcata* Zone); **22.** *Pseudopolygnathus triangulus* Voges, 1959, upper view of MDLCA 30316, sample BTE 10 (Upper *duplicata* Zone); **23.** *Protognathodus meischneri* Ziegler, 1969, upper view of MDLCA 30317, sample BTE 8 (*sulcata* Zone); **24.** *Protognathodus kockeli* Bischoff, 1957, upper view of MDLCA 30318, sample BTE 8 (*sulcata* Zone); **25.** *Protognathodus collinsoni* Ziegler, 1969, upper view of MDLCA 30319, sample BTE 8 (*sulcata* Zone); **26.** *Protognathodus kuehni* Ziegler & Leuteritz, 1970, upper view of MDLCA 30320, sample BTE 8 (*sulcata* Zone).

Plate 7